MONASH University

Investigating the role of SNAIL family of proteins in colorectal cancer

Reyhan Akhtar

B Pharm, M Pharm

A thesis submitted for the degree of

Doctor of Philosophy

in 2018

Monash University

Department of Anatomy and Developmental Biology

Faculty of Medicine, Nursing and Health Sciences

Copyright notice

Contents

Copyright notice 2
List of figures 5
List of tables 8
Publications during enrolment 15
Abstract 16
Declaration 18
Acknowledgement 19
Chapter 1 Introduction 20
1.1 Colorectal cancer 21
1.2 Normal human intestine 35
1.3 SNAIL family of transcription factors 48
1.4 Mouse models for studying intestinal cell biology and tumourigenesis 57
1.5 Intestinal organoids 70
1.6 Conclusion: Challenges and unanswered questions 78
1.7 Hypotheses & aims 79
Chapter 2 - Methods 80
2.1 Collection of primary human colorectal tumour and adjacent normal tissues 81
2.2 Animals 81
2.3 RNA extraction 91
2.4 cDNA synthesis and quantification 91
2.5 Droplet Digital PCR 92
2.6 Immunohistochemistry 95
2.7 H&E staining 96
2.8 Polyp tissue analyses 97
2.9 Histological analyses 98
2.10 Colonic organoid cultures 99
2.11 The Cancer Genome Atlas data analyses 105
2.12 Statistical analyses 105
Chapter 3 - Analysis of SNAIL proteins in primary human colorectal tumours 107
3.1 Introduction 108
3.2 Results 117
3.3 Discussion 148
Chapter 4 – Effects of *Snai1* up-regulation in mouse colonic epithelium and *in vitro* organoid cultures 157

4.1 Introduction 158
4.2 Results 162
4.3 Discussion 182
Chapter 5 - Effects of *Snai1* elevation on intestinal tumourigenesis in the *Apc*$^{flox/flox}$ mouse model of colon cancer 188
5.1 Introduction 189
5.2 Results 200
5.3 Discussion 216
Chapter 6 - General discussion 223
6.1 Introduction 224
6.2 Main findings 224
6.3 Proposed model of SNAI1 function in the colonic epithelium 228
6.4 Future directions 231
6.5 Conclusion 232
References 233

List of figures

Figure 1.1 TNM Staging of colorectal cancer 24
Figure 1.2 Genetic model for colorectal tumourigenesis 26
Figure 1.3 The cancer stem cell model 32
Figure 1.4 Links between molecular factors regulating normal and CSC renewal 34
Figure 1.5 Anatomy of the intestinal wall 35
Figure 1.6 Microscopic anatomy of the mouse colonic epithelium showing crypts 37
Figure 1.7 $Lgr5^{+}$ stem cells in the small intestinal crypts 40
Figure 1.8 The Wnt signalling cascade 45
Figure 1.9 Basic structural organisation of SNAIL family proteins. 49
Figure 1.10 Cre-lox recombination system 59
Figure 1.11 Schematic diagram showing the *VillinCreERT2* construct 61
Figure 1.12 Schematic diagram showing the construct in the *Lgr5CreERT2* mice 62
Figure 1.13 Schematic representation of the construct of the *Cdx2CreERT2* transgene 64
Figure 1.14 Schematic diagram showing the structure of the conditionally targeted allele of *Apc* (Apc^{580s}) 66
Figure 1.15 Schematic diagram showing structure of the conditionally targeted *ROSA26* allele 69
Figure 1.16 Intestinal organoid cultures 72
Figure 1.17 Human colorectal tumour organoids 73
Figure 1.18 Schematic representation of mechanism of inhibition of *Snail*-mediated transcriptional repression of *E-cadherin* by Parnate 77
Figure 3.1 TNM Staging of colorectal cancer 109
Figure 3.2 Intestinal stem cell markers are up-regulated in human colorectal tumours 119
Figure 3.3 Intestinal stem cell markers are up-regulated in a sub-set of human colorectal tumours 120
Figure 3.4 No association of ISC markers with colorectal tumour stage. 122
Figure 3.5 No association of ISC markers with colorectal tumour grade. 123
Figure 3.5 *SNAI1* is up-regulated in human colorectal cancer 125
Figure 3.6 *SNAIL* family members are up-regulated in a subset of human colorectal tumours 126
Figure 3.7 *SNAI1* and *SNAI2* are up-regulated in T3 stage tumours compared to T0 tumours 130
Figure 3.8 *SNAI1* is significantly down-regulated in stage 0 tumours 131
Figure 3.9 Expression of *SNAI1* is significantly lower in adenomas 132
Figure 3.10 Expression of *SNAIL* family members and ISC markers varies across different human colorectal cancer cell lines 134
Figure 3.11 *SNAIL* expression is up-regulated in a subset of colorectal cancer organoid lines 136

Figure 3.12 Assessment of cell viability by PrestoBlue assay in normal, SNAI1^{low} and SNAI1^{high} organoids post treatment with Parnate 139
Figure 3.13 Expression of epithelial markers post treatment (12 hours) with Parnate in normal, SNAI1^{low} and SNAI1^{high} organoids 142
Figure 3.14 cBioPortal OncoPrint summary for *SNAI1*, *SNAI2* and *SNAI3* in the TCGA (Provisional) cohort 143
Figure 3.15 cBioPortal data analysis of frequencies of different genetic alterations of (A) *SNAI1*, (B) *SNAI2* and (C) *SNAI3* across CRCs of different origin 145
Figure 3.16 Overall survival Kaplan-Meier estimate 146
Figure 4.1 Schematic representation of the *RosaSnai1* construct 159
Figure 4.2 Schematic representation of the *VillinCreERT2* construct 160
Figure 4.3 Schematic representation of the *Cdx2CreERT2* construct 160
Figure 4.4 Efficient induction of *Snai1* expression in the small intestine but not in the colon at day 5 in the *VillinCreERT2 RosaSnai1* mice post induction 164
Figure 4.5 Modest up-regulation of *Snai1* in the colon of *VillinCreERT2 RosaSnai1* mice at day 10 165
Figure 4.6 LacZ staining showing patchy recombination in the colon of *VillinCreERT2 Rosa26LacZ* mouse on day 5 165
Figure 4.7 The *Cdx2CreERT2* model drives efficient recombination in the proximal region of the colon 167
Figure 4.8 Lack of induction of *Snai1* up-regulation in the colon at day 5 using the *Cdx2CreERT2* model 168
Figure 4.9 Efficient recombination in the colon achieved at day 10 using the *Cdx2CreERT2* mice 168
Figure 4.10 No obvious phenotypic changes observed in colonic epithelium post *Snai1* up-regulation 169
Figure 4.11 *Snai1* up-regulation induces cell proliferation in colonic crypts 170
Figure 4.12 Colonic crypts over-expressing *Snai1* harbour more proliferative cells 170
Figure 4.13 The expression of CBC stem cell markers is down-regulated following up-regulation of *Snai1* in the colon 172
Figure 4.14 *Snai1* up-regulation in the colon down-regulates +4 stem cell marker expression 173
Figure 4.15 *Snai1* up-regulation in the colon does not affect the expression of enteroendocrine and goblet cell markers 174
Figure 4.16 Colonic organoid grown from a single isolated crypt from wild type mouse epithelium 175
Figure 4.17 The optimal concentration of TAT-Cre to induce efficient recombination in organoids was 8 µM 177
Figure 4.18 Proportion of GFP^{+} cells increases with increase in concentration of TAT-Cre as measured by flow cytometry 178
Figure 4.19 FACS-sorted single TAT-Cre treated colonic epithelial cells give rise to organoids in vitro 178
Figure 4.20 FACS-sorting strategy to collect proliferating cells expressing the *Snai1* transgene 179
Figure 4.21 *Snai1* up-regulation in colonic stem cell-enriched cell population results in activation of EMT in vitro 180

Figure 4.22 *Snai1* up-regulation and loss of Lgr5 expression in transfected proliferative cells *in vitro* 181
Figure 5.1 Functional domains of APC protein 190
Figure 5.2 Genetic model for colorectal tumourigenesis 192
Figure 5.3 Schematic diagram showing the *Lgr5CreERT2* construct 199
Figure 5.4 Schematic representation of the *Cdx2CreERT2* construct 200
Figure 5.5 Schematic diagram showing the structure of the conditionally targeted allele of Apc^{580s} 200
Figure 5.6 Schematic diagram showing the structure of the conditionally targeted *ROSA26* allele 201
Figure 5.7 Representative images of polyps 201
Figure 5.8 Potential *Snai1* overexpression has no effect on the number of polyps formed in the test mice 202
Figure 5.9 Distal small intestine is the site for larger polyps 204
Figure 5.10 *Snai1* overexpression does not affect polyp growth in the distal SI and colon 204
Figure 5.11 *Snai1* transgene does not favour growth of polyps in either distal SI or colon 206
Figure 5.12 PCR analysis of cDNA from polyps 208
Figure 5.13 Insufficient *Snai1* up-regulation in *Lgr5CreERT2* $Apc^{flox/flox}$ *RosaSnai1* mice 209
Figure 5.14 ddPCR analysis revealed that control and test polyps exhibited no significant difference in *Snai1* expression 210
Figure 5.15 Successful *Snai1* up-regulation in polyps 211
Figure 5.16 *Snai1* transgene expression does not affect polyp count in the colon 212
Figure 5.17 Representative images of colonic tissues with polyps 213
Figure 5.18 Expression of *Snai1* transgene promotes growth of polyps 213
Figure 5.19 Over-expression of *Snai1* in polyps promotes cell proliferation 215
Figure 5.20 Polyp regions over-expressing *Snai1* harbour more proliferative cells 215
Figure 6.1 Proposed model for SNAI1 function in the colonic epithelium 230

List of tables

Table 1.1 The TNM staging system for colorectal tumours as defined by the AJCC 24
Table 1.2 Taxonomy of CRC as proposed by Guinney et al. 30
Table 1.3 Markers of adult intestinal stem cells 43
Table 1.4 Members of the *Snail* superfamily 49
Table 1.5 A list of culture media components required for growth of mouse small intestinal and colonic organoids 71
Table 1.6 A list of culture media components required for growth of normal human and colorectal tumour organoids 72
Table 2.1 Summary of the different mouse genotypes used in the study along with their induction regimen 85
Table 2.2 Description of genotyping protocol along with primer sequences for each allele 89
Table 2.3 Components and cycle conditions required for the 2-step reverse transcription protocol 92
Table 2.4 Components of probe and primer reaction mixes for ddPCR along with cycle conditions 93
Table 2.5 Fluorescent probes assay details for ddPCR analysis 93
Table 2.6 Human and mouse primers used for ddPCR analysis 94
Table 2.7 List of antibodies used for immunohistochemistry and immunofluorescence 96
Table 2.8 List of culture media components required for normal human and colorectal tumour organoid cultures 100
Table 2.9 List of culture media components required for mouse colonic organoid cultures 103
Table 2.10 Characteristics of different human colorectal cancer cell lines 104
Table 3.1 TNM staging system of colorectal tumours 110
Table 3.2 Characteristics of colorectal cancer patients (n=68) 118
Table 3.3 Pairwise Pearson correlation of logged fold change values of *SNAIL* family members and ISC markers 128
Table 3.4 Spearman rank order correlation of logged fold change values of *SNAIL* family members and ISC markers 128
Table 3.5 Summary of patients with genetically altered *SNAI1*, *SNAI2* and *SNAI3* 143
Table 3.6 Frequency of samples with co-altered *SNAIL* family genes 144
Table 3.7 Overall survival of CRC patients 146
Table 3.8 Correlation between *SNAI1* and other EMT molecules 147
Table 5.1 APC mutations in colorectal cancer 190
Table 5.2 Examples of genes studied in context of different Apc mutations with description of the location of adenomas and effect on tumour burden and invasion 196
Table 5.3 Summary of localisation of polyps in the intestinal tract in control and test mice 203

Abbreviations

α	Alpha
β	Beta
°	Degree
µg	Micro gram
µl	Micro litre
µm	Micro metre
µM	Micro molar
~	Approximately
<	Smaller/less than
=	Equals to
>	Greater/more than
±	Plus or minus
≥	Greater than or equal to
5-FU	5-Fluorouracil
AJCC	American Joint Committee on Cancer
AML	Acute myeloid leukaemia
APC	Adenomatous polyposis coli
Ascl2	Achaete-scute complex homolog 2
bHLH	Basic helix-loop-helix
Bmi1	Polycomb complex protein
BNF	β-napthoflavone
bp	Base pair
BrdU	5-bromo-2'-deoxyuridine
BSA	Bovine serum albumin
C	Celsius

CBC	Crypt base columnar
cDNA	Complementary DNA
CIMP	CpG island methylator phenotype
CIN	Chromosomal instability
CMS	Consensus molecular subtypes
CRC	Colorectal cancer
CRISPR-Cas9	Clustered regularly interspersed short palindromic repeat (CRISPR)–CRISPR-associated protein 9
CSC	Cancer stem cell
DAB	3,3’-diaminobenzidine
DAPI	4',6-diamidino-2-phenylindole
ddPCR	Droplet digital PCR
DFS	Disease-free survival
DMEM	Dulbecco's Modified Eagle Medium
DNA	Deoxyribonucleic acid
DNase	Deoxyribonuclease
dNTP	Deoxyribonucleotide triphosphate
DPX	Dibutylphthalate polystyrene xylene
E	Embryonic day
EDTA	Ethylenediaminetetraacetic acid
EGFP	Enhances green fluorescent protein
EGFR	Endothelial growth factor receptor
EMT	Epithelial to mesenchymal transition
ENU	N-ethyl-N-nitrosourea
EphB2	Ephrin type-B receptor 2
EtOH	Ethanol
FACS	Fluorescence-activated cell sorting

FAP	Familial adenomatous polyposis
FBS	Foetal bovine serum
fl	Flox
g	G-force/ relative centrifugal force
gDNA	Genomic DNA
GFP	Green fluorescent protein
GSEA	Gene set enrichment analysis
GSK-3β	Glycogen synthase kinase 3 beta
H&E	Haematoxylin and Eosin
HDAC1/2	Histone deacetylases 1 and 2
HEPES	4-(2-hydroxyethyl)-1-piperazineethanesulfonic acid
HMLE	Human mammary epithelial cell
HNPCC	Hereditary nonpolyposis colorectal cancer
HRP	Horseradish peroxidase
i.p.	Intraperitoneal
IBD	Inflammatory bowel disease
IgG	Immunoglobulin G
IHC	Immunohistochemistry
IPC	Internal positive control
IRES	Internal ribosome entry site
ISC	Intestinal stem cell
ISH	In situ hybridisation
kb	Kilo base
KDa	Kilo Dalton
kg	Kilo gram
LEF	Lymphoid enhancer factor
Lgr5	Leucine-rich repeat-containing G-protein coupled receptor 5

LOH	Loss of heterozygosity
loxP	Locus of crossover bacteriophage P1
Lrig1	Leucine-rich repeats and immunoglobulin-like domains protein 1
LRP	Lipoprotein receptor-related protein
LSD1	Lysine-specific demethylase 1
M	Molarity
MAd	Mucinous adenocarcinoma
MAO	Monoamine oxidase
MEC	Mammary epithelial cell
Min	Multiple intestinal neoplasia
MIN	Microsatellite instability
ml	Millilitre
ml	Milli litre
mm	Millimetre
mM	Millimolar
mm	Milli molar
Msi1	Musashi homolog 1
m-tert	Mouse telomerase reverse transcriptase
n	Number
NES	Nuclear export sequence
ng	Nano gram
NLS	Nuclear localisation sequence
ns	Not significant
Olfm4	Olfactomedin 4
OS	Overall survival
PBS	Phosphate buffered saline
PCR	Polymerase chain reaction

PDO	Patient-derived organoid
PDX	Patient-derived xenograft
PFA	Paraformaldehyde
PGK	Phosphoglucokinase
PRC2	Polycomb repressor complex 2
qRT-PCR	Quantitative reverse transcription PCR
RNA	Ribonucleic acid
RNAi	RNA interference
Rnf43	Ring finger protein 43
rpm	Revolutions per minute
RSEM	RNA-Seq by Expectation Maximisation
Rspo2/Rspo3	R-spondin 2/R-spondin 3
RT	Room temperature
RT-PCR	Reverse Transcription-PCR
SCNA	Somatic copy number alterations
SCRA	Signet ring cell adenocarcinoma
SDS	Sodium dodecyl sulphate
SEM	Standard error of the mean
SI	Small intestine
SRD	Serine-rich domain
TA	Transit-amplifying
TAE	Tris-acetate-EDTA
TCF	T-cell factor
TCGA	The Cancer Genome Atlas
TGF-β	Transforming growth factor beta
TNM	Tumour/node/metastasis
UTR	Untranslated region

V	Volts
WHO	World health organisation
WT	Wild-type
x	times/magnification
YFP	Yellow fluorescent protein
ZEB	Zinc-finger E-box binding transcription factor
ZF	Zinc finger
Znrf3	Zinc and ring finger 3

Publications during enrolment

Jardé, T., Kerr, G., **Akhtar, R.** & Abud, H. E. 2018. Modelling intestinal carcinogenesis using in vitro organoid cultures. in: Jenkins, B. J. (Ed.) Inflammation and Cancer: Methods And Protocols. New York, NY: Springer New York.

Horvay, K., Jarde, T., Casagranda, F., Perreau, V. M., Haigh, K., Nefzger, C. M., **Akhtar, R.**, Gridley, T., Berx, G., Haigh, J. J., Barker, N., Polo, J. M., Hime, G. R. & Abud, H. E. 2015. Snai1 regulates cell lineage allocation and stem cell maintenance in the mouse intestinal epithelium. EMBO J, 34, 1319-35.

Abstract

Colorectal cancer (CRC) has a high mortality rate and is the second most common cause of cancer-related deaths in Australia. The majority of the Australian population diagnosed with CRC has a chance of surviving at least 5 years post diagnosis. A high proportion of the CRC patients can be treated successfully when their tumours are diagnosed at early stages, however, fewer than 40% of colorectal tumours are actually detected early. CRC is a progressive disease and each stage of tumourigenesis is marked by mutations in key genes. Mutations in Adenomatous polyposis coli (*APC*) is one of the major drivers of colorectal tumourigenesis. CRCs are believed to originate from intestinal stem cells (ISCs) that undergo genetic alterations leading to uncontrolled cell proliferation in the intestinal epithelium while cancer stem cells (CSCs) are responsible for sustenance of established tumours.

SNAIL family genes – *SNAI1*, *SNAI2* and *SNAI3* - are well known regulators of epithelial to mesenchymal transition (EMT) in embryonic development and also diseased states like cancer metastasis. Recently there has been evidence supporting the contribution of SNAIL family members in acquisition of stem cell properties in non-stem cells and generation of CSCs in various malignancies. This thesis investigates the role of SNAIL family of proteins in regulation of CSCs and maintenance of colorectal tumours. Previous studies and results in this thesis have shown that *SNAI1* is up-regulated in human CRC. Expression of *SNAIL* family members has been shown to correlate with expression of ISC markers *LGR5*, *EPHB2* and *BMI1* in a cohort of 68 primary human colorectal tumours. Significant up-regulation of *SNAI1* has been found to occur during early stages of colorectal tumourigenesis, particularly stage T2 and T3 tumours. cBioPortal data analysis of The

Cancer Genome Atlas (TCGA) cohort of 633 colorectal tumour patients revealed genetic alterations in *SNAIL* genes occur in 21% cases. Patients with altered *SNAIL* genes are associated with lower overall survival. These results suggest that *SNAIL* possibly regulates the stem cell population in tumours and contributes to tumour progression during early stages of tumourigenesis.

This thesis also examines the consequences of *Snai1* up-regulation in the colonic epithelium using mouse models. *Snai1* up-regulation has been shown to enhance cell proliferation in normal colonic epithelial tissues as well as during intestinal polyposis. The functional role of *Snai1* has also been studied *in vitro* using organoid cultures. Over-expression of *Snai1 in vitro* indicated activation of EMT and transformation of a cell population enriched for ISCs into mesenchymal-like cells. Overall, results in this thesis suggest a potential role of SNAIL proteins in regulation of CSCs in CRC. Data presented in this thesis provides an insight into the down-stream effects of SNAI1 up-regulation observed in colorectal tumours and may assist in identifying potential therapeutic targets for CRC prognosis and treatment.

Declaration

This thesis contains no material which has been accepted for the award of any other degree or diploma at any university or equivalent institution and that, to the best of my knowledge and belief, this thesis contains no material previously published or written by another person, except where due reference is made in the text of the thesis.

Reyhan Akhtar

Department of Anatomy and Developmental Biology

Faculty of Medicine, Nursing and Health Sciences

Monash University

Date: 25th September 2018

Acknowledgement

This thesis marks the end of my journey in obtaining a doctorate at Monash University. I would like to express my thanks to all those who contributed in many ways and supported me throughout this journey. I would like to acknowledge the support I received from Monash University in the form the Monash International Postgraduate Research Scholarship and Monash Graduate Scholarship, for giving me the opportunity to pursue doctoral research here in Melbourne. I would like to express my deepest appreciation to my supervisor Associate Professor Helen Abud for her expertise and for believing in me from the start. Helen's patience and understanding, guidance and motivation to push forward is something I will always be grateful for. I appreciate the immense knowledge my associate supervisors Dr. Thierry Jardé and Dr. Katja Horvay shared with me over the last four years. I am thankful to them both for being patient and encouraging during all the ups and downs of my journey.

I would like to thank past and present members of the Abud lab for all the assistance I received throughout my candidature. I feel fortunate to have met them all and made some lovely friends along the way.

Last but definitely not the least, this thesis is the result of the love and never-ending support I have received from my parents. My mum and dad inspired me to make this journey and I will always be grateful to them. Special thanks to my sister for all the love and encouragement she showered me with.

Thank you doesn't seem sufficient but it is said with appreciation and respect for all of you.

Chapter 1 Introduction

Chapter 1 – Introduction

Members of the *SNAIL* family of zinc-finger transcription factors play a central role in morphogenesis and cancer metastasis. They are well known for their importance in the formation of the mesoderm and neural crest during development in several organisms. During recent years, there is increasing evidence of a key role of this family of proteins in regulating stem cells in normal intestinal tissue and tumours. There are still many outstanding questions regarding their precise function in stem cells. Although SNAIL family members are up-regulated in many cancers including colorectal cancer, however, their significance in prognosis and potential as a therapeutic target is still unclear.

1.1 Colorectal cancer

1.1.1 Incidence and types

Colorectal cancer (CRC or bowel cancer) is a disease with a high mortality rate, originating in the epithelial lining of the bowel or large intestine. It is ranked the third most commonly diagnosed cancer and the fourth leading cause of cancer-related deaths worldwide (Arnold et al., 2017). In Australia, CRC is the second most common cause of deaths due to cancer (Australian Institute of and Welfare, 2018). The estimated number of new CRC cases to be diagnosed in Australia in 2018 is 17,004 (accounts for about 12.3% of all new cancer cases diagnosed in 2018). The number of deaths from CRC in 2018 is expected to be 4,129 (8.5% of all cancer-related deaths in 2018). About 69% of the Australian population diagnosed with this cancer has a chance of surviving at least 5 years. The majority of colorectal tumours

(about 90%) can be treated successfully if diagnosed at early stages, unfortunately, less than 40% cases are detected early. Two-thirds of all CRCs arise in the colon while the remainder are rectal cancers (Australian Institute of and Welfare, 2018). Risk factors include increasing age, male sex, personal or family history of colonic polyps or CRC, inflammatory bowel disease (IBD) and environmental factors (e.g. red meat consumption, high-fat diet, inadequate intake of fibre, lack of exercise, obesity, smoking and heavy alcohol consumption) (Haggar and Boushey, 2009).

The most common type of CRCs (95 out of every 100 cases diagnosed), adenocarcinoma, arises in the epithelial cells in the mucosal lining of the bowel (Bosman, 2010). Two less common types of adenocarcinomas are mucinous adenocarcinomas (MAds) and signet ring cell adenocarcinomas (SRCAs). MAds comprise of more than 50% extracellular mucous and are quite often found in colon cancer patients rather than rectal cancer (Hugen et al., 2015). According to the World Health Organisation (WHO) criteria for grading colorectal tumours, MAds are generally considered to be poorly differentiated (Bosman, 2010). SRCAs, on the other hand, represent less than 1% of all colorectal adenocarcinomas and are usually aggressive. There are other rare forms of CRC which include squamous cell cancers, carcinoid tumours, lymphomas and sarcomas.

1.1.2 Histopathological features

The WHO categorises colorectal adenocarcinomas into grades based on the extent of glandular formation (Bosman, 2010). Tumours heterogeneous in differentiation are generally graded based on the least differentiated regions of the tumour, except for regions comprising the invasive tumour front. Well differentiated or grade 1 adenocarcinomas comprise of more

than 95% glandular structures. Moderately differentiated or grade 2 lesions are made up of 50-95% glands. Grade 3 or poorly differentiated tumours consist of less than 50% but more than 5% glands while undifferentiated or grade 4 tumours have less than 5%. MAds and SRCAs are usually categorised as grade 3 adenocarcinomas. It is generally believed that patients with high grade tumours are associated with poor prognosis (Chen et al., 2010, Hyngstrom et al., 2012).

1.1.3 Staging

The selection criteria for appropriate treatment strategies largely depend on the stage of colorectal tumours at the time of diagnosis. The most widely recognised and accepted system for staging colorectal tumours is the tumour/node/metastasis (TNM) staging system devised by the American Joint Committee on Cancer (AJCC). The T-stage indicates the depth of invasion into the bowel wall, the N-stage indicates the extent of lymph node involvement and the M-stage specifies the presence of any distant tumours (Table 1.1 and Figure 1.1). The 8th edition of the TNM classification (effective January 2018) utilises the pathologic or surgical staging (determined by examining tumour tissues removed during surgery) rather than the clinical staging (determined by examining biopsies).

Table 1.1 The TNM staging system for colorectal tumours as defined by the AJCC

Tumour stage	Tumour description
Primary tumour (T)	
T_x	Primary tumour cannot be assessed
T_{is}	Carcinoma in situ
T_1	Tumour invades submucosa
T_2	Tumour invades muscularis propria
T_3	Tumour invades through the muscularis propria into the subserosa
T_4	Tumour directly invades other organs or structures, or perforates visceral peritoneum
Regional lymph nodes	
N_x	Regional lymph nodes cannot be assessed
N_0	No regional lymph node metastases
N_1	Metastases in 1-3 regional lymph nodes
N_2	Metastases in 4 or more regional lymph nodes
Distant metastases	
M_x	Presence or absence of distant metastases cannot be determined
M_0	No distant metastases can be detected
M_1	Distant metastases detected

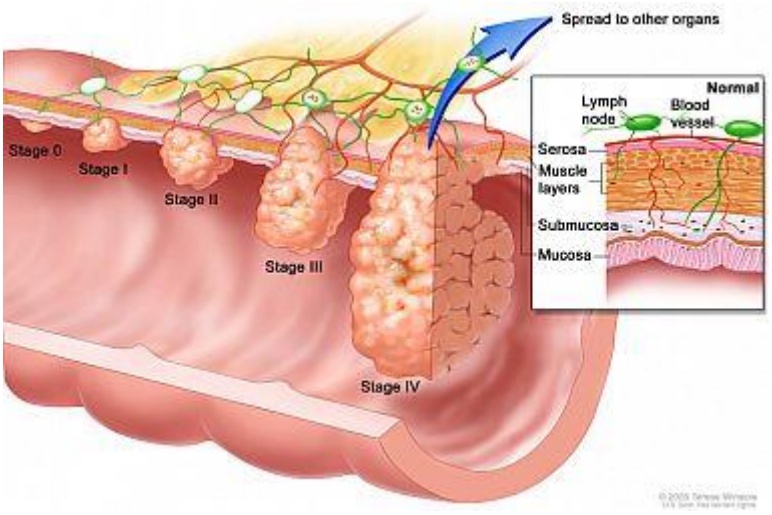

Figure 1.1 TNM Staging of colorectal cancer. Colorectal tumours are categorised into stages based on depth of invasion into the bowel wall, extent of lymph node involvement and presence of secondary tumours or metastasis. Image courtesy: National Cancer Institute.

1.1.4 Initiation and progression of CRC

For decades now, the multi-step adenoma-carcinoma sequence of colorectal carcinogenesis has been widely accepted. CRC arises as a result of accumulation of mutations that occur at specific stages of tumour development (Figure 1.2). A series of mutational events including activation of oncogenes and inactivation of tumour suppressor genes occur during tumourigenesis. Investigations over the last few decades have uncovered several critical genes and pathways- including *WNT*, *RAS-MAPK*, *TP53*, *TGF-β*- involved in the initiation and progression of CRC.

CRC occurs as a result of mutations in key driver genes. Adenomatous polyposis coli (*APC)*, a tumour suppressor and gatekeeper gene, is one of the major and well-known drivers of colorectal tumourigenesis. Role of *APC* as a gatekeeper gene in CRC has been confirmed by several studies which have demonstrated that mutations in other commonly deregulated CRC genes do not result in tumour formation. For instance, the tumour suppressor gene *TP53*, is mutated in more than 80% of all CRCs (Baker et al., 1990). Yet patients with mutated *P53* neither develop polyps nor are at a high risk to develop CRC (Garber et al., 1991). Similarly, *KRAS* is an oncogene which is mutated in 30-50% of colorectal tumours (Bos et al., 1987). However, cells with mutant *K-ras* have little or no potential to form colorectal tumours (Sansom et al., 2006). This implies that mutations in other genes do not lead to significant deregulation of growth among cells in the presence of a normal gatekeeper gene. Other gatekeeper tumour suppressor genes have been implicated in other cancers, however, these genes do not appear to play a gatekeeper function in CRC. *PTEN* is one such tumour suppressor gene which is commonly mutated in other malignancies like endometrial cancers and is thought to play a gatekeeper function in the endometrium (Kinzler and Vogelstein,

1997). Other gatekeeper tumour suppressor genes include the retinoblastoma (*RB*) gene in the retina and von Hippel-Lindau (*VHL*) in kidney (Cavenee et al., 1985, Mandriota et al., 2002).

Genomic instability is a hallmark of malignant tumours. Chromosomal instability (CIN) and microsatellite instability (MIN) are characteristic features of familial CRCs – Familial adenomatous Polypososis (FAP) and Hereditary nonpolyposis colorectal cancer (HNPCC) respectively. CIN has been suggested to occur as a result of mutations in *APC* and *TP53* (Fodde et al., 2001, Iacopetta, 2003). Almost three decades ago, Fearon and Vogelstein proposed a model identifying the molecular events underlying the initiation and progression of CRC based on the commonly occurring genetic alterations in CRC (Figure 1.2) (Fearon and Vogelstein, 1990). This model suggests that although, it is the accumulation of mutations that results in a malignant tumour, there are mutations that occur at characteristic phases during tumour progression.

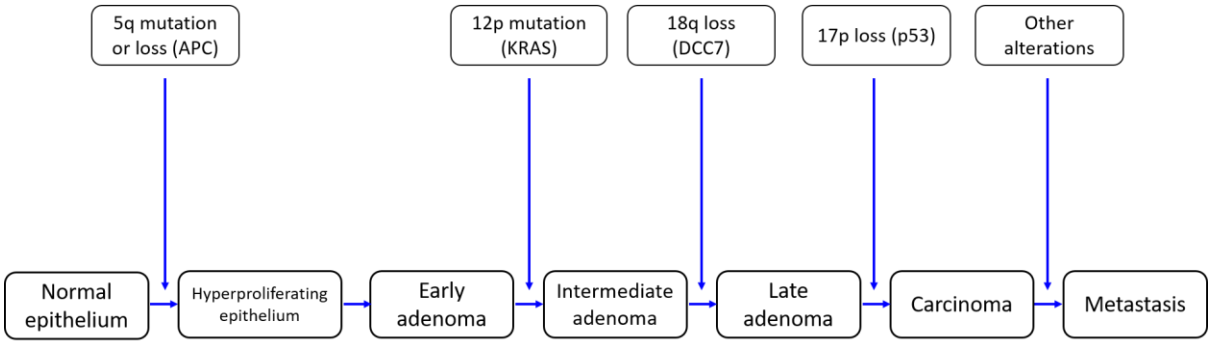

Figure 1.2 Genetic model for colorectal tumourigenesis as proposed by Fearon and Vogelstein. Adapted from (Fearon and Vogelstein, 1990).

Standard chemotherapy usually includes combination regimens of 5-fluorouracil (5-FU), irinotecan, oxaliplatin and leucovorin. When diagnosed at an early stage the cancer is usually curative and treatment options include surgical resection or anastomosis, chemotherapy and radiation therapy alone or in combination. For patients diagnosed with metastatic CRC treatment is often directed at extending life and keeping the patients comfortable. However, not all patients respond to chemotherapy in a similar manner and oncologists face a number of challenges in terms of diagnosis and optimising treatment especially for patients with stage II and III CRC. So far, *KRAS* mutations have been established as a major predictive biomarker for resistance to treatment of advanced CRC as these patients are resistant to anti-EGFR therapy. Although substantial progress has been made in colorectal cancer over the last decade, current research should be aimed at identifying molecules that can act as biomarkers to aid selection of patients that are likely to respond to therapy, thereby rationalising treatments and improving outcomes in these patients.

1.1.5 Molecular subtypes of CRC

Colorectal cancer is a heterogeneous disease and a great deal of variability exists in prognosis and drug response between patients with same stage tumours. There is considerable effect of presence (or absence) of certain genetic alterations on the characteristics of a tumour and in turn its response to chemo or radiotherapy. The relationship between these alterations and clinical response is not well defined. Inconsistencies with respect to response to drug therapies has been a major challenge to overcome. Keeping in mind the extensive heterogeneity present in CRC and variations between individual treatment responses, it is imperative to develop novel targeted therapeutic agents so as to offer personalised cancer medicine and prevent overtreatment and adverse effects in patients. In order to attempt to

resolve these discrepancies, researchers have proposed different systems of classification of colorectal tumours based on their molecular profile. Two such recently proposed systems are discussed in this section.

The Cancer Genome Atlas (TCGA) project characterised frequently occurring somatic mutations by analysing a large cohort of colorectal tumours (Cancer Genome Atlas, 2012). Two main subsets were identified – hypermutated tumours which represented 16% of all sporadic cases and non-hypermutated tumours which accounted for 84% of all cases analysed. Overall, 32 frequently mutated somatic genes were identified in hypermutated and non-hypermutated tumour groups. The most recurrently mutated genes among the non-hypermutated tumours included *APC*, *TP53* and *KRAS* among others, while the two most commonly mutated genes in hypermutated tumours included *ACVR2A* and *APC*. *APC* was the only gene that was found to be mutated in majority of hypermutated and non-hypermutated tumours (51% and 81% respectively). *WNT* signalling was the most frequently altered pathway (93% and 97% of non-hypermutated and hypermutated cases respectively), which included biallelic inactivation of *APC* or activating mutations of *CTNNB1* in approximately 80% of the tumours. Apart from *APC* and *CTNNB1*, alterations in 14 other *WNT* pathway genes including *SOX9* and *AXIN2* were found, confirming the significance of this pathway in CRC. Extensive epithelial cell proliferation is a major consequence of aberrant WNT activation which is also detected in most colorectal cancers (Fodde and Brabletz, 2007). As a result, WNT target genes are likely to have key role in mediating tumourigenesis in the intestine. Up-regulation of Frizzled, a WNT receptor, was found in 17% of the tumours, with some tumours exhibiting a 100-fold increase in expression over normal tissues (Cancer Genome Atlas, 2012). Another commonly deregulated signalling pathway in CRC is the *P53* pathway with a *TP53*

mutation rate of 59% in non-hypermutated cases (Cancer Genome Atlas, 2012). Furthermore, TCGA analysis suggests potential therapeutic approaches like inhibitors of WNT signalling and other proteins like ERBB2 and ERBB3. Although, TCGA classification identifies the recurrently occurring genetic alterations in CRC, this information is not sufficient to be able to predict drug response.

Guinney and colleagues formulated a consensus classification of CRC subtypes based on gene expression data from 18 different CRC datasets (Guinney et al., 2015). CRCs can be classified into four consensus molecular subtypes (CMSs) – CMS1, CMS2, CMS3 and CMS4. CMS1 or MSI-immune tumours represented 14% of all CRCs, were hypermutated and included majority of the microsatellite instable or MSI tumours. Higher levels of chromosomal instability measured by somatic copy number alterations (SCNA) was observed in CMS2-CMS4 tumours. Copy number gain of oncogenes and loss of tumour suppressor genes occurred more frequently in CMS2 tumours. Mutations in *KRAS* occurred more frequently in CMS3 tumours and almost 30% of these tumours were hypermutated. Lastly, CMS4 tumours displayed over-expression of an EMT signature. A summary of significant biological differences in gene expression among these subtypes is given in Table 1.2.

Associations between these subtypes and clinicopathological and prognostic parameters have been reported. For instance, CMS1 tumours are associated with a higher histopathological grade and occur more frequently in females with right-sided lesions. These patients have very poor survival rates after tumour relapse while CMS2 patients mainly develop tumours on the left side and have relatively higher post-relapse survival rates (Guinney et al., 2015). Not only do CMS4 tumours tend to be diagnosed at later stages (stage III and IV) of development, patients diagnosed with CMS4 tumours were found to have worse

relapse-free as well as overall survival (Guinney et al., 2015, Song et al., 2016). Intriguingly, a recent study has shown that this classification can be extended to *in vitro* models of CRC suggesting that these cancer cells faithfully recapitulate the intrinsic features of primary tumours. Linnekamp and colleagues examined a panel of 43 human CRC cell lines, 33 primary cell cultures and 34 patient-derived xenograft (PDX) models and reported that even in absence of the adjoining stromal compartment, the tumour epithelial cells retain their functional characteristics and can be stratified into the different CMS groups, that too in a similar pattern as observed in primary tumours (Linnekamp et al., 2018). The CMS classification is considered to be the most robust system of classification for CRCs so far.

Table 1.2 Taxonomy of CRC as proposed by Guinney et al. (Guinney et al., 2015)

Types	CMS1 MSI immune	CMS2 Canonical	CMS3 Metabolic	CMS4 Mesenchymal
Proportion of all CRCs	14%	37%	13%	23%
Genomic aberrations	MSI, CIMP high, hypermutation	SCNA high	Mixed MSI status, SCNA low, CIMP low	SCNA high
Common mutations	BRAF	-	KRAS	-
Pathway involved	Immune infiltration and activation	WNT and MYC activation	Metabolic deregulation	Stromal infiltration, TGF-β activation, angiogenesis
Survival	Worse survival after relapse	Better survival after relapse	-	Worse relapse-free and overall survival

CIMP = CpG island methylator phenotype, MSI = microsatellite instability, SCNA = somatic copy number alterations

Some studies have investigated the idea whether categorisation of tumours into CMS groups can help predict response to drug therapies. A clinical trial examining the association between molecular subtypes of CRC and benefits of combination therapy of oxaliplatin added to 5-FU and Leucovorin therapy demonstrated that a subset of CMS2 tumours (consisting of enterocytes) responded to oxaliplatin treatment while the other tumour subtypes were resistant (Song et al., 2016). Although both classification systems have potential clinical relevance for use in clinical trials, they still cannot predict differential drug response. Further validation by the transcriptional signatures is necessary to improve sub-classification of colorectal tumours.

1.1.6 Cancer stem cells

Colorectal tumours, like other solid malignancies, harbour a heterogeneous subset of neoplastic cells that are capable of maintaining tumourigenesis and driving tumour growth. These cells are referred to as cancer stem cells (CSCs) and resemble normal tissue stem cells in that they also exhibit self-renewal and lineage-specific differentiation potential. When isolated from the primary tumour, they give rise to new tumours which resemble the primary tumour in terms of heterogeneity (Figure 1.3). The cancer stem cell model, as outlined by Visvader and Lindeman in 2012, proposes categorisation of cells based on hierarchy in such a way that a small population of highly dynamic CSCs, bear the ability to sustain a neoplasm.

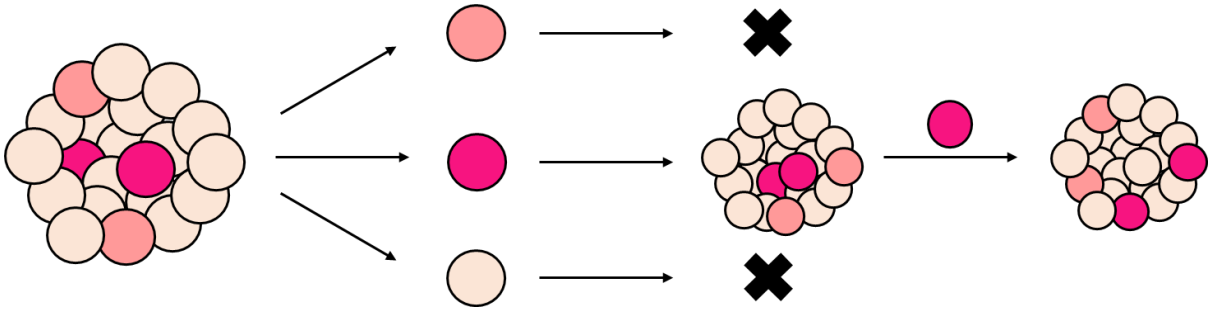

Figure 1.3 The cancer stem cell model. CSCs refers to a small population of cells within a tumour that have the capacity to self-renew and differentiate. In the example shown above, a mutation in a progenitor cell (dark pink) endows the tumour cell with stem cell-like properties. These cells can be isolated and transplanted in an organism giving rise to tumours resembling primary tumours in heterogeneity. Adapted from (Visvader and Lindeman, 2012)

It is important to note here that the cell of origin and CSCs are two different concepts. CSCs may not always arise from normal tissue stem cells. Acquisition of mutations by epithelial progenitor cells can result in transformation of these progenitors into CSCs (Figure 1.3). Moreover, there is emerging evidence supporting the idea of existence of an equilibrium between neoplastic progenitor cells and CSCs. A number of molecules have been proposed to play a role in acquisition of stem cell-like properties by non-stem cells (Figure 1.4). One such family of molecules is the *Snail* family of transcriptional regulators. *Snail* family, composed of three members – *Snai1*, *Snai2* and *Snai3* – are well known regulators of epithelial to mesenchymal transition (EMT). EMT is a crucial process in not only normal tissue development but also plays a role in advanced stages of tumourigenesis involving migration of tumour cells to other organs. *Snail*, along with other EMT transcription factors like *Zeb1* cause repression of *E-cadherin*, a gene that is a fundamental component of the adherens junctions between epithelial cells (Figure 1.4). Thus, repression of *E-cadherin* acts as an

important link between the epithelial characteristics and acquisition of stemness. CSCs have the ability to act as the cells of origin or tumour initiating cells in secondary tumours and are critically important for colonisation following metastatic dissemination. Association between induction of EMT and acquisition of stem cell-like properties by non-stem cells seems counter-intuitive as this suggests that epithelial stem cells express mesenchymal markers. This poses as a double threat in the context of cancer as EMT can impart (a) self-renewal capacity and (b) mesenchymal traits to tumour cells, thus contributing to invasiveness and resistance to therapeutic interventions.

Studies have suggested a contributory role of CSCs to resistance to chemotherapy (and/or radiotherapy) and recurrence of tumours, the two major challenges today in cancer research. For instance, one possible explanation for tumour relapse in patients could be attributed to the quiescent nature of some CSCs. This means that some CSCs bear the intrinsic ability of escaping therapeutic interventions eventually resulting in tumour relapse. Furthermore, the existence of molecularly distinct CSC populations has been identified in individual patients with acute myeloid leukaemia (AML) (Goardon et al., 2011). However, the underlying mechanism leading to resistance of CSCs to drug and radiotherapies is largely unknown.

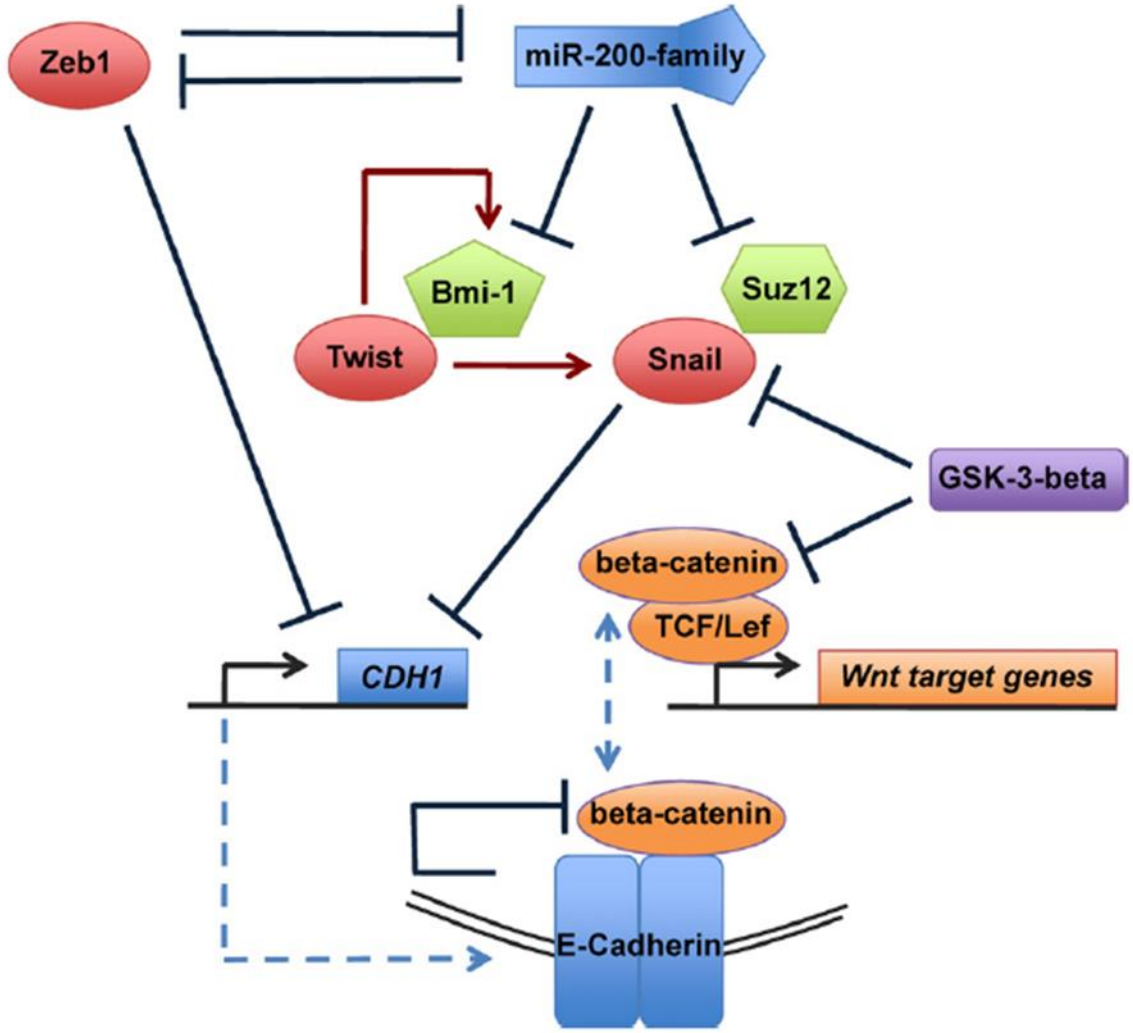

Figure 1.4 Links between molecular factors regulating normal and CSC renewal. In the absence of an active *Wnt* signalling, Snail and β-catenin undergo phosphorylation by GSK-3β resulting in their subsequent ubiquitination and destruction in the proteasome. Snail and Zeb1, both EMT molecules along with Twist, cause repression of E-cadherin (CDH1). E-cadherin binds to β-catenin resulting in its inactivation, thus preventing its association with TCF/LEF transcription factors (dashed blue line) and subsequent activation of *Wnt* target genes in the nucleus. Blue arrows indicate inhibitory activity, red arrows represent activation. Image courtesy (Scheel and Weinberg, 2012).

1.2 Normal human intestine

The mammalian intestine consists of two anatomically and functionally distinct parts- small and large intestine. The small intestine is composed of duodenum, jejunum and ileum whereas, the large intestine is formed by caecum, colon and rectum. The intestinal wall comprises of multiple layers as shown in Figure 1.5.

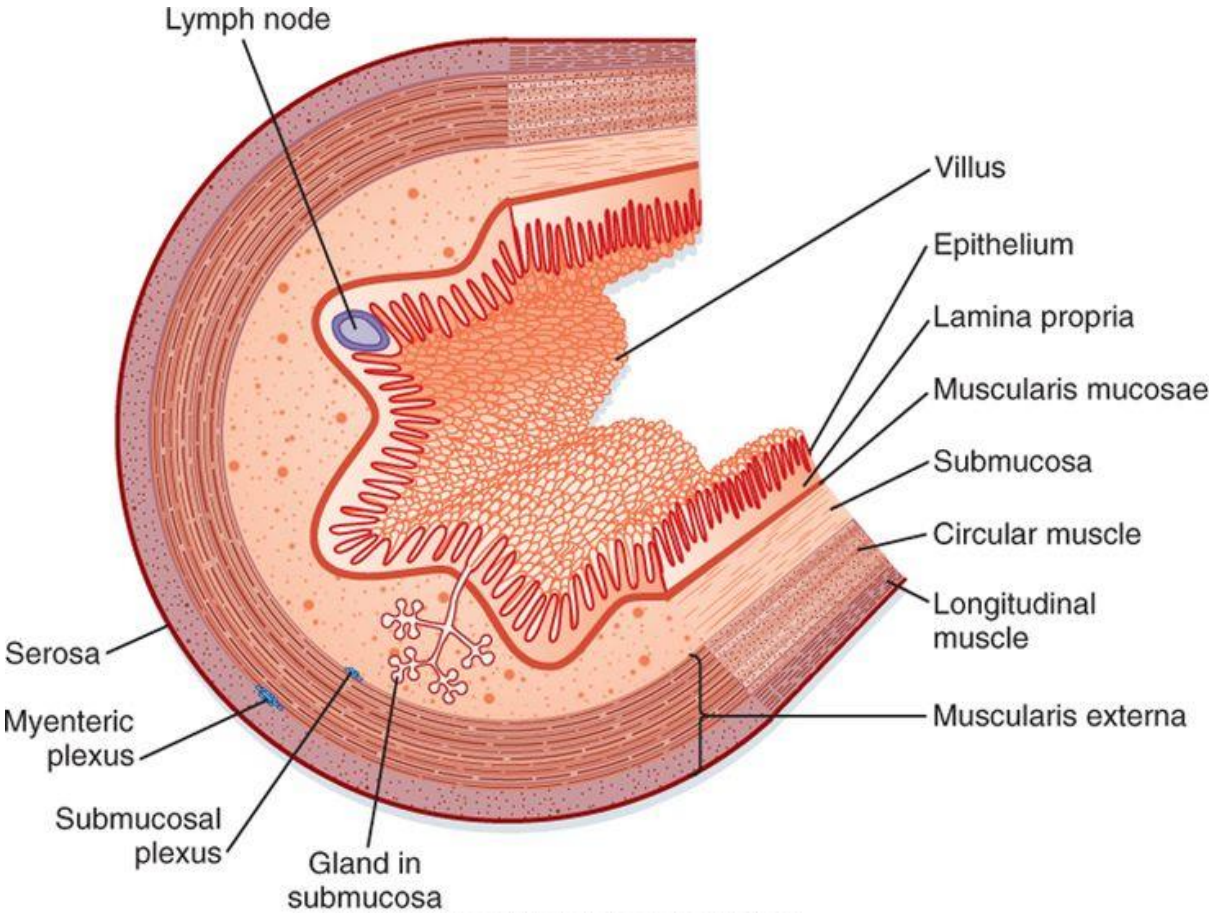

Figure 1.5 Anatomy of the intestinal wall. Image courtesy Berne and Levy Physiology (Koeppen and Stanton, 2008).

1.2.1 Intestinal epithelium

The intestine plays a critical role in the body and is responsible for absorption of nutrients and water. The innermost lining of the mammalian intestinal wall, the epithelium, is a single cell layer which separates the lumen from the underlying stromal compartment. It is a highly regenerative and multifunctional tissue which renews itself every 3-5 days. The small intestinal epithelium consists of numerous crypt-villus units. Villi are finger-like structures that project into the lumen and maximise surface area for absorption. At the base of each villus, there are multiple invaginations known as crypts of Lieberkühn (or simply known as crypts) which harbour the intestinal stem cells (ISCs). The epithelium of the colon lacks villi and is only composed of crypt structures. Small intestinal and colonic crypts contain both proliferative and differentiated cell types that perform highly specialised functions. Regeneration and homeostasis in the epithelium is maintained by a small population of ISCs residing in the base of the crypts and are referred to as crypt base columnar (CBC) cells and have the ability to give rise to the differentiated cell types (Figure 1.6).

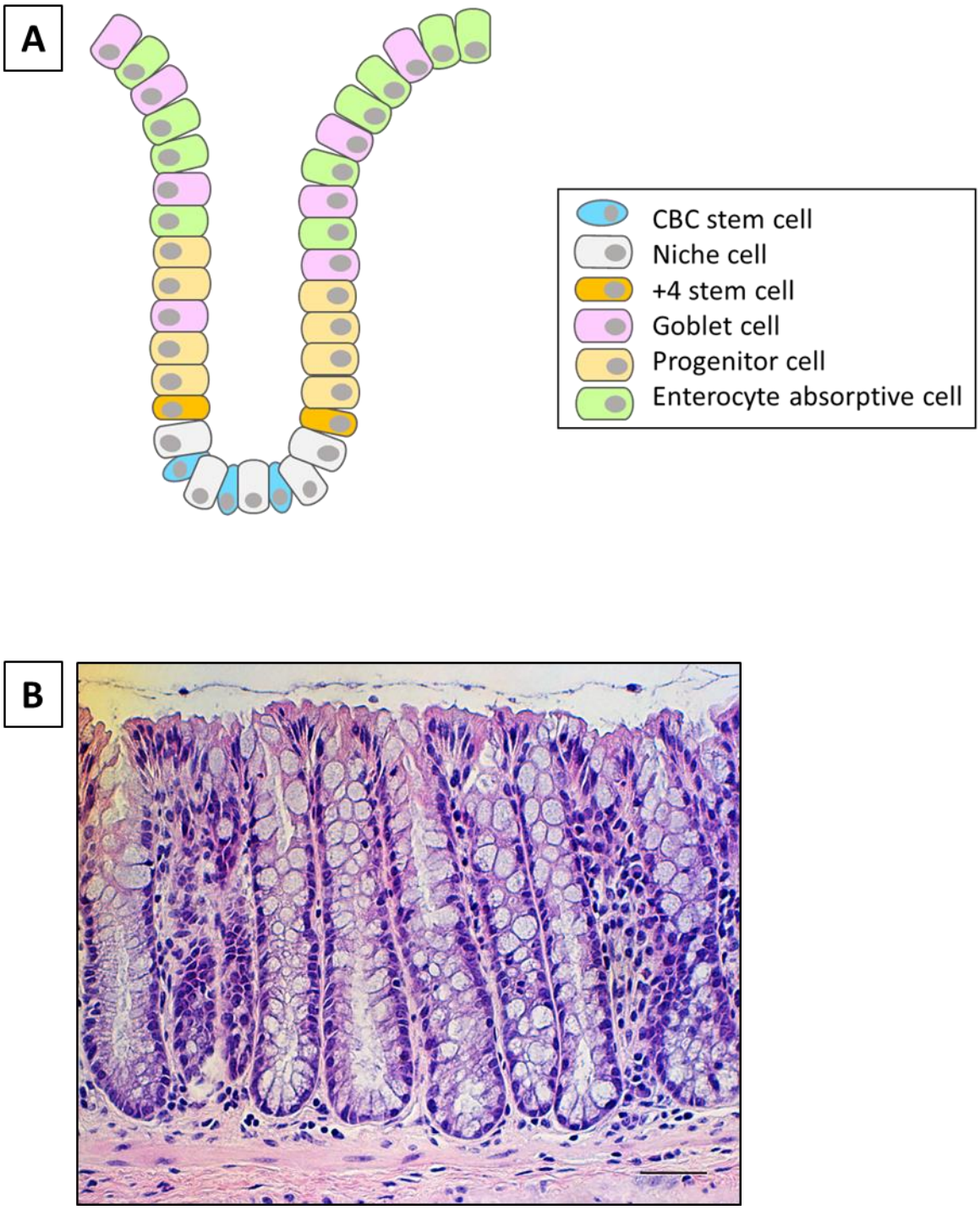

Figure 1.6 Microscopic anatomy of the mouse colonic epithelium showing crypts. (A) Schematic representation of the colonic crypt architecture showing the different cell types including the ISCs and differentiated cells. (B) Colonic epithelium stained with Haematoxylin and Eosin. The epithelium of the colon lacks villi. Scale bar 20 µm.

At the level of a single stem cell, two experimental approaches can assess “stemness”: genetic lineage tracing and transplantation. In the small intestine, two different intestinal stem cell models have been formulated: the stem cell zone model and the +4 model. The stem cell zone model as defined by Cheng and Leblond identifies the existence of a population of active stem cells referred to as the crypt base columnar stem or CBC cells located at the base of the crypts. The experiment involved ^{3}H-thymidine exposure to normal control animals, following which many CBC cells died, and were eventually phagocytosed by the viable CBC cells. The resulting radioactive phagosomes were later observed in the differentiated cells population. This was the first lineage tracing experiment and was considered as evidence for stemness of the CBC cells (Cheng and Leblond, 1974). Bjerknes and Cheng later confirmed these results while examining short-lived and long-lived clones originating from marked intestinal crypt cells (Bjerknes and Cheng, 1999, Bjerknes and Cheng, 2002). Marked CBC cells were found to consistently give rise to clones comprising all four major cell lineages in the crypt.

The +4 model, originally proposed by Potten more than four decades ago, suggests the presence of label-retaining cells (LRC) at positions ranging from +2 to +7 (average +4) positions from the crypt base (Potten, 1977). Interestingly, there is no well-defined +4 stem cell population in the colon. Repair and regeneration of epithelial cells in the colon is thought to be driven mainly by a small population of the CBC cells. These stem cells divide and give rise to all the epithelial cell lineages including the absorptive and secretive cell lineages. The stem cells divide and give rise to progenitors called the transit-amplifying (TA) cells which migrate upwards along the crypt and eventually die by apoptosis. The progenitor cells undergo terminal differentiation and give rise to one of the various differentiated cell types – goblet, enteroendocrine, enterocytes and Paneth (present only in the small intestine) cells.

1.2.2 ISC markers

Over the years, a multitude of marker genes have been proposed to mark the adult CBC and +4 ISC populations. Numerous studies have provided experimental evidence in support of the presence of the two stem cell populations in the intestinal crypt thus confirming the existence of the populations. However, their nature and relationship to one another is debatable. Moreover, there are considerable differences in the expression pattern of these markers in the small intestine and colon and also between species (mouse versus human). While some of the markers have been detected in the human colonic epithelium, there are some differences in expression patterns with respect to species. For instance, *Olfm4* expression is confined to the small intestinal crypts in mouse but is present in small intestinal and colonic epithelial crypts in humans (Kosinski et al., 2007, van der Flier et al., 2009a). Details of some of these ISC markers are discussed in the section below. A summary of CBC and +4 stem cell markers is given in Table 1.3.

1.2.2.1 *Lgr5*

The *Lgr5* (leucine-rich-repeat-containing G-protein-coupled receptor 5) gene encodes a 7-transmembrane protein, is a downstream target of *Wnt* signalling and acts a receptor for *Wnt* pathway ligands called *R-spondins*. Barker and colleagues demonstrated *in vivo* lineage tracing in CBC stem cells using an *Lgr5-EGFP-IRES-CreERT2* mouse crossed to *Rosa26RlacZ* reporter mouse where tamoxifen induced Cre activity led to activation of the lacZ reporter in the $Lgr5^+$ cells (Barker et al., 2007). Expression of the *Lgr5-lacZ* transgene was observed in slender cells at the base of the small intestinal and colonic crypts. $Lgr5^+$ cells yielded blue clones which originated from the crypt bottom and differentiated into goblet cells and

colonocytes and these clones remained unchanged over the 60-days experimental period. $Lgr5^+$ cells in the colon were found to be more quiescent than their small intestinal counterparts as the blue staining was restricted to the crypt bottom at day 5 post induction with tamoxifen. $Lgr5^+$ cells divide actively and are uniform in morphology. Sato *et al.* have further confirmed the stem cell nature of the $Lgr5^+$ cells by isolating these cells and demonstrating that a single $Lgr5^+$ cell is capable of giving rise to self-organising epithelial structures called organoids which are reminiscent of the normal gut (Sato et al., 2009). Gene expression profiling of FACS-sorted Lgr5-EGFP cells has identified an *Lgr5* ISC signature (Munoz et al., 2012, Van der Flier et al., 2007). Figure 1.7 shows the $Lgr5^+$ cells in the small intestinal epithelium of *Lgr5-EGFP-IRES-CreERT2* mouse detected by anti-GFP immunohistochemistry (IHC). To this day, *Lgr5* is considered to be the gold standard among ISC marker genes.

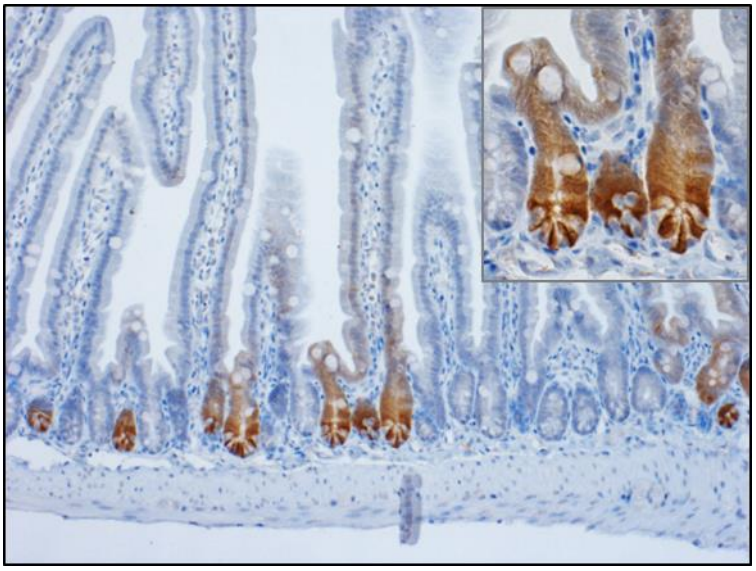

Figure 1.7 $Lgr5^+$ stem cells in the small intestinal crypts marked by expression of GFP in *Lgr5-EGFP-IRES-CreERT2* mouse. Tissue sections were stained for GFP using an anti-GFP antibody. Magnification 10x and inset 20x.

1.2.2.2 *Bmi1*

Bmi1 gene, a member of the polycomb group gene family (polycomb-repressing complex 1 or PRC1), is considered to be a marker of the +4 ISCs. Using lineage tracing experiments Sangiorgi and Capecchi showed a prominent $Bmi1^+$ lineage in the small intestine (Sangiorgi and Capecchi, 2008). To identify $Bmi1^+$ cells in the intestine, Bmi1Cre-ER mice were crossed to *Rosa26LacZ* reporter mice and $Bmi1^+$ LacZ stained cells was examined. Out of the 91 stained cells analysed, 86 were located at positions +4, +5 from the base of the crypts. Lineage tracing revealed that these $Bmi1^+$ cells were able to give rise to differentiated cells confirming their role as a stem cell marker. Moreover, studies suggest that *Bmi1* plays a role in regulation of ISCs. Loss of *Bmi1* has been shown to reduce proliferation in the intestinal stem cell compartment (Lopez-Arribillaga et al., 2015). Furthermore, *Bmi1* is essential for self-renewal of colorectal cancer initiating cells (Kreso et al., 2014).

1.2.2.3 *EphB2*

The receptor tyrosine kinase Ephrin type-B receptor 2 (*EphB2*) is a WNT target gene. Based on experiments performed by Sato *et al*. (2011), Merlos-Suarez and colleagues isolated and cultured single cells from mouse small intestine expressing high or medium levels of *EphB2* and reported the formation of complex multicellular organoid structures *in vitro* (Merlos-Suarez et al., 2011). An *EphB2*-ISC gene signature (including *Lgr5* and *Ascl2* genes) was identified which was found to be over-expressed in human CRCs. Gene Set Enrichment Analysis (GSEA) of 340 primary colon tumours revealed strong association of expression of *EphB2*-ISC signature with metastatic tumours compared to non-metastatic tumours. Furthermore, poorly differentiated colon tumours were enriched for the *EphB2*-ISC and proliferation signatures compared to relatively benign well-differentiated tumours. In

addition, genes associated with predicting the risk of relapse following curative therapy were enriched in the *EphB2*-derived ISC signature. These studies elucidate the role of *EphB2* not just in the normal intestine but also in tumours as a marker of CSCs.

1.2.2.4 *Olfm4*

Olfactomedin-4 (*Olfm4*) is a glycoprotein that belongs to the olfactomedin-related protein family (Zhang et al., 2002). Olfm4 has been proposed to be a robust marker for crypt base columnar cells in the intestine (van der Flier et al., 2009b). Although OLFM4 expression has not been detected in the mouse colon, Van der Flier *et al*. demonstrated high expression of OLFM4 in CBC cells in human small intestine and colon and also in cells within colorectal tumours (van der Flier et al., 2009a). Similar pattern of OLFM4 expression was observed in human and mouse small intestine. Tumour cells expressed relatively much higher levels of OLFM4 compared to wildtype CBC cells. This is suggestive of a possible function of OLFM4 in CSCs.

1.2.2.5 *Ascl2*

The Achaete scute-like 2 (*Ascl2*) gene encodes a basic helix-loop-helix (bHLH) transcription factor. Its expression is mainly detected in extraembryonic tissues (Guillemot et al., 1994). Van der Flier *et al*. identified *Ascl2* as a marker of the $Lgr5^{+}$ stem cells in the intestine. *Ascl2* was enriched in the GFP^{hi} stem cell population of the colon isolated from the *Lgr5-EGFP-IRES-CreERT2* mice (van der Flier et al., 2009b). Moreover, loss of *Ascl2* in *in vitro* organoid cultures resulted in reduction in stem cell proliferation (Schuijers et al., 2015).

1.2.2.6 Rnf43 and Znrf3

Ring finger protein 43 (RNF43) and Zinc and ring finger 3 (ZNRF3) are E3 ubiquitin ligase proteins which negatively regulate the Wnt signalling pathway (Koo et al., 2012). Using *in situ*

hybridisation in the mouse small intestinal crypt, Koo *et al*. confirmed the expression of *Rnf43* and *Znrf3* in CBC cells.

1.2.2.7 CD44

CD44 is a cell surface adhesion receptor. Gracz *et al*. confirmed CD44 as an intestinal stem cell marker when they isolated and subjected CD44-expressing intestinal epithelial cells to culture conditions and showed that these single cells were able to form enterosphere structures while the CD44 negative population failed to do so (Gracz et al., 2013).

Table 1.3 Markers of adult intestinal stem cells

CBC markers	+4 markers
Lgr5 (Barker et al., 2007, Sato et al., 2009) **EphB2** (Merlos-Suarez et al., 2011) **Ascl2** (van der Flier et al., 2009b) **CD44** (Gracz et al., 2013) **Olfm4** (van der Flier et al., 2009a) **Rnf43** (Koo et al., 2012) **Znrf3** (Hao et al., 2012) **Troy** (Fafilek et al., 2013) **Msi1** (Potten et al., 2003)	**Bmi1** (Lopez-Arribillaga et al., 2015, Sangiorgi and Capecchi, 2008) **Hopx** (Munoz et al., 2012) **Tert** (Montgomery et al., 2011) **Lrig1** (Powell et al., 2012)

1.2.3 *Wnt* signalling in the intestine

Wnt signalling plays a critical role in maintenance of intestinal homeostasis and induction of colorectal tumours. The canonical *Wnt* pathway regulates the ISC population in the normal small intestinal and colonic epithelium. A *Wnt* signalling gradient exists in the intestinal epithelium with strong WNT signalling activity at the base of crypts which gradually weakens moving upwards along the crypt-villus axis. As a result, the morphologically distinct ISC and differentiated cell compartments express varying levels of *Wnt* genes (Gregorieff and Clevers,

2005). Short-range signalling, lipid-modified WNT ligands are secreted by Paneth cells in the epithelium and the surrounding ISC niche which bind to the Frizzled transmembrane receptors and Lrp5 and 6 co-receptors (Alexandre et al., 2014, Gross et al., 2012). R-spondins are WNT ligands which are responsible for positive regulation of *Wnt* signalling and stabilisation of the Frizzled receptors against degradation by the transmembrane E3 ubiquitin ligases *Rnf43*/*Znrf3* (Hao et al., 2012, Koo et al., 2012).

Apc is an important component of the *Wnt* (or Wnt-β-catenin) pathway and loss of *Apc* results in activation of *Wnt* signalling (Figure 1.8). Over-activation of *Wnt* signalling is a characteristic feature of colorectal tumours. Mutations in *APC* generally result in loss of domains of the APC protein which are essential for binding to β-catenin and microtubules. In normal conditions, β-catenin binding at these sites occurs only after phosphorylation of each site by GSK3β, while β-catenin forms a complex with APC and another *Wnt* target gene, Axin and promotes GSK3β-mediated phosphorylation of its own serine and threonine residues. Following phosphorylation, β-catenin undergoes proteolytic degradation. However, in the absence of a functional APC protein which occurs in most CRCs, the complex is constitutively dissociated, and β-catenin is not phosphorylated resulting in its accumulation in the cellular cytoplasm and subsequent migration into the nucleus. Nuclear β-catenin binds to the transcription factor T-cell factor 4 (TCF4) resulting in subsequent activation of transcription of *Wnt* target genes like Lgr5 and Axin2 (Barker and Clevers, 2006, Morin et al., 1997). Aberrant transcriptional activation of genes by β-catenin is responsible for not only tumour initiation but also plays a role in invasion and metastasis (Gavert and Ben-Ze'ev, 2007). Thus, APC is a key component of the Wnt/β-catenin signalling pathway. A schematic representation of the *Wnt* signalling cascade in given in Figure 1.8.

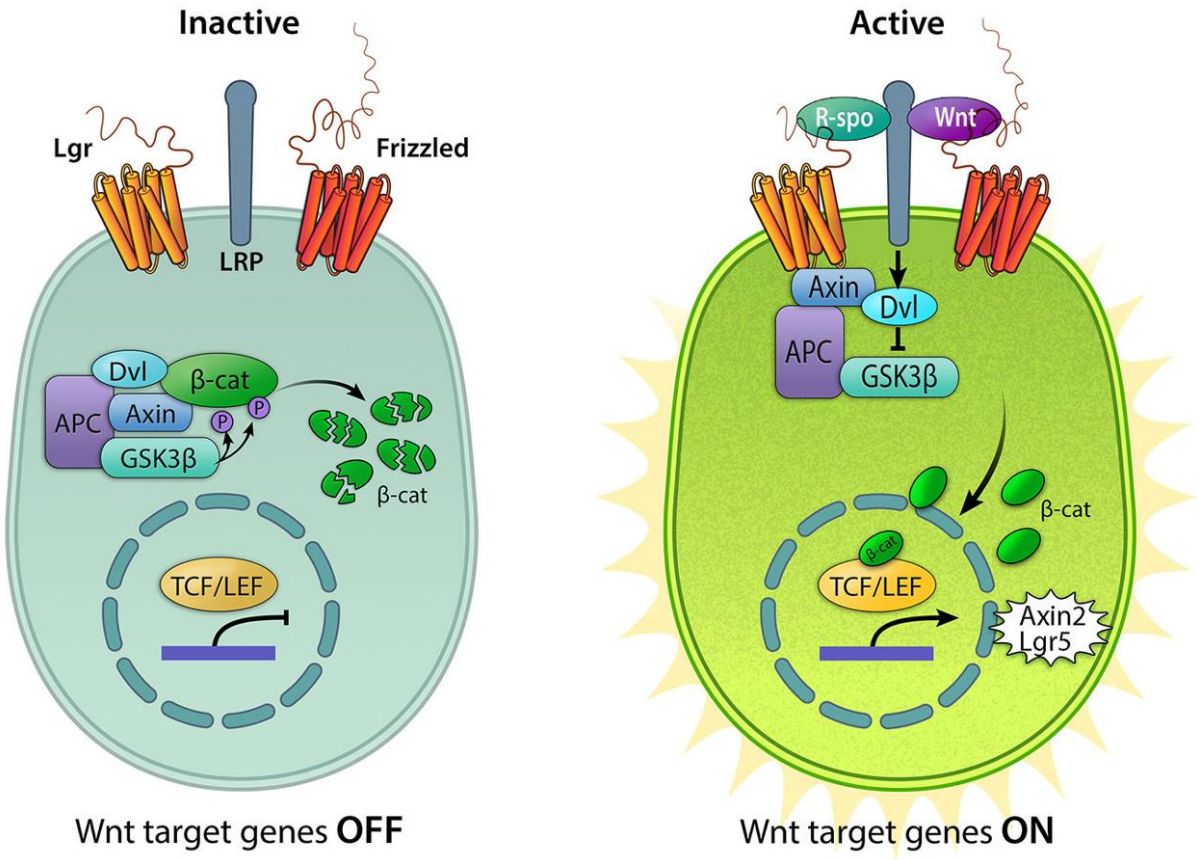

Figure 1.8 The Wnt signalling cascade. In the absence of WNT ligands (left), APC-GSK3β-Axin-Dvl form a destruction complex in the cytoplasm and bind to β-catenin resulting in phosphorylation and subsequent degradation of β-catenin. As a result, T cell factor/lymphoid enhancer-binding factor (TCF/LEF) remain inactive in the "off" state. Activation of the pathway (right) occurs when WNT ligands bind to the Frizzled receptors and the co-receptor lipoprotein receptor-related protein (LRP) 5/6. This leads to dissociation of the destruction complex allowing translocation of β-catenin into the nucleus where it binds to TCF/LEF transcription factors and activates transcription of WNT target genes. Image courtesy Jansson *et al*. (Jansson et al., 2015).

1.2.4 Role of intestinal stem cells in cancer

To identify the cellular origins of cancer, transgenic or conditionally targeted gene models in mouse have been used to explore the effects of oncogenes and tumour suppressor genes in different types of cancers. Lineage tracing experiments in mouse models have shown that stem cells act as cells of origin in intestinal cancer (Barker et al., 2009). Barker *et al.* studied the appearance and development of intestinal adenomas over a period of 36 days using β-catenin and enhanced green fluorescent protein (EGFP) immunohistochemistry in progenies resulting from a cross between the stem cell-specific *Lgr5-EGFP-IRES-CreERT2* knockin mice and $Apc^{flox/flox}$ mice (Cre activated by a single intraperitoneal injection of tamoxifen). Transformation of stem cells by loss of *Apc* favoured development of intestinal adenomas. This was in contrast to results obtained from *AhCre/*$Apc^{flox/flox}$*/Rosa26R* mice, where loss of *Apc* occurred in the transit-amplifying (TA) cells as Cre expression was induced by oral administration of β-napthoflavone (BNF) and not by injection into the peritoneum of the mouse. No macroscopic adenomas were formed as a result of recombination in the TA cells, thus confirming that crypt stem cells act as cells of origin in CRC. It could be argued that oral administration of BNF resulted in its inability to access the intestinal stem cells which are located much deeper in the base of the crypts as compared to the easily accessible TA cells.

Numerous studies have reported up-regulation of LGR5 in CRC (Fan et al., 2010, Jarde et al., 2015, Kleist et al., 2011, McClanahan et al., 2006, Uchida et al., 2010). Moreover, over-expression of LGR5 in colorectal tumours has been linked to poor prognosis (He et al., 2014, Takahashi et al., 2011). Uchida *et al*. analysed the expression of LGR5 in 50 stage II/III colorectal tumours and found a 3-fold increase in LGR5 expression in 70% of these tumours as compared to matched normal mucosal tissues. Histological analysis of *LGR5* mRNA in

tumour sections revealed *LGR5* staining diffused throughout the tumour with detection of *LGR5* mRNA at the invasive front of tumours also while no signal was detected in the adjoining stromal compartment. Moreover, up-regulation of LGR5 was reported in 100% of human CRC cell lines (n = 4) derived from metastatic tumours (Uchida et al., 2010). A previous study performed in our laboratory demonstrated up-regulation of intestinal stem cell markers *LGR5*, *EPHB2* and *CD44* in a cohort of 50 colorectal tumours (Jarde et al., 2015). Furthermore, qRT-PCR analysis of 89 paired primary colorectal tumour and adjacent normal tissues revealed positive correlation between *LGR5* mRNA and expression of oncogene *c-MYC* (Takahashi et al., 2011). Expression of the LGR5 protein was detected in crypt-like regions at the periphery of the tumours and at the tumour-host interface. As discussed previously in this chapter, CSCs are believed to play a crucial role in tumour invasion and metastasis by migrating to the invasive front. Detection of expression of LGR5 at the invasive front of tumours suggests a role of LGR5 in regulation of CSCs.

Correlation between the stem cell signature and cancer prognosis has been reported in context of CRC. Colorectal tumours expressing high levels of the ISC marker gene *EPHB2* are more aggressive and are more likely to give rise to new tumours following cessation of treatment. Gene Set Enrichment Analysis (GSEA) of a cohort of 340 primary colorectal tumours has shown the *EphB2*-ISC gene signature to be strongly linked to metastatic rather than non-metastatic tumours. Comparing tumour morphology, poorly differentiated tumours were found to be enriched for the *EphB2*-ISC gene signature rather than benign well-differentiated tumours (Merlos-Suarez et al., 2011). Associations between expression of BMI1 and survival of CRC patients have been investigated. The 5-year disease-free survival (DFS) and 5-year overall survival (OS) for patients with BMI1-positive colon tumours was

significantly less than that for patients with BMI1-negative tumours. Moreover, significantly higher number of patients with BMI1-positive tumours developed metastases or tumour relapse compared to patients with BMI1-negative tumours (Li et al., 2010). These studies along with numerous others confirm the role of stem cells in the initiation and progression of colorectal tumours.

1.3 SNAIL family of transcription factors

Snail family members are transcriptional regulators of the zinc-finger type (C_2H_2 type). All three members (*Snai1*, *Snai2* and *Snai3*, also called *Snail*, *Slug* and *Smuc* respectively) share a similar structural organisation with a highly conserved carboxy terminal domain which contains four to six zinc fingers and an amino terminal domain (Figure 1.9). A summary of *Snail* family members across different species is given in Table 1.4. *Snail* genes are well known regulators of epithelial to mesenchymal transition or EMT. EMT is a process during which epithelial cells lose their junctions and apical-basal polarity and transition into mesenchymal cells with enhanced migratory capacity and invasiveness. EMTs can be classified into three different subtypes (Kalluri and Weinberg, 2009). Type 1 EMTs occur during embryo formation, implantation and organ development. Type 2 EMTs occur during wound healing, tissue regeneration and organ fibrosis constitutes the second type of EMT. Type 3 EMTs occur in tumour cells and is associated with invasion of these cells to other organs (metastasis).

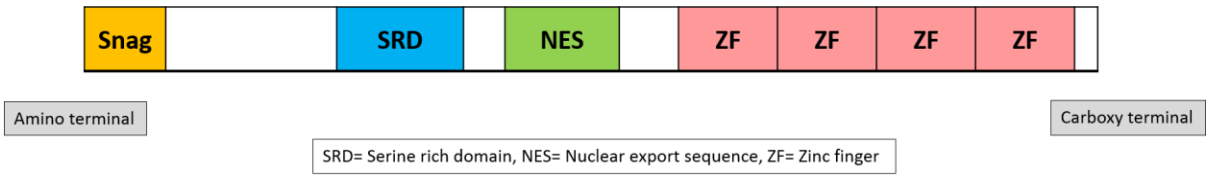

Figure 1.9 Basic structural organisation of SNAIL family proteins. The SNAG domain at the amino terminal is critical for interaction of SNAIL with histone lysine-specific demethylase 1 (LSD1) (Lin et al., 2010). The carboxy terminal is composed of four to six zinc fingers (ZFs).

Table 1.4 Members of the *Snail* superfamily (Nieto, 2002)

Species	Common name	Gene	Synonyms
Caenorhabditis elegans	Nematode	snail-like scratch-like	K02D7.2 C55C2.1
Drosophila melanogaster	Fruitfly	snail escargot worniu scratch scratch-like 1 scratch-like 2	 CG12605 CG17181
Danio rerio	Zebrafish	snail1 snail2 slug scratch	
Mus musculus	Mouse	Snail Slug Scratch Smuc	Slugh Zfp293
Homo sapiens	Human	SNAIL SNAILP SLUG SMUG SCRATCH1 SCRATCH2	SNAIL1, SNAILH SNAI1P SLUGH, SNAIL2 SNAIL3

1.3.1 Normal physiological role

Identification of homologues of *Snail* in various species including humans suggests a conserved role for *Snail*. *Snail* was identified in *Drosophila* as a gene critical for mesoderm formation (Alberga et al., 1991). Being key regulators of EMT, *Snail* genes play an important role in morphogenesis in several species. Several studies have acknowledged a role of these genes in neural crest formation (LaBonne and Bronner-Fraser, 2000, Nieto et al., 1994). As part of their role as EMT mediators, *Snail* genes are known to induce a phenotypic change in epithelial cells by binding to E-box of DNA sequences in target genes through their zinc-finger domains. The functional requirement of *Snail* in activation of EMT in mammals has been established by several independent experimental approaches. SNAIL directly represses *E-cadherin* expression resulting in conversion of epithelial cells into mesenchymal cells in mice (Cano et al., 2000). In addition to *E-cadherin*, *Snail* family members down-regulate other epithelial markers like *Desmoplakin*. Transcription of mesenchymal markers like *Vimentin* and *Fibronectin* is activated by *Snail* (Cano et al., 2000).

It has been proposed that *Snail* family members play different roles within the same species. Carver *et al*. examined the phenotype in mice carrying a mutant *Snail* allele (deletion of exons 1 and 2) and reported normal development of heterozygotes $Snail^{+/-}$ while no homozygotic mutants were obtained in the litter (Carver et al., 2001). Further investigation of the embryos at different time-points during development revealed that by E8.5 $Snail^{-/-}$ embryos were severely retarded in growth compared to the heterozygotic and wildtype littermates and were being resorbed suggesting that *Snail* knockdown results in defects in EMT during gastrulation. In contrast, studies suggest that *Snai2* does not play a role in formation of the mesoderm and neural crest. Jiang and colleagues generated mice carrying the $Slugh^{lacZ}$

(*Snai2*^{lacZ}) fusion allele (created by replacing portions of exon 2 and 3 encoding the zinc finger domain with β-galactosidase gene) which results in a *Snai2* loss-of-function mutation (Jiang et al., 1998). At E7.5 no β-gal staining was detected in the primitive streak. Moreover, homozygous mice (*Slugh*$^{lacZ/lacZ}$), although significantly smaller in size compared to littermates, were viable indicating that *Slug* does not play a critical role in gastrulation. Distinct roles of *Snai1* and *Snai2* have been identified in mammary gland. Ye and colleagues studied endogenous expression of *Snai1* and *Snai2* in context of breast cancer by FACS sorting Snai1^{+} and Snai2^{+} cells using knockin IRES-YFP reporters for *Snai1* and *Snai2* (Ye et al., 2015). On one hand, higher expression of SNAI2 was observed in normal mammary stem cell-enriched basal mammary epithelial cells, whereas, SNAI1 expression was detected in stromal fibroblasts with no expression in basal and luminal mammary epithelial cells. In addition, expression of SNAI1 was found to be activated in tumour cells while SNAI2 expression was associated with normal mammary gland cells in mice. These studies suggest that *Snail* family members perform different functions within the same tissues.

Evolutionary conservation suggests that *Snail* family members are likely to perform similar functions in different organisms with respect to maintenance of ISCs. Interestingly, however, members of the *Snail* family have been reported to perform some other divergent roles in different species. Moreover, *Snail* family members are not always expressed in the same tissues. While *Snai2* is expressed in the primitive streak and premigratory neural crest precursor cells in chick embryos, *Snail* expression has not been detected in these tissues (Nieto et al., 1994). However, in mouse embryos, *Snail* expression was detected in both of these tissues (Sefton et al., 1998). It was thus proposed that the EMT-associated function of

Snai2 in chick is performed by *Snai1* in mice. Observations made by Carver *et al*. are in support of this statement (Carver et al., 2001).

The role of *Snail* and *Slug* in EMT is not restricted to the development of mesoderm and neural crest. Studies by Chen and Gridley demonstrated that *Snai1* and *Snai2* have redundant functions in embryonic long bone development in mice (Chen and Gridley, 2013). Mouse embryos carrying $Snai2^{lacZ}$ null allele and embryos with $Snai1^{flox}$ conditional alleles ($Snai1^{flox/flox}$) did not present with any obvious defects in long bone development. However, combining limb-bud specific *Snai1* deletion with *Snai2* null deletion resulted in substantial defects in the long bones of the limbs in these mice including 20% reduction in bone length of femurs and other long bones of the forelimbs and hindlimbs along with delayed ossification of digits as well as tibia. These changes in phenotype were attributed to occur as a result of defects in chondrocyte proliferation. Another study investigated the effect of loss of *Snai1* along with *Snai2* on palate development in mice. *Snai2* null ($Snai2^{-/-}$) mice with neural crest specific deletion of *Snai1* presented with cleft palate and multiple craniofacial defects (Murray et al., 2007).

Members of the *Snail* family are expressed in several multipotent cell populations such as intestinal (Horvay et al., 2011, Micchelli and Perrimon, 2006), mammary (Mani et al., 2008) and neural stem cells (Southall and Brand, 2009). There is emerging evidence supporting the notion that *Snail* plays a role in regulation of stem cells in different tissues. SNAI1 has been shown to co-localise with CBC stem cell marker *Lgr5* in intestinal crypt base in *Lgr5-EGFP-IRES-CreERT2* mice (Horvay et al., 2011). In the small intestine, up-regulation of *Snai1* has been shown to increase the number of stem and proliferative cells in the crypts. However, SNAI1 over-expression on its own is not sufficient to induce tumourigenesis in the intestine

as reported by a study performed in our laboratory (Horvay et al., 2015). Function of *Snail* family genes is believed to be conserved through evolution as studies in *Drosophila* midgut have demonstrated that *Snail* genes are a necessity for maintenance of ISCs (Korzelius et al., 2014).

As such, *Snail* genes have a number of EMT-independent functions as well. One such role of *Snail* is as a cell survival factor. Kajita *et al*. induced expression of exogenous SNAI1 and SNAI2 in MCF7 breast carcinoma cells which usually express very low levels of endogenous SNAI1 and SNAI2 (Kajita et al., 2004). As expected, there was a reduction in expression of E-CADHERIN and OCCLUDIN in both SNAI1- and SNAI2 expressing cells. Down-regulation of *p53* mRNA was observed in both of these genetically altered cell types. Furthermore, ectopic expression of *Snai1* or *Snai2* led to transcriptional repression of *p53* target genes including *Caspase 6*. Conversely, depletion of SNAI1 in A375 human melanoma cells led to a moderate up-regulation of *p53*. In response to DNA damage-induced programmed cell death, a 7-fold increase in the number of apoptotic cells was observed in *Snai1*-depleted A375 cells (Kajita et al., 2004). Another study investigating the role of *Snai2* in normal haematopoietic progenitor cells reported that *Snai2* knockout in mice renders these progenitors susceptible to apoptosis and acts as a survival-promoting factor (Inoue et al., 2002).

1.3.2 Role in cancer

Another type of EMT process occurs during metastasis when cells of the primary tumour disseminate through blood vessels and colonise at a distant site. Several studies have suggested a crucial role of EMT in the acquisition of malignant phenotypes by tumour cells. Although EMT is fundamental to normal processes like embryonic development it is becoming

increasingly evident that EMT mechanisms are an integral component of the progression of many tumours of epithelial origin including colorectal cancer.

A number of molecules have been known to cause repression of the epithelial phenotype and activation of the mesenchymal phenotype in cells. These changes in gene expression can be attributed to regulators including SNAIL, TWIST, zinc-finger E-box binding (ZEB) transcription factors. EMT can also be triggered by other signalling molecules such as epidermal growth factor (EGF), transforming growth factor β (TGFβ), WNTs and NOTCH.

SNAIL proteins are up-regulated in many human cancers and have been shown to facilitate an invasive tumour phenotype in mice. *Snail*-induced EMT leads to repression of E-cadherin transcription in tumours and is considered to be a marker of a poor clinical outcome and a more invasive phenotype in many malignancies like breast, gastric and oesophageal squamous cell carcinoma (Kuo et al., 2012, Shin et al., 2012, van Nes et al., 2012). Moreover studies have suggested an inverse correlation between the expression of *Snail* and *E-cadherin* and the prognosis of patients with breast and oral squamous cell cancer (Blanco et al., 2002, Yokoyama et al., 2001). Blanco *et al*. reported *Snail* expression in 47% (8 out of 17 infiltrating ductal breast carcinomas) while its expression was non-detectable in normal breast epithelial tissues. Expression of E-cadherin was lower in regions with *Snail* expression in tumours suggesting that *Snail* expression inversely correlates with expression of *E-cadherin* in breast cancer. Furthermore, with respect to tumour differentiation, Snail expression was detected in more than half of grade 2 tumours and majority of grade 3 tumours with no detectable expression in grade 1 tumours (Blanco et al., 2002). This suggests a trend in *Snail* expression in later stages of tumour development. The fact that SNAI1 and SNAI2 are not expressed in

normal thyroid cells but are expressed during thyroid carcinogenesis (Hardy et al., 2007) reinforces the functional role of these genes in tumour development.

Recent studies in a variety of skin cancers demonstrated the role of *Snail* in tumour initiation and progression. Sustained over-expression of SNAI1 in the basal layer of skin in mice led to formation of spontaneous tumours which was further accelerated and became aggressive on a *p53* knockout background. In addition to this, *Snail* expression contributed to expansion and survival of skin stem cells *in vivo* (De Craene et al., 2014). Our recent study suggests that loss of *Snai1* in the mouse intestinal epithelium results in a decrease in epithelial cell proliferation, loss of CBC stem cells and the inability to form *in vitro* organoids. Loss of *Snai1* in the intestine also impaired regeneration following damage induced by radiation due to loss of the CBC stem cells (Horvay et al., 2015). These studies confirm the role of *Snail* genes in regulation of stem cells and induction of tumours.

An increasing amount of scientific evidence suggests that tumour growth is maintained by a small subpopulation of CSCs. These CSCs exhibit a self-renewing capacity, are considered to be resistant to conventional chemotherapy and are also thought to be responsible for therapy failure and relapse in patients (Jones et al., 2004). SNAIL proteins have been implicated to play a role in generation of CSCs. Mani *et al*. have reported a link between activation of EMT and stemness of mammary epithelial cells. Reversible activation of *SNAIL* led to the development of a mesenchymal morphology and increase in expression of mesenchymal marker *VIMENTIN* in human mammary epithelial cells (HMLEs) as a result of activation of EMT. CD24 and CD44 are cell surface markers associated with normal human mammary epithelial cells and mammary CSCs when present in a $CD44^{high}/CD24^{low}$ configuration. Development of $CD44^{high}/CD24^{low}$ marker phenotype was observed in HMLE-SNAIL cells, in

addition to a 10-fold increase in ability to form mammospheres. Interestingly, SNAIL expression in FACS-sorted single cells was sufficient to convert $CD44^{low}/CD24^{high}$ cells to stem-like $CD44^{high}/CD24^{low}$ cells (Mani et al., 2008). Transient ectopic expression of SNAI2 in primary mammary epithelial cells (MECs) induced EMT and generated 17 times more organoids than control-vector-expressing MECs. In addition, transient expression of SNAI2 in luminal progenitors led to a 50-fold increase in the organoid-forming capability of these cells in contrast to differentiated luminal cells, in which SNAI2 expression failed to induce any organoid-forming ability (Guo et al., 2012). Induction of ectopic expression of SNAIL in ACT1 human anaplastic thyroid cancer cells led to repression of E-CADHERIN and acquisition of a mesenchymal morphology. On transplantation of ACT1 and ACT1 –SNAIL cells into nude mice, no significant difference in frequency of tumours generated by these two cell types was reported. Nevertheless, there was enhanced ability (3-fold increase) of ACT1-SNAIL cells to form spheres *in vitro* (Yasui et al., 2013). These results can be attributed to a possible role of SNAIL proteins in expansion of the stem cell population or acquisition of stem cell-like characteristics by non-stem cells in different tissue systems. Hwang *et al*. have reported the CSC characteristics-inducing role of *SNAIL* in human colorectal cancer cell lines (Hwang et al., 2011) but the same needs to be confirmed *in vivo*. Hwang *et al*. demonstrated that SNAI1 overexpression in SW480 human CRC cell line induced the expression of CD44 stem cell marker and resulted in a higher self-renewal ability while its knockdown in primary colonospheres or HT29 human CRC cells depleted CD44 mRNA (Hwang et al., 2011). Similar results were obtained in a study by Hwang and colleagues in 2014, where they showed that *SNAIL* knockdown in sphere-derived cancer stem cells significantly reduced the sphere-forming frequency and tumour-initiating capability of these cells (Hwang et al., 2014).

1.3.3 Gaps in literature

Although SNAIL proteins are up-regulated in a number of cancers including colorectal cancer, little is known about the role that these proteins play in normal regenerating tissues. The role of *Snai1* in the small intestine has been recently studied in our laboratory, however, these results cannot be extrapolated to the colon without confirmational evidence. Hence, it is crucial to expand our understanding about their function in the colon, as in humans the colon is the site of tumour origin. Moreover, SNAIL proteins have been associated with induction of stem cell properties in epithelial cells, however, the underlying mechanism by which SNAIL induces this "stemness" is not fully understood.

1.4 Mouse models for studying intestinal cell biology and tumourigenesis

As mentioned above, the intestine is a vital organ in the body, responsible for absorption of nutrients. Any changes in the pathways regulating homeostasis in the intestine can adversely affect intestinal function and eventually the organism. To circumvent this problem many strategies have been developed to generate conditional knockout mouse models to study intestinal cell biology and mechanisms of tumour initiation.

1.4.1 Cre-lox system for recombination

The generation of genetically engineered mouse mutants by site-specific recombination has made great contributions to the understanding of the biological function of a diverse category of molecules. One commonly used system for generating conditional gene knockouts is the Cre/lox system (Figure 1.10). Cre recombinase, an enzyme from the bacteriophage P1, catalyses recombination between two loxP sites by excising the intervening DNA sequence (Sauer and Henderson, 1988). Cre-lox system involves the use of both a Cre driver mouse

expressing Cre under tissue specific reporter and a mouse with two loxP sites inserted at the selected locus of interest, intercrossing these two results in progeny expressing Cre with the excision of the intervening DNA between the loxP sites. The tamoxifen-dependent recombinase construct, Cre-ERT2, is based on the fusion of Cre with the mutated ligand-binding domain of the human estrogen receptor (ER) and is normally present in the cytoplasm. Administration of tamoxifen results in binding of tamoxifen to the Cre-ERT2 construct, facilitating nuclear localisation of this complex and subsequent activation of the Cre enzyme. This tamoxifen-inducible system allows us to control the time and site of recombination and can be used to initiate transcription of the target gene at any particular time.

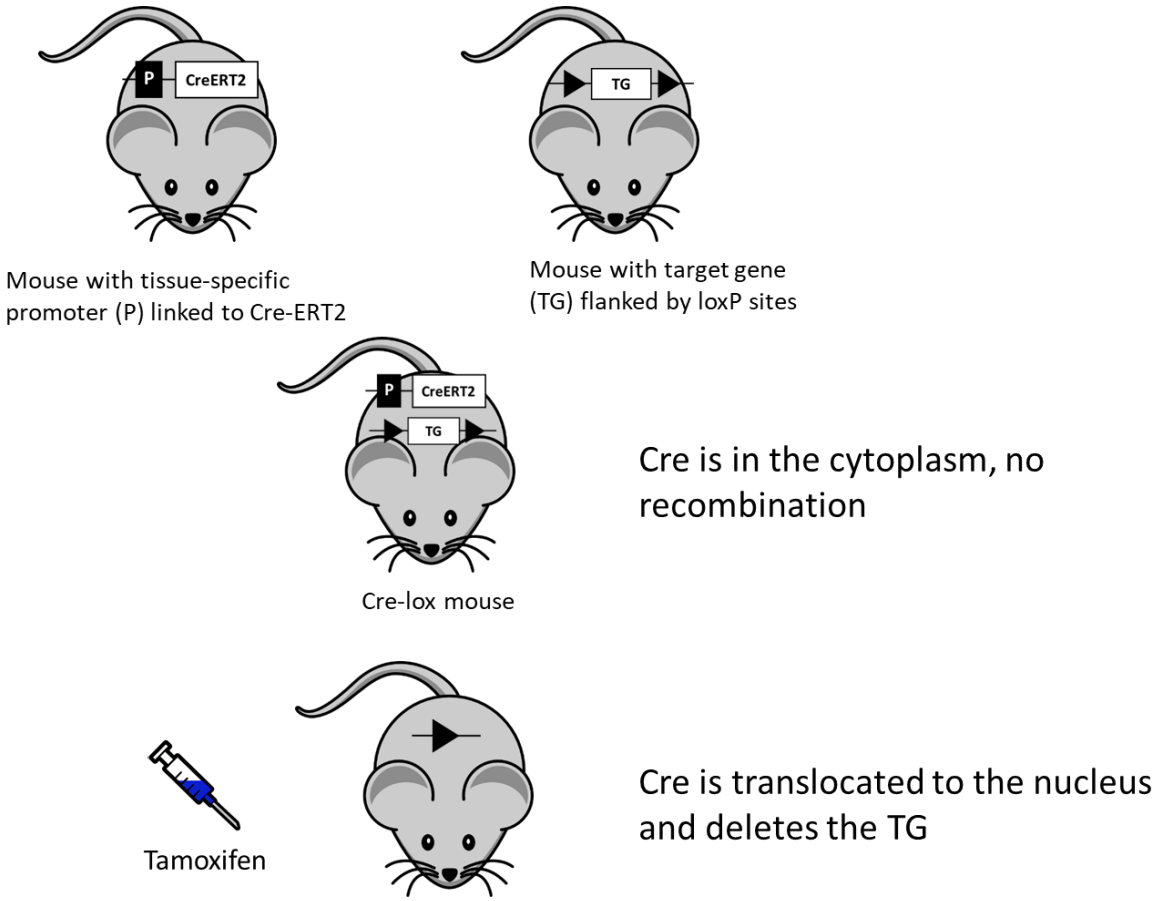

Figure 1.10 Cre-lox recombination system. In the absence of tamoxifen, Cre enzyme remains in the cytoplasm and is inactive. However, in the presence of tamoxifen, Cre-ERT2 translocates into the nucleus and induces excision of the floxed target gene (TG) under the tissue-specific promoter.

1.4.2 Intestinal tissue-specific promoters

The rapidly renewing intestinal epithelial lining poses a challenge for efficient conditional gene modifications. Targeting Cre activity in the differentiating cell compartment would not produce an obvious phenotypic change as the desired level of transgene expression would not be achieved as a result of recombined cells being rapidly lost to apoptosis. However, recombined alleles have been shown to persist after many epithelial renewal cycles when ISCs

are targeted. Nevertheless, recombination is never 100% efficient. Although several strategies are available for tissue-specific deletion of genes flanked by loxP sites which preferentially target the small intestine in mice, these cannot be considered ideal for studying the gene function in the colon. It is important to note here that majority of Cre drivers (with the exception of a very few) available today achieve more efficient recombination in the small intestine compared to the colon. Some of the commonly used intestine-specific Cre promoters are described below. Schematic representation of the Cre driver constructs used in the current study is given in Figures 1.11, 1.12 and 1.13.

1.4.2.1 VillinCre

Villin is a cytoskeletal protein and its expression has been reported in the epithelial cell lineages of the digestive and urogenital tracts (Maunoury et al., 1992). El Marjou and colleagues generated a tamoxifen-dependent recombination system, *VillinCreERT2*, to achieve site-specific activation or inactivation of genes in the mouse gut. The *VillinCreERT2* construct (Figure 1.11) consists of a 9-kb regulatory region of the Villin promoter and Cre recombinase fused to the mutated ligand-binding domain of the human oestrogen receptor (ER) (el Marjou et al., 2004). Administration of tamoxifen results in excision of the loxP flanked target DNA sequence by Cre recombinase in the small intestine and colon. Cre localisation studies in intestinal tissues harvested from *VillinCreERT2* mice post induction with tamoxifen revealed nuclear staining in the epithelial cells along the crypt-villus axis, while no staining was observed in the non-epithelial cells of the gut. Interestingly, at day 60 post induction there was a two-fold increase in the proportion of recombined crypts in the small intestine compared to the colon as observed by X-gal staining (el Marjou et al., 2004). This difference in Cre efficiency in the small intestine and colon was confirmed by another study. Conditional

inactivation of *Apc* under the inducible VillinCre promoter (*VillinCreERT2*) revealed extensive dysplasia in the crypt compartment throughout the small intestine while a less severe phenotype was observed in the colon (Andreu et al., 2005). In a previous study done in our laboratory, *Snai1* up-regulation in the small intestinal epithelium using the *VillinCreERT2 RosaSnai1* mice was confirmed (Horvay et al., 2015), however, no examination of the colonic tissues was performed at the time.

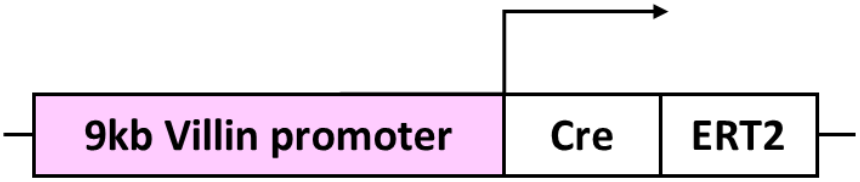

Figure 1.11 Schematic diagram showing the *VillinCreERT2* construct.

1.4.2.2 AhCre

Under the CYP1A1 promoter of the rat cytochrome P4501A1 gene, following administration of β-Naphtoflavone (BNF), AhCre mice direct expression of the Cre enzyme in all epithelial cells of the liver and small intestine except for the Paneth cells. Ireland *et al*. generated these mice to study gene function in the intestinal epithelium. Cre efficiency using the AhCre was determined by examining β-gal staining post intraperitoneal injection of BNF (5 daily injections) in progenies of AhCre mice crossed to ROSA26 reporter mice (Ireland et al., 2004). Extensive staining was observed in the oesophagus, lining of the fundus and antrum, gall bladder, liver, pancreas and proximal small intestine (except Paneth cells). A mosaic pattern of staining was observed in the colon which was indicative of less efficient recombination in this tissue. Cre activity in the small intestine using the AhCre is mainly restricted to the TA cell compartment. Surprisingly, oral administration of BNF in AhCre $Apc^{flox/flox}$ mice (to induce loss

of *Apc* gene in the TA cells) did not produce any adenomas in these mice (Barker et al., 2009). This could be attributed to either, oral administration of BNF being ineffective, or *Apc* deletion in the TA cells being insufficient to produce adenomas.

1.4.2.3 Lgr5Cre

Barker *et al*. developed the *Lgr5-EGFP-IRES-CreERT2* mice to specifically target, visualise and study the 'stemness' of the $Lgr5^+$ CBC cells (Barker et al., 2007). These mice were generated by integrating an EGFP-IRES-creERT2 cassette at the ATG translational start codon in Exon 1 of *Lgr5* (Figure 1.12). These mice were intercrossed with mice carrying the *Rosa26R-lacZ* reporter allele and Cre activity was induced by tamoxifen resulting in expression of *LacZ* in the $Lgr5^+$ cells. This allows lineage tracing of the progenies originating from the marked $Lgr5^+$ stem cell in the small intestine and colon. Comparing the expression pattern of *LacZ* on day 5 post induction, clear differences were observed between the small intestinal and colonic tissues. $LacZ^+$ cells were observed much higher along the crypt-villus axis in the small intestine while staining was restricted to crypt bottoms in the colon. This is indicative of the quiescent nature of the $Lgr5^+$ stem cells in the colon compared to those in the small intestine. Although the Lgr5-Cre promoter directs recombination in the stem cells of the small intestine and colon, it is associated with a mosaic pattern of expression which suggests that not all stem cells are targeted.

Figure 1.12 Schematic diagram showing the construct in the *Lgr5CreERT2* mice. UTR, untranslated region; EGFP, enhanced green fluorescent protein; IRES, internal ribosome entry site.

1.4.2.4 A33Cre

The intestine-specific expression pattern of the A33 antigen was reported by Johnstone *et al*. (Johnstone et al., 2002). The A33Cre employs a Cre recombinase fused to the ligand binding domain of the progesterone receptor knocked into the A33 locus where Cre activity is induced by the progesterone antagonist RU486 (Malaterre et al., 2007). Malaterre and colleagues used the A33Cre mice to selectively target loss of *c-Myb* to the distal colon and rectum. Cre activity was induced by feeding mice chow mixed with RU486 for up to 4 weeks which resulted in loss of *c-Myb* in regions of the distal colon. Ablation of *c-Myb* resulted in decrease in crypt length in the distal colon whereas no effect on crypt and villus formation in the small intestine was observed. Although recombination using the A33Cre is not absolute in the colon, it does display a colon-specific pattern of Cre expression.

1.4.2.5 Cdx2Cre

The constitutive Cdx2Cre model was generated by Hinoi *et al*. where they observed Cre recombinase activity in the epithelium of distal ileum all the way down to distal colon. Moreover, localisation of majority of the polyps following loss of *Apc* under the Cdx2Cre promoter was observed in the colon compared to small intestinal localisation in VillinCre $Apc^{flox/+}$ mice (Hinoi et al., 2007). The tamoxifen inducible *Cdx2CreERT2* transgene has been shown to direct Cre expression in the proximal colon (Feng et al., 2013). A roughly 9.5 kb fragment of Cdx2 is present upstream of CreERT2 (Figure 1.13). Tamoxifen-induced (three daily i.p. injections) *Cdx2CreERT2 Rosa26R-LacZ* mice resulted in detection of β-gal expression in the caecum and proximal colon by day 6 and patchy staining in the distal ileum by 2 months.

These studies confirm the colon-specific expression of Cre recombinase using the Cdx2Cre driver.

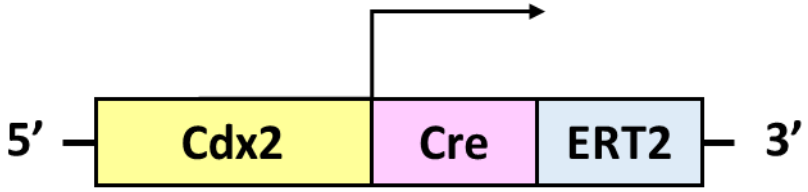

Figure 1.13 Schematic representation of the construct of the *Cdx2CreERT2* transgene.

1.4.3 Modelling tumourigenesis in the intestine

Mutations in *APC* commonly occur in a majority of sporadic and familial adenomatous polyposis (FAP) colorectal cancers (CRCs) (Aoki and Taketo, 2007). Germline mutations in *APC* are found in FAP patients, while somatic mutations are associated with sporadic CRCs. More than 95% of these mutations (in both FAP and sporadic cancer patients) lead to premature truncation of the protein (Galiatsatos and Foulkes, 2006). As mutations in *APC* are quite common in CRC, mouse models of CRC available so far are designed to mimic loss of *Apc* in mice. Over the years, there have been several studies that have shown that mutation of APC is a crucial early event in tumourigenesis and the contribution of other oncogenes/tumour suppressor genes is often only revealed in the context of an *Apc* mutation. A description of the most commonly used mouse models of intestinal polyposis is given below.

1.4.3.1 *Apc$^{min/+}$*

Apc$^{min/+}$ is a very commonly used mouse model for FAP and was generated by random mutagenesis using an alkylating agent - N-ethyl-N-nitrosourea (ENU) (Moser et al., 1990, Moser et al., 1995). An autosomal dominant mutation in one *Apc* allele (transversion at codon

850) leads to premature protein truncation resulting in phenotypic and genetic similarities to human FAP. *Apc*$^{min/+}$ mice are heterozygous for this mutation. Loss of heterozygosity (LOH) of the wild type *Apc* allele results in development of multiple intestinal adenomas in these mice. On a C57BL/6 background, *Apc*$^{min/+}$ mice have been shown to develop more than 50 adenomas throughout the intestinal tract (Moser et al., 1990). Although widely used, this model has certain critical drawbacks as it does not fully recapitulate the human FAP phenotype. These mice develop adenomas predominantly in the small intestine while FAP patients have adenomas localised to the colon. Moreover, *Apc*$^{min/+}$ mouse polyps occasionally develop into invasive adenocarcinoma. This is in contrast to adenomas observed in FAP patient tumours which routinely progress to adenocarcinoma (Halberg et al., 2000). This can be attributed to differences in intestinal cell biology between these two species. Most CRC patients do not show any symptoms of the disease until very late stages, thus, making it essential to model the earliest stages of tumourigenesis.

1.4.3.2 *Apc*$^{flox/flox}$

Apc$^{flox/flox}$ mice were first generated by Shibata *et al*. in 1997 using Cre-loxP-mediated inactivation of *Apc* which led to formation of colorectal adenomas (Shibata et al., 1997). A schematic representation of the construct is given in Figure 1.14. Conditional inactivation of *Apc* in these mice produces a 480 amino acid truncated protein which is similar to the truncating *APC* mutations observed in human CRC. Examination of tumour pathology in these mice revealed tumour invasion into the submucosal layer in about 50% of the tumours which were identified as adenocarcinomas. Homozygous deletion of *Apc* using different Cre drivers has been studied in models of intestinal polyposis (Sansom et al., 2004, el Marjou et al., 2004, Barker et al., 2009). Sansom *et al*. investigated the phenotype following conditional deletion

of *Apc* in the proliferative cell compartment of mouse small intestine using Cyp1A (AhCre) promoter (Sansom et al., 2004). Cre activity in AhCre $Apc^{flox/flox}$ mice was induced by four daily injections of β-napthoflavone which resulted in recombination in both *Apc* alleles. Histological analysis of intestinal tissues revealed altered crypt-villus architecture suggesting disruption of intestinal homeostasis, increase in cell proliferation and accumulation of nuclear β-catenin confirming activation of *Wnt* signalling. These observations concur with the findings reported by Andreu and colleagues using the Villin promoter (Andreu et al., 2005). Hyperproliferation and delayed migration of cells to the villus tip was observed in the small intestine while no obvious phenotype was observed in the colon. It is important to point out here that homozygous deletion of *Apc* using the Villin- and Ah-Cre drivers causes a severe phenotype in the small intestine, as a result these mice do not form tumours and die early. Targeting the ISC population for loss of *Apc* is one possible solution. Loss of *Apc* in the $Lgr5^{+}$ population using the Lgr5-EGFP-IRES-creERT2 $Apc^{flox/flox}$ resulted in formation of microadenomas in the intestine. As these mice have been shown to survive up to 36 days post induction with tamoxifen, this model could be to study early stages of tumourigenesis in the intestine.

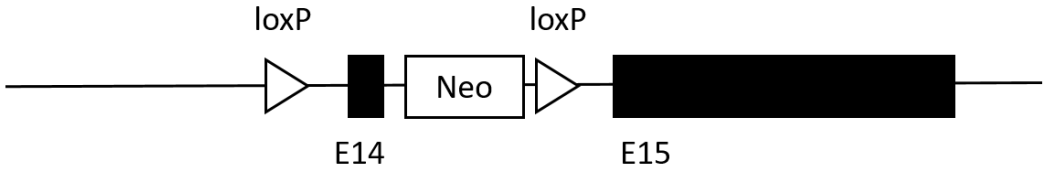

Figure 1.14 Schematic diagram showing the structure of the conditionally targeted allele of *Apc* (*Apc^{580s}*). The targeting vector was constructed by inserting one loxP site into intron 13 and the other, with a PGK-Neo cassette (Neo) into intron 14, resulting in exon 14 flanked by the loxP sites.

Several studies have examined the role of other genes including *K-ras* and *p53* in an APC deficient setting in mouse models of CRC. Halberg and colleagues investigated the effects of lack of *p53* function on tumour progression in $Apc^{min/+}$ mice (Halberg et al., 2000). While $Apc^{min/+}$ $p53^{+/-}$ mice develop more tumours (compared to $Apc^{min/+}$ $p53^{+/+}$ control), all tumours were benign. Homozygous deletion of *p53* ($Apc^{min/+}$ $p53^{-/-}$) resulted in formation of small intestinal and colonic tumours. 22% of the colonic tumours resembled *in situ* carcinomas with respect to tumour characteristics whereas 5% of the small intestinal tumours were invasive and invaded the muscularis mucosal layer. This suggests that loss of *p53* is necessary for tumour progression as is the case in human CRC where mutation in *P53* during late stages contributes to progression of tumourigenesis. While mutation of *K-ras* alone has no effect on intestinal homeostasis, however, in combination with *Apc* deletion, *K-ras* expression has been shown to be associated with accelerated tumourigenesis and increased invasiveness (Sansom et al., 2006). Loss of *Pten*, a tumour suppressor gene mutated in 5-14% of CRCs (Berg et al., 2010), has no effect on normal intestinal homeostasis (Marsh et al., 2008). However, AhCreERT $Pten^{flox/flox}$ $Apc^{flox/+}$ mice developed adenocarcinomas which invaded through the sub-epithelial layers of the small intestinal wall into the peritoneal serosa. In contrast, the AhCreERT $Pten^{+/+}$ $Apc^{flox/+}$ control mice developed benign and non-invasive intramucosal adenomas. Not only do these studies reinforce the role of *APC* as one of the major drivers of tumourigenesis, they also highlight the contribution of other genes towards cancer progression.

1.4.4 Mouse models for studying *Snail* function

A number of conditionally-expressing *Snail* genes mouse models have been generated over the years. While some have been used to study the role of these genes in gastrulation (Carver

et al., 2001, Murray et al., 2007), others have been used to analyse the role of these genes in cancer and metastasis (De Craene et al., 2014, Knab et al., 2014). Although, previously studies have looked at the role of these proteins in the small intestine, not much is known regarding their function in the colon.

1.4.4.1 Loss of function

Using the Cre-Lox system, Murray and colleagues achieved conditional inactivation of *Snai1* by inserting the LoxP-FRT-PGKneo-FRT cassette upstream of exon 1 and while the second LoxP site was introduced between exons 2 and 3 in the *Snai1* locus (Murray et al., 2006). Cre-mediated excision of the $Snai1^{floxneo}$ allele resulted in generation of the $Snai1^{del2}$ allele which is similar to that generated by Carver and colleagues (Carver et al., 2001). While $Snai1^{floxneo}$ homo- and heterozygotes were viable without any obvious phenotypic abnormalities, $Snai1^{del2}$ homozygotes died during gastrulation due to defects in mesoderm. Similar observations were reported by Carver *et al*. $Snai1^{del}$ mice have since then been used to study *Snai1* function in different systems including embryonic neural precursors and small intestine (Horvay et al., 2015, Zander et al., 2014). Zander *et al*. showed that inducible deletion of *Snail* leads to neuronal deficits and decrease in adult neural precursor cells. Studies in our lab have shown that conditional deletion of *Snai1* in the small intestine results in loss of CBC stem cells and increase in number of enteroendocrine and Paneth cells in mice (Horvay et al., 2015).

1.4.4.2 Gain of function

Activation of *Snai1* in mice has been investigated in different tissues. Nyabi *et al*. generated the RosaSnai1 mice which carry a construct (Figure 1.15) with the *Snai1* cDNA inserted into the Rosa26 locus and the expression is dependent on tamoxifen induced Cre-mediated

excision of a PGK-neo-STOP cassette flanked by two loxP sites (Nyabi et al., 2009). Overexpression of *Snai1* in the mouse intestine results in expansion of the CBC stem cell population accompanied by an increase in number of enteroendocrine and Paneth cells and crypt cell proliferation. Interestingly, elevated levels of *Snai1* leads to non-viability of organoids in *in vitro* cultures and a significantly higher level of apoptosis which can be rescued by addition of WNT3a (a growth factor secreted by Paneth cells in the small intestine) to the organoids (Horvay et al., 2015). While no tumour growth was observed in the small intestine following over-expression of *Snai1*, ectopic expression of *Snai1* in skin was sufficient to induce initiation of spontaneous tumours and promoted epidermal stem and progenitor cell population expansion (De Craene et al., 2014). Consequences of *Snai1* over-expression have been examined in the developing bone. de Frutos *et al*. utilised mice expressing the pcDNA3-Snail1-ERT2 construct which comprises of the *Snai1* coding sequence fused to a mutated of the ligand-binding domain of the human estrogen receptor. Induction with tamoxifen resulted in an active exogenous SNAI1 protein (de Frutos et al., 2007). *Snai1* activation in embryos resulted in transcriptional repression of *E-cadherin* and at E18.5 embryos presented with short limbs as a result of reduction in length of long bones.

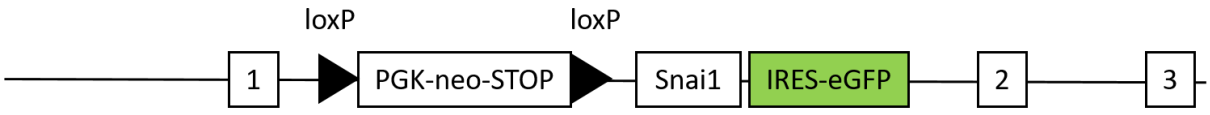

Figure 1.15 Schematic diagram showing structure of the conditionally targeted *ROSA26* allele. Cre mediated deletion of the intervening loxP flanked PGK-neo-STOP cassette results in the ROSA26-locus based expression of an exon1-Snai1-IRES-eGFP fusion transcript.

1.5 Intestinal organoids

Almost a decade ago, Sato *et al.* designed a culture system in which crypts isolated from normal intestinal tissues give rise to organoid structures with buds when seeded in Matrigel (Sato et al., 2009). Intestinal organoids or "mini-guts" are irregular structures which essentially recapitulate all aspects of a self-renewing epithelium *in vitro*.

1.5.1 Mouse and human intestinal organoid cultures

Crypt cultures from *Lgr5–EGFP–IRES–CreERT2* mouse small intestine revealed the presence of Lgr5-GFP^{+} cells intermingled with Paneth cells in the bud-like regions (Sato et al., 2009). Organoids can also be generated from Lgr5-GFP^{hi} single cells sorted by FACS. Organoids generated from FACS-sorted single cells were identical in morphology compared to organoids derived from isolated whole crypts. Moreover, presence of differentiated cell types of the epithelium including Paneth, enteroendocrine, goblet cells and enterocytes and absence of stromal cells has been confirmed in intestinal organoids (Sato et al., 2009). Sato and colleagues optimised the culture conditions for both normal and tumour mouse intestinal organoids (Sato et al., 2011). Organoids can be derived from colonic crypts in a similar way with addition of exogenous WNT ligand (WNT3A) to crypt cultures to compensate for the absence of Paneth cells in the colonic epithelium (Sato et al., 2011). A list of growth factors necessary for mouse organoid cultures is given in Table 1.5. We have been successfully growing mouse small intestinal and colonic as well as normal human and colorectal tumour organoids in our laboratory. A representation of growth of mouse small intestinal organoids starting seeding of crypts to mature organoids is given in Figure 1.16 (Jardé et al., 2018). Representative images of organoids established from three different human primary

colorectal tumours are given in Figure 1.17. Organoids can be derived from normal human and colorectal tumour tissues *in vitro* (Sato et al., 2011). A list of culture conditions required for growth of normal human and tumour organoids is given in Table 1.6.

Table 1.5 A list of culture media components required for growth of mouse small intestinal and colonic organoids. Note: Addition of exogenous WNT3A is not required for growing small intestinal organoids.

Component	Final concentration
DMEM/F12	To make up volume
GlutaMax	1/100
Hepes	1x
Penicillin/Streptomycin	1/100
N2 supplement	1x
B27 supplement	1x
Fungizone	1/500
Mouse recombinant EGF	50 ng/ml
Mouse recombinant Noggin	100 ng/ml
R-spondin-1 conditioned media	10%
Wnt3a conditioned media	50%

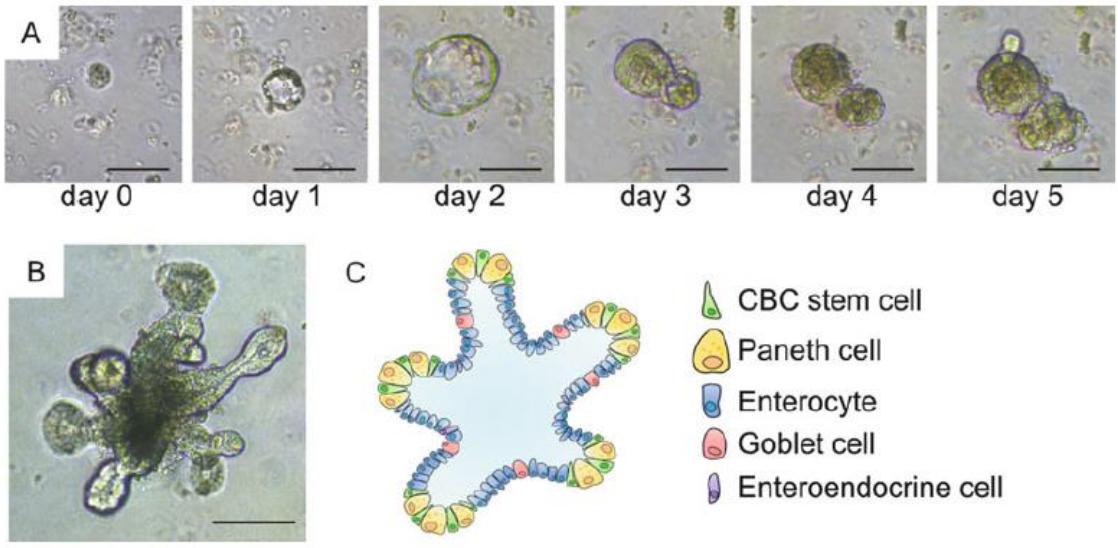

Figure 1.16 Intestinal organoid cultures. (A) Growth of intestinal organoids over a period of 5 days starting from seeding isolated crypts in Matrigel (day 0), (B) Mature small intestinal organoid in culture at day 8 and (C) Schematic diagram of an organoid with the different cell types. Scale bars 100 µm. Image courtesy Jardé *et al*. (Jardé et al., 2018).

Table 1.6 A list of culture media components required for growth of normal human and colorectal tumour organoids. Note: Addition of exogenous WNT3A is not required for growing tumour organoids.

Component	Final concentration
Advanced DMEM/F12	To make up volume
GlutaMax	1/100
Hepes	1x
Penicillin/Streptomycin	1/100
N2 supplement	1x
B27 supplement	1x
Fungizone	1/500
Human recombinant EGF	50 ng/ml
Human recombinant Noggin	100 ng/ml
R-spondin-1 conditioned media	20% (normal) 10% (tumour)
Wnt3a conditioned media	50% (normal only)
Gastrin	10 nM
Nicotinamide	10 mM
N-acetylcysteine	1.25 mM
A83-01	500 nM

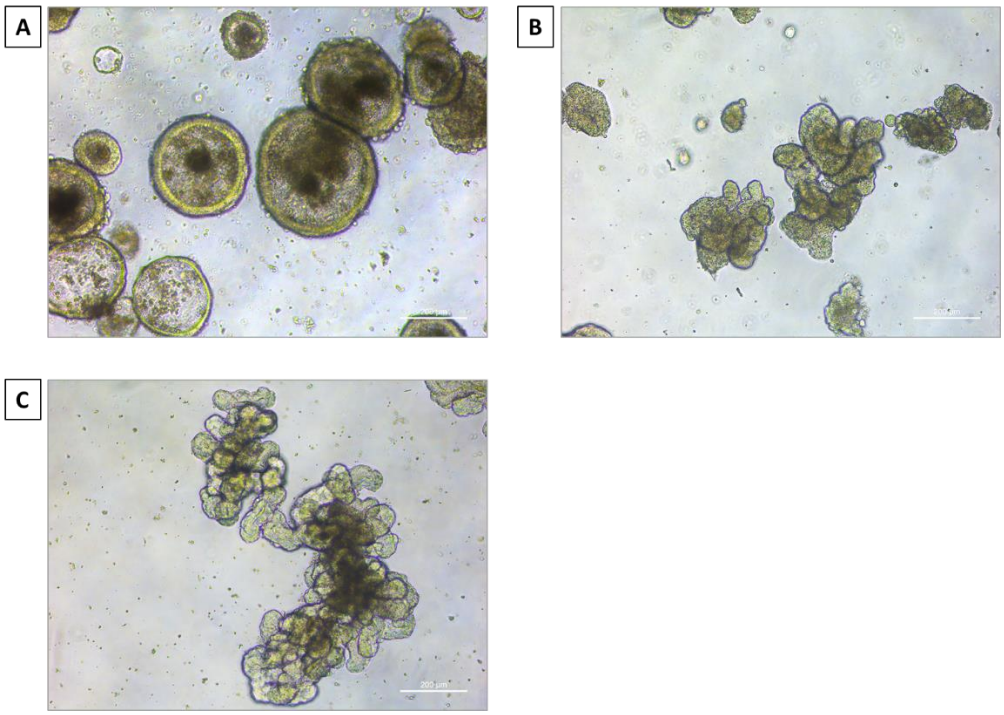

Figure 1.17 Human colorectal tumour organoids. Representative images of organoids derived from three (A, B, C) different primary tumours. Tumour organoids generated from different tumour tissues generally differ in morphology depending on the tumour characteristics. While organoids in (A) have a cystic morphology, (B) and (C) organoids have more "budding". Scale bars 200 µm.

1.5.2 Modelling CRC using organoids cultures

There is emerging evidence in support of the idea that tumour cells isolated from primary tumours and grown in culture recapitulate the primary tumour. A recent study has demonstrated that cell cultures derived from primary tumour tissues recapitulate the CMS characteristics of the primary tumour (Linnekamp et al., 2018). Out of the 8 patient tumour-primary culture pairs examined, 7 primary cultures recapitulated expression patterns that were specific to individual patients suggesting that tumour cells retain the characteristics of the original patient tumour *in vitro*. Furthermore, organoids derived from primary tumours

recapitulate patient response to treatment. A recent study by Vlachogiannis *et al*. examined phenotypic and genotypic characteristics of patient-derived organoids (PDOs) compared to original tumours from patients recruited in a Phase 1/2 clinical trial (Vlachogiannis et al., 2018). With respect to phenotype, similarities in morphology between patient biopsies and PDOs generated from these biopsies were observed. Similar expression pattern of CDX2 and CK7 (commonly used diagnostic markers of CRC) by immunohistochemistry was observed in PDOs and parental biopsies. Next-generation sequencing analysis of a cohort of 23 paired PDOs and parental biopsies revealed a 96% overlap in the mutational spectrum. Interestingly, these findings can be extrapolated to the two groups when it comes to response to drug therapies. Not only did PDOs mimic primary tumour in terms of drug response but also with respect to resistance to specific drugs (Vlachogiannis et al., 2018). It is important to note here that *in vitro* organoid cultures are not a true representation of the tumour in *vivo* and results from these studies do not take into account the contribution of the adjoining stromal tissue to tumour heterogeneity and drug response. Nevertheless, PDOs serve as an efficient platform for modelling CRC *in vitro* and studying the mechanism of regulation of CSCs.

1.5.3 Manipulating gene function in organoid cultures

As discussed in the previous section, *in vitro* modelling of colorectal cancer has many advantages over animal use in research as it allows us to study the disease mechanism much more efficiently. Several studies have utilised genetically engineered organoids to examine gene function in mouse and human intestine. Onuma *et al*. adopted the RNA interference (RNAi) approach to induce loss of APC in mouse intestinal organoids. Post-knockdown organoids (mixed with Matrigel) were injected into nude mice, following which development of solid round nodules with accumulation of β-catenin in the nuclei was observed suggesting

that loss of APC in organoids recapitulates APC loss in *vivo* (Onuma et al., 2013). Matano and colleagues utilised the clustered regularly interspersed short palindromic repeat (CRISPR)–CRISPR-associated protein 9 (Cas9) genome editing approach to knockdown commonly mutated CRC genes in human intestinal organoids. Sequential mutations in *APC*, *SMAD4*, *TP53* and *KRAS* in organoids was found to mimic *in vivo* the multi-step process of tumourigenesis (Matano et al., 2015).

Cre recombinase has been widely utilised to genetically manipulate DNA *in vivo*, however, one of the most commonly encountered problems with using an *in vivo* system has been the difficulty to achieve efficient delivery and consistent expression of the Cre enzyme in mammalian cells. A previous study in our laboratory used tamoxifen to induce Cre-mediation excision of the target gene in *in vitro* organoid cultures (Horvay et al., 2015). Successful recombination was confirmed by X-gal staining observed in organoids derived from Rosa26LacZ-Cre reporter mice. *In vitro* loss of *Snai1* was induced by treating intestinal organoids generated from VillinCreERT2 *Snai1*$^{flox/flox}$ mice with tamoxifen. Compared to untreated controls, tamoxifen-treated organoids displayed diminished growth and an increase in apoptosis as a result of loss of *Snai1* function (Horvay et al., 2015). Although, tamoxifen successfully induces recombination *in vitro*, its cytotoxicity should be taken into account as tamoxifen is a potent anti-cancer drug. To overcome the cytotoxic effects of tamoxifen, using a cell permeable, biologically active Cre recombinase enzyme is a good alternative. Direct delivery of the TAT-Cre enzyme (up to 2 µM) to mammalian cells has been shown to be highly efficient in inducing recombination in hiPSCs *in vitro* (Kadari et al., 2014). TAT-Cre is a recombinant cell-permeant fusion Cre-recombinase protein. As nuclear localisation of the Cre enzyme is essential for its activity, the TAT sequence mediates

penetration of the protein into the cell while the nuclear localisation sequence (NLS) regulates its localisation into the nucleus. In the current study, up-regulation of *Snai1* in mouse colonic organoids was induced by TAT-Cre. Results from these experiments have been published (in part) recently (Jardé et al., 2018).

Pharmacological inhibition of gene function *in vitro* is another alternative approach. Chemical inhibitors have been used to inhibit the catalytic activity of enzymes. One such inhibitor utilised in the current study is Tranylcypromine (or Parnate). Parnate is a monoamine oxidase/lysine-specific demethylase 1 (MAO/LSD1) inhibitor which has been shown to block the interaction between LSD1 and the SNAG domain of *Snail in vitro* (Ferrari-Amorotti et al., 2013). A schematic model of mechanism of Parnate-induced inhibition of *Snail*-mediated transcriptional repression of *E-cadherin* is depicted in Figure 1.18. Treatment of human CRC cell lines HCT116 and Colo205 with Parnate resulted in increased expression of genes, which are downstream targets of *SNAIL* - *E-CADHERIN*, *OCCLUDIN* and *DESMOPLAKIN* and decrease in expression of mesenchymal markers *VIMENTIN* and *N-CADHERIN* suggesting induction of EMT characteristics (Ferrari-Amorotti et al., 2013).

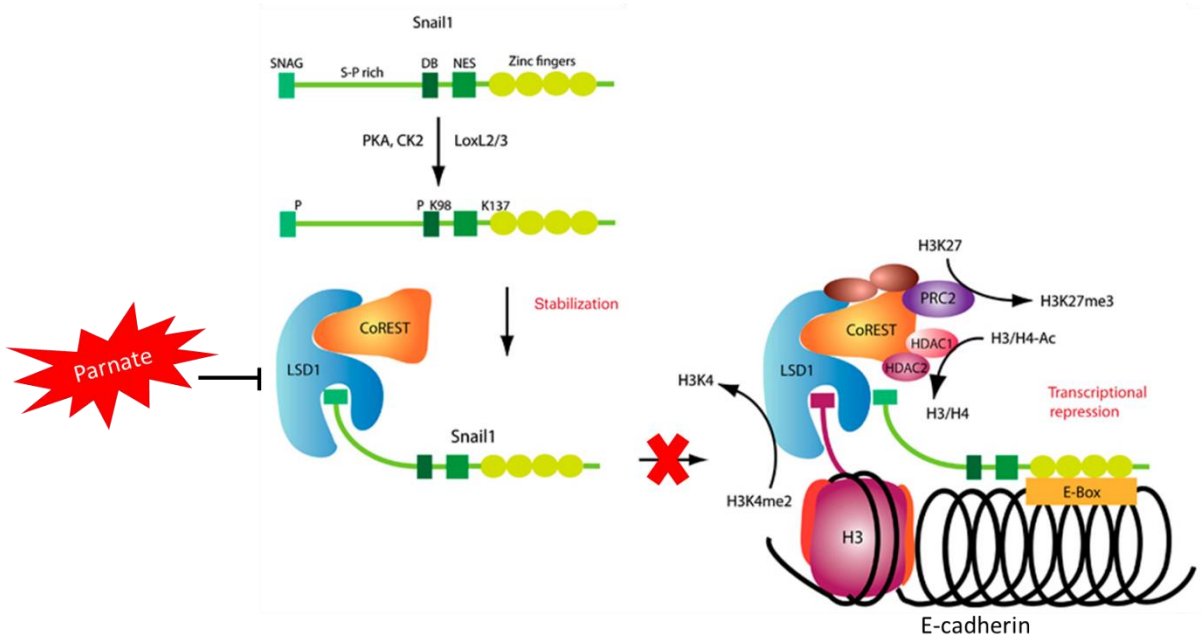

Figure 1.18 Schematic representation of mechanism of inhibition of *Snail*-mediated transcriptional repression of *E-cadherin* by Parnate, adapted from Christofori 2010 (Christofori, 2010). In normal conditions, Snail is phosphorylated and binds to LSD1 via its SNAG domain forming a Snail-LSD1-CoREST complex. This complex is recruited to E-boxes of the Snail target gene E-cadherin, where LSD1 binds to histone H3 resulting in demethylation of lysine 4 (H3K4). On the other hand, histone deacetylases 1 and 2 (HDAC1/2) deacetylate histones 3 and 4, and the polycomb repressor complex 2 (PRC2) trimethylates lysine 27 of histone 3 (H3K27). Altogether, this results in repression of the *E-cadherin* gene. In presence of Parnate, LSD1 activity is inhibited resulting in its inability to bind to the SNAG domain of *Snail*. This leads to failure of the downstream steps to occur resulting in inhibition of *Snail*-mediated repression of *E-cadherin*.

1.6 Conclusion: Challenges and unanswered questions

SNAIL proteins are known to be up-regulated in a number of different malignancies including colorectal cancer. However, consequences of this up-regulation remain largely undefined. Whether these proteins have a role in regulating the cancer stem cell population in colorectal tumours will be an interesting aspect to look at as SNAI1 has been shown to be up-regulated in colorectal cancer. Studies investigating their potential as therapeutic targets in the management and treatment of colorectal cancer are crucial. Moreover, the significance of these proteins in predicting aggressiveness and recurrence of tumours needs to be further investigated. Results from the current study will provide a deeper insight into whether the expression of SNAIL family proteins correlates with ISC markers, tumour stage and morphology in patients with CRC. Furthermore, the downstream effects of *Snai1* up-regulation and its role particularly in colon tumour initiation and progression will be examined.

1.7 Hypotheses & aims

1.7.1 Hypotheses

Based on the literature discussed in this chapter, we hypothesise that SNAIL proteins play a critical role in promotion of "stemness" characteristics in CRC. It is also hypothesised that SNAIL proteins are essential for maintenance of cancer stem cells and their expression correlates with ISCs in CRC. In addition, ectopic expression of *Snai1* can accelerate polyposis when combined with loss of *Apc* in mice.

1.7.2 Aims

1.7.2.1 To determine the relative expression levels of SNAIL family members and ISC markers in a cohort of 68 primary colorectal tumours with adjacent normal tissues.

1.7.2.2 To determine whether expression of SNAIL family members correlates with ISC markers expression and whether the expression of these markers correlates with tumour stage and morphology in CRC.

1.7.2.3 To examine the phenotype and determine the effect of ectopic expression of *Snai1* in the colonic epithelium using transgenic mice induced for over-expression of *Snai1*.

1.7.2.4 To determine the effect of *Snai1* up-regulation *in vitro* using colonic organoid cultures derived from transgenic mice.

1.7.2.5 To determine whether *Snai1* elevation is sufficient to accelerate polyposis in $Apc^{flox/flox}$ mouse model of intestinal tumourigenesis.

Chapter 2 - Methods

Chapter 2 – Methods

2.1 Collection of primary human colorectal tumour and adjacent normal tissues

Collection of samples from colorectal cancer patients that had surgical resections at Cabrini Hospital, Melbourne was approved by the Cabrini Human Ethics Committee and the Monash University Ethics Committee. All patients provided written informed consent. Clinical samples collected included benign polyps, primary tumour samples at various stages and adjacent normal tissues with clinical data. Normal and tumour tissues were snap frozen for further analyses and were also fixed in 4% paraformaldehyde (PFA) for histological analyses.

2.2 Animals

All protocols were approved by the Monash Animal Research Platform Ethics Committee. Investigations conformed to the National Health and Medical Research Council/ Commonwealth Scientific and Industrial Research Organisation/Australian Agricultural Council Code of Practice for the Care and Use of Animals for Experimental Purposes and were approved by the Monash Animal Research Platform Committee on Ethics in Animal Experimentation. Different transgenic mouse lines were utilised to study the function of *Snai1* in both normal tissues and models of intestinal polyposis. A description of the different mouse strains is given below. Schematic representation of each construct has been given in the introduction (Chapter 1) section.

2.2.1 *VillinCreERT2*

El Marjou *et al*. combined the Cre-lox recombination system with the tissue specificity of the Villin promoter to achieve site-specific excision of the target gene in the small and large intestine along the crypt-villus axis (el Marjou et al., 2004). The construct was injected into C57BL/6 x DBA/2 hybrid cells. The *VillinCreERT2* construct consists of a 9-kb regulatory region of the Villin promoter and Cre recombinase fused to the mutated ligand-binding domain of the human oestrogen receptor (ER). This results in excision of the loxP flanked target DNA sequence by Cre recombinase in the intestine in the presence of tamoxifen.

2.2.2 *Lgr5CreERT2*

Lgr5CreERT2 is an inducible Cre recombinase (Cre is bound to the mutated ligand-binding domain of the oestrogen receptor) that mediates recombination of target genes in the intestinal stem cells ($Lgr5^+$ cells) at any chosen time (Barker et al., 2007). These mice were generated on a pure C57BL/6 background by integrating a *EGFP-IRES-creERT2* cassette at the ATG translational start in exon 1 of the *Lgr5* locus. The construct contains an internal ribosome entry site (IRES) fused to the CreERT2 domain that allows the production of the Cre protein containing an ERT2 domain critical for nuclear translocation in the presence of tamoxifen. The tamoxifen-mediated inducible system allows Cre recombinase activity in the nucleus of the $Lgr5^+$ intestinal stem cells to induce recombination.

2.2.3 *Cdx2CreERT2*

Hinoi *et al*. generated mice carrying the Cdx2 elements to confer colon-preferential expression of the transgene in mice (Hinoi et al., 2007). The construct consists of a 9.5 kb fragment of the Cdx2 gene present upstream of CreERT2. This transgene was injected into

C57BL/6J x SJL/J hybrid cells. Cre activity under the Cdx2 promoter in the presence of Tamoxifen has been reported in the region from terminal ileum to rectum with the strongest induction of Cre activity in the caecum and proximal colon (Feng et al., 2013).

2.2.4 *RosaSnai1*

These mice were generated on a mixed background by Nyabi and colleagues by conditionally targeting the ROSA26 locus (Nyabi et al., 2009). A STOP cassette flanked by two LoxP sites, a Snai1 cDNA cassette and an IRES-eGFP cassette were introduced in exon 1, resulting in Cre-mediated deletion of the STOP cassette enabling expression of the *Snai1* transgene. In the current study, *Snai1* function was examined by inducing expression of the *Snai1* transgene in normal colonic tissues and $Apc^{flox/flox}$ mouse model of intestinal tumourigenesis

2.2.5 $Apc^{flox/flox}$

To study the role of *Snai1* in context of intestinal polyposis *RosaSnai1* mice were crossed with *Apc* mutant mice. Inactivation of *Apc* in mice was achieved by conditional targeting by inserting a pair of loxP sites into introns 13 and 14 of the *Apc* gene (Shibata et al., 1997). Cre mediated homologous recombination deletes a region encompassing exon 14 of *Apc* and induces a frameshift mutation at codon 580, resulting in a non-functional protein.

2.2.6 $ZsGreen1^{flox/+}$

These mice are hemizygous for ZsGreen1 conditional allele introduced into the *ROSA26* locus. In the absence of Cre recombinase, a loxP-flanked STOP cassette prevents transcription of the ZsGreen1 green fluorescent protein (GFP). When these mice are crossed with mice expressing the Cre enzyme, the resulting offspring will have the STOP cassette excised in the tissues expressing Cre recombinase, resulting in expression of ZsGreen1 in that tissue (Madisen et

al., 2010). ZsGreen1 fluorescence is extremely bright and can be visualised microscopically without the use of a specific antibody.

2.2.7 Administration of Tamoxifen

Cre recombinase activity in all experimental groups was induced by tamoxifen. Mice were injected intraperitoneally with Tamoxifen (Sigma Aldrich) (80 mg/kg) dissolved in sunflower oil at 37 °C. Table 2.1 summarises the injection regimens for the different experimental groups. Adult mice (male and female) aged 6-8 weeks were injected with tamoxifen and monitored closely and culled by cervical dislocation by trained personnel at different time-points or when they presented symptoms related to intestinal tumour burden as mentioned in Table 2.1. Mice induced for development of intestinal tumours were monitored daily for any signs or symptoms of sickness including loss of weight, abdominal swelling, hunched appearance, intestinal prolapse, anaemia (pale foot pads), diarrhoea or rectal bleeding.

Table 2.1 Summary of the different mouse genotypes used in the study along with their induction regimen

Genotype	VillinCreERT2	VillinCreERT2; RosaSnai1
Tamoxifen injection regimen	Four daily injections	
End-point/tissue collection	Day 5 and 10	
Number of animals (n)	3 (day 5 and 10)	4 (day 5) 3 (day 10)

Genotype	Cdx2CreERT2; ZsGreen1$^{fl/+}$
Tamoxifen injection regimen	Four daily injections
End-point/tissue collection	Day 5 and 10
Number of animals (n)	4 (day 5) 2 (day 10)

Genotype	Cdx2CreERT2	Cdx2CreERT2; RosaSnai1
Tamoxifen injection regimen	Four daily injections	
End-point/tissue collection	Day 5 and 10	
Number of animals (n)	4 (day 5) 10 (day 10)	9 (day 5) 10 (day 10)

Genotype	Lgr5CreERT2; Apc$^{fl/fl}$	Lgr5CreERT2; Apc$^{fl/fl}$; RosaSnai1
Tamoxifen injection regimen	Four daily injections	
End-point/tissue collection	Day 36	
Number of animals (n)	6	9

Genotype	Cdx2CreERT2; Apc$^{fl/fl}$	Cdx2CreERT2; Apc$^{fl/fl}$; RosaSnai1
Tamoxifen injection regimen	Three daily injections	
End-point/tissue collection	Mice culled when sick, average day 28	
Number of animals (n)	4	6

2.2.8 Collection of mouse tissues

Mice were humanely culled by cervical dislocation by trained personnel for tissue collection. Colonic tissues were harvested from mice immediately after culling and cut open longitudinally. Tissues were washed in ice-cold 1X phosphate-buffered saline (PBS) to remove all faecal content. Tail tips were collected for re-genotyping.

2.2.9 Tissue processing and embedding

Based on the genotype of the animals, normal and polyp tissues collected were processed for analyses.

2.2.9.1 Normal colonic tissues

Normal colonic tissues were cut and segmented into proximal and distal colon. Tissues were rolled into "Swiss rolls" as previously described by Moolenbeek and Ruitenberg (Moolenbeek and Ruitenberg, 1981) and fixed in 4% PFA (Merck, Darmstadt, Germany) at 4 °C overnight prior to processing. Tissues were placed in a cassette and processed using an automatic processor (Leica autostainer XL, North Ryde, NSW, Australia). Tissues were washed and dehydrated through a series of ethanol washes first (2 hours in 70% Ethanol (EtOH), 2 hours in 90% EtOH and 3 x 2 hours in 100% EtOH), followed by 3 x 2 hours washes in xylene (APS Ajax Finechem, Taren Point, Australia). Tissues were permeated in paraffin wax at 58 °C for at least 30 minutes and then removed from the cassettes and embedded manually in paraffin wax which was allowed to solidify on an ice plate. 4 µm thick sections were cut for immunohistochemistry and H&E staining.

2.2.9.2 Polyp tissues

Polyp tissues were collected and cut into two pieces (proximal and distal colon) and incubated with fixative for 16 hours at 4 °C followed by staining with methylene blue solution (Sigma Aldrich) for 30 minutes at room temperature. Post staining, polyp tissues were washed with 1X PBS and imaged using a Zeiss stereo microscope (Carl Ziess, Göttingen, Germany) and processed for embedding. Tissues were placed in a cassette and processed using an automatic processor (Leica autostainer XL, North Ryde, NSW, Australia) as described above. 4 µm thick sections were cut for immunohistochemistry and H&E staining.

2.2.10 Epithelial crypt preparation

Only *VillinCreERT2* and *VillinCreERT2 RosaSnai1* small intestinal and colonic tissues were used for crypt preparations. For isolation of crypt fractions, freshly isolated colonic tissues were washed with ice-cold 1X PBS and cut longitudinally to remove all faecal content. Tissues were cut into 5 mm long fragments and incubated in freshly prepared ethylenediaminetetraacetic acid (EDTA) buffer (250 mM EDTA in 1X PBS) and placed on a rotating wheel at 4 °C for one hour. EDTA/PBS was discarded, and tissue pieces were gently washed in 1X PBS twice. The digested tissue fragments were then placed in 20 ml 1X PBS in a 50 ml Falcon tube and shaken vigorously to dislodge the epithelial crypts. The tissues were removed and the suspension enriched for epithelial cells was centrifuged at 1500 rpm for 5 minutes at 4 °C. The supernatant was discarded and the process was repeated twice, collecting epithelial cells from three suspension fractions. After removal of the supernatant, the pellet was transferred to 1.5 ml Eppendorf tubes and stored at -80 °C for RNA isolation.

2.2.11 Genomic DNA extraction

To isolate genomic DNA (gDNA) from mice, tail tip samples were incubated in filter sterilised tail lysis buffer containing 50 mM Tris-hydrochloride (Tris-HCl, pH=8), 100 mM EDTA, 100 mM sodium chloride and 1% sodium dodecyl sulfate (SDS) in milliQ water with 200 µg/ml proteinase K for at least 5 hours or overnight at 55 °C. Suspensions were vortexed with 250 µl 5 M sodium chloride and then centrifuged (14,000 x g for 25 minutes) causing all cellular debris to precipitate. The supernatant containing gDNA was removed and transferred to new Eppendorf tubes containing 500 µl isopropanol and inverted causing the DNA to precipitate. The tubes were centrifuged (7000 x g for 15 minutes) and the supernatant tipped off. Pellets were washed in 500 µl 70 % EtOH and centrifuged again (10,000 x g for 15 minutes) to remove any excess salt. Pellets were then air dried for 5 minutes to remove ethanol and then re-dissolved in 200 µl sterile milliQ water and incubated for 1 hour at 37 °C. gDNA samples for stored at 4 °C.

2.2.12 Genotyping

2 µl of each gDNA sample was used for genotyping PCR. A previously determined mutant gDNA sample was included in every PCR screen as a positive control, and a sample without any DNA (water) was used as a negative control. Each PCR mix consisted of Platinum taq DNA Polymerase or Dream Taq Polymerase (Invitrogen, Carlsbad, USA), 10X reaction buffer (Invitrogen, Carlsbad, USA), 50 mM $MgCl_2$ (Invitrogen, Carlsbad, USA), 10 mM dNTPs (Invitrogen, Carlsbad, USA), 10 µM forward primer and 10 µM reverse primer for the gene of interest. Bio-Rad™ thermal cycler (Bio Rad laboratories, NSW, Australia) and SimpliAmp™ thermal cycler (Applied Biosystems, Thermo Scientific) were used for thermal cycling. The

primer sequences and the PCR programs for each allele used are given in Table 2.2. PCR products were mixed with DNA loading dye and electrophoresed on 2% agarose gels at 90 V and visualised using a Fuji LAS3000 Gel Doc System.

Table 2.2 Description of genotyping protocol along with primer sequences for each allele

Genotyping allele		VillinCreERT2
Forward primer		CAAGCCTGGCTCGACGGCC
Reverse primer		CGCGAACATCTTCAGGTTCT
Expected band size		200 bp
Reaction mix		**Thermocycling conditions**
Component	**Volume used**	95 °C 3 minutes 94 °C 30 seconds 65 °C 30 seconds x 30 cycles 72 °C 30 seconds 72 °C 5 minutes 11 °C hold
gDNA	2 µl	
10x reaction buffer	2.5 µl	
$MgCl_2$ (50 mM)	0.7 µl	
dNTPs (10 mM)	0.5 µl	
F primer (10 µM)	0.5 µl	
R primer (10 µM)	0.5 µl	
Platinum Taq DNA Polymerase	0.2 µl	
MilliQ water	18.1 µl	
Total volume	**25 µl**	

Genotyping allele		Lgr5CreERT2
Forward primer		CACTGCATTCTAGTTGTGG
Reverse primer		CGGTGCCCGCAGCGAG
Expected band size		200 bp
Reaction mix		**Thermocycling conditions**
Component	**Volume used**	94 °C 5 minutes 94 °C 30 seconds 61 °C 30 seconds x 35 cycles 72 °C 30 seconds 72 °C 10 minutes 4 °C hold
gDNA	2 µl	
10x reaction buffer	2.5 µl	
$MgCl_2$ (50 mM)	0.75 µl	
dNTPs (10 mM)	0.5 µl	
F primer (10 µM)	0.8 µl	
R primer (10 µM)	0.8 µl	
Platinum Taq DNA Polymerase	0.1 µl	
MilliQ water	17.75 µl	
Total volume	**25 µl**	

Genotyping allele		Cdx2CreERT2
Forward primer (transgene)		CATGGTGAGGTCTGCTGATG
Reverse primer (transgene)		CATGTCCATCAGGTTCTTGC
Forward primer (internal +ve control)		CTAGGCCACAGAATTGAAAGATCT
Reverse primer (internal +ve control)		GTAGGTGGAAATTCTAGCATCATCC
Expected band size		200 bp (transgene), 324 bp (IPC)
Reaction mix		**Thermocycling conditions**
Component	**Volume used**	94 °C 2 minutes
gDNA	2 µl	
10x reaction buffer	3.25 µl	94 °C 20 seconds 65 °C 15 seconds x 10 cycles 68 °C 10 seconds
$MgCl_2$ (50 mM)	1.3 µl	
dNTPs (10 mM)	0.13 µl	94 °C 15 seconds 60 °C 15 seconds x 28 cycles 72 °C 10 seconds
F primer (10 µM)	1.25 µl	
R primer (10 µM)	1.25 µl	
Platinum Taq DNA Polymerase	0.1 µl	72 °C 2 minutes 11 °C hold
MilliQ water	15.72 µl	
Total volume	**25 µl**	

Genotyping allele		RosaSnai1
Forward primer (transgene)		AAAGTCGCTCTGAGTTGTTAT
Reverse primer (WT)		GGAGCGGGAGAAATGGATATG
Reverse primer (transgene)		GCGAAGAGTTTGTCCTCAACC
Expected band size		220 bp (transgene), 550 bp (WT)
Reaction mix		**Thermocycling conditions**
Component	**Volume used**	95 °C 3 minutes
gDNA	2 µl	
10x reaction buffer	2.5 µl	95 °C 30 seconds 60 °C 30 seconds x 34 cycles 72 °C 45 seconds
$MgCl_2$ (50 mM)	0.8 µl	
dNTPs (10 mM)	0.8 µl	
F primer (10 µM)	0.8 µl	72 °C 5 minutes 11 °C hold
R primer (10 µM)	0.8 µl	
Platinum Taq DNA Polymerase	0.1 µl	
MilliQ water	17.2 µl	
Total volume	**25 µl**	

Genotyping allele		ZsGreen1 flox
Forward primer (transgene)		AACCAGAAGTGGCACCTGAC
Reverse primer (transgene)		GGCATTAAAGCAGCGTATCC
Forward primer (WT)		AAGGGAGCTGCAGTGGAGTA
Reverse primer (WT)		CCGAAAATCTGTGGGAAGTC
Expected band size		199 bp (transgene), 297 bp (WT)
Reaction mix		**Thermocycling conditions**
Component	**Volume used**	94 °C 2 minutes
gDNA	2 µl	
10x reaction buffer	2.4 µl	94 °C 20 seconds 65 °C 15 seconds x 10 cycles 68 °C 10 seconds
$MgCl_2$ (50 mM)	1 µl	
dNTPs (10 mM)	0.5 µl	94 °C 15 seconds 60 °C 15 seconds x 28 cycles 72 °C 10 seconds
F primer (10 µM)	1.2 µl	
R primer (10 µM)	1.2 µl	
Platinum Taq DNA Polymerase	0.1 µl	72 °C 2 minutes 11 °C hold
MilliQ water	15.6 µl	
Total volume	**24 µl**	

Genotyping allele		Apc flox
Forward primer		GTTCTGTATCATGGAAAGATAGGTGGTC
Reverse primer		CACTCAAAACGCTTTTGAGGGTTGATTC
Expected band size		314 bp (transgene), 226 bp (WT)
Reaction mix		Thermocycling conditions
Component	Volume used	94 °C 3 minutes 94 °C 30 seconds 59 °C 30 seconds x 30 cycles 72 °C 40 seconds 72 °C 10 minutes 11 °C hold
gDNA	2 µl	
10x reaction buffer	2.5 µl	
$MgCl_2$ (50 mM)	0.6 µl	
dNTPs (10 mM)	0.5 µl	
F primer (10 µM)	0.5 µl	
R primer (10 µM)	0.5 µl	
Dream Taq DNA Polymerase	0.2 µl	
MilliQ water	18.2 µl	
Total volume	**25 µl**	

2.3 RNA extraction

Total RNA was extracted from epithelial crypt cell pellets, proximal colonic tissue fragments and polyps using the RNeasy® Mini Kit (Qiagen, Hilden, Germany). The protocol followed was as per the manufacturer's instructions given in the RNeasy® Mini Handbook. RNA was eluted in 30 µl RNase-free water. To isolate RNA from human CRC cell lines, normal human and colorectal tumour and mouse colonic organoids, RNeasy® Micro Kit (Qiagen) was used following the protocol described in the RNeasy® Micro Handbook and eluted in 14 µl RNase-free water. The quality and concentrations of the isolated RNA samples were determined spectrophotometrically (NanoDrop 1000 Spectrophotometer) using 1 µl RNA. RNA samples were stored at -80 °C until further used for cDNA synthesis.

2.4 cDNA synthesis and quantification

To synthesise complementary DNA (cDNA) from RNA samples, the QuantiTect® Reverse Transcription (RT) Kit (Qiagen) was used. For human and mouse tissues 1 µg RNA and for organoids 500 ng RNA was reverse transcribed to cDNA as per the manufacturer's instructions. Components of the gDNA elimination reaction and reverse transcription reaction along with thermocycling conditions are given in Table 2.3. Post-RT cDNA samples were

quantified spectrophotometrically using the QIAxpert system (Qiagen) and placed at -20 °C for short-term and -80 °C for long term storage.

Table 2.3 Components and cycle conditions required for the 2-step reverse transcription protocol

Component	Volume used	Thermocycling conditions
gDNA elimination reaction		
7x gDNA wipeout buffer	2 µl	42 °C for 2 minutes Hold at 4 °C
Template RNA	500 ng or 1 µg	
RNase-free water	Variable	
Total volume of reaction	**14 µl**	
RT Master Mix		
Quantiscript Reverse Transcriptase	1 µl	42 °C for 15 minutes 95 °C for 15 minutes Hold at 4 °C
5x Quantiscript RT buffer	4 µl	
RT Primer mix	1 µl	
gDNA elimination reaction including template RNA	14 µl (from above)	
Total volume of reaction	**20 µl**	

2.5 Droplet Digital PCR

Expression of genes of interest in human and mouse tissues and organoid samples was measured by Droplet Digital PCR (ddPCR) system developed by Bio-Rad™ (Hindson et al., 2011). Expression of *SNAIL* family members and ISC markers mRNA in normal and colorectal tumour tissues was analysed using fluorescent tagged probes from Integrated DNA Technologies (IDT) (Iowa, USA) (Table 2.5). Analyses of mRNA expression in human and mouse organoids and mouse tissues was performed using primers obtained from IDT (Table 2.6). PCR mixes were prepared using either Supermix for probes (without dNTPs) or Supermix for EvaGreen (Bio-Rad). Table 2.4 summarises the components of the PCR mix and thermocycling conditions for both probes and EvaGreen reaction mixes.

Table 2.4 Components of probe and primer reaction mixes for ddPCR along with cycle conditions

Reaction mix for probes (25 µl)		**Thermocycling conditions**
Component	**Volume used**	95 °C 5 minutes
Supermix for Probes (no dUTPs) FAM probe (25 µM) HEX probe (25 µM) cDNA MilliQ water	12.5 µl 0.25 µl 0.25 µl 2 µl 8 µl	95 °C 30 seconds x 40 cycles 59 °C 1 minute 4 °C 5 minutes 90 °C 5 minutes 12 °C hold
Reaction mix for primers (25 µl)		**Thermocycling conditions**
Component	**Volume used**	95 °C 10 minutes
Supermix for EvaGreen Forward primer (10 µM) Reverse primer (10 µM) cDNA MilliQ water	12.5 µl 0.25 µl 0.25 µl 2 µl 10 µl	94 °C 30 seconds x 39 cycles 60 °C 1 minute 98 °C 10 minutes 12 °C hold

Table 2.5 Fluorescent probes assay details for ddPCR analysis

Gene	**Assay ID**	**Forward primer**	**Reverse primer**	**Fluorescent channel**
SNAI1	Hs.PT.58.2984401	GCA CTG GTA CTT CTT GAC ATC T	GGC TGC TAC AAG GCC AT	FAM
SNAI2	Hs.PT.58.1772559	CAG ATG AGC CCT CAG ATT TGA C	AGG ACA CAT TAG AAC TCA CAC G	HEX
SNAI3	Hs.PT.58.39730475.g	ACT CCG CCT CAT CCC AA	CAC ACA CTC AAA CAT GTA CAC AC	FAM
LGR5	Hs.PT.58.20842190	TTG AAG GCT TCG CAA ATT CTG	AAC GCT CTG ACA TAC ATT CCC	FAM
EPHB2	Hs.PT.58.21222743	CGC ACC TGG AAG ACA TAG ATG	GTG ATC CTG GAC TAT GAG CTG	HEX
BMI1	Hs.PT.56a.18691455	TGT TCG ATG CAT TTC TGC TTG	GCA TTC ATT TTC TGC TGA ACG A	HEX

Table 2.6 Human and mouse primers used for ddPCR analysis

Species	Gene	Forward primer	Reverse primer
Homo sapiens	*E-cadherin*	CCG CTG GCG TCT GTA GGA AGG	GGC TCT TTG ACC ACC GCT CTC C
	Occludin	GCC GGT TCC TGA AGT GGT T	CGA GGC TGC CTG AAG TCA TC
	Desmoplakin	GCT AAA CGC CGC CAG GAT	CCG CAT GAC TGT GTT GGA AT
	Plakoglobin	AAG GTG CTA TCC GTG TGT CC	GTT GTT GCA TGT CAG GTT GG
	Vimentin	CCA GCC GCA GCC TCT ACG	GCG AGA AGT CCA CCG AGT CC
	N-cadherin	CTG TGG GAA TCC GAC GAA TGG	GTC ATT GTC AGC CGC TTT AAG G
Mus musculus	*Snai1*	CAACTATAGCGAGCTGCAGGA	AGGAGAGAGTCCCAGATGAGG
	Lgr5	CCTTGGCCCTGAACAAAATA	ATTTCTTTCCCAGGGAGTGG
	EphB2	AGAATGGTGCCATCTTCCAG	GCACATCCACTTCTTCAGCA
	Bmi1	ATGCATCGAACAACCAGAATC	GTCTGGTTTTGTGAACCTGGA
	Ascl2	CAGGAGCTGCTTGACTTTTCCA	GGGCTAGAAGCAGGTAGGTCCA
	mTert	CGTGGTACAGCTGCTTAGGTC	CTGACCTCCTCTTGTGACAGC
	Axin2	GCAGCTCAGCAAAAAGGGAAAT	TACATGGGGAGCACTGTCTCGT
	ChgA	TCCCCACTGCAGCATCCAGTTC	CCTTCAGACGGCAGAGCTTCGG
	Muc2	AGGGCTCGGAACTCCAGAAA	CCAGGGAATCGGTAGACATCG

Following preparation of the PCR mix (as shown in Table 2.4), sample droplets were generated in the QX100 droplet generator (Bio-Rad). 20 µl each of prepared PCR mix was used and transferred to the sample wells of the cartridge for droplet generation along with 70 µl of droplet generator oil (specific for probes or EvaGreen) pipetted into the bottom wells of the cartridge. The cartridge was covered with a gasket and placed into the QX100 droplet generator. Once droplet generation was complete, the cartridge and gasket were removed and 40 µl of droplets from the droplet wells were pipetted into a 96-well PCR plate (Eppendorf) for thermocycling. This was repeated till droplets were generated for all the samples and transferred to the PCR plate. The plate was sealed with foil using a Bio-Rad PX1™ PCR Plate sealer at 180 °C and placed in the thermal cycler (Bio-Rad C1000 Touch™ thermal cycler) for amplification. Post PCR amplification, the PCR plate was transferred to the QX100™ Droplet Reader (Bio-Rad). The droplet reader quantifies the number of target DNA copies in each sample droplet using the QuantaSoft™ software and expresses the concentration as

copies per µl. Analysis of expression of SNAIL family members and other markers using ddPCR has proven advantageous in the current study as it has a smaller sample requirement than conventional quantitative-PCR (qPCR) and allows absolute quantification while negating the need for technical replicates. No reference gene was used for analysis as the mRNA expression data in the human and mouse studies was normalised against the concentration of cDNA and have been presented as either copies per µl or copies per µg.

2.6 Immunohistochemistry

To analyse the localisation of different proteins in the colonic epithelium, immunohistochemistry (IHC) was performed. Paraffin embedded tissues were cut into 4 µm thick sections and mounted on Superfrost Plus Poly-L-Lysine (PLL) coated slides (Menzel-Glaser, Btaunschweig, Germany). Sections were dewaxed in histosol and serially rehydrated in EtOH. Antigen retrieval was performed in 1.5 L 10 mM citrate buffer pH=6 (Merck, Darmstadt, Germany), in a pressure cooker (Tefal, Wentworth Point, Australia) for 10 minutes on a high pressure setting. Sections were allowed to cool and transferred to warm 1X PBS before incubating in 1% hydrogen peroxide (H_2O_2) for 30 minutes at room temperature to destroy endogenous peroxidases. Sections were blocked in 5% bovine serum albumin (BSA) in PBS for one hour and incubated overnight with primary antibody diluted in 1% BSA/PBS in a humidified chamber at 4 °C. Slides were rinsed in 1X PBS to remove excess unbound primary antibody and incubated with a horseradish peroxidase (HRP) secondary antibody for an hour at room temperature. Presence of peroxidase was detected using 3,3'-diaminobenzidine (DAB) (Dako, Glostrup, Denmark) as substrate as per manufacturer's protocol which produces a brown precipitate. Sections were counterstained with haematoxylin for 30 seconds, rinsed

in water, followed by dehydration in EtOH and histosol and mounted under coverslips using DPX (Sigma, Aldrich, St Louis, USA) as a mountant.

For immunofluorescence, sections were incubated with a fluorescently labelled secondary antibody in a dark chamber protected from light for one hour at room temperature. Sections were counterstained with 4',6-diamidino-2-phenylindole (DAPI) (Thermo Scientific) to mark the nuclei, washed with 1X PBS twice for 5 minutes each and mounted with a fluorescent mounting medium (Dako, Glostrup, Denmark) followed by cover slipping. Details of the primary and secondary antibodies used are given in Table 2.7.

Table 2.7 List of antibodies used for immunohistochemistry and immunofluorescence

Antibody	Species raised in	Dilution for IHC	Manufacturer	Catalogue number
Primary				
Snai1	Mouse	1:300	GeneTex	GTX125918
BrdU	Mouse	1:300	BD Biosciences	555627
GFP	Goat	1:2000	Rockland	600-106-215
E-cadherin	Mouse	1:300	BD Biosciences	610182
β-catenin	Mouse	1:300	BD Biosciences	610154
Secondary				
Goat anti-mouse IgG (H+L) HRP	Goat	1:500	Invitrogen	G21040
Donkey anti-goat Alexa Fluor® 568	Donkey	1:500	Invitrogen	A-11057
Donkey anti-mouse Alexa Fluor® 488	Donkey	1:500	Invitrogen	A-21202

2.7 H&E staining

Tissue morphology was examined by staining sections with haematoxylin and eosin (H&E) performed at the Monash Histology Platform. Slides were dewaxed in xylene (3 x 2 minutes),

followed by 100% EtOH (3 x 2 minutes). Sections were stained with haematoxylin (Sigma Aldrich, St Louis, USA) for 2-3 minutes, followed by rinsing in running tap water for 2 minutes to remove excess stain. Slides were dipped in acid alcohol briefly (few seconds), rinsed in tap water and then in Scott's tap water (2-3 seconds), followed by rinsing in tap water again. Sections were counterstained with an aqueous solution of eosin (Amber Scientific) for 3 minutes, followed by dehydration in 100% EtOH (3 x 2 minutes) and xylene (3 x 2 minutes). Slides were mounted with coverslips using DPX mounting medium (Sigma, Aldrich, St Louis, USA).

2.8 Polyp tissue analyses

Small intestinal and colonic tissues harvested from *Lgr5CreERT2 Apc$^{flox/flox}$* and *Lgr5CreERT2 Apc$^{flox/flox}$ RosaSnai1* mice and colonic tissues isolated from *Cdx2CreERT2 Apc$^{flox/flox}$* and *Cdx2CreERT2 Apc$^{flox/flox}$ RosaSnai1* mice were fixed in 4% PFA and stained with methylene blue (Sigma Aldrich, St Louis, USA). Absorptive dyes like methylene blue allow for better visualisation of polyps as they define the edges and also the depth of the polyp. Tissues were pinned on to wax plates and imaged. Images were acquired using the Zeiss stereo microscope (Carl Ziess, Göttingen, Germany). Bright field images were taken using the Axio Cam MRc5 digital camera running AxioVision Rel. 5.0 software (Carl Ziess, Göttingen, Germany) and images were analysed using the ImageJ2 software (NIH).The number of polyps was measured using the ImageJ2 software while the polyp diameter was measured by using the AxioVision Rel. 5.0 software. The AxioVision software converts image pixels to a metric scale. Images of methylene blue stained tissue pieces with polyps were used and the size along the longest linear line over the length of each polyp (in mm) was measured.

2.9 Histological analyses

Quantification of number of proliferative ($BrdU^+$) cells after up-regulation of *Snai1* in the normal colon and $Apc^{flox/flox}$ colonic polyp tissues was performed for both groups after imaging tissue sections post co-immunofluorescence with anti-GFP, anti-BrdU antibodies and counter-staining with DAPI.

2.9.1 Normal colonic tissues (*Cdx2CreERT2 RosaSnai1*)

To examine any changes in cell proliferation in colonic tissues over-expressing *Snai1* on day 10 post induction with tamoxifen, recombined (green crypts expressing Snai1-eGFP) versus non-recombined (crypts not expressing Snai1-eGFP) were analysed. At least 10 each recombined and non-recombined crypts were analysed per animal. To allow accurate representation of cell proliferation, only crypts which were completely open were chosen for analysis. The number of $BrdU^+$ cells (red channel) was counted in each of these crypts using the cell counter plugin of the ImageJ2 software. The average number of proliferative cells in GFP^+ and GFP^- crypts was calculated for each of the 10 animals in the group.

2.9.2 Colonic polyp tissues (*Cx2CreERT2* $Apc^{flox/flox}$ *RosaSnai1*)

Differences in cell proliferation were analysed in $Apc^{flox/flox}$ mice expressing the *Snai1* transgene. The number of $BrdU^+$ proliferative cells was quantified in polyps over-expressing *Snai1* (indicated by Snai1-eGFP staining) and polyps expressing endogenous *Snai1* (non-green polyps). The ImageJ2 software was utilised to measure the area of polyps and count the number of $BrdU^+$ cells in these polyps. The number of proliferative cells was calculated in 0.01 mm^2 area of polyps for both control and test polyps for each mouse.

2.10 Colonic organoid cultures

2.10.1 Human normal and colorectal tumour organoids

Collection of samples from colorectal cancer patients that had surgical resections at Cabrini Hospital, Melbourne was approved by the Cabrini Human Ethics Committee and the Monash University Ethics Committee. All patients provided written informed consent.

2.10.1.1 Collection of tissues and establishing cultures

Clinical samples collected included benign polyps, primary tumour samples at various stages and adjacent normal tissues with clinical data recorded in the Cabrini database. Samples were collected the day of surgery and processed for organoid cultures by Dr Genevieve Kerr and Dr Rebekah Engel. Adjoining mesenchymal tissue was carefully removed using surgical scissors and the epithelium was utilised to generate organoids after a series of tissue dissociation steps. Normal and tumour cells from tissues were re-suspended in Matrigel and seeded in culture in 24-well plates (Nunc) and fresh culture media supplemented with required growth factors (Table 2.8) was added every alternate day. Once organoids were established, an aliquot of normal and tumour organoid from different organoid lines was collected and expanded in culture for Parnate assay.

Table 2.8 List of culture media components required for normal human and colorectal tumour organoid cultures

Component	Manufacturer	Catalogue number	Final concentration
Advanced DMEM/F12	Gibco	12634028	To make up volume
GlutaMax	Gibco	35050061	1/100
Hepes	Gibco	15630130	1x
Penicillin/Streptomycin	Gibco	15140122	1/100
N2 supplement	Gibco	17502048	1x
B27 supplement	Gibco	17504044	1x
Fungizone	Gibco	15290018	1/500
Human recombinant EGF	Peprotech	100-15	50 ng/ml
Human recombinant Noggin	Peprotech	120-10C	100 ng/ml
R-spondin-1 conditioned media	Prepared in-house	-	20% (normal) 10% (tumour)
Wnt3a conditioned media	Prepared in-house	-	50% (normal only)
Gastrin	Sigma Aldrich	10047-33-3	10 nM
Nicotinamide	Sigma Aldrich	98-92-0	10 mM
N-acetylcysteine	Sigma Aldrich	616-91-1	1.25 mM
A83-01	Tocris	2939	500 nM

2.10.1.2 Parnate assay

Organoids generated from primary colorectal tumour tissues were screened for *SNAI1* expression by ddPCR. Organoids expressing high levels of SNAI1 ($SNAI1^{high}$) were selected for sensitivity to Parnate. Normal colonic organoids and organoids expressing low levels of SNAI1 ($SNAI1^{low}$) were used as controls. Assays for both control and $SNAI1^{high}$ organoids were performed in 96-well plates (Nunc). Organoids were treated with 100 µM of Parnate (Sigma Aldrich, St. Louis, USA) dissolved in RNase-free water (filter sterilised prior to use). Parnate was added to culture media in each organoid well (5 wells for PrestoBlue assay + 4 wells for RNA) every two hours for 12 hours with a final dose at 24 hours. RNase-free water treated organoids were used as control for each assay. After 12 hours, organoids were harvested for RNA. Cell viability was measured at different time points during the assay – 0, 12, 24 and 48

hours using the PrestoBlue® reagent (Invitrogen). Expression of a number of epithelial and mesenchymal markers including *E-CADHERIN, OCCLUDIN, PLAKOGLOBIN, DESMOPLAKIN, VIMENTIN AND N-CADHERIN* (Table 2.6) was analysed in control and Parnate-treated organoids 12 hours post treatment.

2.10.1.3 Cell viability assay

To measure any changes in organoid growth post treatment with Parnate, PrestoBlue® assay was performed as per the manufacturer's instructions. PrestoBlue® reagent contains a cell-permeant resazurin-based solution which is virtually non-fluorescent. PrestoBlue® reagent is rapidly taken up by cells when added to media. The reducing power of viable cells converts resazurin to an intensely red-fluorescent compound, resorufin. This change in fluorescence can be measured using a fluorescence reader. The PrestoBlue® working solution was prepared by diluting the PrestoBlue® solution (Invitrogen) 10 times in human basal media and incubated at 37 °C for 5 minutes protected from light. Culture media was removed from the organoid plate and PrestoBlue® solution was added to each well working in quintuplicates. Wells without any organoids were used as blank. Plate was incubated with the PrestoBlue® solution for 30 minutes at 37 °C. PrestoBlue® solution was collected from each well and transferred to a dark plate (Nunc) protected from light. PrestoBlue® fluorescence was measured using a PHERAstar® (BMG Labtech) fluorescence plate reader at excitation 540 nm and emission 590 nm wavelengths. This assay was performed for each organoid line at fixed time-points throughout the Parnate assay - 0, 12, 24 and 48 hours of culture.

2.10.2 Mouse colonic organoids

Organoids were generated from colonic crypts isolated from transgenic mice and manipulated genetically *in vitro*.

2.10.2.1 Establishing cultures

Generation of intestinal organoids has previously been described (Sato et al., 2009). In the current study colonic organoids were generated from *RosaSnai1* and *ZsGreen1*$^{flox/+}$ mice. Fresh colonic tissues were harvested and washed in ice-cold 1X PBS and cut open longitudinally. All fragments of adipose tissue were removed using surgical scissors. Faecal contents were removed and the tissue was gently scraped using a coverslip to remove any leftover mucous. The tissues were cut into small fragments and incubated with 4 mM EDTA in 1X PBS in 50 ml Falcon tubes at 4 °C for 30 minutes. Epithelial crypt enriched fractions were collected by pipetting tissue pieces vigorously in the tube and centrifuging at 1500 rpm for 5 minutes at 4°C. Supernatant was discarded and the pellet was re-suspended in 10 ml 1X PBS and transferred to a new tube using a 70 µm cell strainer (Becton Dickinson, New Jersey, USA) to remove any mucous and large clumps of cells. The crypt enriched suspension was centrifuged at 1500 rpm for 5 minutes at 4 °C. The pellet collected was re-suspended in Matrigel (Corning, NY, USA) and seeded in a pre-warmed 24-well plate (Nunc, Roskilde, Denmark). Pre-warmed colonic organoid culture medium was added and the plate was kept in an incubator at 37 °C with 5% CO_2 in a humidified atmosphere. Culture media supplemented with growth factors was replaced every alternate day. Details of the culture media components is given in Table 2.9.

Table 2.9 List of culture media components required for mouse colonic organoid cultures

Component	Manufacturer	Catalogue number	Final concentration
DMEM/F12	Gibco	11320033	To make up volume
GlutaMax	Gibco	35050061	1/100
Hepes	Gibco	15630130	1x
Penicillin/Streptomycin	Gibco	15140122	1/100
N2 supplement	Gibco	17502048	1x
B27 supplement	Gibco	17504044	1x
Fungizone	Gibco	15290018	1/500
Mouse recombinant EGF	Peprotech	315-09	50 ng/ml
Mouse recombinant Noggin	Peprotech	250-38	100 ng/ml
R-spondin-1 conditioned media	Prepared in-house	-	10%
Wnt3a conditioned media	Prepared in-house	-	50%

2.10.2.2 TAT-Cre assay

Expression of ZsGreen1 GFP and *Snai1* transgene was induced in mouse colonic organoids using a cell permeable Cre recombinase enzyme, TAT-Cre (Merck Millipore). Organoids were dissociated using TrypLE Express (Invitrogen) and incubated with 8 µM TAT-Cre added to culture media in a 1.5 ml Eppendorf tube for 4 hours at 37 °C in an incubator. Cells were centrifuged at 1500 rpm for 5 minutes at 4 °C and the pellet was re-suspended in Matrigel. Cells were seeded in 48-well plates and allowed to grow in culture media for 5 days, replacing with fresh media every other day. On day 5, organoids were visualised for GFP expression using a fluorescent microscope (Carl Zeiss, Göttingen, Germany).

2.10.2.3 FACS analyses

Transfected organoids were processed for FACS analysis on day 5 post treatment with TAT-Cre. Organoids were mechanically dissociated from the Matrigel using a P1000 pipette and centrifuged with 1X PBS for (1500 rpm for 5 minutes) at 4 °C. The pellet was re-suspended in

a cocktail of TrypLE Express (1 ml), 10 µM Rock inhibitor (RKI) (Tocris) and 50 Units DNAse I (Roche) and incubated at 37 °C for 2 minutes in a water bath. Cold DMEM/F12 was added to the tube and the suspension was centrifuged (1500 rpm for 5 minutes) at 4 °C. Cells were re-suspended in FACS buffer consisting of DMEM/F12, 10% fetal bovine serum (FBS) (Bovogen) and 10 µM RKI and FACS analysis was performed. For optimisation studies, ZsGreen1 GFP^+ cells were sorted and collected. To examine the effect of *Snai1* up-regulation in colonic stem cells, $CD24^{med}/GFP^+$ and $CD24^{med}/GFP^-$ cell populations were collected and re-seeded in culture and analysed on day 8.

2.10.3 Human CRC cell lines

Expression of *SNAIL* family members and ISC markers was analysed across a set of human colorectal cancer cell lines by ddPCR. A description of origin of each cell line chosen is given in Table 2.10.

Table 2.10 Characteristics of different human colorectal cancer cell lines

Cell line	Description	Tissue	Catalogue/Code number
LIM1215	Colorectal carcinoma cell line	Omental metastasis, CRC transcending colon	CBA-1215
LIM1899	Columnar cell adenocarcinoma of the colon	Colon	CBA-0163
LIM2405	Adherent cell line derived from a poorly differentiated adenocarcinoma of the caecum	Caecum/Colon	CBA-0165
LIM2550	Colon carcinoma	Colon	CBA-0169
CACO-2	Colorectal adenocarcinoma	Colon	09042001
SW480	Dukes' type B, colorectal adenocarcinoma	Colon	87092801

2.11 The Cancer Genome Atlas data analyses

The database was accessed in July-August 2017 to analyse specific gene sets within the TCGA Colorectal Adenocarcinoma (Provisional) dataset consisting of 633 samples where mutations, copy number alteration and mRNA expression data are included. The RNA Seq Version 2 (RNA-Seq by Expectation Maximisation [RSEM]) was used for each selected gene (Z-score threshold ± 2). Genetic alterations and overall survival data for patients with mutated *SNAIL* family members were accessed for analysis.

2.12 Statistical analyses

2.12.1 Human samples

The analyses for normal and tumour tissues were performed in a blinded manner and correlated with clinical characteristics for each patient at Cabrini Hospital. All statistical analyses were conducted by a Biostatistician, Margaret Staples, at Cabrini Hospital. Fold changes between tumour and matched normal samples were calculated as the ratio of gene expression in tumour versus normal using non-parametric tests. Associations between gene expressions were assessed using Wilcoxon signed-rank tests. To test the significance of fold changes between normal and tumour samples, one sample paired t-tests were performed. Associations between *SNAIL* family members and ISC markers were assessed using Pearson and Spearman rank correlations. To investigate associations between marker gene expression and tumour characteristics, linear regression modelling using the logarithm of the marker gene fold changes as the dependent variable was used. Comparisons between control and Parnate treated organoids was made using paired student's t-tests and 2-way ANOVA. A p-value <0.05 was considered statistically significant.

2.12.2 Mouse samples

Statistical analyses were conducted using GraphPad Prism 6 software for Windows, (version 6.07, San Diego, USA). Student's t-tests were used for all quantitative analyses in mouse tissues and organoids to determine significance between groups. Comparisons between the control and test mice were made by unpaired Student's t-test assuming unequal variance (Welch's correction) unless mentioned as otherwise. The use of paired or unpaired t-test has been specified for each experiment in the results section. A p-value <0.05 was considered statistically significant. Data is represented as mean ± standard error of the mean (SEM).

Chapter 3 - Analysis of SNAIL proteins in primary human colorectal tumours

Chapter 3 – Analysis of SNAIL proteins in primary human colorectal tumours

3.1 Introduction

3.1.1 Colorectal cancer: Incidence and staging

Colorectal cancer (CRC or bowel cancer) is the third most commonly diagnosed cancer in both men and women worldwide. In Australia, it was estimated that it will become the second most commonly occurring cancer in 2017 (Australian Institute of and Welfare, 2018). The projected number of new CRC cases diagnosed in Australia in 2018 will be 17,004. The 5-year survival rates for bowel cancer patients is 69% (Australian Institute of and Welfare, 2018), which is far less than those for other common cancers like breast and prostate with survival rates of around 90%. This is in part due to the fact that more than 60% of bowel cancer cases are detected at advanced stages (Bowel Cancer Australia). Nevertheless, for cases that are diagnosed early, chances of successful treatment are as high as 90%. The most common type of CRC (95 out of every 100 cases diagnosed), adenocarcinoma, arises in the epithelial cells that line the large intestinal wall. There are other forms of CRC which do not occur as often, which include squamous cell cancers, carcinoid tumours, lymphomas and sarcomas. Extensive heterogeneity exists in colorectal tumours and there is considerable variation among tumours with respect to response to drug treatments. This heterogeneity translates into variable drug response even for same stage tumours. Tumours are staged at the time of diagnosis based on

a universal staging system, the TNM staging system for colorectal tumours devised by the American Joint Committee on Cancer (AJCC). It is based on depth of invasion of the bowel wall, extent of regional lymph node involvement and presence of distant tumours (Figure 3.1). Table 3.1 summaries the different stages. Associations between tumour stages and marker genes were analysed in this study.

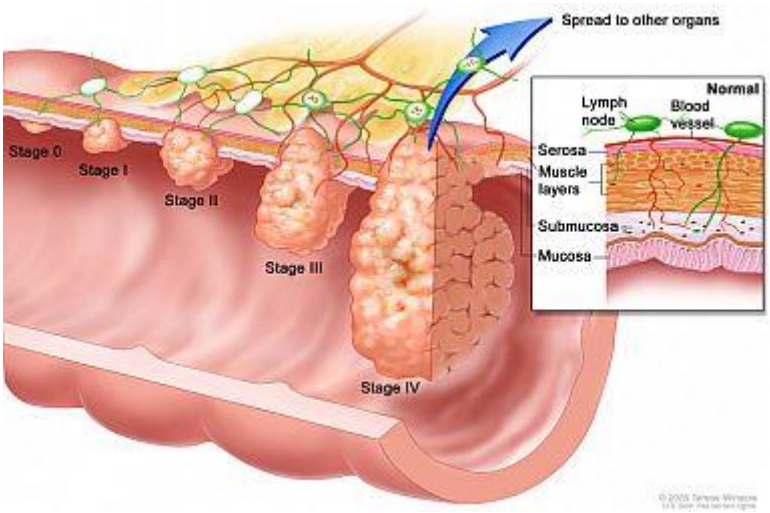

Figure 3.1 TNM Staging of colorectal cancer. Colorectal tumours are categorised into stages based on depth of invasion into the bowel wall, extent of lymph node involvement and presence of secondary tumours or metastasis. Image source: National Cancer Institute.

Table 3.1 TNM staging system of colorectal tumours

Tumour stage	Tumour description
Primary tumour (T)	
T_x	Primary tumour cannot be assessed
T_{is}	Carcinoma in situ
T_1	Tumour invades submucosa
T_2	Tumour invades muscularis propria
T_3	Tumour invades through the muscularis propria into the subserosa
T_4	Tumour directly invades other organs or structures, or perforates visceral peritoneum
Regional lymph nodes	
N_x	Regional lymph nodes cannot be assessed
N_0	No regional lymph node metastases
N_1	Metastases in 1-3 regional lymph nodes
N_2	Metastases in 4 or more regional lymph nodes
Distant metastases	
M_x	Presence or absence of distant metastases cannot be determined
M_0	No distant metastases can be detected
M_1	Distant metastases detected

Variations in response to drug therapies as a result of tumour heterogeneity can be attributed to somatic mutations occurring within tumours. The Cancer Genome Atlas characterised somatic alterations in colorectal cancer by conducting a genome scale analysis of 276 samples and identified two tumour sets – hypermutated (16% of all tumours analysed) and non-hypermutated tumours (84% of tumours) (Cancer Genome Atlas, 2012). About 32 somatic genes were found to frequently mutated in these hypermutated and non-hypermutated cancers. The most recurrently mutated genes among the non-hypermutated tumours included *APC*, *TP53* and *KRAS* among others, while the two most commonly mutated genes in hypermutated tumours included *ACVR2A* and *APC*. *APC* was the only gene that was found to

be mutated in the majority of hypermutated and non-hypermutated tumours (51% and 81% respectively). WNT signalling was the most frequently altered pathway (93% of cases), which included biallelic inactivation of *APC* or activating mutations of *CTNNB1* in approximately 80% of the tumours.

3.1.2 Role of stem cells in colorectal cancer

Intestinal stem cells are a small population of actively dividing cells present at the base of the intestinal crypts in normal epithelium. These stem cells were first identified in the small intestine and are also known as crypt base columnar (CBC) cells or $Lgr5^{+}$ cells as these cells can be detected by marker gene *Lgr5* (Barker et al., 2007). Other ISC marker genes include *Olfm4* (van der Flier et al., 2009b), *Ascl2* (van der Flier et al., 2009b), *EphB2* (Merlos-Suarez et al., 2011), *Bmi1* (Sangiorgi and Capecchi, 2008) and *Lrig1* (Powell et al., 2012), among others.

There is some evidence that intestinal tumours arise as a result of mutations accumulating in ISCs (Barker et al., 2009). Support for this concept was demonstrated by Barker and colleagues when the *Apc* tumour suppressor gene was knocked out in ISCs and transit amplifying (TA) cells in mice. Loss of *Apc* in the ISC population resulted in the rapid formation of intestinal adenomas whereas no adenomas were formed in mice with *Apc* deletion in the TA cell compartment, thus confirming that the ISCs can act as cells of origin in intestinal cancer. Cancer stem cells (CSCs) have also been identified in established tumours. The cancer stem cell model outlined by Visvader and Lindeman has been discussed in section 1.1.6 (Chapter 1). Resistance to chemotherapy (and/or radiotherapy) and recurrence of tumours, the two major challenges today in cancer research, are thought to occur as a result of these CSCs. For instance, one possible explanation for tumour relapse could be attributed to the quiescent

nature of some CSCs. This means that some CSCs are capable of escaping therapeutic interventions eventually resulting in tumour relapse. Not only that, existence of molecularly distinct CSC populations has been identified within individual patients with acute myeloid leukaemia (AML) (Goardon et al., 2011). Therefore, it is crucial to deconstruct mechanisms that lead to resistance of CSCs to drug and radiotherapies. Therefore, markers which identify tumours with a cancer stem cell signature may be helpful in providing information about drug resistance and the chance of tumour recurrence.

Correlation between the stem cell signature and cancer prognosis has been reported in context of colorectal cancer. Colorectal tumours expressing high levels of the ISC marker gene EPHB2 are more aggressive and are more likely to give rise to new tumours following cessation of treatment. Gene Set Enrichment Analysis (GESA) of a cohort of 340 primary colorectal tumours has shown the EPHB2-ISC gene signature to be strongly linked to metastatic rather than non-metastatic tumours. Comparing tumour morphology, poorly differentiated tumours were found to be enriched for the EPHB2-ISC gene signature rather than benign well-differentiated tumours (Merlos-Suarez et al., 2011). There is emerging evidence for other markers which are present in stem cell populations as potential predictors of disease outcome. This includes regulators of EMT, in particular the *SNAIL* family of transcription factors.

3.1.3 SNAIL proteins and cancer

A number of molecules – including SNAIL proteins - have been known to play a role in regulation and maintenance of the ISC population. The *SNAIL* family of transcription factors is composed of three members – *SNAI1*, *SNAI2* and *SNAI3*. Snail genes are well known for their

role in regulation of epithelial-mesenchymal transition (EMT) in both normal and diseased states. SNAIL proteins are up-regulated in many human cancers and have been shown to play a role in induction of an invasive phenotype in mouse models of cancer (Nieto, 2002). SNAIL-induced EMT results in suppression of E-cadherin transcription in tumours and is considered to be a marker of a poor clinical outcome and a more invasive phenotype in many malignancies including breast cancer (van Nes et al., 2012), gastric (Shin et al., 2012) and oesophageal squamous cell carcinoma (Kuo et al., 2012). Although SNAI1 plays a critical role in driving EMT especially in cancer, there has been emerging evidence suggesting that SNAI1 plays a role in the regulation of the stem cell population in different tissues. For instance, up-regulation of *Snai1* in the small intestinal crypts results in increase in number of stem cells as well as proliferative cells. However, *Snai1* over-expression was not sufficient to induce tumour formation in these mice (Horvay et al., 2015). Role of SNAIL has been studied in context of skin cancers where SNAIL proteins were found to contribute to expansion and survival of skin stem cells *in vivo* (De Craene et al., 2014). Examination of the transcriptome profile of CRC colonospheres revealed significant SNAI1 up-regulation, with high expression of SNAI1 in HT29 colonospheres positive for stem cell marker CD44 compared to $CD44^{-}$ colonospheres (Hwang et al., 2011). Moreover, overexpression of SNAI1 in SW480 human CRC cell line has been shown to induce expression of CD44 resulting in enhanced self-renewal ability while its knockdown in primary colonospheres or HT29 human CRC cells decreased CD44 expression. The function of *Snail* has also been studied in the mammary gland where its expression was essentially detected in the $CD44^{high}/CD24^{low}$ normal human mammary epithelial stem cell and mammary CSC populations (Al-Hajj et al., 2003, Mani et al., 2008, Sleeman et al., 2006). Ectopic expression of SNAIL in immortalised human mammary epithelial

cells has been shown to result in activation of EMT and acquisition of a $CD44^{high}/CD24^{low}$ expression pattern in these cells (Mani et al., 2008). Although *Snail* has been shown to induce stem cell properties, however, one of the many unanswered questions still remains – whether *Snail* plays a role in maintaining cancer stem cells in mammalian intestinal cancer. In this chapter, the associations between ISC markers and SNAIL expression with tumour stage and morphology are examined in primary colorectal tumours.

3.1.4 Human colorectal tumour organoids as a model to study SNAIL function

One of the approaches to study the function of *Snail* in context of human colorectal tumours is by targeting *Snail* or *Snail*-induced transcription in organoids generated from isolated human colorectal tumour tissues. Sato *et al.* have developed an intestinal epithelial organoid culture system in which crypts from normal tissues or cancer cells from colorectal tumours form organoid structures in Matrigel (Sato et al., 2011). *In vitro* modelling of colorectal cancer has many advantages over animal use in research as it permits rapid analysis of drug response in a readily accessible *in vitro* system. Tranylcypromine (or Parnate) is a monoamine oxidase/LSD1 inhibitor which has been shown to block the interaction between LSD1 and the SNAG domain of SNAIL (Ferrari-Amorotti et al., 2013), therefore, treating cancer cells with Parnate should mimic the changes in expression of epithelial and mesenchymal markers induced by down-regulation of *SNAIL* function. Treatment of human CRC cell lines HCT116 and Colo205 with Parnate resulted in increased expression of *SNAIL* downstream target genes, *E-CADHERIN*, *OCCLUDIN* and *DESMOPLAKIN* and a decrease in expression of mesenchymal markers *VIMENTIN* and *N-CADHERIN* suggesting induction of EMT characteristics (Ferrari-Amorotti et al., 2013). These experiments validate the potential of Parnate to inhibit the function of SNAIL. Therefore, we decided to look at the consequences

of *SNAIL* downregulation in SNAI1^{high} human colorectal tumour organoids following treatment with Parnate to assess any changes in expression of these target genes and in organoid proliferative capacity.

3.1.5 cBioPortal for Cancer Genomics

Considering the heterogeneity among human colorectal tumours, studying gene function in specific tumour sub-types can be limited by small sample size. To overcome this, researchers have access to databases like cBioPortal for Cancer Genomics to widen the scope of their studies. The cBioPortal for Cancer Genomics is an open-access resource for studying a wide range of cancer genomics data sets. The portal stores DNA copy-number data, mRNA and microRNA expression data, protein-level and phosphoprotein level (RPPA) data, DNA methylation data, and limited de-identified clinical data (Cerami et al., 2012, Gao et al., 2013). The TCGA provisional datasets are directly sourced from TCGA data centre. The cBioPortal is an important resource for examining the expression of candidate genes in a large dataset and correlating these with patient outcomes. However, the cBioPortal only has mRNA/protein expression data and does not give any information as to where in the tumours these genes are expressed. The available data in cBioPortal is utilised in this chapter to examine correlation of SNAIL family members with patient outcome data.

3.1.6 Significance of this study

Numerous studies so far have implicated a role of SNAIL in tumour progression and tissue invasion. However, the association of SNAIL expression with stem cells and patient outcome in colorectal cancers is still unclear. This study investigates the role of SNAIL family members

in colorectal tumours and their association with cancer stem cell markers, tumour stage and patient outcome.

3.1.7 Hypothesis

This chapter investigates the hypothesis that SNAIL expression is associated with cancer stem cells in colorectal cancer and may play a role in regulation of stem cells in these tumours.

3.2 Results

3.2.1 Intestinal stem cell markers are up-regulated in human colorectal cancer

Several studies have shown up-regulation of stem cell markers in CRC (Lugli et al., 2005, Merlos-Suarez et al., 2011, Uchida et al., 2010, Jarde et al., 2015). To verify these findings in the current patient cohort, the expression of intestinal stem cell markers was studied in a set of primary tumours and adjacent normal tissues obtained from colorectal cancer patients. The study cohort consisted of 68 patients who consented to donate tumour tissue and adjacent normal tissue after surgical resections at Cabrini Hospital, Melbourne. The clinical characteristics of patients are summarised in Table 3.2.

Table 3.2 Characteristics of colorectal cancer patients (n=68)

	Frequency	Percent
Gender		
Female	45	60.8
Male	29	39.2
Grade		
Adenoma	5	7.4
Well differentiated	2	2.9
Moderately differentiated	47	69.1
Poorly differentiated	13	19.1
Undifferentiated	1	1.5
Stage		
0	5	7.4
I	14	20.6
II	29	42.6
III	12	17.6
IV	8	11.8
T stage		
0	5	7.4
1	5	7.4
2	11	16.2
3	39	57.4
4	8	
N stage		
0	49	72.1
1	15	22.1
2	4	5.9
M stage		
0	60	88.2
1	8	11.8

Tumour staging showed most of these tumours were at stage II (42.6%) and stage I (20.6%), and relatively fewer tumours at stage III (17.6%) and IV (11.6%). Pathological analysis of these tumours revealed that most tumours were graded as moderately differentiated (69.1%). Expression of stem cell markers in tumour tissue was compared to normal tissue in each patient. ddPCR analysis of the expression levels of *LGR5*, *EPHB2* and *BMI1* demonstrated up-regulation of the intestinal stem cell markers at the RNA level in the majority of tumour tissues

(Figure 3.2). Tumour samples with two-fold or higher increase in expression of marker genes compared to matched normal tissue were classified as samples with up-regulated marker mRNA expression. *LGR5* was up-regulated in 71% of the tumour samples, whereas *EPHB2* and *BMI1* were up-regulated in 60% and 42% of the tumour tissues respectively (Figure 3.3).

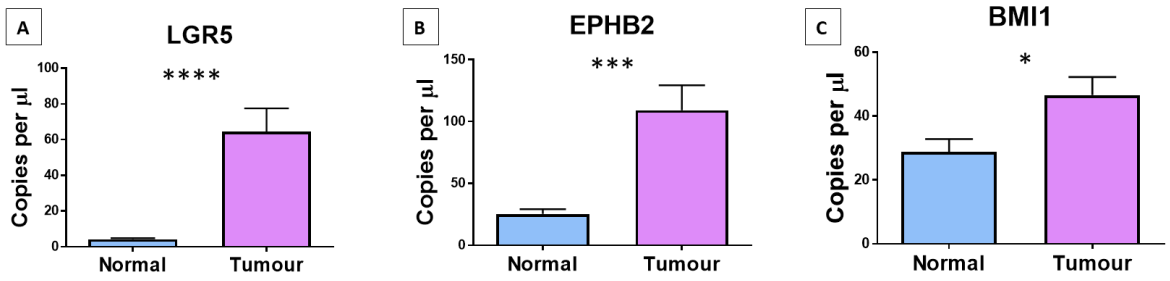

Figure 3.2 Intestinal stem cell markers are up-regulated in human colorectal tumours. Expression of intestinal stem cell markers (A) *LGR5* (p<0.0001), (B) *EPHB2* (p=0.0001) and (C) *BMI1* (p=0.0119) in primary colorectal tumour tissues versus adjacent normal tissue (n=68). Data was analysed by paired t-test and is represented as the mean ± SEM.

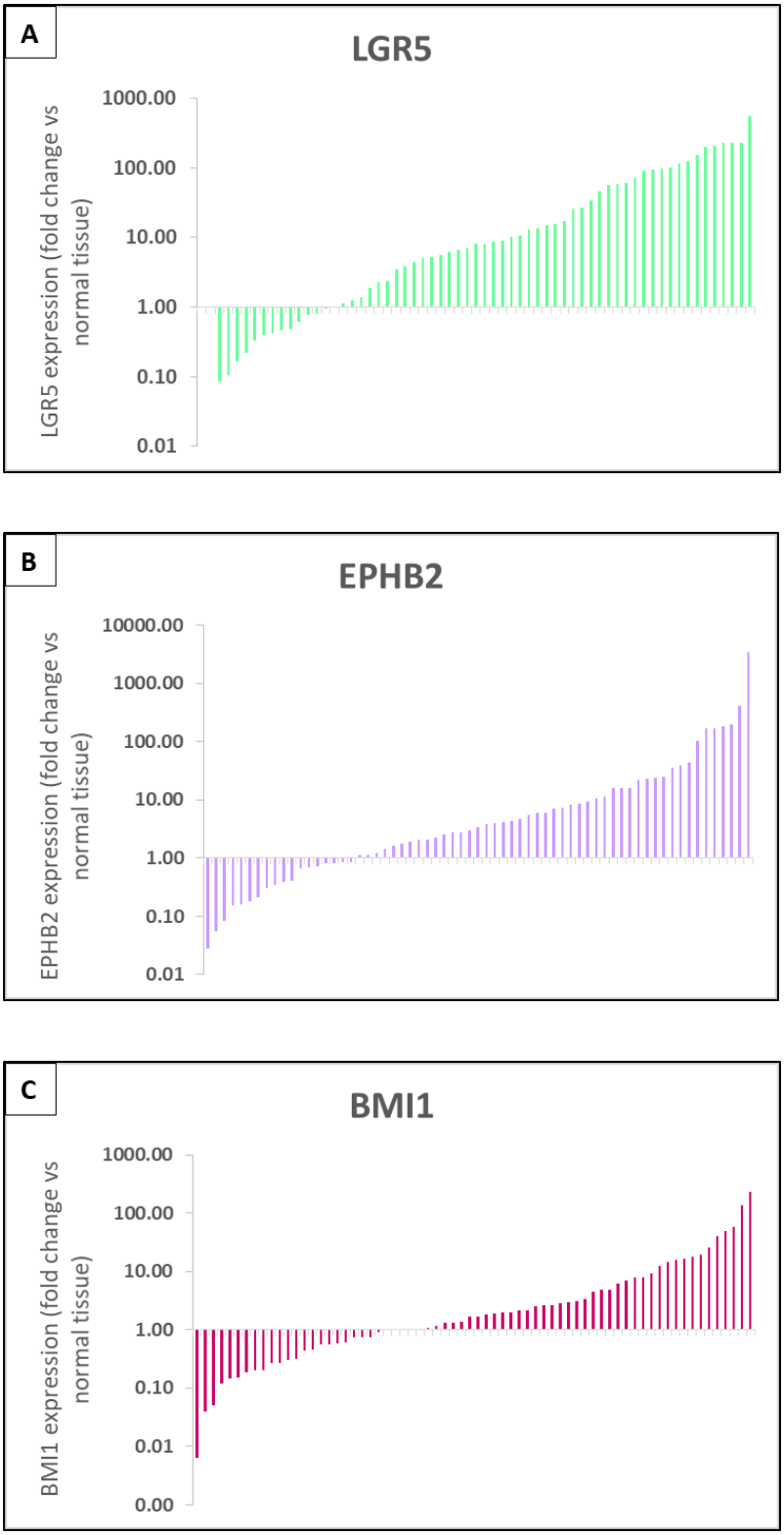

Figure 3.3 Intestinal stem cell markers are up-regulated in a sub-set of human colorectal tumours. Waterfall plots of fold change expression of intestinal stem cell markers (A) *LGR5*, (B) *EPHB2* and (C) *BMI1* versus adjacent normal tissue analysed in 68 tissue sample pairs. Two-fold or higher increase in expression of *LGR5* was observed in 71% of the tumours, 60% tumours for *EPHB2* and in 42% of tumours or *BMI1* expression.

Linear regression analysis revealed that there was no association of ISC markers expression with tumour stage and tumour grade (Figure 3.4 and 3.5). This analysis confirmed the up-regulation of ISC markers described in other studies within the cohort of tumours utilised in this study.

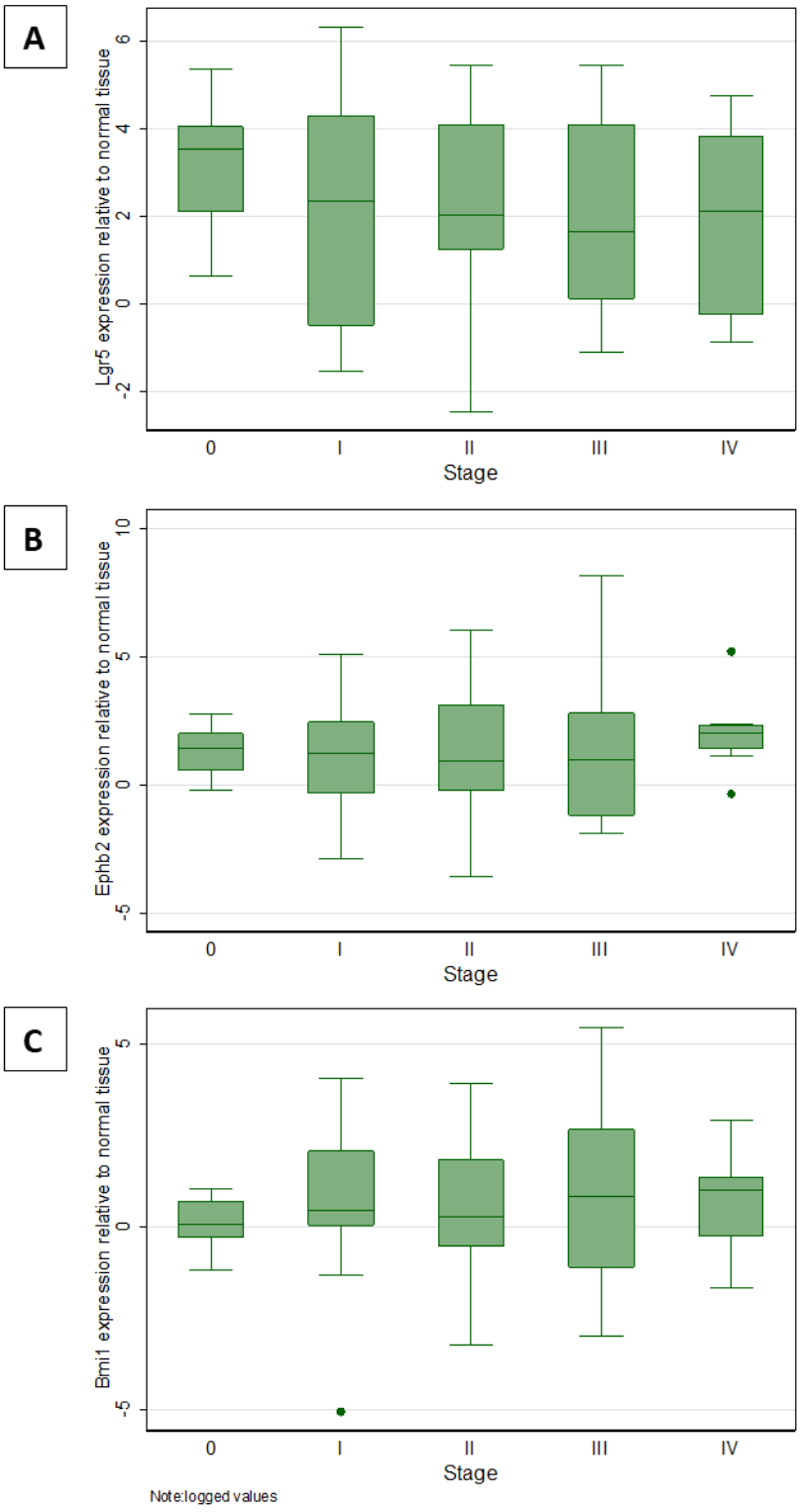

Figure 3.4 No association of ISC markers with colorectal tumour stage. Boxplots of mRNA expression fold change values of ISC markers (A) *LGR5*, (B) *EPHB2* and (C) *BMI1* across different stages of colorectal tumours. Error bars represent the minimum and maximum of all data points excluding outliers.

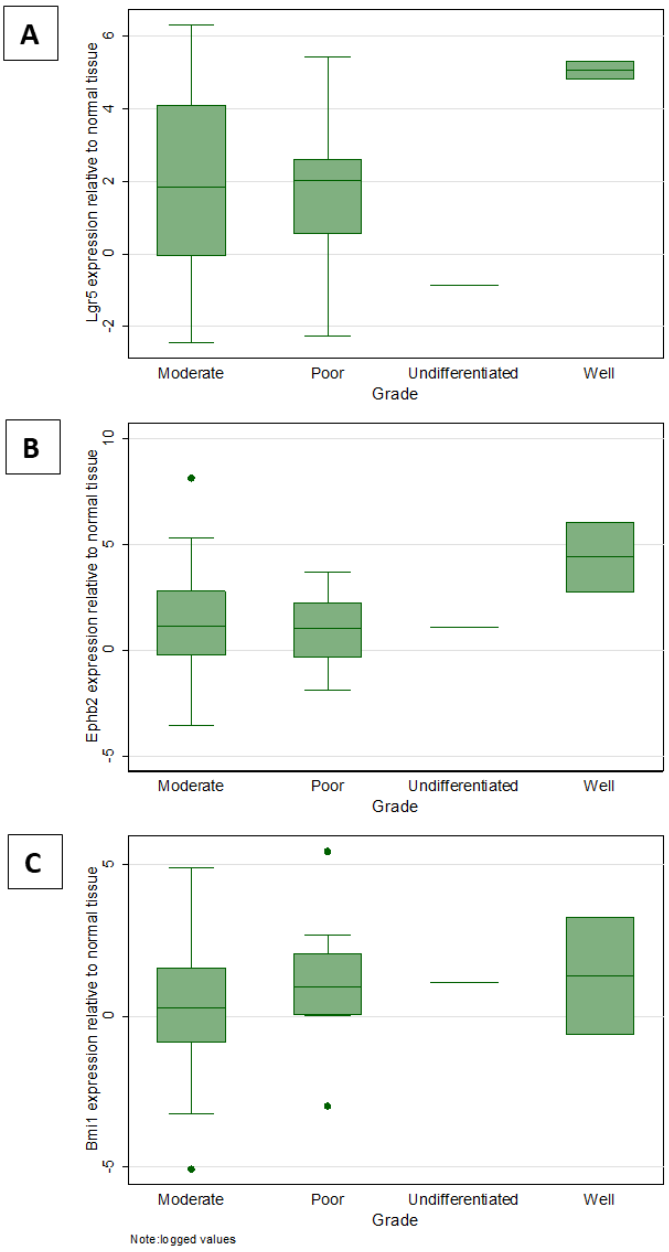

Figure 3.5 No association of ISC markers with colorectal tumour grade. Boxplots of mRNA expression of ISC markers (A) *LGR5*, (B) *EPHB2* and (C) *BMI1* relative to normal tissue across different grades of colorectal tumours. Error bars represent the minimum and maximum of all data points excluding outliers.

3.2.2 SNAI1 is up-regulated in human colorectal cancer

SNAIL genes have been proposed to play a role in progression of tumours and maintenance of cancer stem cells. Following analysis of intestinal stem cell markers, expression of *SNAIL* family members was analysed in tumour tissue and adjacent normal tissue. Overall, the expression of *SNAI1* was significantly up-regulated in tumours compared to normal tissues in this patient cohort. Interestingly, no significant difference in *SNAI2* or *SNAI3* expression overall in tumours compared to normal tissues was observed (Figure 3.5). Although normal and tumour samples expressed relatively low levels of the *SNAI1* transcript as compared to *SNAI2* and *SNAI3*, expression of *SNAI1* mRNA was up-regulated (two-fold or higher) in 36/68 (52%) of individual tumour samples as compared to normal tissues. *SNAI2* and *SNAI3* mRNA expression was found to be up-regulated (two-fold or higher increase versus normal tissues) in 24/68 (35%) and 25/68 (36%) of individual tumour tissues respectively suggesting there is hetergeneity among tumours as there are subsets of tumours within this cohort which overexpress *SNAI2* and *SNAI3* (Figure 3.6). Overall, 19% (13/68) of the tumours demonstrated up-regulation of all three *SNAIL* family members. Analysing individual tumours with up-regulated *SNAI1* (36 samples out of 68), 50% (18/36) presented with up-regulation of *SNAI2* and *SNAI3* as well.

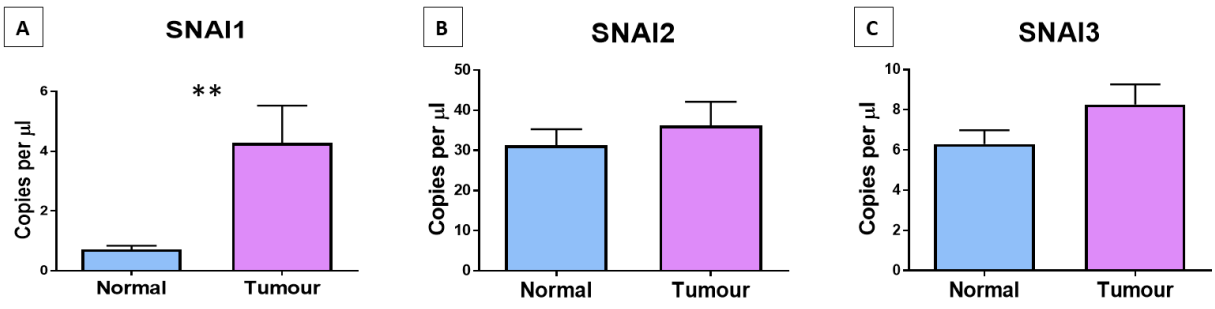

Figure 3.5 *SNAI1* is up-regulated in human colorectal cancer. Expression of *SNAIL* family members (A) *SNAI1* ($p<0.01$), (B) *SNAI2* and (C) *SNAI3* in primary colorectal tumour tissues versus adjacent normal tissue (n= 68). Data was analysed by paired t-test and is represented as the mean ± SEM.

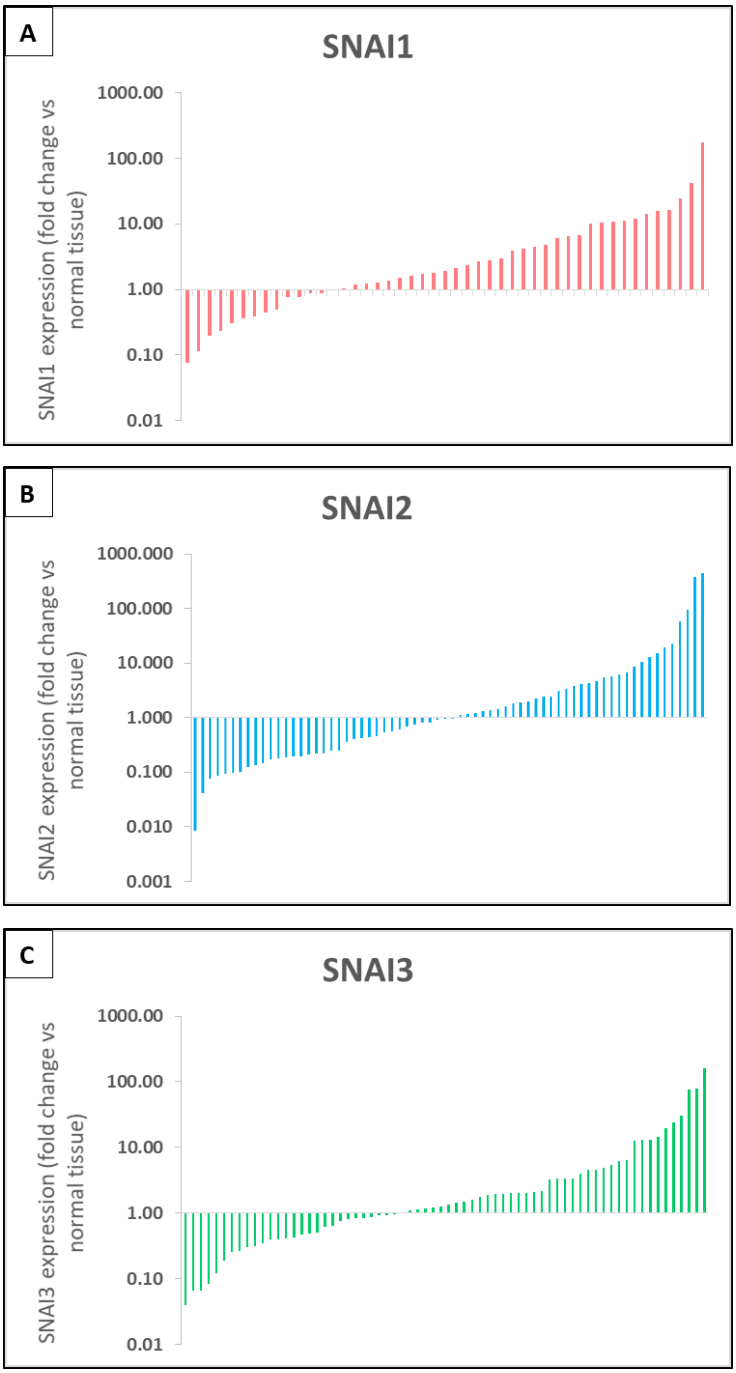

Figure 3.6 *SNAIL* family members are up-regulated in a subset of human colorectal tumours. Waterfall plots of fold change expression of *SNAIL* family members (A) *SNAI1*, (B) *SNAI2* and (C) *SNAI3* in tumours versus adjacent normal tissues (n= 68). The proportion of patients with two-fold or higher increase in expression of *SNAI1* was 52%, 35% for *SNAI2* and 36% for *SNAI3*.

3.2.3 Expression of *SNAIL* family members correlates with intestinal stem cell markers in primary colorectal tumours

Relationship between variables can be assessed by either using Pearson's coefficient (measures the linear relationship between two variables) or Spearman's rank order coefficient (evaluates the monotonic relationship between two variables). Correlations between mRNA fold changes (normal vs tumour) of *SNAI1*, *SNAI2* and *SNAI3* and the intestinal stem cell markers were assessed using both Pearson correlation test (Table 3.3) and Spearman rank order correlation test (Table 3.4). Similar outcomes were obtained from both tests. Expression of *SNAIL* family members correlated with expression of all three intestinal stem cell markers. Moreover, expression of *SNAIL* family members correlated with each other. This suggests that although *SNAI1* was up-regulated in a subset of tumour tissues, these tumours also express higher levels of intestinal stem cell markers. Similarly, tumours overexpressing *SNAI2* and *SNAI3* mRNA also expressed high levels of *SNAI1* and the intestinal stem cell markers.

Table 3.3 Pairwise Pearson correlation of logged fold change values of *SNAIL* family members and ISC markers

		SNAI1	SNAI2	SNAI3	LGR5	BMI1
SNAI2	Correlation	0.67				
	p-value	<0.001				
	n	47	68			
SNAI3	Correlation	0.54	0.80			
	p-value	0.0001	<0.001			
	n	47	68	68		
LGR5	Correlation	0.43	0.53	0.59		
	p-value	0.0035	<0.001	<0.001		
	n	44	61	61	61	
BMI1	Correlation	0.70	0.80	0.74	0.57	
	p-value	<0.001	<0.001	<0.001	<0.001	
	n	47	68	68	61	68
EPHB2	Correlation	0.67	0.69	0.84	0.81	0.77
	p-value	<0.001	<0.001	<0.001	<0.001	<0.001
	n	47	65	65	59	65

Table 3.4 Spearman rank order correlation of logged fold change values of *SNAIL* family members and ISC markers

		SNAI1	SNAI2	SNAI3	LGR5	BMI1
SNAI2	Correlation	0.73				
	p-value	<0.001				
	n	49	68			
SNAI3	Correlation	0.47	0.73			
	p-value	0.0006	<0.001			
	n	49	68	68		
LGR5	Correlation	0.41	0.52	0.65		
	p-value	0.005	<0.001	<0.001		
	n	47	63	63	61	
BMI1	Correlation	0.69	0.74	0.74	0.55	
	p-value	<0.001	<0.001	<0.001	<0.001	
	n	49	68	68	63	68
EPHB2	Correlation	0.63	0.63	0.77	0.82	0.77
	p-value	<0.001	<0.001	<0.001	<0.001	<0.001
	N	49	65	65	61	65

3.2.4 Expression of *SNAI1* and *SNAI2* correlates with T stage of colorectal tumours

Tumour tissues were graded based on the TNM staging system devised by the American Joint Committee on Cancer (AJCC). Linear regression analysis of *SNAI1, SNAI2* and *SNAI3* mRNA with tumour stage revealed association of *SNAI1* and *SNAI2* levels with T-stage of colorectal tumours (Figure 3.7). T-stages 2 and 3 had significantly higher levels of *SNAI1* relative to T0 tumours whereas SNAI2 was up-regulated in T-stage 3. However, there was no association with the N- and M-stages. On comparing expression of *SNAI1* with respect to overall tumour stages, stage 0 tumours had significantly lower *SNAI1* expression fold change values compared to more advanced staged (stage I, II, III and IV) tumours (Figure 3.8).

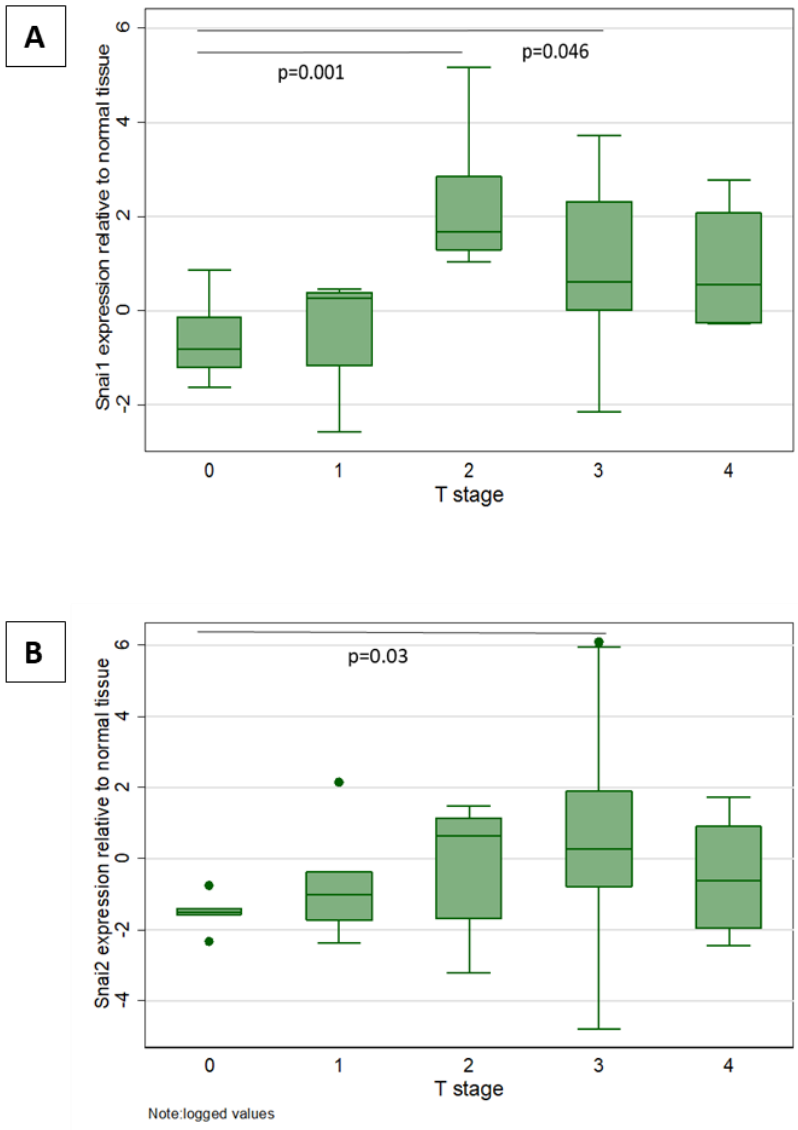

Figure 3.7 *SNAI1* and *SNAI2* are up-regulated in T3 stage tumours compared to T0 tumours. Boxplots of (A) *SNAI1* and (B) *SNAI2* expression fold change values across different T stage tumours (n = 47 and 68 respectively). Error bars represent the minimum and maximum of all data points excluding outliers.

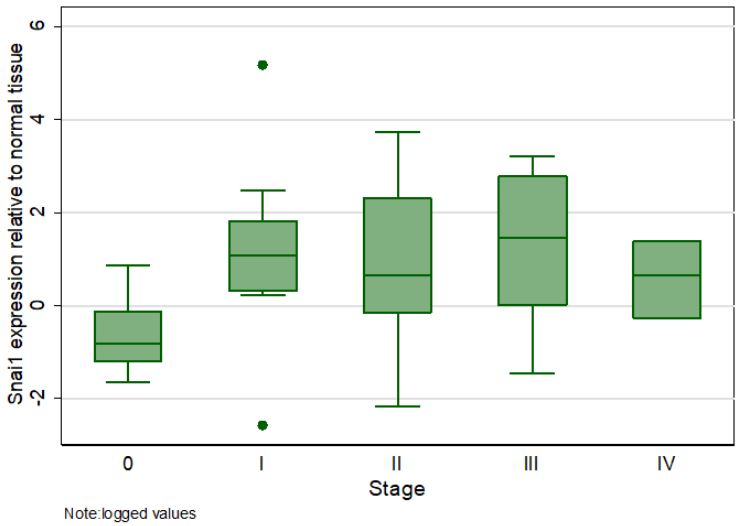

Figure 3.8 *SNAI1* is significantly down-regulated in stage 0 tumours (p = 0.042). Boxplot showing *SNAI1* expression fold change values across tumours (n = 47) of different stages starting from stage 0 to IV. Error bars represent the minimum and maximum of all data points excluding outliers.

3.2.5 Adenomas are associated with low levels of *SNAI1* as compared to adenocarcinomas

SNAIL family members mRNA expression data was analysed for associations with tumour morphology. Out of the 68 tumours analysed in this study, majority of these were adenocarcinomas (92.6%) while the remaining tumours were adenomas (7.4%). Expression of *SNAI1* was found to be significantly lower in adenomas when compared to adenocarcinomas (Figure 3.9). However, there was no association of *SNAI2* and *SNAI3* with tumour morphology.

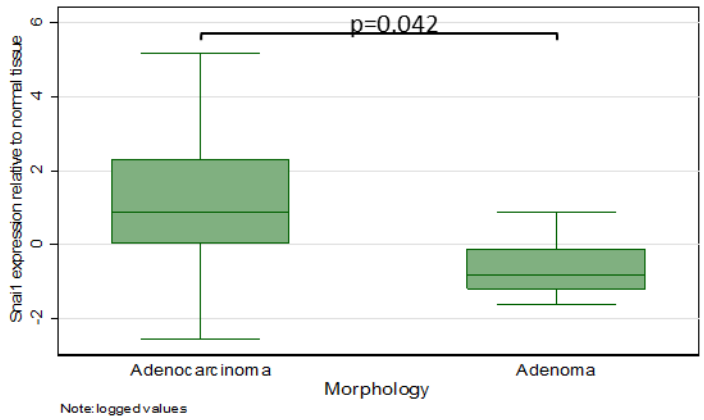

Figure 3.9 Expression of *SNAI1* is significantly lower in adenomas. Boxplot of *SNAI1* expression fold change values for adenomas and adenocarcinomas (n = 47). Linear regression analysis was conducted using log fold change values of *SNAI1* expression and tumour morphology (p = 0.034).

3.2.6 SNAIL and ISC markers expression in human colorectal cancer cell lines

To further study the expression profiles of *SNAIL* family members and intestinal stem cell markers in human colorectal tumours, CRC cell lines originating from different patients with diverse characteristics were chosen for analysis (Table 3.4). ddPCR analysis was carried out to determine the expression of these markers in a panel of 6 different primary CRC cell lines (Figure 3.10). Expression of *SNAI1* and *SNAI3* varied across these cell lines, however, *SNAI2* mRNA was only detected in SW480 cells. This is in contrast to primary CRC tissues, where *SNAI2* was the most abundantly expressed SNAIL family member, whereas, *SNAI1* and *SNAI3* were detected at relatively lower levels of expression (section 3.3.2). Overall in hCRC cell lines, there was approximately a 14-16-fold increase in average expression of *SNAI1* and *SNAI3* compared to *SNAI2*. LIM2405 expressed the highest level of *SNAI1* mRNA, whereas LIM1215 expressed high level of *SNAI3* mRNA. LIM1215 cells also expressed high levels of *LGR5*. *EPHB2* mRNA was detected in all but one cell line analysed. No *EPHB2* was detected in LIM2405.

BMI1 was expressed in all 6 cell lines. Marker expression data was analysed to determine correlation between *SNAIL* family members and ISC markers. No association between *SNAIL* family and ISC marker expression was observed across these cell lines. Notably, however, there was considerable variation within groups. The high variation within groups could be because the RNA used for each sample was isolated from cell lines at different passages which may have resulted in variation in expression levels of these markers.

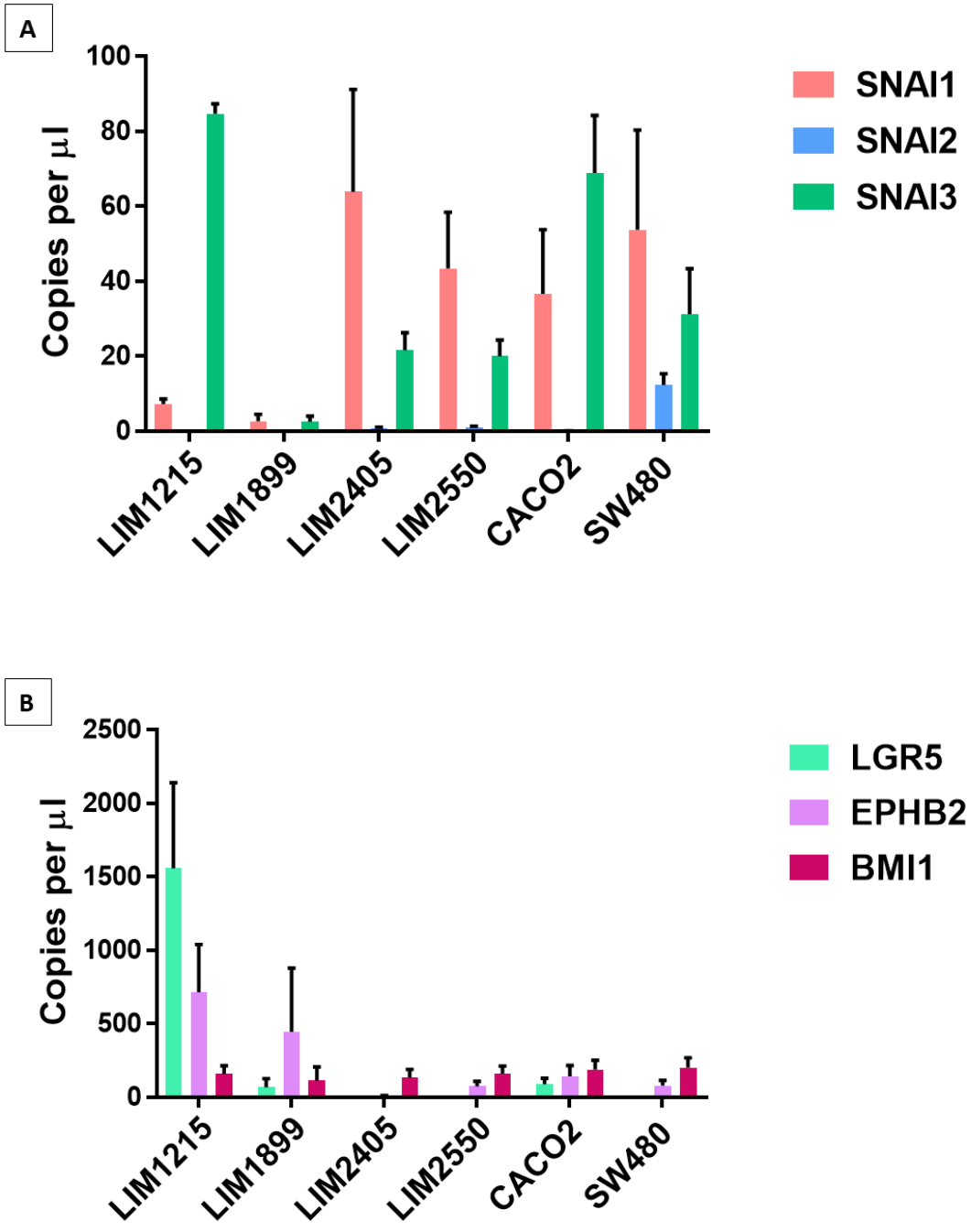

Figure 3.10 Expression of *SNAIL* family members and ISC markers varies across different human colorectal cancer cell lines. Marker expression was analysed in triplicates for each cell line. Data is represented as mean ± SEM.

3.2.7 Expression of *SNAIL* in human colorectal tumour organoid lines

Following analysis of markers in human CRC cell lines, expression of *SNAIL* was analysed in organoids generated from human colorectal tumour tissues collected from patients admitted for surgery at Cabrini Hospital. Colorectal tumour organoids prove advantageous in that they allow study of gene function *in vitro* without interference from the surrounding stromal tissue. Expression of *SNAIL* was analysed across a set of 13 tumour and one normal organoid line (Figure 3.11). While majority of these organoids did not express very high levels of *SNAI1*, only two organoid lines, ORG50T and ORG64T demonstrated clear SNAI1 up-regulation. While ORG53T and ORG73T expressed medium levels (expression values close to the overall average) of *SNAI1*, these were not chosen for further analysis as the *SNAI1* expression levels were still much lower than those detected in ORG50T and 64T. No obvious differences in organoid morphology or organoid growth rate were observed when comparing organoids expressing high levels of *SNAI1* versus those expressing relatively low levels.

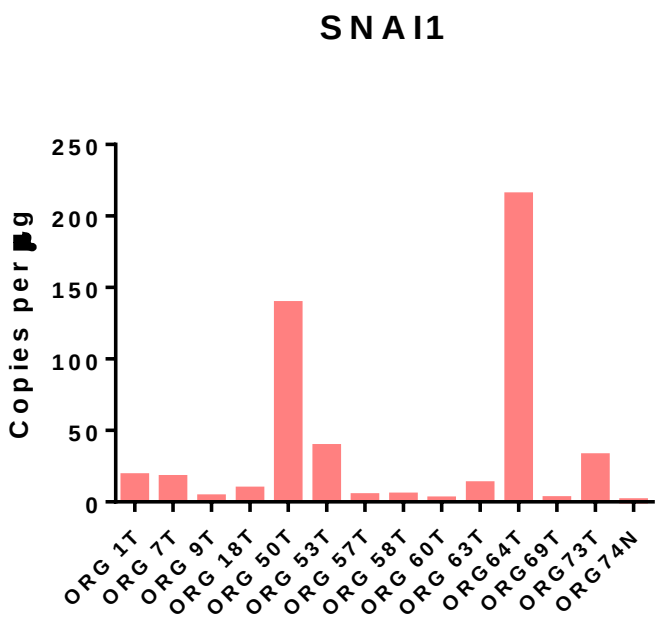

Figure 3.11 *SNAIL* expression is up-regulated in a subset of colorectal cancer organoid lines. *SNAI1* mRNA copy number was assessed by ddPCR in 13 tumour organoid lines and 1 normal colon organoid line.

3.2.8 Parnate assay

Human colorectal tumour organoids expressing high levels of *SNAI1* mRNA were treated with 100 µM Parnate, whereas normal and SNAI1^{low} organoids were used as controls. To assess any changes in cell viability post treatment with Parnate, PrestoBlue assay was carried out at 0, 12, 24 and 48 hours of treatment (Figure 3.12). There was a significant decrease in cell viability when ORG50T SNAI1^{high} organoids were treated with Parnate, while no difference in viability was observed for ORG64T SNAI1^{high} organoids. No effect on viability of SNAI1^{low} organoids (ORG58T and ORG63T only) was found, however, ORG57T SNAI1^{low} organoids viability decreased 24- and 48-hours post treatment with Parnate. Contrary to these results, viability of organoids generated from normal colorectal tissue (ORG74N) increased during treatment with Parnate and then declined when Parnate treatment was stopped. As the

effect on cell viability in these organoids was not related to expression of *SNAI1*, the changes in viability observed could be due to the cytotoxic effects of Parnate.

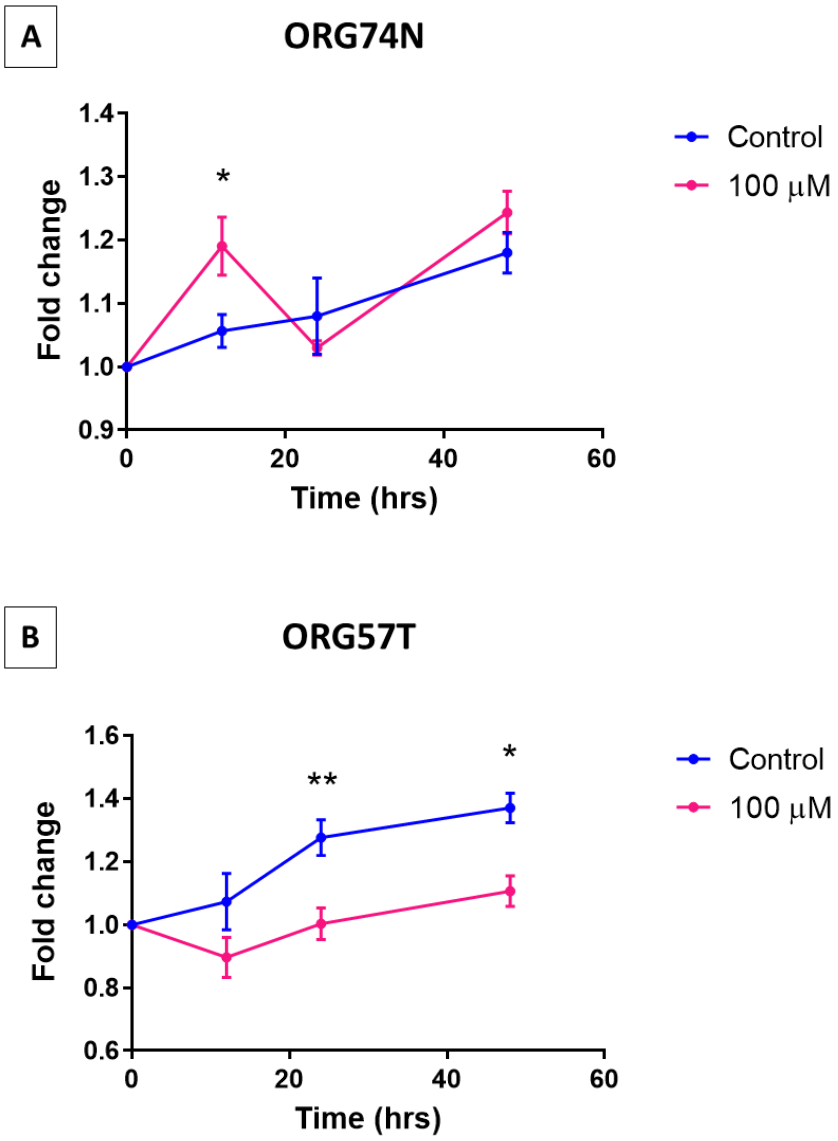

C

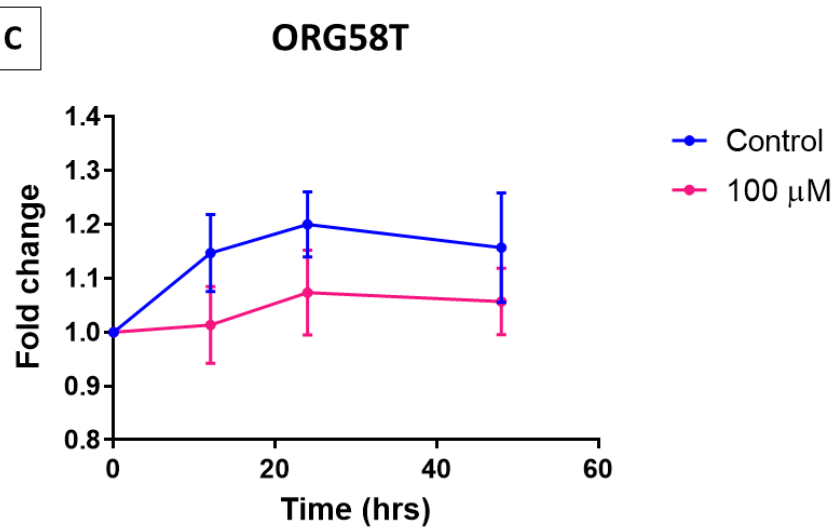
ORG58T
Fold change
1.4
1.3
1.2
1.1
1.0
0.9
0.8
0
20
40
60
Time (hrs)
Control
100 µM

D

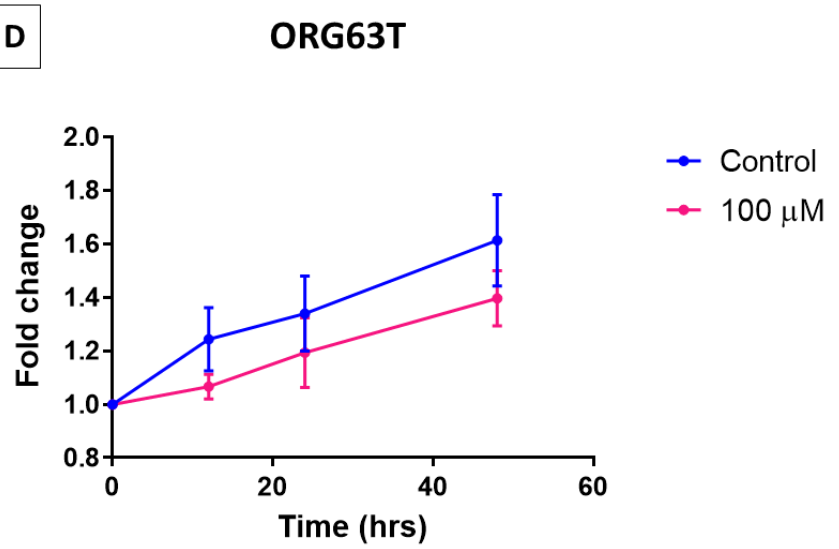
ORG63T
Fold change
2.0
1.8
1.6
1.4
1.2
1.0
0.8
0
20
40
60
Time (hrs)
Control
100 µM

E

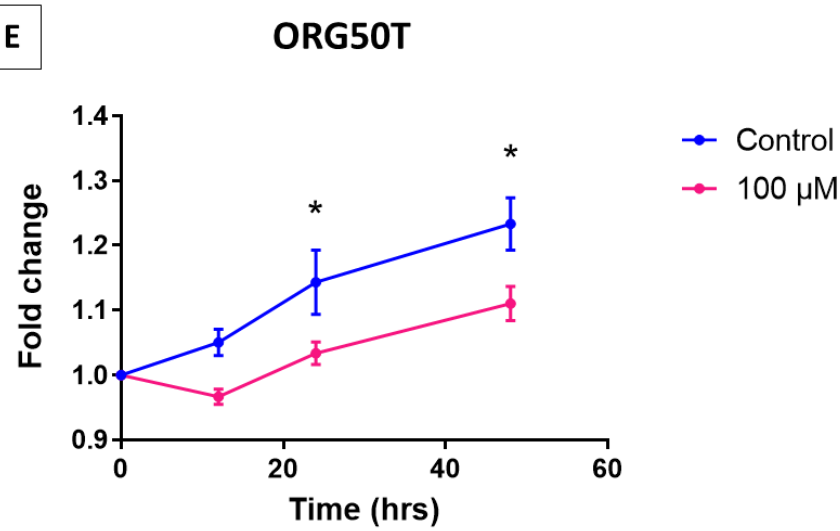
ORG50T
Fold change
1.4
1.3
1.2
1.1
1.0
0.9
*
*
0
20
40
60
Time (hrs)
Control
100 µM

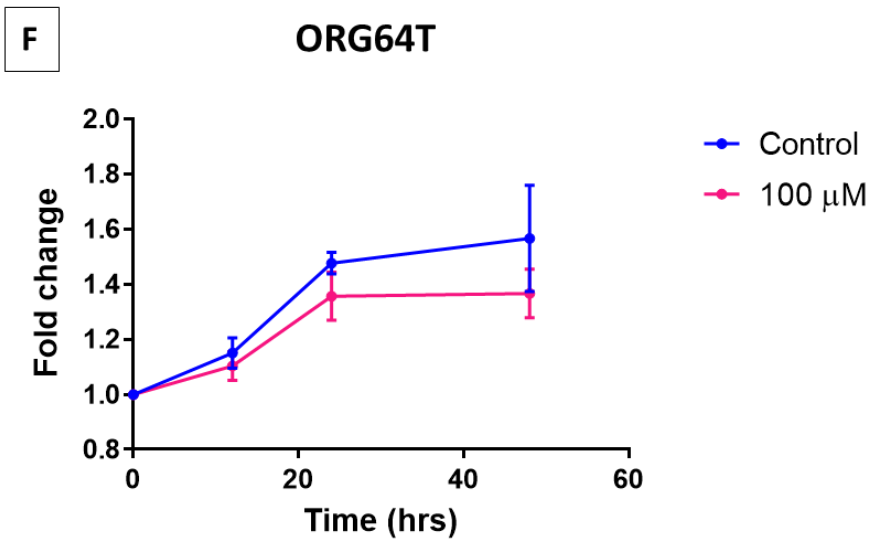

Figure 3.12 Assessment of cell viability by PrestoBlue assay in normal, SNAI1^{low} and SNAI1^{high} organoids post treatment with Parnate. Normal (A) ORG74N (p = 0.045), SNAI1^{low} organoids (B) ORG57T (p = 0.0087, 0.0115 resp.), (C) ORG58T (ns), (D) ORG63T (ns) and SNAI1^{high} (E) ORG50T (p = 0.0402, 0.0194 resp.) and (F) ORG64T (ns) were treated with Parnate for 12 hours with a final dose at 24 hours. Cell viability was measured by PrestoBlue assay at 0, 12, 24 and 48 hours of culture. Experiments were performed in triplicates (n = 3) for each organoid line. Data was analysed by two-way ANOVA (Sidak's multiple comparisons test) and is represented as mean ± SEM. ns = not significant.

One of the well-known functions of *SNAIL* genes is to repress transcription of epithelial marker genes. Following treatment of organoids with Parnate expression of various epithelial marker genes including *E-CADHERIN*, *OCCLUDIN*, *PLAKOGLOBIN* and *DESMOPLAKIN* was assessed by ddPCR as these genes are downstream targets of Snail-induced transcriptional repression (Figure 3.13). Expression of mesenchymal genes *N-CADHERIN* and *VIMENTIN* was also analysed, however, these genes were undetectable in these organoids. While all three organoid groups (normal, SNAI1^{low} and SNAI1^{high}) varied in degree of responsiveness to addition of Parnate, treatment with Parnate did not result in significant change in expression of epithelial marker genes in these organoid lines suggesting that the concentration of

Parnate used (although quite high for an inhibitor) may have been insufficient to cause blockade of SNAIL-induced transcriptional repression in these tumour organoid lines.

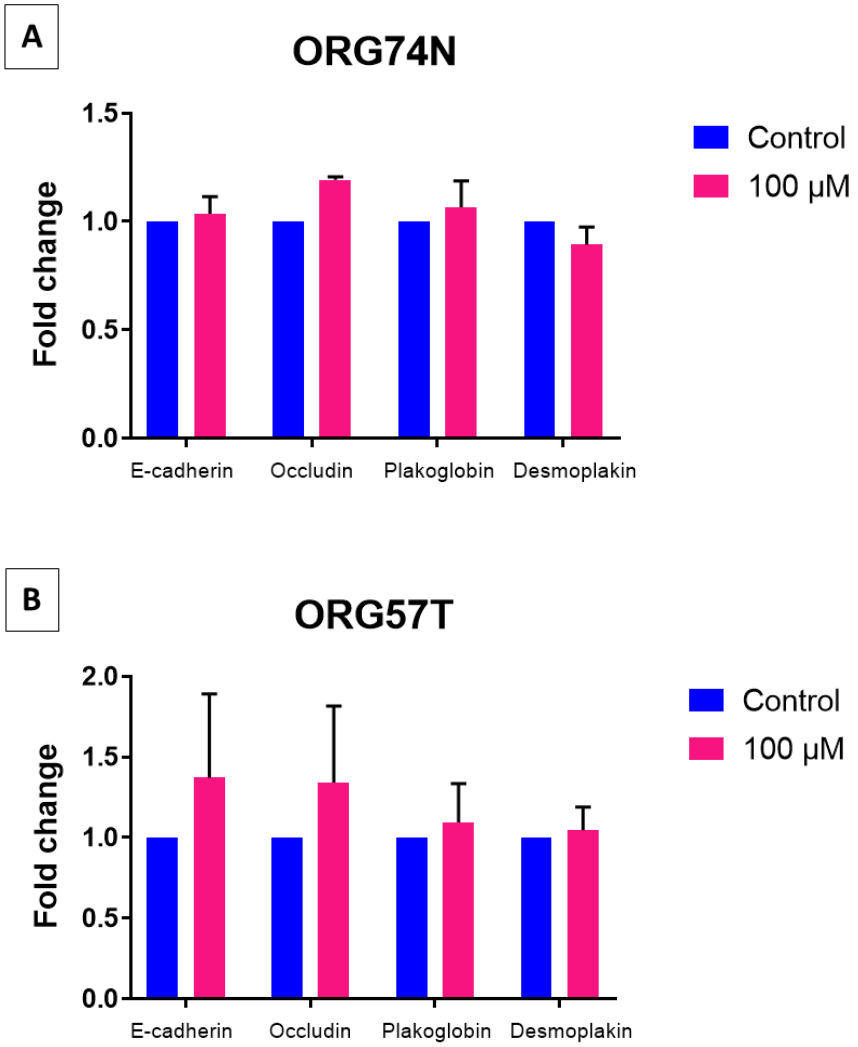

C

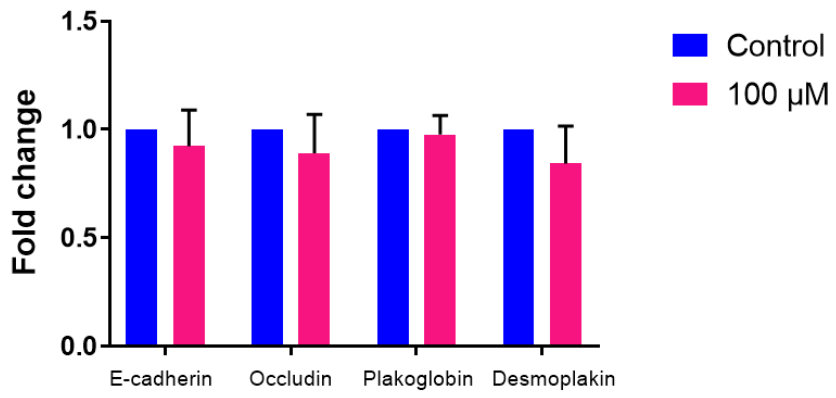
ORG58T
Fold change
1.5
1.0
0.5
0.0
E-cadherin
Occludin
Plakoglobin
Desmoplakin
Control
100 µM

D

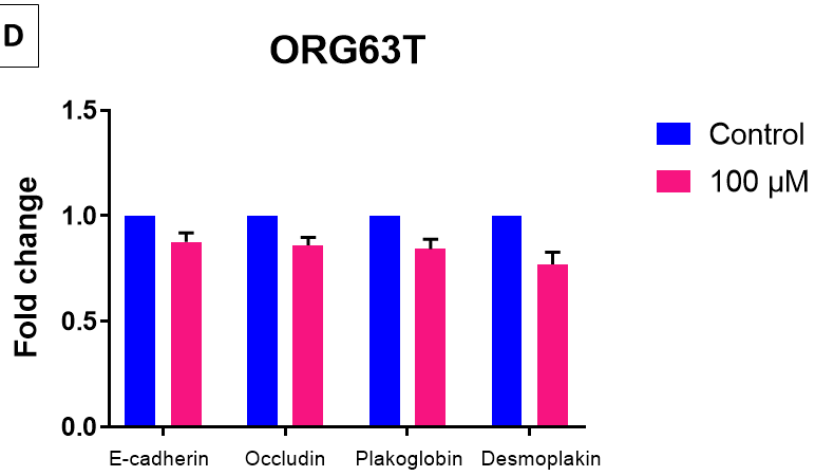
ORG63T
Fold change
1.5
1.0
0.5
0.0
E-cadherin
Occludin
Plakoglobin
Desmoplakin
Control
100 µM

E

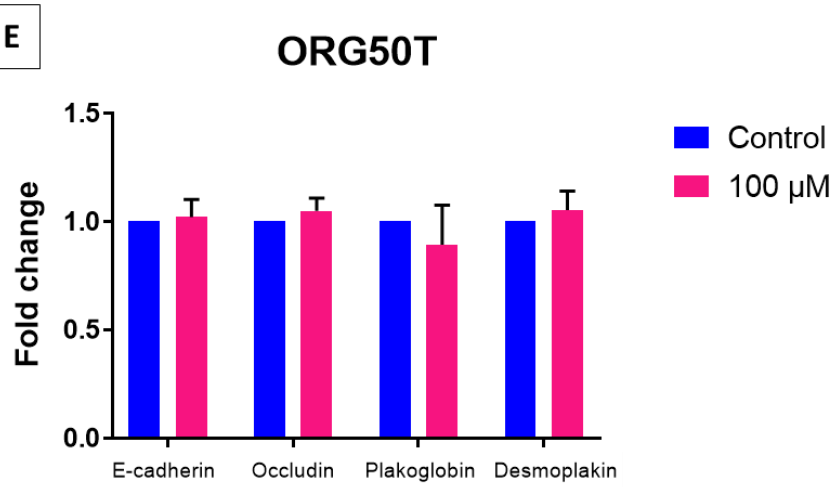
ORG50T
Fold change
1.5
1.0
0.5
0.0
E-cadherin
Occludin
Plakoglobin
Desmoplakin
Control
100 µM

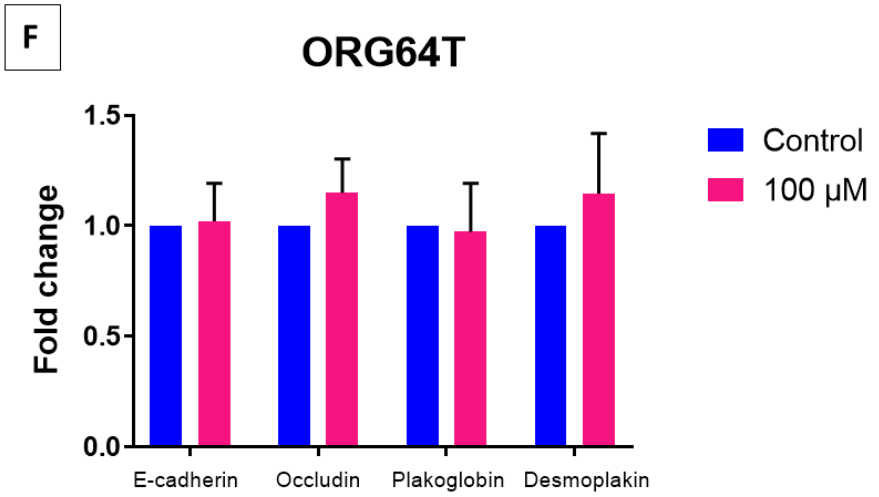

Figure 3.13 Expression of epithelial markers post treatment (12 hours) with Parnate in normal, SNAI1^{low} and SNAI1^{high} organoids. Normal (A) ORG74N, SNAI1^{low} organoids (B) ORG57T, (C) ORG58T, (D) ORG63T and SNAI1^{high} (E) ORG50T and (F) ORG64T were treated with Parnate for 12 hours and organoids were harvested for RNA at this point. Experiments were performed in triplicates (n = 3) for each organoid line. Data was analysed by paired t-test and is represented as mean ± SEM. Data was not significant.

3.2.9 The Cancer Genome Atlas data analysis

To compare these findings to a larger cohort of colorectal patients, data from the cBioPortal for Cancer Genomics was utilised. Data from the TCGA (Provisional) dataset with a sample size of 633 patients with colorectal adenocarcinoma was used. Of the 633 samples, 61.3% (388/633) were colorectal adenocarcinomas, 26.38% (167/633) were rectal adenocarcinomas, 10.43% (66/633) were mucinous adenocarcinoma of the colon and rectum and 1.9% (12/633) were colorectal adenocarcinomas. Figure 3.14 and Table 3.5 gives a summary of cases with altered *SNAI1, SNAI2* and *SNAI3* protein or mRNA expression in 629 sequenced cases. Of note, majority of the altered cases resulted in up-regulation of expression at the mRNA and protein levels. *SNAIL* family member genes were very rarely mutated.

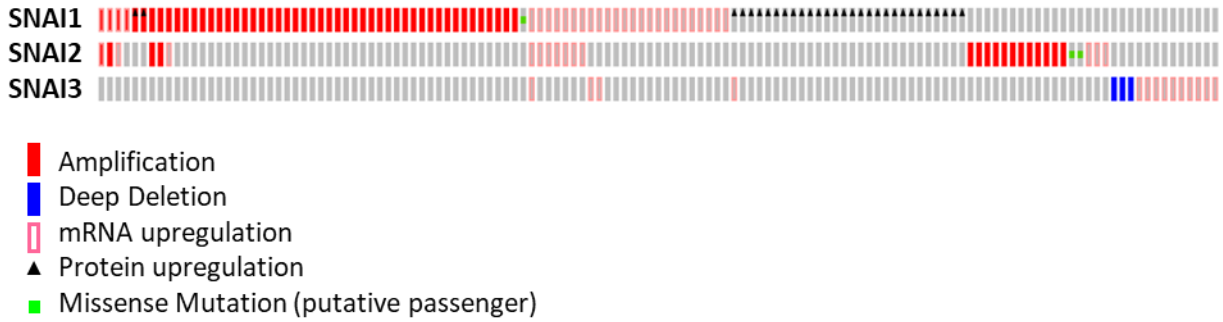

Figure 3.14 cBioPortal OncoPrint summary for *SNAI1*, *SNAI2* and *SNAI3* in the TCGA (Provisional) cohort. The OncoPrint is a graphical summary of genomic alterations for a gene across a set of tumour samples where each column represents a patient sample and rows represent genes. Of the 629 sequenced samples analysed for *SNAI1*, *SNAI2* and *SNAI3* genes, 21% of cases had at least one altered gene.

Table 3.5 Summary of patients with genetically altered *SNAI1*, *SNAI2* and *SNAI3*

Type of genetic alteration	SNAI1	SNAI2	SNAI3
Amplification	7.95%	2.54%	Nil
Deep deletion	Nil	Nil	0.48%
mRNA up-regulation	4.45%	2.06%	2.22%
Protein up-regulation	4.77%	Nil	Nil
Missense mutation	0.16%	0.32%	Nil
Total	16%	5%	2.7%

Intriguingly, the chances of occurrence of *SNAI1* alteration with altered *SNAI2* within the same tumour were highly probable (Table 3.6) indicating that alterations in one family member could lead to alterations in the other. While alterations in *SNAI1* and *SNAI3*, and *SNAI2* and *SNAI3* tended to co-occur, these associations were not statistically significant.

Table 3.6 Frequency of samples with co-altered *SNAIL* family genes

Gene A	Gene B	Neither	A not B	B not A	Both	Log odds ratio	Tendency	p-value
SNAI2	SNAI1	513	17	90	13	1.472	Co-occurrence	**<0.0001**
SNAI1	SNAI3	517	99	13	4	0.474	Co-occurrence	0.294
SNAI2	SNAI3	587	29	16	1	0.235	Co-occurrence	0.567

With respect to different CRC types, mucinous adenocarcinomas of the colon and rectum presented with majority of the alterations resulting in *SNAI1* and *SNAI3* mRNA/protein up-regulation whereas *SNAI2* mRNA up-regulation was observed mostly in colorectal adenocarcinomas (Figure 3.15). Genetic alterations resulting in amplification of *SNAI1* and *SNAI2* were mostly found in colorectal adenocarcinomas. Mutations in *SNAI1* and *SNAI2*, although rare, were mostly found in mucinous adenocarcinomas.

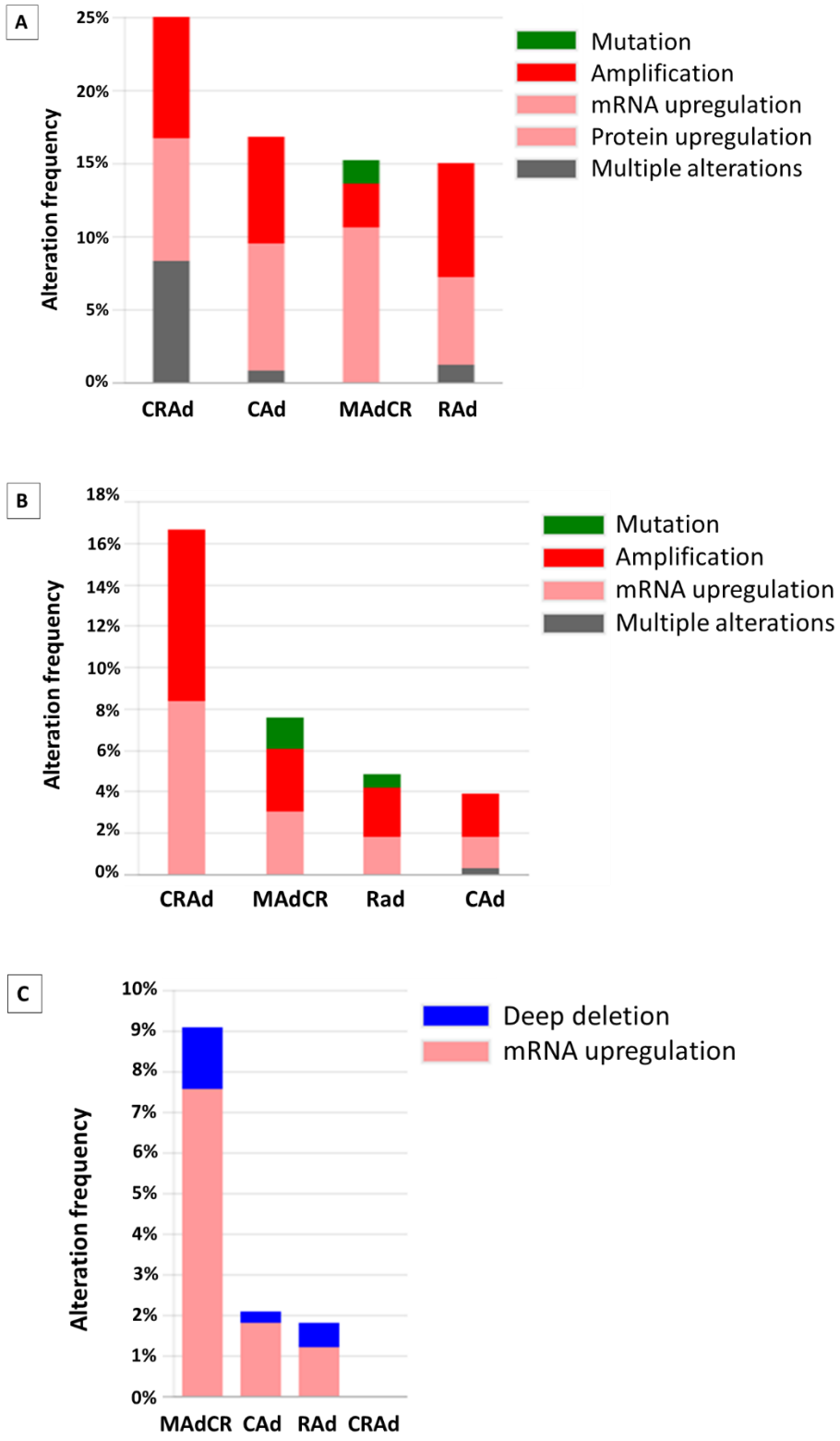

Figure 3.15 cBioPortal data analysis of frequencies of different genetic alterations of (A) *SNAI1*, (B) *SNAI2* and (C) *SNAI3* across CRCs of different origin. CRAd = colorectal adenocarcinoma, CAd = colon adenocarcinoma, MAdCR = mucinous adenocarcinoma of the colon and rectum, RAd = rectal adenocarcinoma.

Comparing overall survival of these 130 (21%) patients with and without genetic alterations in *SNAI1*, *SNAI2* and *SNAI3*, patients with alterations died much sooner with a median survival of 49.38 months as compared to 83.18 months for the cohort with no genetically altered *SNAIL* family members (Figure 3.16 and Table 3.7). No significant difference in disease/progression-free survival between patients with altered (84.23 months) versus unaltered (78.65 months) *SNAIL* family genes was observed.

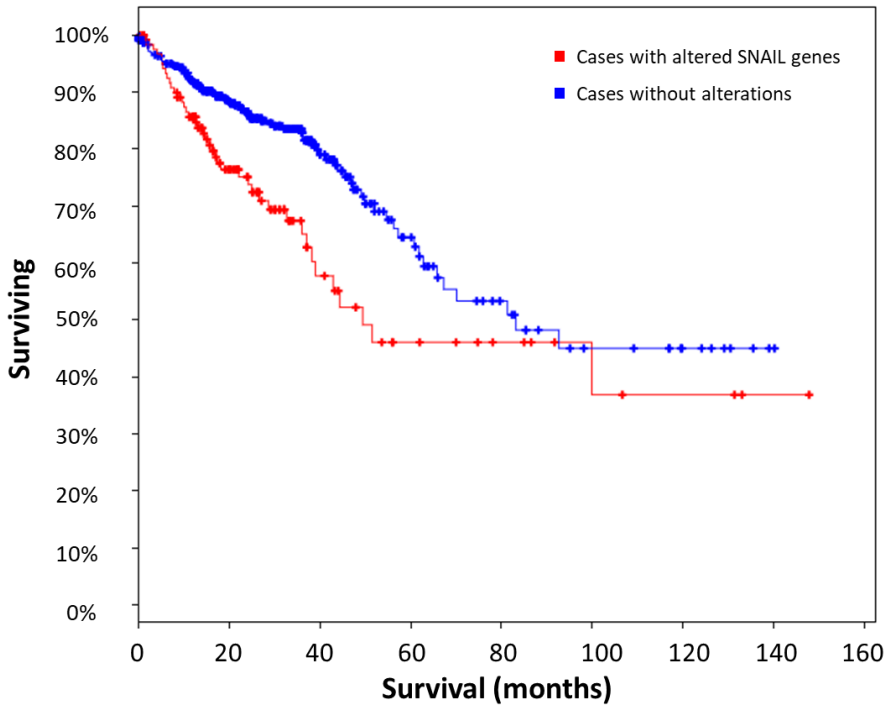

Figure 3.16 Overall survival Kaplan-Meier estimate. Patients with genetically altered *SNAIL* genes demonstrated significantly shorter overall survival (p=0.00210).

Table 3.7 Overall survival of CRC patients

	Total number of cases	Number of deceased cases	Median survival (months)
Cases with alterations	130	41	49.38
Cases without alterations	489	88	83.18

As EMT is an important process during cancer progression, mRNA expression of *SNAI1* was compared to other EMT molecules including *ZEB1* and *TWIST* using data available on the cBioPortal (n = 629). Of note, the cBioPortal only provides the correlation coefficient data when the test values are greater than 0.3 and does not indicate whether the association is significant or not. mRNA expression data for *SNAI1* and *ZEB1* was also analysed for correlation in the Cabrini patient cohort (n=63) (Table 3.8). Overall, the expression of *SNAI1* was found to correlate with these EMT markers both in the TCGA cohort as well as in the Cabrini cohort of colorectal tumours.

Table 3.8 Correlation between *SNAI1* and other EMT molecules

Gene 1	Gene 2	Pearson correlation coefficient	Spearman rank correlation coefficient
cBioportal (n = 629)			
SNAI1	ZEB1	0.40	0.44
SNAI1	ZEB2	0.45	0.45
SNAI1	TWIST1	0.45	0.54
SNAI1	TWIST2	0.53	0.54
Cabrini (n = 63)			
SNAI1	ZEB1	0.37 ($p<0.01$)	0.72 ($p<0.0001$)

3.3 Discussion

3.3.1 Intestinal stem cell markers are up-regulated in colorectal cancer

Numerous studies over the years have confirmed the up-regulation of stem cell markers in colorectal cancer (Lugli et al., 2005, Merlos-Suarez et al., 2011, Uchida et al., 2010, Jarde et al., 2015). Uchida *et al*. analysed the expression of LGR5 in 50 stage II/III colorectal tumours and found there was a 3-fold increase in LGR5 expression in 70% of these tumours as compared to matched normal mucosal tissues. Histological analysis of LGR5 mRNA in tumour sections revealed LGR5 staining diffused throughout the tumour with detection of LGR5 mRNA at the invasive front of tumours also while no signal was detected in the adjoining stromal compartment. Moreover, up-regulation of LGR5 was reported in 100% of human CRC cell lines (n = 4) derived from metastatic tumours (Uchida et al., 2010). A previous study done in our laboratory demonstrated up-regulation of intestinal stem cell markers LGR5, EPHB2 and CD44 in a cohort of 50 colorectal tumours (Jarde et al., 2015). The current study concurs with the previous findings as the expression of ISC markers *LGR5*, *EPHB2* and *BMI1* was significantly higher in colorectal tumours when compared to adjacent normal tissue. This could be occurring as a result of hyper-activation of WNT signalling in these tumours which leads to subsequent up-regulation of downstream targets of WNT including *LGR5*, *EPHB2* and *CD44*. Moreover, colorectal cancer patients with tumours enriched for the ISC gene signature have been found to be more prone to relapse compared to patients expressing low levels of ISC marker genes (Merlos-Suarez et al., 2011).

3.3.2 *SNAI1* is up-regulated in CRC and its expression correlates with ISC markers

SNAIL proteins are up-regulated in a number of human cancers. Of the three SNAIL family members, SNAI1 or SNAIL in particular has been implicated in the progression of tumours and cancer metastasis. Apart from its role as a key EMT regulator in cancer metastasis, SNAI1 expression in tumours has been associated with a poor clinical outcome and a more aggressive phenotype in malignancies such as breast (van Nes et al., 2012) and gastric cancers (Shin et al., 2012). Up-regulation of SNAI1 in SW480 human CRC cell line has been shown to induce expression of ISC marker CD44 (Hwang et al., 2011). In this study, *SNAI1* was found to be up-regulated in the majority of colorectal tumours and human CRC cell lines. This is in accordance with previous studies in human cancers including colorectal cancer (Roy et al., 2005). Expression of *SNAI2*, on the other hand, was not up-regulated in most tumours and was not detected in 5 of the 6 human CRC cell lines analysed in this study. This could possibly be due to the fact that Snai2 is not expressed in the intestinal epithelium, rather Snai2 expression has been shown to be limited to the mesenchyme in mice (Horvay et al., 2015). This indicates that the current cohort (Cabrini) of colorectal tumours quite possibly consists of a large proportion of mesenchymal tissue and is not purely epithelial. qPCR/ddPCR analysis of epithelial and mesenchymal markers in these tumours could give more insight into the nature of tumour tissues. Furthermore, these studies could be extended to immunostaining of tissue sections to establish if SNAIL family members are restricted to epithelial or mesenchymal cell compartments. This was not possible in this study due to a lack of reliable antibodies to analyse expression in human tissue.

Expression of SNAI1 has been shown to induce cancer stem cell-like properties in mammary epithelial cells (Mani et al., 2008). SNAIL proteins have previously been reported to contribute

to expansion and survival of stem cells of skin in mice (De Craene et al., 2014). To investigate any association between *SNAIL* family members and ISC markers in colorectal tumours, mRNA expression data was analysed for any correlation between these two groups. Interestingly, expression of *SNAIL* family members correlated with ISC markers expression in these tumours. This implies that tumours with up-regulation of *SNAIL* family members also overexpressed ISC marker genes. This suggests that SNAIL could possibly play a role in regulation and/or maintenance of cancer stem cells in colorectal tumours. It is interesting to note that although *SNAI2* and *SNAI3* were up-regulated in a small sub-set of tumours, these tumours also overexpressed the ISC marker genes suggesting that these molecules may be playing a similar role as SNAI1 in these tumours. It remains unclear whether SNAI1 and ISC markers are co-localised within tumours. Due to lack of specific antibodies against SNAI1 (numerous anti-SNAI1 antibodies were tested), expression of SNAI1 could not be examined in tumour tissue sections. Dual RNA in situ hybridisation/immunohistochemistry for SNAI1/LGR5 or SNAI1/EPHB2 is one alternative which could help us identify the subsets of cells expressing these markers. It would be interesting to see whether SNAIL family members co-localise with CSC markers in colorectal tumours.

3.3.3 Early stages of colorectal tumour formation are associated with higher levels of SNAI1 and SNAI2 mRNA

As mentioned earlier in this chapter, the colorectal tumours are staged based on the TNM staging system by AJCC. The TNM staging system groups tumours based on depth of invasion into the bowel wall (T- stage), extent of regional lymph node involvement (N- stage) and presence of metastatic tumours (M- stage). SNAIL family members are key regulators of EMT that have been implicated in cancer metastasis, which suggests that these proteins are likely

to play a role in advanced stages of tumourigenesis. To verify this, expression of SNAIL family members (fold change versus normal tissue) was analysed for any association with TNM stages of colorectal tumours in the current patient cohort. Surprisingly, expression of SNAI1 was significantly higher in T-stage 2 and 3 tumours compared to T0 tumours whereas SNAI2 was up-regulated in T-stage 3 tumours. This finding suggests a role of SNAIL in earlier stages of tumour development and not just advanced stages as has been believed so far. In T-stage 2 and 3 tumours, tumour cells invade the muscularis propria and subserosal layers of the gut. On comparing expression of SNAI1 and SNAI2 in stage T2 versus T3, both SNAI1 and SNAI2 were expressed at relatively higher levels at T2 than T3. It may be possible that SNAIL is a critical regulator of stem cell maintenance, and via this mechanism, SNAI1 allows stem cell-mediated tumour development and invasion of tumour cells into the deeper layers of the intestinal wall. Although there is evidence which supports the idea that SNAI1 is involved in cancer progression *in vitro*, not much is known about the contribution of *Snai1* towards early onset of tumours *in vivo*. In the context of breast cancer, functions of endogenously encoded *Snai1* and *Snai2* have been studied using knock-in IRES-YFP reporters for *Snai1* and *Snai2* (Ye et al., 2015). Ye *et al.* utilised a transgenic mouse model which mimics the human mammary tumour progression in mice and found that Snai1-YFP expression was present in early-stage lesions whereas the relative proportion of Snai2-YFP+ cells was significantly lower in these lesions compared to normal tissue. Using a mouse model (K14-Snai1) with skin-specific expression of an HA-tagged SNAI1 protein (tagged to distinguish the transgene from endogenous Snai1), De Craene *et al*. demonstrated that ectopic expression of *Snai1* is sufficient to induce formation of spontaneous skin tumours in mice (De Craene et al., 2014).

These studies along with ours suggest that SNAI1 plays a role in the early stages of tumourigenesis.

3.3.4 Difficulties in interpreting data observed in human CRC cell lines

My results observed in human colorectal cancer cell lines suggest that these hCRC cell lines are not a good model for investigating gene function in the context of cancer as these cells have been maintained in culture over several years and are likely to have lost the heterogeneity observed in primary colorectal tumours. Moreover, cell cultures are a 2D system, thus, not a true representation of the tumours which is why a 3D model – colorectal tumour organoids – was employed to study SNAIL function in colorectal tumours *in vitro*.

3.3.5 Treating SNAI1^{high} colorectal tumour organoids with Parnate results in reduced viability

As it has now been confirmed that SNAI1 is up-regulated in CRC, effects of inhibiting SNAI1-induced transcriptional repression were assessed *in vitro* using human colorectal tumours organoids. Parnate is a known inhibitor of the enzyme lysine-specific demethylase 1, also known as LSD1. Studies involving knock-down of LSD1 have reported that loss of LSD1 expression results in a decrease in growth of cancer cells as well as their invasion and migratory potential (Lv et al., 2012). Moreover, interaction of SNAIL/SLUG and LSD1 is required for SNAIL/SLUG-mediated transcription of downstream target genes. Treatment of human CRC cells with Parnate has previously been shown to result in inhibition of Slug-dependent transcriptional repression of EMT markers like E-cadherin and blocks the migration and invasion of these tumour cells *in vitro* (Ferrari-Amorotti et al., 2013). In the current study, treatment of human colorectal tumour organoids expressing both high and low

levels of SNAI1 with 100 µM Parnate resulted in reduction in cell viability suggesting that this decrease in viability is independent of SNAIL. Reduction in viability of organoids could be due to the cytotoxic effects of Parnate. Comparing expression of epithelial markers genes in organoids post treatment with Parnate, no significant differences were observed. One possible explanation for this could be that Parnate, although an irreversible inhibitor of LSD1, is not LSD1-specific. Structurally, the catalytic sites of LSD1 resemble those of the monoamine oxidase (MAO) class of enzymes, as a result Parnate also inhibits MAO-A and MAO-B enzymes (Schmidt and McCafferty, 2007). Furthermore, the concentration of Parnate used in the current study was chosen based on that used in a previous article where treatment of HCT116 and Colo205 human CRC cells with 100 µM Parnate resulted in increased expression of *E-CADHERIN*, *OCCLUDIN* and *DESMOPLAKIN* (Ferrari-Amorotti et al., 2013). An inhibitor concentration of 100 µM is very high for cells *in vitro* which explains the loss of viability in these organoids following treatment with Parnate. Moreover, the sample number (SNAI1^{high} and normal organoids) in the current study was very small and more organoid lines need to be tested to confirm these results. The current results show no evidence that Parnate treatment blocked SNAIL function within colorectal organoids so the function of SNAIL in regulating colonic organoid growth is yet to be determined.

To study consequences of blockade of SNAI1-induced transcription *in vitro*, more potent selective inhibitors of LSD1 can be utilised. GSK2879552 is one such molecule which irreversibly targets LSD1. The IC50 (concentration of an inhibitor at which the response is reduced to half) for Parnate is 950 nM whereas IC50 for GSK2879552 is 16 nM which is approximately a 60-fold decrease in concentration compared to Parnate. Very weak inhibitory effect of GSK2879552 has been reported for MAO-A and MAO-B. The anti-tumour activity

associated with GSK2879552-mediated catalytic inhibition of LSD1 has been examined in a range of cancer cell types (Mohammad et al., 2015). Treatment of small cell lung carcinoma (SCLC) cells with 1 µM GSK2879552 resulted in growth inhibition *in vitro*. However, expression of Snail downstream targets was not analysed in this study. As tumour organoids serve as an excellent model for *in vitro* study of gene function, other alternative approaches for studying LSD1/Snail-mediated transcriptional repression like RNA interference and CRISPR could be employed.

3.3.6 Analysis of gene expression data using the cBioPortal

The majority of the genetic alterations observed in the TCGA cohort of colorectal tumours (n = 633) resulted in either amplification or up-regulation of mRNA/protein of SNAIL family members. This suggests that colorectal tumours are more likely to overexpress *SNAIL* family genes rather than result in down regulation of *SNAIL* genes. This is in agreement with previous studies which have reported *SNAIL* up-regulation in colorectal cancer (Roy et al., 2005). A tissue array of 59 colorectal tumours of different stages and location was pathologically examined using antibodies against SNAI1 (production of these antibodies has been discontinued by Santa Cruz Biotechnology). The majority of these tumours (78%) were found to over-express SNAI1. Moreover, an increase in the proportion of SNAI1-positive tumours was reported among stage III (15/23) and IV (6/6) tumours (Roy et al., 2005). This reinstates the notion that SNAIL plays a role in cancer metastasis. The expression of SNAI1 has previously been associated with increased risk of tumour relapse and poor survival in patients with mammary tumours (Moody et al., 2005).

In the TCGA study, the median overall survival of patients with genetically altered *SNAIL* family members was significantly lower compared to patients with wildtype *SNAIL*. In addition the frequency of different alterations in *SNAIL* family members was analysed in different CRC types. Mucinous adenocarcinomas presented with the highest frequency of *SNAI1* alterations resulting in mRNA/protein up-regulation. Mucinous adenocarcinomas account for about 10-15% of all CRCs and are associated with poor drug response compared to adenocarcinomas and are quite often diagnosed at advanced stages (Hugen et al., 2016). Further investigation revealed that the majority of all alterations resulting in gain in copy number (87%) and very high amplification (87.5%) of SNAI1 occurred in stage T2 and T3 tumours. Similar observations were made for SNAI2 where stage T2 and T3 tumours presented with the majority of amplification (80%) and gain in copy number (87%) alterations. Although this is copy number data and not mRNA expression, these findings share a pattern similar to what was observed in the Cabrini cohort where SNAI1 and SNAI2 (mRNA expression) were significantly higher in stage T2 (SNAI1 only) and T3 (SNAI2 and SNAI2) tumours. Furthermore, alterations in *SNAI1* and *SNAI2* tend to co-occur. This reinforces the idea that *SNAIL* family members play a crucial role in earlier stages of colorectal tumourigenesis. Moreover, patients with alterations were associated with poor survival with a median survival of 49.38 months compared to 83.18 months for the latter. SNAIL-induced EMT has been shown to lead to transcriptional repression of epithelial marker E-cadherin in tumours and is considered to be an indicator of poor clinical outcome and associated with a more aggressive tumour phenotype in several malignancies like gastric cancers (Shin et al., 2012), oesophageal squamous cell carcinoma (Kuo et al., 2012), and mammary cancers (van Nes et al., 2012). Additionally, expression of Snai1 in a skin-specific p53-null background results in enhanced tumourigenesis and more

aggressive carcinosarcomas which metastasise to the lungs (De Craene et al., 2014). These studies add further confirmation to the notion that *SNAIL* genes play a critical role in induction of invasive characteristics in tumours.

Taken together, results in this chapter suggest that SNAI1 may be contributing to progression of colorectal tumours during early stages of tumour development and could possibly play a role in regulation of cancer stem cells in CRC. Further investigation into the function of SNAIL in regulation of CSCs is essential. Co-localisation studies examining expression of SNAIL and CSC markers like LGR5 in tumour sections would help identify the subsets of cell populations expressing these markers and reveal whether SNAIL is expressed in CSCs. Analysis of CSCs isolated from tumours for enrichment of *SNAIL* genes would give us an insight into the role of SNAIL in the regulation and maintenance of these cells.

3.3.7 Chapter Conclusion

The data in this chapter confirms up-regulation of *SNAI1* and its association with expression of intestinal stem cell markers and tumour stage in colorectal cancer. Results from this study and cBioPortal data analysis confirm a critical role of *SNAI1* in earlier stages of tumour progression. Further analysis is required to understand the role of *SNAIL* in regulation and maintenance of CSCs. Additional studies examining the role of *SNAI1* in colorectal tumours using *in vitro* organoid cultures are required.

Chapter 4 – Effects of *Snai1* up-regulation in mouse colonic epithelium and *in vitro* organoid cultures

Chapter 4 – Effects of *Snai1* up-regulation in mouse colonic epithelium and *in vitro* organoid cultures

4.1 Introduction

4.1.1 Background

As discussed previously in Chapter 3, *SNAI1* was found to be the only family member significantly up-regulated in a cohort of human colorectal cancers compared to normal tissue and patients with mutated *SNAIL* genes are associated with poor survival. However, the consequences of *SNAIL* up-regulation are not well understood.

Apart from having key roles in normal development, aberrant expression of *Snail* in tissues has been shown to contribute to tumour formation and induction of stem cell properties in non-stem cells. Numerous studies have established a link between *Snail* expression and stem cell-like phenotype. Studies in mammary cells expressing elevated levels of *Snail* family members have shown to result in acquisition of stem cell properties by these cells (Guo et al., 2012, Mani et al., 2008). In regard to tumourigenesis, ectopic expression of *Snai1* in the epidermis has been shown to cause epidermal hyperproliferation and induction of spontaneous tumours in the skin (De Craene et al., 2014). Although SNAI1 is absent in normal mammary epithelial cells, its expression has been shown to be tightly associated with a tumour-initiating cell phenotype in breast cancer (Ye et al., 2015).

In normal mouse small intestine, SNAI1 has been found to co-localise with the intestinal stem cell (ISC) marker gene *Lgr5* in the crypt base columnar (CBC) stem cells (Horvay et al., 2011).

Studies in our laboratory suggest that loss of *Snai1* in the mouse intestinal epithelium results in a decrease in epithelial cell proliferation, loss of CBC stem cells and an inability to form *in vitro* organoids in culture. In contrast, an opposite effect was seen when *Snai1* expression was up-regulated in the small intestine which resulted in expansion of the CBC stem cell pool (Horvay et al., 2015). This suggests that *Snai1* plays a role in maintenance of the ISC population and regulation of proliferation. It should be noted here that these studies investigated the role of *Snai1* in the small intestine and these results cannot necessarily be extrapolated to the colon. The small intestine and colon differ in numerous ways including tissue morphology, cellular composition and stem cell dynamics. It is essential to expand our understanding about the function of *Snai1* in normal colonic tissue as colon is the site of origin of tumours in humans while tumours in the small intestine are rare.

In order to model the up-regulation of *SNAI1* expression observed in colorectal tumours, we decided to examine the consequences of *Snai1* over-expression in normal mouse colonic epithelia. Two different experimental approaches were followed. First, an inducible mouse model, which allows tamoxifen-dependent Cre-mediated expression of the *Snai1* transgene (RosaSnai1) in the colonic epithelia *in vivo*, was utilised (Figure 4.1). The *RosaSnai1* mice were generated by Nyabi and colleagues by insertion of the Snai1 cDNA-IRES-eGFP sequence, downstream of a floxed PGK-neo-STOP cassette, into the Rosa26 locus (Nyabi et al., 2009).

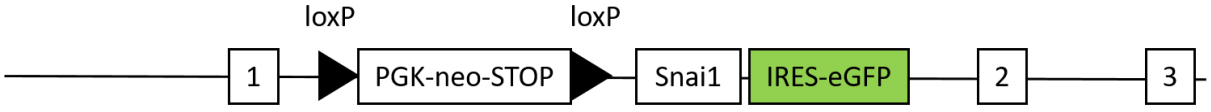

Figure 4.1 Schematic representation of the *RosaSnai1* construct.

Two intestinal tissue-specific inducible Cre promoters were used, namely *VillinCreERT2* and *Cdx2CreERT2*. Schematic diagrams of the constructs are given in Figure 4.2 and 4.3 respectively and a detailed description of the transgenes is given in sections 1.4.2.1 and 1.4.2.5 respectively (Chapter 1).

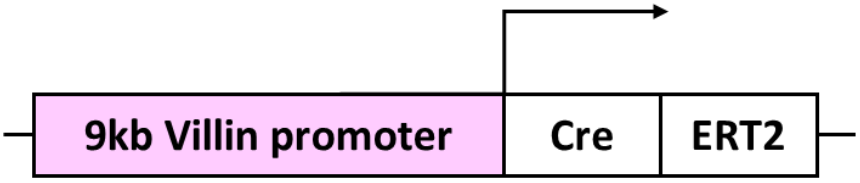

Figure 4.2 Schematic representation of the *VillinCreERT2* construct.

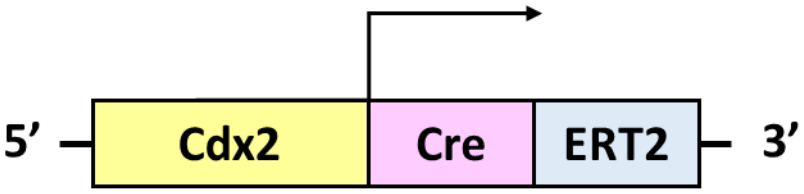

Figure 4.3 Schematic representation of the *Cdx2CreERT2* construct.

The second was an *in vitro* approach, where *Snai1* over-expression was induced in mouse colonic organoids using a cell-permeant TAT-Cre recombinase. The eGFP sequence in the *RosaSnai1* construct allows tracing of the Snai1^{+} cells detected by GFP expression in both *in vivo* and *in vitro* systems.

4.1.2 Mouse intestinal organoids

Cre recombinase has been widely utilised to genetically manipulate DNA *in vivo*, however, one of the most commonly encountered problems with using an *in vivo* system is the inconsistent expression of the active enzyme in mammalian cells. Sato *et al.* established an intestinal epithelial organoid culture system where single Lgr5^{+} cells were able to give rise to

self-organising structures which essentially recapitulate all the aspects of a self-renewing epithelium (Sato et al., 2009). Intestinal organoid cultures present with a unique opportunity to study gene function in an efficient manner. One of the ways we can alter gene expression in this system is by using a cell permeable Cre recombinase enzyme known as TAT-Cre which mediates excision of floxed DNA sequences resulting in transgene expression in cells *in vitro*. Organoids are a good model for inducing efficient gene recombination in culture and studying gene function in the intestinal stem cell compartment.

4.1.3 Significance of this study

Previous studies have investigated the role of *Snai1* in the small intestine, however, these results cannot be applied to the colon due to morphological and cellular differences. In addition, we have observed that *SNAI1* levels are up-regulated in Stage 2 colorectal tumours compared to stage 0 (Chapter 3), which suggests a role for SNAI1 in driving early carcinogenesis. The consequences of SNAI1 up-regulation in supporting colorectal tumour initiation and growth as well as its interplay with the stem cell compartment are not clearly understood. For these reasons, the current study examines the effects of ectopic expression of *Snai1* in the normal colonic epithelia in order to define whether *Snai1* is sufficient to drive aberrant proliferation and initiates tumour formation. Using both *in vivo* and *in vitro* approaches will provide a deeper understanding of the downstream effects of *Snai1* up-regulation which will further expand our understanding about its functional role and association with stem cells in colorectal cancer.

4.1.4 Hypothesis

This chapter investigates the hypothesis that *Snai1* up-regulation in the colon alters morphology of the epithelium by affecting the stem cell population and cellular proliferation.

4.2 Results

4.2.1 Tamoxifen induced Cre mediated recombination using the Villin promoter targets the small intestine rather than colon in mice

Previously, Marjou *et al*. have combined the Cre recombination system with the intestinal tissue specificity of the murine Villin promoter in *VillinCreERT2* mice, a tamoxifen-dependent recombinase model (el Marjou et al., 2004) which allows spatial and temporal control of Cre recombinase activity. Using this model, efficient Cre activity was reported in the small intestine and colon (el Marjou et al., 2004).

In order to investigate the effects of Snai1 up-regulation, the *VillinCreERT2* mice were crossed with the *RosaSnai1* mice. *RosaSnai1* mice carry a construct containing a PGK-neo-STOP cassette flanked by two loxP sites in front of a Snai1 cassette inserted into the Rosa26 locus. The expression of *Snai1* is dependent on tamoxifen induced Cre-mediated excision of the floxed STOP cassette. Details of the *RosaSnai1* and *VillinCreERT2* mouse models along with schematic representations of the construct have previously been discussed in Chapter 1 (Section 1.4.4.2 and 1.4.2.1 respectively).

We have previously used the Villin promoter in our laboratory to induce up-regulation of *Snai1* in the small intestine (Horvay et al., 2015). To confirm the activity of tamoxifen in up-regulating *Snai1* expression in induced animals, I first examined the expression of *Snai1* in small intestinal tissue from *VillinCreERT2 RosaSnai1* mice compared to *VillinCreERT2* controls following 4 daily tamoxifen injections (Figure 4.4). Indeed, the expression level of *Snai1* was effectively up-regulated (32 to 102-fold increase) as expected and previously reported. However, there was no difference in the level of *Snai1* transgene expression in the colonic

epithelium between the control and the test group on day 5 post induction with tamoxifen (Figure 4.4). As a result, I decided to examine colonic tissues at a later time-point – day 10 post induction as cell turnover in the colon is slower. Although a colonic up-regulation (4-fold increase) of *Snai1* expression in the test group was observed at day 10 compared to controls (Figure 4.5), this was much lower than that observed in the small intestinal tissues at day 5. While the average level of *Snai1* expression in the small intestine was 150 copies/µg at day 5, this value was much lower in the colon (19 copies/µg) even at day 10. In other words, the expression of *Snai1* in the test colonic tissues was very low and not representative of the level of expression observed in colorectal cancer samples. It is likely that the level of expression is not sufficient to produce any phenotypic changes in the epithelium. The lack of induction of *Snai1* in the colon could be due to insufficient Cre-mediated recombination. In order to examine the pattern of Cre activity in the colon, *VillinCreERT2* mice were crossed with *Rosa26LacZ* reporter mice. Induction with tamoxifen resulted in expression of β-galactosidase (β-gal) in the recombined epithelial cells and was used as indicator of recombination efficiency. Analysis of β-gal expression revealed staining in a small number of cells throughout the colonic epithelium (Figure 4.6). Taken together, these findings confirm efficient Cre activity in the small intestinal epithelium with significantly lower efficiency observed in the colon using the *VillinCreERT2* mice. This level of recombination was not adequate to analyse possible phenotypic consequences of induction of *Snai1* expression in the intestinal epithelium.

As Cre activity observed in the colon was not sufficient for the current study, no further experiments were performed using the *VillinCreERT2* mice and a Cre driver with relatively

more colon-specific activity, i.e. the *Cdx2CreERT2*, was chosen for analysing the effects of *Snai1* over-expression in the colon.

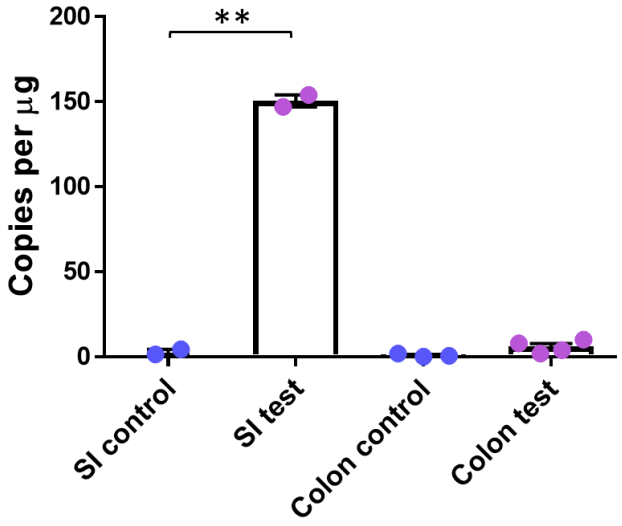

Figure 4.4 Efficient induction of *Snai1* expression in the small intestine but not in the colon at day 5 in the *VillinCreERT2 RosaSnai1* mice post induction. Mice were injected i.p. with four daily tamoxifen doses. Expression of Snai1 was significantly up-regulated (32 to 102-fold increase) in the small intestine (n= 2 each, p= 0.0050) whereas no change in Snai1 expression was observed in the colonic tissues of test (*VillinCreERT2 RosaSnai1*, n= 4) versus control mice (*VillinCreERT2*, n= 3, p= 0.0651). Data was analysed by unpaired t-test and is represented as the mean ± SEM.

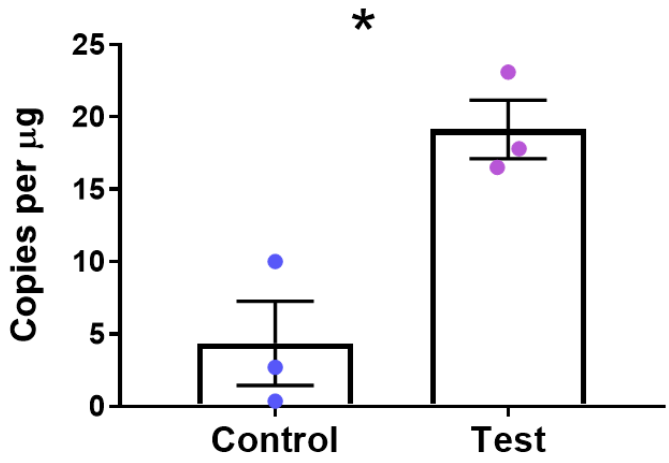

Figure 4.5 Modest up-regulation of *Snai1* in the colon of *VillinCreERT2 RosaSnai1* mice at day 10. Mice were given 4 daily i.p injections of tamoxifen. *Snai1* expression was significantly higher in the test group (4-fold increase) compared to the controls (n= 3 each, p= 0.0176). Data was analysed by unpaired t-test and is represented as the mean ± SEM.

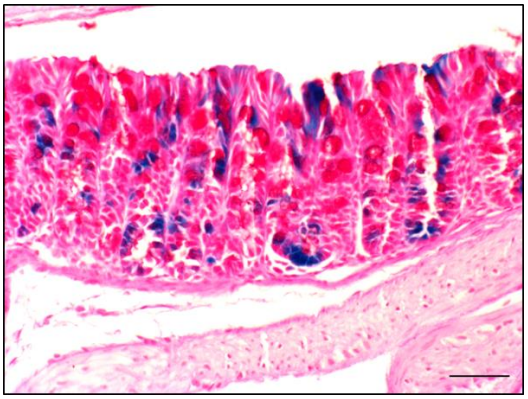

Figure 4.6 LacZ staining showing patchy recombination in the colon of *VillinCreERT2 Rosa26LacZ* mouse on day 5. Cells stained in blue indicate successful recombination. Scale bar 50 µm.

4.2.2 Cdx2 promoter directs recombination in proximal part of the colon in mice following induction with Tamoxifen

The Cdx2P-NLS-Cre, which was first reported by Hinoi and colleagues in 2007, was shown to preferentially target the colonic epithelium in mice (Hinoi et al., 2007). The Cdx2P-NLS-Cre with one *Apc* floxed allele has been reported to result in formation of tumours predominantly in the colon and rectum (Hinoi et al., 2007). To investigate the extent of recombination in my mice, *Cdx2CreERT2* mice were crossed to a GFP reporter (ZsGreen1) mouse. The ZsGreen1 mice used in this study carry a hemizygous ZsGreen1 conditional allele knocked into the *ROSA26* locus (Madisen et al., 2010). Crossing these mice with CreERT2 mice leads to deletion of the floxed STOP cassette present upstream of the *ZsGreen1* sequence in the presence of tamoxifen resulting in expression of the GFP. One advantage of using these mice was that ZsGreen1 is an extremely bright GFP which can be visualised in tissues microscopically without the use of a specific antibody. In the current study, Cre activity was induced in *Cdx2CreERT2 ZsGreen1*$^{flox/+}$ mice by four daily injections of tamoxifen and colon was harvested on day 10. Upon analysing the tissue under a fluorescent microscope, it was observed that the proportion of recombined (GFP^{+}) crypts was higher in the proximal part of the colon, and this declined moving closer to the distal colon (Figure 4.7). This confirmed that the Cdx2 promoter targets the colon and the recombination efficiency is optimal to study *Snai1* function in the proximal colon.

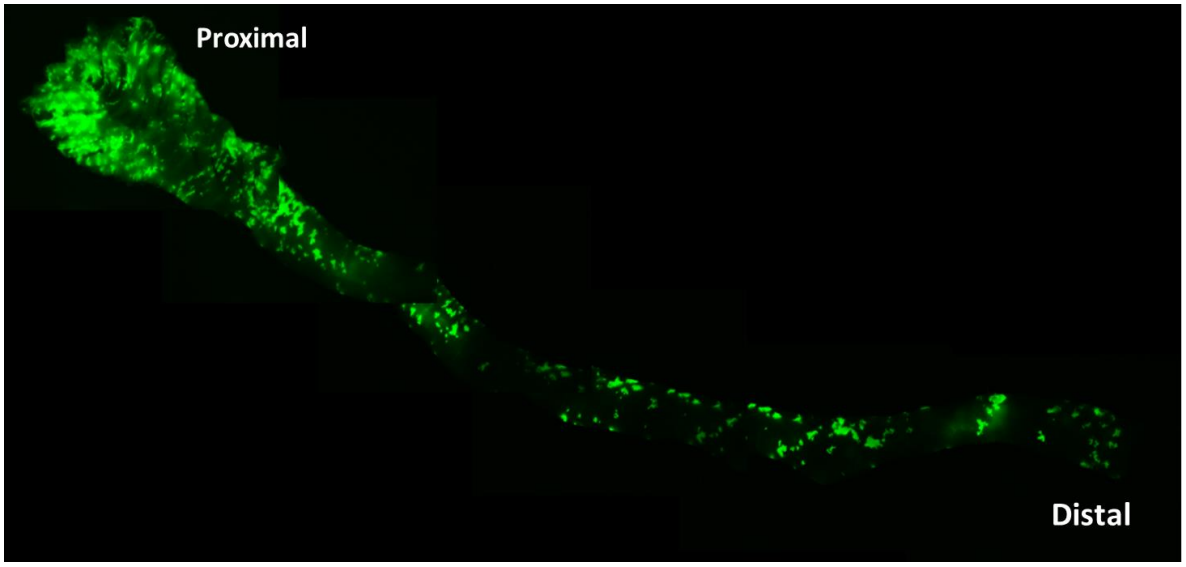

Figure 4.7 The *Cdx2CreERT2* model drives efficient recombination in the proximal region of the colon. ZsGreen1 GFP expression in the *Cdx2CreERT2 ZsGreen1*$^{flox/+}$ mice was induced by four daily injections of tamoxifen followed by collection of colonic tissues on day 10. GFP expression was mainly concentrated in the proximal colon with relatively fewer green cells observed towards the medial and distal regions of the colon.

4.2.3 Up-regulation of *Snai1* in the mouse colon using the Cdx2 promoter

The proximal part of the colon was chosen for further analysis. After 4 daily injections with tamoxifen, colonic tissues were harvested from control (*Cdx2CreERT2*) and test (*Cdx2CreERT2 RosaSnai1/RosaSnai1* (RS/RS)) mice on day 5 and day 10. The expression level of *Snai1* was investigated by Droplet Digital PCR (ddPCR). No significant change in *Snai1* expression was observed on day 5 in test *versus* control mice (Figure 4.8). However, significant elevation in *Snai1* expression in the colon was observed in test mice with an overall average of 359 copies/µg (approx. 6-fold increase) compared to the controls (average 66 copies/µg) harvested on day 10 (n= 10, p= 0.0210, Figure 4.9). The expression level in different individual test mice was variable with expression up to 100-fold. No noticeable phenotypic changes (analysed by H&E staining) in the colonic epithelia were observed in test mice at day 10 (Figure 4.10).

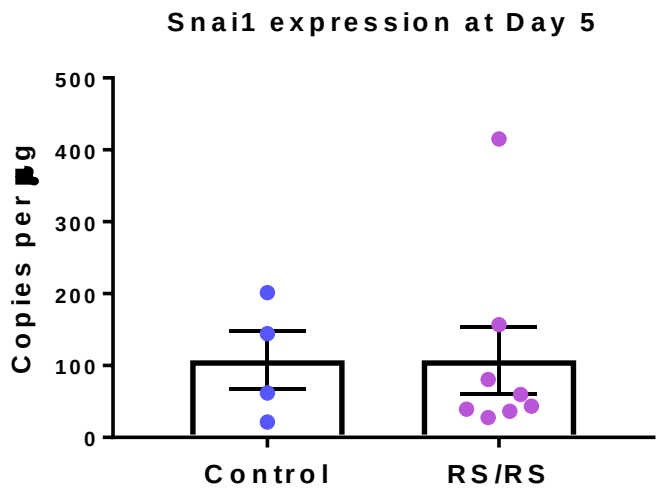

Figure 4.8 Lack of induction of *Snai1* up-regulation in the colon at day 5 using the *Cdx2CreERT2* model. Control and test mice were injected with four daily tamoxifen doses. At day, 5 no significant difference in colonic expression of *Snai1* was observed between the control (n= 4) and test group (n= 8, p= 0.9981). Data was analysed by unpaired t-test and is represented as the mean ± SEM.

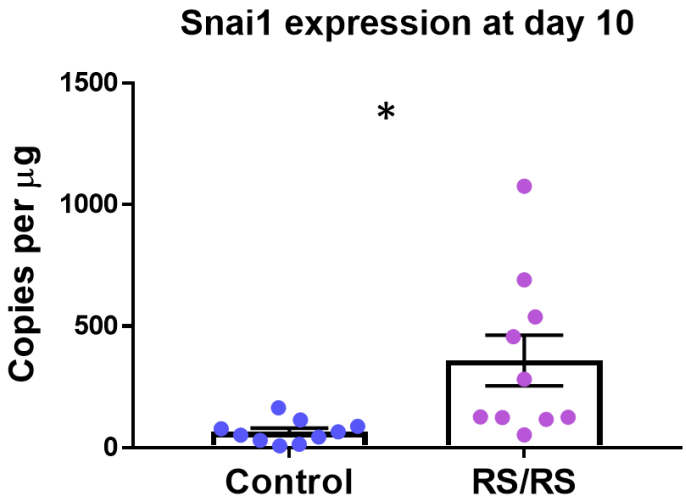

Figure 4.9 Efficient recombination in the colon achieved at day 10 using the *Cdx2CreERT2* mice. Tamoxifen regimen included four daily doses injected intraperitoneally. Expression of *Snai1* increased significantly (approx. 6-fold increase between the average test *versus* control values) in the colonic tissues in the test group at day 10 post induction when compared to the control mice (n= 10 per group, p= 0.0210). Data was analysed by unpaired t-test and is represented as the mean ± SEM.

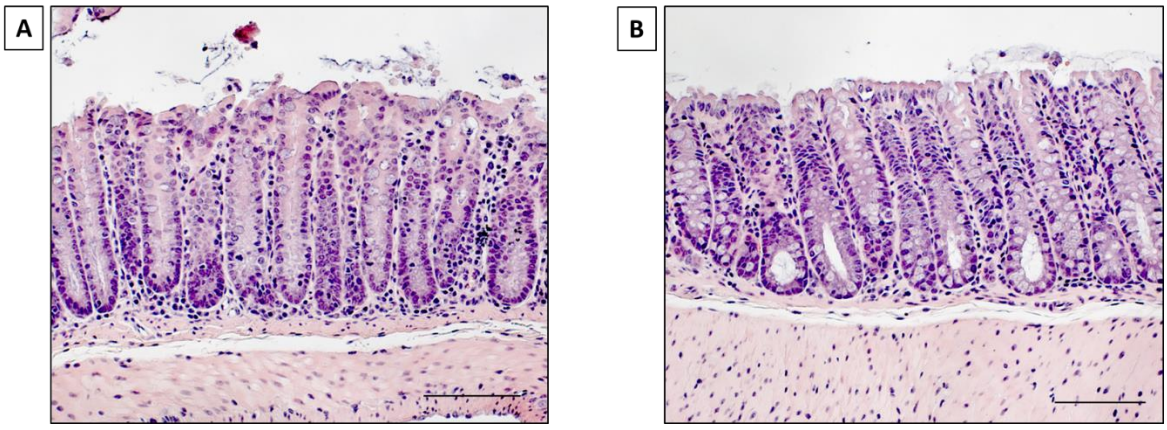

Figure 4.10 No obvious phenotypic changes observed in colonic epithelium post *Snai1* up-regulation. Representative images from Haematoxylin and Eosin (H&E) stained colonic tissues from (A) *Cdx2CreERT2* (control) and (B) *Cdx2CreERT2 RS/RS* (test) mice at day 10 post induction with tamoxifen. Scale bars 50 µm.

4.2.4 Analysis of cell proliferation in colonic epithelium expressing the *Snai1* transgene

Cdx2CreERT2 control and *Cdx2CreERT2 RS/RS* test mice culled on day 10 were injected with BrdU 2 hours prior to dissection to enable analysis of cell proliferation. As the *RosaSnai1* construct contains an eGFP cassette, it allows visualisation of regions with up-regulated *Snai1* via GFP expression. Upon staining with anti-BrdU and anti-GFP antibody (and counter-staining with DAPI), the number of $BrdU^+$ cells were counted in the colonic epithelium of test mice. Open crypts where all the crypt cells expressed GFP formed the test group (hereby referred to as GFP^+) and crypts negative for GFP staining in the same animal were considered as controls (referred to as GFP^-). When comparing the number of actively proliferating cells in recombined (GFP^+) versus non-recombined (GFP^-) crypts, it was found that colonic crypts expressing elevated levels of Snai1 harbour a higher number of proliferating cells than non-recombined GFP^- crypts (mean 8.2 and 5.35 cells per crypt respectively, Figure 4.11). Figure

4.12 (A) and (B) shows representative images of the control and test colonic tissues respectively showing an increase in the number of BrdU$^+$ cells in crypts over-expressing *Snai1*.

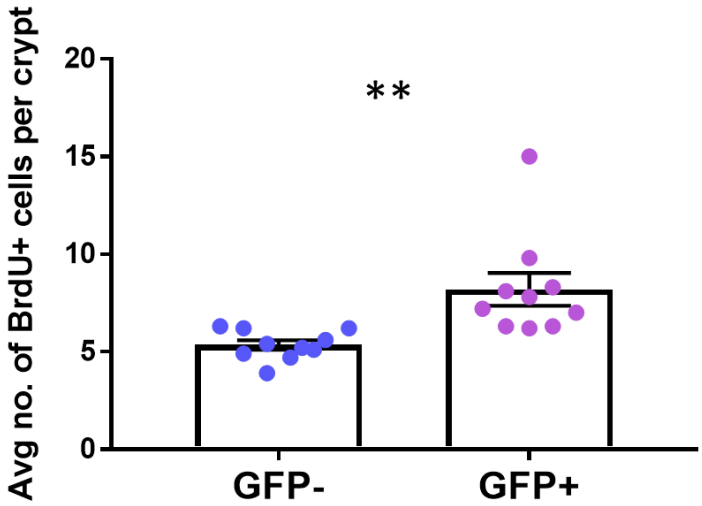

Figure 4.11 *Snai1* up-regulation induces cell proliferation in colonic crypts. The number of BrdU$^+$ cells was quantified in GFP$^-$ and GFP$^+$ crypts (≥ 10 each) in the same animal (n= 10) and was found to be higher in GFP$^+$ crypts (p= 0.0032). Data was analysed by paired t-test and is represented as the mean ± SEM.

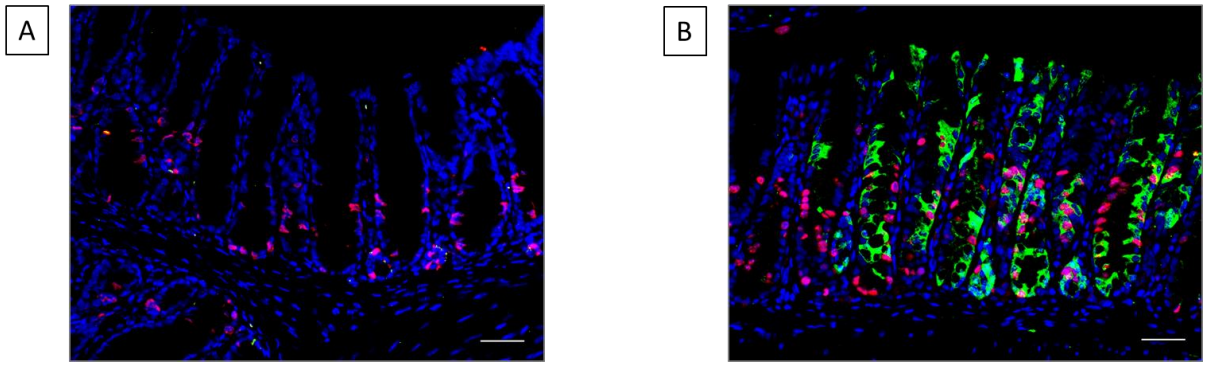

Figure 4.12 Colonic crypts over-expressing *Snai1* harbour more proliferative cells. Representative co-immunofluorescence images showing the BrdU$^+$ proliferative cells (red) in (A) Snai1-eGFP$^-$ or non-recombined crypts and (B) Snai1-eGFP$^+$ (green) or recombined crypts from the same animal, counterstained with DAPI (blue). Scale bars 20 µm.

4.2.5 Analysis of intestinal stem cell markers in colonic tissues overexpressing *Snai1*

To assess whether increased crypt cell proliferation mediated by *Snai1* up-regulation was inducing changes in the stem cell pool, the expression of ISC markers in control and test mice was investigated by ddPCR analysis. Expression of well-known CBC (*Lgr5, EphB2, Axin2* and *Ascl2*) and +4 (*Bmi1* and *mTert*) ISC marker genes was analysed in proximal colonic tissues collected from control and test mice. Expression of *Lgr5*, *EphB2* and *Bmi1* was found to be significantly down-regulated in tissues expressing higher levels of *Snai1* as compared to the control mice (Figure 4.13 (A), (B) and Figure 4.14 (A)). However, there was no significant difference in the expression of other CBC stem cell markers *Axin2* and *Ascl2* between the control and test group (Figure 4.13 (C) and (D)). In addition, expression of *mTert*, a +4 stem cell marker, remain unchanged following Snai1 up-regulation (Figure 4.14 (B)). It is important to note here that in the previous chapter, *SNAI1* expression was found to correlate with *LGR5*, *EPHB2* and *BMI1* stem cell marker expression in CRC. Based on these results, it could be suggested that *Snai1* up-regulation affects *Lgr5, EphB2* and *Bmi1* expression in the colon. In other words, expression of *Lgr5*, *EphB2* and *Bmi1* may be regulated by *Snai1* or the expression of *Snai1* in the stem cell compartment drives stem cell proliferation and differentiation rather than expansion of the stem cell pool. On the other hand, no difference in expression of *Axin2*, *Ascl2* and *mTert* could mean that *Snai1* does not play a direct role in regulation of these genes.

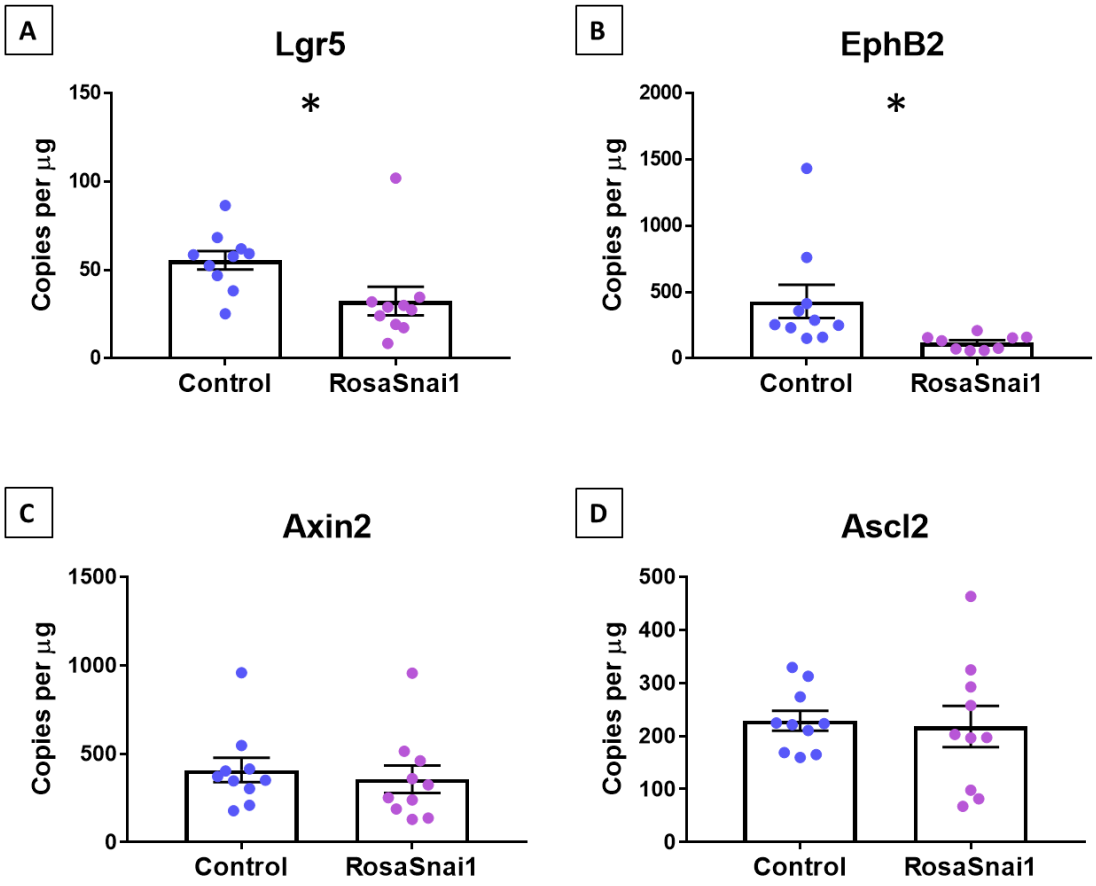

Figure 4.13 The expression of CBC stem cell markers is down-regulated following up-regulation of *Snai1* in the colon. Significant decrease in expression of ISC marker genes (A) *Lgr5* (p= 0.0303), (B) *EphB2* (p= 0.0351) was observed while no change in (C) *Axin2* (p= 0.6226) and (D) *Ascl2* (p= 0.8083) expression was detected in test *versus* control group (n= 10 per group) analysed by ddPCR. Data was analysed by unpaired t-test and is represented as the mean ± SEM.

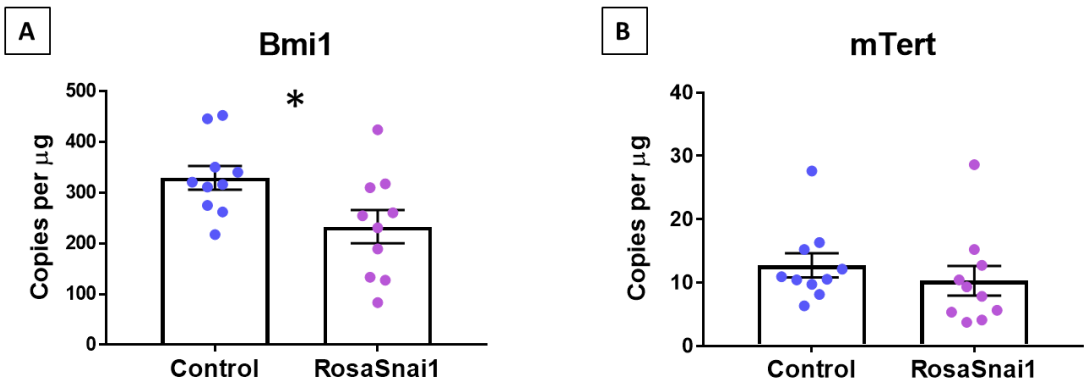

Figure 4.14 *Snai1* up-regulation in the colon down-regulates +4 stem cell marker expression. Expression of (A) *Bmi1* (p= 0.0294) was down-regulation while no effect on expression of (B) *mTert* (p= 0.4318) was observed in the test *versus* control group (n= 10 per group) analysed by ddPCR. Data was analysed by unpaired t-test and is represented as the mean ± SEM.

4.2.6 Overexpression of *Snai1* has no effect on expression of differentiated cells markers

To further study the effect of *Snai1* up-regulation in normal colonic epithelium, expression of differentiated cell population markers was analysed. No difference in the expression of enteroendocrine cell marker *Chromogranin A* (Figure 4.15 (A)) or goblet cell marker *Muc2* (Figure 4.15 (B)) was observed when analysed by ddPCR suggesting that over-expression of *Snai1* does not affect these terminally differentiated cell types. Quantification of these different cell populations in the colonic epithelia is required to make further conclusions.

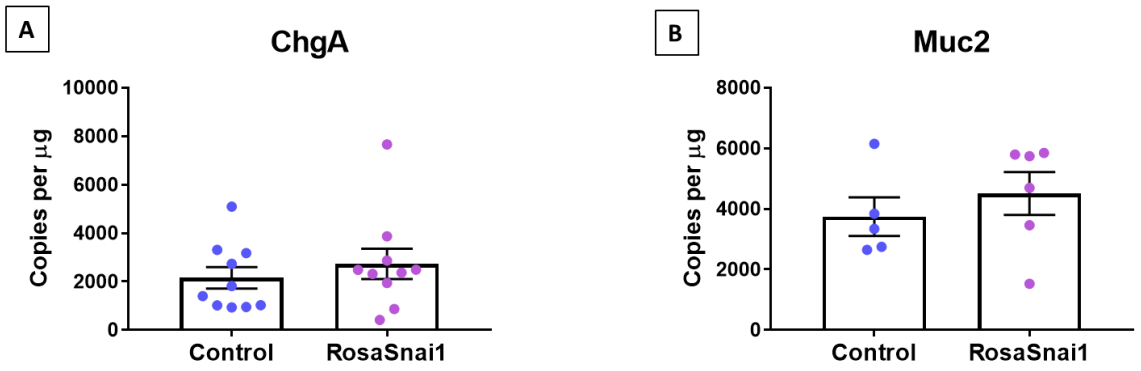

Figure 4.15 *Snai1* up-regulation in the colon does not affect the expression of enteroendocrine and goblet cell markers. Expression of enteroendocrine and goblet cell markers (A) *Chromogranin A* (n= 10 per group, p= 0.4591) and (B) *Muc2* (n ≥ 5, p= 0.4429) respectively in the test group compared to the control group. Data was analysed by unpaired t-test and is represented as the mean ± SEM.

4.2.7 Generation of colonic organoids from crypts isolated from mice

To further analyse the function of *Snai1*, I utilised an *ex-vivo* organoid system. Sato *et al.* originally described an intestinal epithelial organoid culture system where single $Lgr5^{+}$ cells were able to give rise to self-organising structures which essentially recapitulate all the aspects of a self-renewing epithelium (Sato et al., 2009). Organoids can be generated from either single stem cells or isolated crypts from small intestine and colon. Small intestinal and colonic organoids essentially require similar culture media conditions, including the *Wnt* signalling potentiator R-spondin, the EGF signalling activator EGF and the BMP signalling inhibitor Noggin. However, the culture media for colonic organoids requires addition of WNT3a as colonic crypts lack Paneth cells, thus have no source of intrinsic *Wnt* signalling activators for growth. Figure 4.16 shows an image of a mature colonic organoid cultured in growth media containing 50% Wnt3a conditioned media (CM), 10% Rspondin1 CM, 100 ng/ml

noggin, 50 ng/ml EGF and basal media for 8 days. Structures marked by yellow arrows represent the crypts and are called 'buds' whereas the middle region represents the lumen.

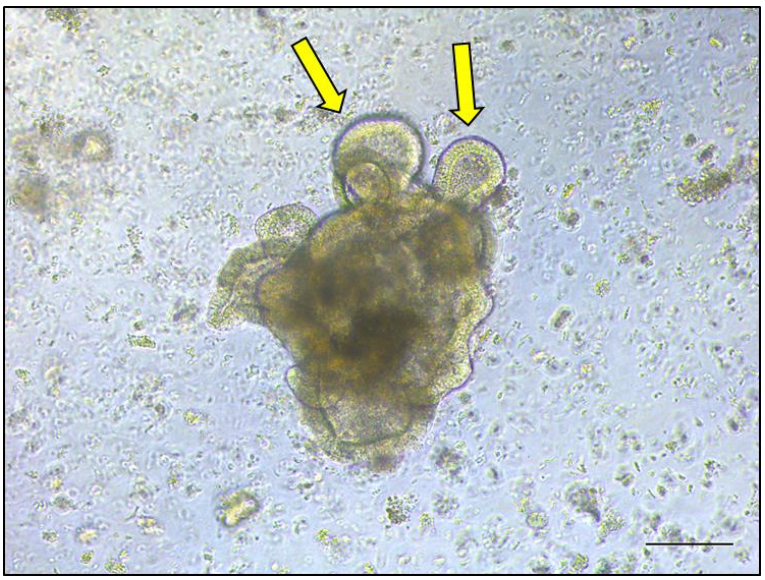

Figure 4.16 Colonic organoid grown from a single isolated crypt from wild type mouse epithelium. Crypts harvested from mice were seeded in Matrigel and grown in culture media supplemented with growth factors. This resulted in formation of these irregular structures with buds known as organoids or 'mini-guts'. This image shows a mature colonic organoid on day 8 where the arrows represent crypts, also called 'buds' which contain the stem cells, and the central or luminal region consists of the differentiated cells. Scale bar 100 µm.

4.2.8 Analysing the effects of *Snai1* up-regulation in colonic organoids using TAT-Cre

In order to induce *Snai1* expression in organoids established from *RosaSnai1* mice, I designed an experiment utilising TAT-Cre. TAT-Cre recombinase is a recombinant cell permeant fusion cre-recombinase which can be added to cultures to induce recombination and subsequent expression of the transgene *in vitro*. Considerable variation exists among different batches of commercially available TAT-Cre and the optimal concentration of the enzyme required to induce efficient recombination varies among different cell types. Before commencing my experiment, it was necessary to determine the optimal dose and protocol to produce efficient

recombination in the organoid cultures. To assess efficiency of TAT-Cre-induced recombination in my colonic organoids culture system, organoids were generated from GFP reporter mice and treated with different concentrations of TAT-Cre recombinase. Post treatment with TAT-Cre, the proportion of GFP^+ cells was analysed by flow cytometry as a measure of successful recombination. Untreated organoids were used as a control. The optimum concentration of TAT-Cre required for efficient recombination was found to be 8 µM as the percentage of GFP^+ cells using this concentration was highest (68%) as compared to 4 µM (36%) and 6 µM (55%) (Figure 4.17 and 4.18). The figure depicts a qualitative increase in TAT-Cre efficiency as seen by the number of GFP+ organoids in the different panels. An obvious difference in the number of GFP+ organoids can be seen in second and third panel using the lowest and highest concentration of TAT-Cre recombinase. A higher magnification image has been included in the third panel to show organoid morphology as this concentration was selected for further analysis.

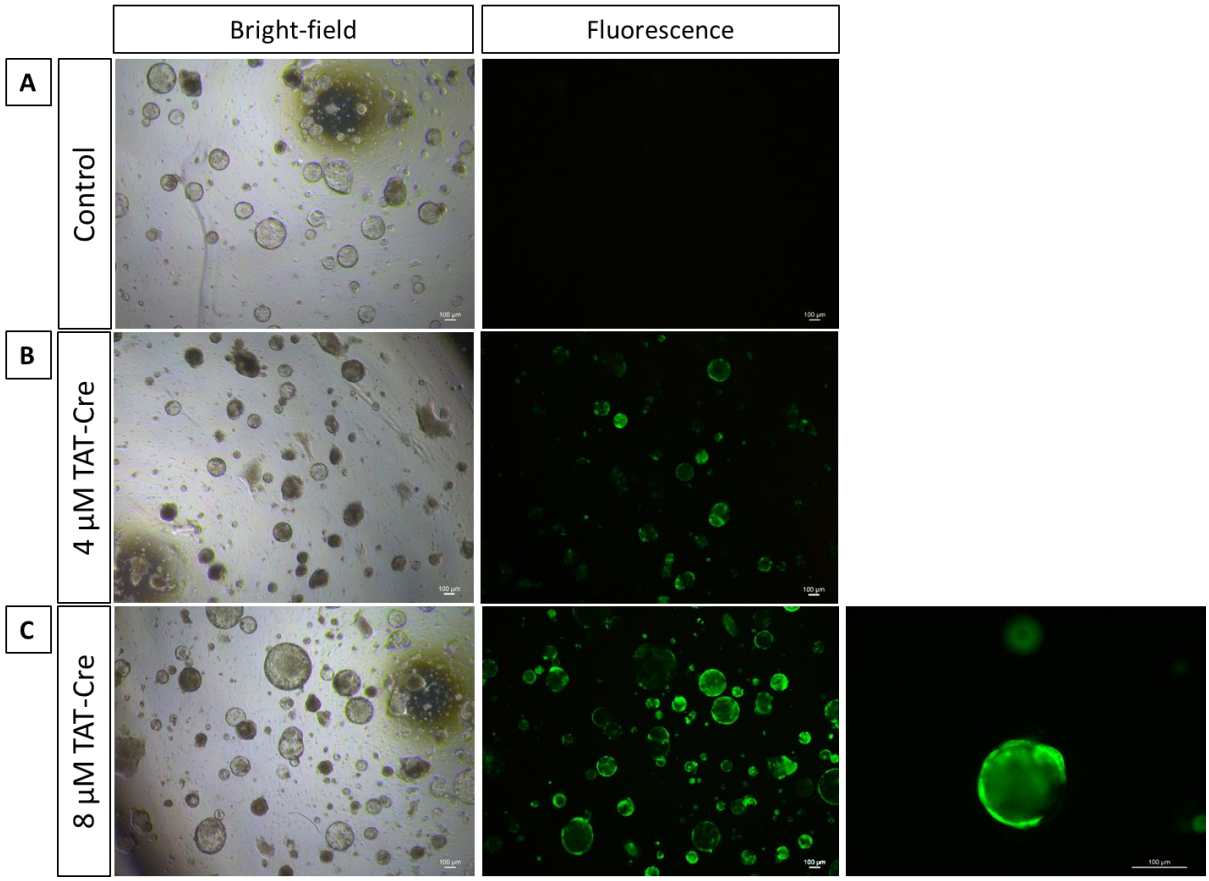

Figure 4.17 The optimal concentration of TAT-Cre to induce efficient recombination in organoids was 8 µM. Colonic organoids were dissociated and treated with different concentrations (4, 6 and 8 µM) of TAT-Cre recombinase for 4 hours at 37 °C. Post-treatment cells were re-seeded in Matrigel and grown in culture for 5 days. Organoids were examined for GFP expression on day 5. Representative bright-field and fluorescent images showing the proportion of GFP^+ organoids on day 5 post treatment with (B) 4 µM and (C) 8 µM TAT-Cre as compared to (A) untreated control organoids. An obvious difference in the proportion of GFP^+ organoids can be seen in the second and third panel using the lowest (4 µM) and highest (8 µM) concentration of TAT-Cre. A higher magnification in the third panel has been included to show organoid morphology as this concentration was selected for further analysis. Scale bars 100 µm.

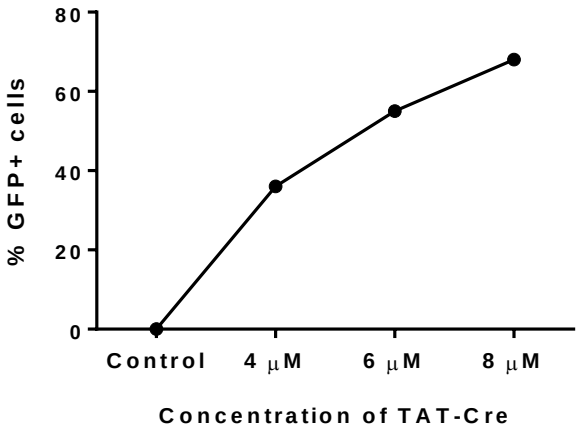

Figure 4.18 Proportion of GFP⁺ cells increases with increase in concentration of TAT-Cre as measured by flow cytometry. Recombination efficiency was highest (68%) with 8 μM TAT-Cre.

Following FACS analysis, sorted single GFP⁺ cells were re-seeded in Matrigel to determine whether these single cells have the ability to form secondary organoids. Indeed, these single GFP⁺ cells were able to give rise to entire GFP⁺ spherical organoids by day 8 in culture as seen in Figure 4.19.

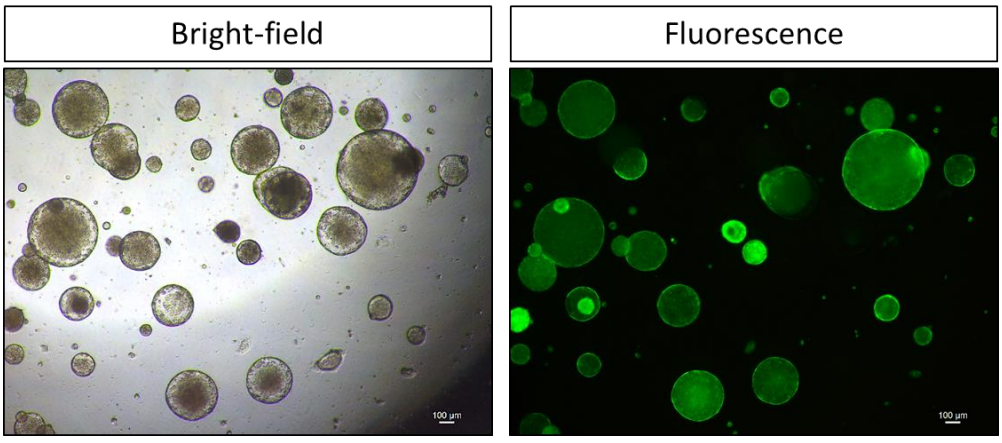

Figure 4.19 FACS-sorted single TAT-Cre treated colonic epithelial cells give rise to organoids in vitro. Single cells sorted by FACS re-seeded in Matrigel generated cystic organoids. Representative bright-field and fluorescent images of GFP⁺ organoids on day 8 post FACS. Scale bars 100 μm.

4.2.9 *Snai1* up-regulation in colonic epithelium transforms ISCs into mesenchymal cells *in vitro*

Following assessment of the optimum TAT-Cre concentration required for efficient recombination, organoids were generated from RosaSnai1 mouse colonic crypts and treated with 8 µM TAT-Cre. After 5 days in culture, the treated organoids were dissociated, and single cell isolated by FACS. This was possible due to the presence of an IRES-GFP in the *RosaSnai1* construct. In order to isolate cells with organoid-forming capabilities, the CD24 marker was utilised as a medium level of CD24 expression marks a population of proliferative cells, including ISCs (Nefzger et al., 2016). These $CD24^{med}$ cells were then further separated, based on the expression of the GFP cassette, into $CD24^{med}/GFP^{+}$ cells expressing the *Snai1* transgene and $CD24^{med}/GFP^{-}$ control cells. Figure 4.20 depicts the strategy used for FACS analysis for these organoids.

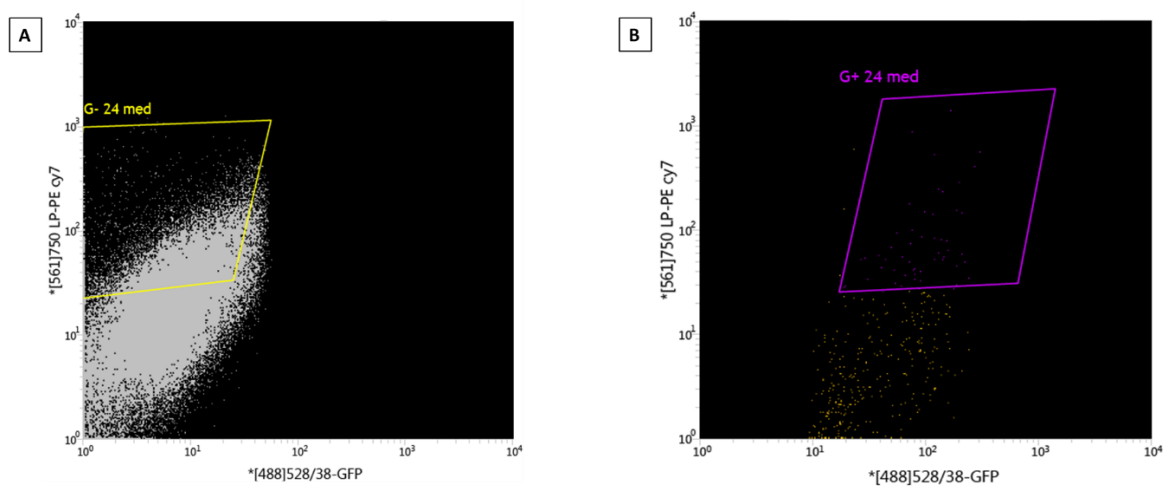

Figure 4.20 FACS-sorting strategy to collect proliferating cells expressing the *Snai1* transgene. Two different colonic epithelial cell populations were sorted based on GFP (Snai1) and PeCy7 (CD24) fluorescence, one (A) expressing endogenous *Snai1* ($CD24^{med}/GFP^{-}$) and the other (B) expressing elevated levels of *Snai1* ($CD24^{med}/GFP^{+}$). Cells expressing medium level of CD24 were collected as $CD24^{med}$ marks the proliferative cells including the stem cells.

The two cell populations collected by FACS were re-seeded in Matrigel and allowed to grow in normal colonic organoid culture media up to day 8. As expected, numerous spherical organoids were observed in wells seeded with the control cell population not expressing the *Snai1* transgene ($CD24^{med}/GFP^{-}$) (Figure 4.21 (A)). Surprisingly, wells seeded with the $CD24^{med}/GFP^{+}$ cells expressing elevated levels of *Snai1* did not show organoid forming ability. Instead, clusters of cells resembling fibroblasts in morphology were observed (Figure 4.21 (B)), suggesting that *Snai1* up-regulation in these cells resulted in activation of EMT, leading to transformation of these epithelial cells into mesenchymal cells.

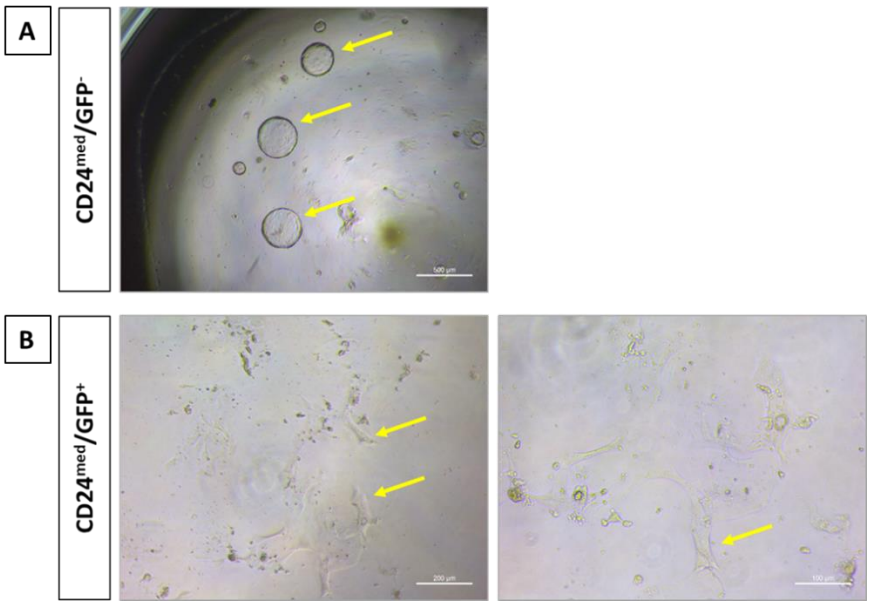

Figure 4.21 *Snai1* up-regulation in colonic stem cell-enriched cell population results in activation of EMT in vitro. (A) Cells expressing endogenous *Snai1* formed spherical organoids (marked by yellow arrows) by day 8 whereas (B) Cells expressing the *Snai1* transgene transformed into fibroblasts seen as clusters of cells marked by yellow arrows and no spherical organoids were observed. Scale bars (A) 500 µm, (B) 200 µm (left) and 100 µm (right).

To confirm *Snai1* up-regulation in the CD24^{med}/GFP^{+} cell population versus the CD24^{med}/GFP^{-} control population, ddPCR analysis was performed to quantify the expression level of *Snai1* in these cell populations. As expected, there was an almost 2-fold increase in expression of *Snai1* in the CD24^{med}/GFP^{+} cell population compared to CD24^{med}/GFP^{-} cells (Figure 4.22 (A)). In order to confirm that these cells expressing the *Snai1* transgene had indeed transformed into mesenchymal cells, *Lgr5* expression was analysed. No *Lgr5* mRNA was detected in the transformed cell population whereas the non-transformed epithelial cells expressed over 150 copies/µg of the *Lgr5* mRNA (Figure 4.22 (B)). This suggests that the epithelial cell population lost its epithelial identity and acquired a mesenchymal profile, although this needs to be tested using a mesenchymal marker such as vimentin and repeated (n=1 only).

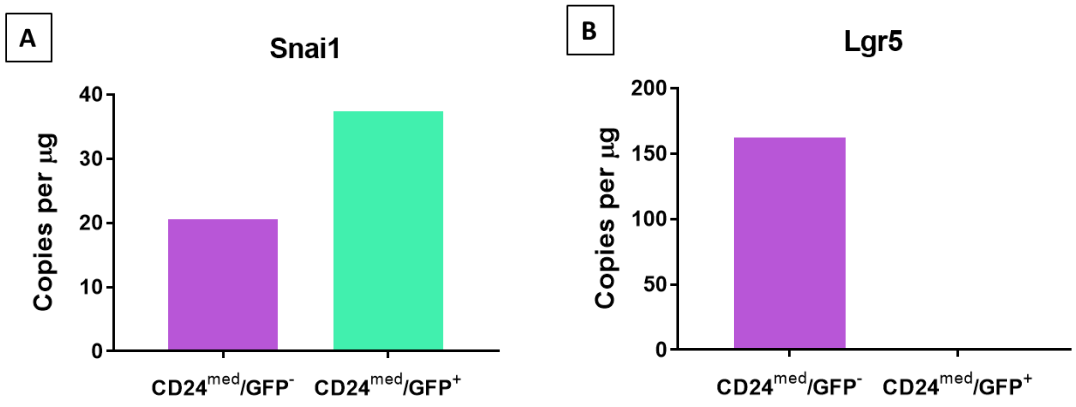

Figure 4.22 *Snai1* up-regulation and loss of Lgr5 expression in transfected proliferative cells *in vitro*. Expression of (A) *Snai1* and (B) *Lgr5* in the recombined cell population versus the non-recombined stem cells (n=1).

4.3 Discussion

4.3.1 Tissue-specific Cre-mediated recombination in mice using the Villin and Cdx2 promoter

One of the major challenges facing researchers examining gene function in the colon is the lack of robust colon-specific Cre drivers. The vast majority of epithelial functional studies largely or exclusively target the small intestine to study the role of key molecules in normal tissues or during intestinal tumourigenesis. Adenoviral delivery of Cre to target the colonic tissues in mice is a technically challenging approach, and, as a result, has not been widely utilised. The *VillinCreERT2* construct is based on fusion of the Cre recombinase to the mutated ligand-binding domain of the human oestrogen receptor which results in tamoxifen dependent activity of the Cre enzyme. Several studies have utilised this model to target transgene expression in the small intestine and colon. Using the *VillinCreERT2* system, Cre expression has been reported to be detectable by immunoblotting in tissue lysates from the mouse small intestine and colon (el Marjou et al., 2004). Several studies have observed efficient recombination in the colon using the *VillinCreERT2* model (Eckmann et al., 2008, Schwitalla et al., 2013). Eckmann *et al*. reported efficient deletion of IKKβ in the small intestinal and colonic epithelium confirmed by immunoblotting using anti-IKKβ antibody in the *VillinCreERT2* mice (Eckmann et al., 2008). Schwitalla and colleagues evaluated the effects of (intestinal epithelial cell-specific) loss of *p53* ($Tp53^{\Delta IEC}$) combined with carcinogen azoxymethane (AOM)-induced activating mutation of β-catenin in the colon using *VillinCreERT2* mice (Schwitalla et al., 2013). Deletion of p53 under the Villin promoter in the AOM-induced tumourigenesis model resulted in invasion of ≥50% of the colonic tumours into the submucosa. Altogether, findings by Eckmann *et al*. and Schwitalla *et al*. indicate efficient

recombination in the colon, enough to produce a phenotype, using the *VillinCreERT2* model. As a result, we decided to use this model to study the effects of Snai1 up-regulation in the colon. However, in my study, recombination efficiency was much higher in the small intestine resulting in significant increase (32-102-fold increase) in *Snai1* expression in these tissues whereas very low up-regulation (4-fold increase) of *Snai1* expression was detected in the colonic tissues. Analysis of recombination efficiency revealed that Cre activity under the Villin promoter is very limited in the colon. Loss of *Apc* in the colon did not result in a dramatic phenotype in the colon compared to the small intestine and hyperproliferative crypt units were only observed in small patches throughout the colon, which suggest inefficient recombination using the *VillinCreERT2* system (Andreu et al., 2005). These differences in Cre efficiency in the colon under the Villin promoter observed in different studies could be attributed to differences in genetic backgrounds of mice and variability in the ability of Cre to promote recombination in different floxed alleles. This highlights the importance of monitoring recombination in each experiment.

Another model, the *Cdx2CreERT2* system has been reported to demonstrate colonic epithelium-preferential Cre recombinase activity in adult mice (Hinoi et al., 2007). Hinoi *et al*. assessed somatic activation of a floxed *Apc* allele in the gastrointestinal tract of *Cdx2Cre* $Apc^{flox/+}$ and *VillinCre* $Apc^{flox/+}$ mice. In the *Cdx2Cre* $Apc^{flox/+}$ mice, the Cre targeted *Apc* allele was found to be present along with the wild-type *Apc* allele in normal mucosa from distal small intestine to the rectum, whereas, in *VillinCre* $Apc^{flox/+}$ mice the *Apc* allele was present from the duodenum to the rectum. The majority of the adenomas formed in the *Cdx2Cre* $Apc^{flox/+}$ mice were found in the large intestine as compared to the *VillinCre* $Apc^{flox/+}$ mice which mostly developed small intestinal adenomas (Hinoi et al., 2007). Interestingly, the bulk

of tumours observed in the *Cdx2Cre Apc*$^{flox/+}$ mice were localised in the distal part of the colon with very few polyps detected in the proximal colon. An opposing pattern of Cre efficiency was observed in my study, where Cre activity was highest in the proximal colon with minimal efficiency in the distal regions. Another study examined *Cdx2CreERT2* activity in mice carrying an EYFP-Cre reporter construct (Feng et al., 2013). EYFP expression was found in epithelial cells from terminal ileum to rectum with the strongest induction of Cre activity in the caecum and proximal colon. This concurs with the results described in this chapter where the strongest Cre activity was observed in the proximal part of the colon. The regional differences associated with the *Apc* phenotype may be due to the effect of genetic background or the expression of co-operating genes that promote polyp formation preferentially in the distal region of the colon. Taken together, these results suggest that, efficient gene recombination is achieved in the proximal colon using the tamoxifen inducible *Cdx2CreERT2*, which will allow studying the effects of *Snai1* over-expression in the proximal colon.

4.3.2 *Snai1* up-regulation results in increased cell proliferation in the colonic epithelium

Several studies have examined the effects of *Snai1* up-regulation during development and in various adult tissues. During gastrulation, ectopic expression of *Snai1* in developing bones of mouse embryos results in growth defects including shortness of limbs, which occurs as a result of reduction of long bone length (de Frutos et al., 2007). In addition, a reduction in proliferation of chondrocytes and impaired hypertrophic chondrocyte differentiation was reported to occur. This decrease in proliferation and impaired differentiation during early stages of development could be due to activation of EMT following up-regulation of *Snai1*. On the other hand, in adult tissues, an increase in cell proliferation following *Snai1* up-regulation has been demonstrated in various tissues (Horvay et al., 2015). The consequences of *Snai1*

up-regulation have been documented in adult mouse tissues including the skin where ectopic *Snai1* in the epidermis drives hyperproliferation and formation of spontaneous tumours (De Craene et al., 2014). Up-regulation of *Snai1* has been previously studied in the mouse small intestine in our laboratory. Results from the study demonstrated an increase in cell proliferation measured by counting the number of $PCNA^+$ proliferative cells by immunofluorescence (Horvay et al., 2015). Similar findings were observed in the experiments described in this chapter where an increase in cell proliferation was found in colonic crypts expressing elevated levels of *Snai1* as compared to wild-type crypts in the same mice after 10 days of induction. These findings suggest that in both the small intestine and colon elevation of SNAI1 levels promotes cell proliferation.

4.3.3 Up-regulation of *Snai1* results in reduced expression of ISC markers, no effect on differentiated cell markers

Elevated levels of *Snai1* in the small intestine have been shown to result in increased expression of CBC ISC markers *Lgr5* and *Olfm4* and an increase in number of $CD44v6^+$ CBC stem cells (Horvay et al., 2015). In contrast, the expression of CBC ISC markers *Lgr5, EphB2* and +4 stem cells marker *Bmi1* was significantly reduced following *Snai1* up-regulation in the colon. This difference in expression of ISC makers in the small intestine and colon following up-regulation of Snai1 could be, in part, due to the difference between the small intestinal and colonic epithelial tissue architecture. The small intestinal epithelium consists of crypt and villus units and the ISC niche is composed of Paneth cells, alternating with the stem cells at the crypt base, and the surrounding mesenchyme, which secrete ligands responsible for regulation of the ISC population. The colonic epithelium, on the other hand, lacks Paneth cells but contains other niche cells that do not secrete the same complement of growth factors.

For example, colonic niche cells do not produce WNT3A (Sasaki et al., 2016). Differences in co-operating niche factors or downstream effectors may contribute to differences in the functional dynamics of Snai1 in different regions of the intestine. Another possible explanation for down-regulation of ISC markers in the colon could be that the increase in cell proliferation observed occurs as a result of increased division among these stem cells leading to 'exhaustion' of some of these stem cells and down-regulation of key markers. qRT-PCR analysis does not show if there is any change in stem cell numbers but measures overall abundance of transcripts within tissues. It would be interesting to examine if the decrease in expression of the stem cell markers is due to a reduction in the number of stem cells in these tissues or whether there is an overall decrease in the expression of these genes while the stem cell number remains constant. One approach to investigate these possibilities would be by examining the stem cells at earlier time-points, perhaps day 5, to 'capture' the proliferation event of active stem cell division and quantify the number of $CD44v6^{+}/BrdU^{+}$ (proliferating stem cells) cells. Alternatively, in order to evaluate the number of stem cells in the epithelium, the number of $Lgr5^{+}$ colonic cells could be assessed by flow cytometry using a cell surface marker mediated stem cell isolation protocol (Nefzger et al., 2016). The proliferation potential of these $Lgr5^{+}$ cells could also be assessed by performing an EdU cell proliferation assay combined with flow cytometry analysis.

No significant differences in the expression of CBC stem cell markers *Ascl2*, *Axin2* and +4 marker *mTert* was observed. One possible explanation could be that *Snai1* regulates *Lgr5*, *EphB2* and *Bmi1* expression and not *Ascl2*, *Axin2* and *mTert* expression. Furthermore, down-regulation of *Lgr5* and *EphB2* expression could mean a decrease in *Wnt* signalling at the crypt base which, in turn, could be a compensatory mechanism for the increase in cell proliferation

observed in the crypts. Or the converse could be true, decrease in ISC marker expression could result in increase in cell proliferation to compensate for the loss in *Wnt* signalling. No difference in the expression of *ChgA* and *Muc2* suggests that *Snai1* does not affect the terminally differentiated enteroendocrine and goblet cells. Again, it would be interesting to see whether there is any change in the number of enteroendocrine and goblet cells in crypts expressing the *Snai1* transgene as a decrease in number of enteroendocrine cells has been reported in the small intestinal epithelium in *RosaSnai1* mice (Horvay et al., 2015).

4.3.4 *Snai1* up-regulation in colonic stem cells and progenitors results in activation of EMT *in vitro*

Manipulation of gene expression in organoids using TAT-Cre recombinase has never been carried out before and we are the first ones to design a robust protocol for transfection of colonic organoids using this system (Jardé et al., 2018). Transfecting organoids using TAT-Cre is an efficient way of manipulating gene function *in vitro*. Successful transfection was achieved in colonic organoids using this technique as observed by up-regulation of *Snai1* in culture. Interestingly, up-regulation of *Snai1* in these cells did not produce an increase in cellular proliferation but resulted in a change of morphology resembling activation of EMT with a loss of polarity and conversion of the epithelial cells into mesenchymal cells. Loss of epithelial stem cell characteristics was further confirmed by failure to detect *Lgr5*, a robust ISC marker gene and epithelial marker, while epithelial cells not expressing the *Snai1* transgene maintained their epithelial characteristics and formed spherical organoids. Further validation of these observations by analysing the expression of mesenchymal markers, like *Vimentin*, in the *Snai1* transgene-expressing cells is required.

Snail family members are well-known as regulators of EMT and as discussed in Chapter 3, SNAI1 is up-regulated in a number of cancers. Several studies have investigated the role of SNAI1 in the context of EMT in cancer cell lines. For instance, overexpression of SNA1 in A431 human squamous cell carcinoma (SCC) results in loss of expression of epithelial cell marker E-CADHERIN, loss of apical polarity and resemblance to fibroblasts in morphology (Yokoyama et al., 2003).

It is important to note here that studying gene function in *in vitro* intestinal organoids has its advantages and limitations compared to *in vivo* approaches. Crypts in the epithelium are believed to be in close contact with the underlying mesenchyme that creates a specialised cellular microenvironment supporting the ISCs. Organoid cultures allow evaluation of gene function in the epithelial cells without interference from the underlying mesenchyme. However, organoids are not a true representation of the epithelial tissue *in vivo*. Moreover, the contributory role of the interaction of genes that play a key role in maintenance of epithelial cells with the mesenchyme cannot be taken into account when working with organoids. Although there was induction of EMT upon *Snai1* up-regulation in colonic epithelium *in vitro*, no activation of EMT occurred when *Snai1* was overexpressed in the epithelium *in vivo.* This could possibly be due to the threshold of *Snai1* expression in these two systems. The observed levels of *Snai1* expression required for maintenance of epithelial stem cells in the intestine is significantly lower than level observed in cell lines undergoing *Snai1*-induced EMT. Another explanation for the difference could be the influence of surrounding niche signals *in vivo* that are not present in the *in vitro* organoid system. *Wnt* signalling plays a key role in the maintenance of epithelial cell identity in the intestine. The underlying mesenchyme secretes WNT ligands required for maintaining intestinal

homeostasis. It is possible that for epithelial cells to transition into cells resembling mesenchymal cells in morphology *in vitro*, a much lower level of *Snai1* expression is required as there is no surrounding mesenchyme to compensate for this change. Whereas *in vivo*, as the surrounding mesenchyme is intact, a much higher level of *Snai1* expression would be required to see any such effect. However, this is just speculation at the moment and a deeper investigation into the role of *Snai1* in both systems and the resulting phenotypes is essential.

4.3.5 Chapter Conclusion

The data in this chapter confirms colonic specificity of the Cdx2 promoter for Cre-mediated recombination. One could argue that the increase in cell proliferation observed in mouse colon could be extrapolated to CRC suggesting a possible increase in proliferation in colorectal tumours as a result of SNAI1 up-regulation. *Snai1* up-regulation in the colonic epithelium *in vivo* leads to down-regulation of ISC marker genes. However, this is in contrast to CRC, where ISC markers are up-regulated which could be due to hyper-activated WNT signalling in the tumours. It is unclear whether the decrease in expression of the stem cell markers in mouse is due to a reduction in the number of stem cells in the colonic crypts or whether there is an overall down-regulation in the expression of these genes in the ISCs while the stem cell number remains constant. Effect of *Snai1* up-regulation on stem cells could be further investigated by examining the stem cells at an earlier time-point and quantifying the number of actively proliferating stem cells. *In vitro*, Snai1 up-regulation results in activation of EMT by converting proliferating epithelial cells into clusters of mesenchymal-like cells. This difference in phenotype observed in these two systems could be attributed to different threshold levels of exogenous Snai1 *in vivo* and *in vitro*. Additional studies investigating the effects of Snai1

up-regulation both *in vivo* and in *in vitro* organoid cultures are required to clarify these hypotheses.

Chapter 5 - Effects of *Snai1* elevation on intestinal tumourigenesis in the $Apc^{flox/flox}$ mouse model of colon cancer

Chapter 5 – Effects of *Snai1* elevation on intestinal tumourigenesis in the *Apc*$^{flox/flox}$ mouse model of colon cancer

5.1 Introduction

This chapter examines the interaction between ectopic *Snai1* expression and loss of *Apc* in the intestinal epithelium. As *SNAI1* over-expression was observed in earlier stages of tumourigenesis in CRC (Chapter 3), consequences of induction of *Snai1* up-regulation during early stages of polyp formation in a mouse model of intestinal tumourigenesis were investigated in this chapter.

5.1.1 Background

Adenomatous Polyposis Coli (*APC*), is a multi-functional tumour suppressor gene which encodes a 312 kDa protein, and is mutated in approximately 80% of sporadic and familial adenomatous polyposis (FAP) colorectal cancers (CRCs) (Fearnhead et al., 2001). The APC gene was first identified in 1991 by positional cloning of the FAP locus (Groden et al., 1991, Kinzler et al., 1991). Germline mutations in *APC* are found in FAP patients, while somatic mutations are associated with sporadic CRCs (Table 5.1). Majority of the germline and somatic mutations occur in exon 15 of the *APC* gene, which comprises of more than 75% of its coding sequence (Beroud and Soussi, 1996). Germline mutations mostly occur at codons 1061 and 1309, whereas, over 60% of all somatic mutations occur in the mutation cluster region (MCR) which represents the region between codon 1286 and 1513 (Beroud and Soussi, 1996,

Miyoshi et al., 1992a). The APC protein is composed of an N-terminal region consisting of an oligomerisation domain and an armadillo region, a series of 15- and 20-amino acid repeats, and a basic domain and EB1 and the human disc large protein binding sites at the C-terminal (Fearnhead et al., 2001) (Figure 5.1).

Table 5.1 APC mutations in colorectal cancer

	FAP	Sporadic adenomas	Sporadic Cancers
Prevalence of APC mutation	>85% (Powell et al., 1992)	>80% (Jen et al., 1994)	>80% (Smith et al., 1993)
Type of mutations	Germline mutations	Somatic mutations	Somatic mutations
Truncating	96% (Nagase and Nakamura, 1993)	89% (Miyoshi et al., 1992b, Powell et al., 1992)	98% (Miyoshi et al., 1992b, Powell et al., 1992)
Missense	4% (Nagase and Nakamura, 1993)	11% (Miyoshi et al., 1992b, Powell et al., 1992)	2% (Miyoshi et al., 1992b, Powell et al., 1992)

Adapted from (Kinzler and Vogelstein, 1996)

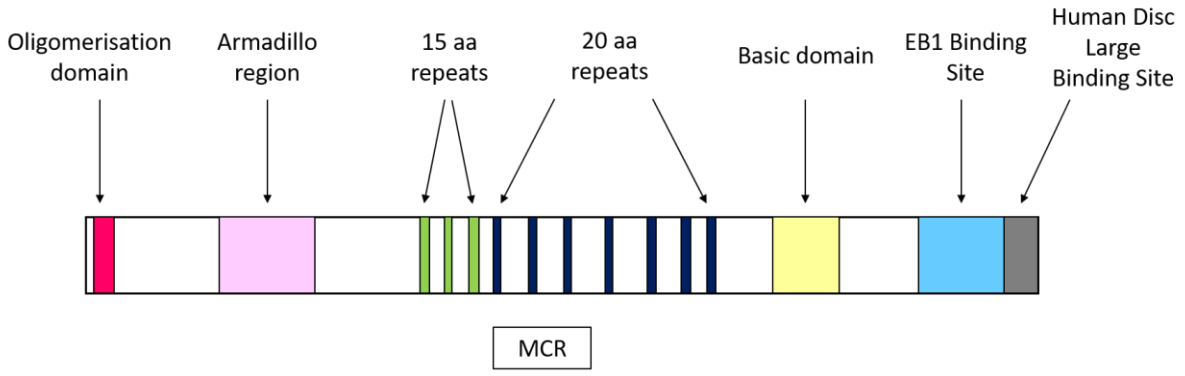

Figure 5.1 Functional domains of APC protein. The 15- and 20-amino acid repeats provide binding sites for β-catenin. Image adapted from Fearnhead *et al*. (Fearnhead et al., 2001).

The location of the inherited *APC* mutation is often associated with occurrence of specific manifestations in FAP patients. For instance, mutations within codons 1250 and 1464 usually result in development of severe polyposis (Nagase et al., 1992) as compared to patients with APC mutations in other locations. More than 95% of these mutations (in both FAP and sporadic cancer patients) lead to premature truncation of the protein (Galiatsatos and Foulkes, 2006). These truncations result in loss of domains (15- and 20-amino acid repeats) which are required for binding to β-catenin and microtubules. β-catenin forms a complex of proteins with APC and AXIN (called the destruction complex) which promotes GSK3β-mediated phosphorylation of β-catenin serine and threonine residues leading to its degradation by the proteasome. In the absence of a functional APC protein, the destruction complex is constitutively dissociated, β-catenin is not phosphorylated and therefore not degraded, resulting in its accumulation in the cellular cytoplasm and subsequent migration into the nucleus. Nuclear β-catenin binds to the transcription factor T-cell factor 4 (TCF4) resulting in activation of Wnt target genes (Barker and Clevers, 2006, Morin et al., 1997). Thus, APC is a key component of the Wnt/β-catenin signalling pathway.

Over the years, *APC*, a gatekeeper gene, has emerged as one of the major drivers of colorectal tumourigenesis. One line of evidence in support of this statement is provided by the tumour suppressor gene *p53*, which is mutated in more than 80% of all CRCs (Baker et al., 1990). Yet patients with mutated *p53* neither develop polyps nor are at a high risk to develop CRC (Garber et al., 1991). Similarly, cells with mutant *KRAS* are quite common in the colonic epithelium, however, these cells have little or no potential to form colorectal tumours (Shpitz et al., 1996). This implies that mutations in other genes do not lead to significant perturbation in growth in the presence of a wild-type *Apc* gatekeeper. However, about 15% of all colorectal

tumours develop independent of an *APC* mutation. Gene fusions involving R-spondin 2 (RSPO2) and R-spondin 3 (RSPO3) occur in about 10% of CRCs and are responsible for sustained activation of WNT signalling in these tumours. Moreover, RSPO2/RSPO3 gene fusions have been found to be mutually exclusive with mutated *APC* (Seshagiri et al., 2012). Similarly, activating mutation in *BRAF* occurs in 10-15% of CRCs and is considered a driver in the serrated pathway (Rad et al., 2013).

More than two decades ago, Fearon and Vogelstein proposed a model identifying the molecular events underlying the initiation and progression of colorectal cancer (Fearon and Vogelstein, 1990) suggesting that, although accumulation of mutations results in a metastatic tumour, these mutations occur at characteristic phases of tumour progression (Figure 5.2). Importantly, they suggested that loss of APC was the initial genetic alteration leading to CRC development.

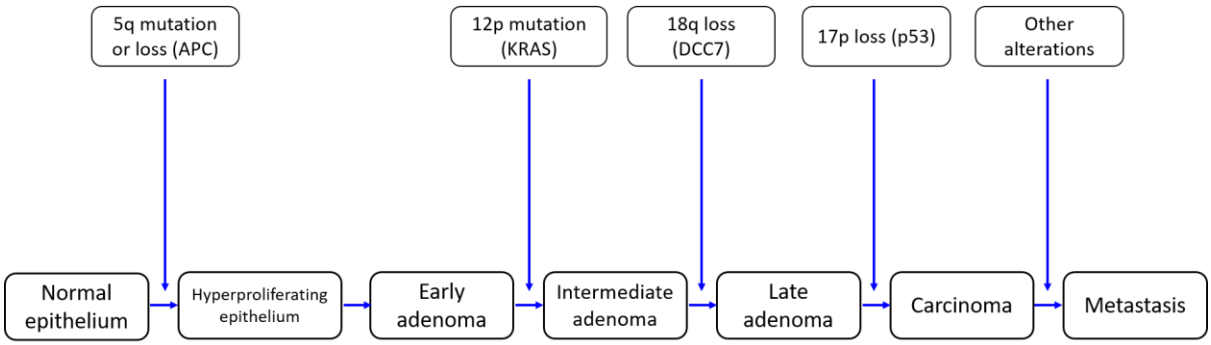

Figure 5.2 Genetic model for colorectal tumourigenesis as proposed by Fearon and Vogelstein. Image adapted from (Fearon and Vogelstein, 1990).

Apc$^{min/+}$, a widely used mouse model for FAP, carries an autosomal dominant mutation in *Apc* (transversion at codon 850) causing premature protein truncation (Moser et al., 1990, Moser et al., 1995). These mice were generated by random mutagenesis using N-ethyl-N-nitrosourea (ENU). These mice are heterozygous for this mutation and develop tumours which are genetically and phenotypically similar to human FAP tumours. Spontaneous loss of heterozygosity (LOH) of the wild type *Apc* allele results in formation of multiple intestinal adenomas in these mice. However, *Apc*$^{min/+}$ mice do not fully mimic the human FAP phenotype as localisation of majority of the adenomas developed in these mice is restricted to the small intestine, while FAP tumours localised to the colon. Moreover, most CRC patients do not show any symptoms of the disease until very late stages, thus, making it essential to model the earliest stages of tumourigenesis.

Conditional inactivation of APC at a given time point allows for the study of the phenotype at an early stage. *Apc*$^{flox/flox}$ mice were first generated by Shibata et al in 1997 by using Cre-loxP-mediated inactivation of *Apc* which resulted in formation of colorectal adenomas (Shibata et al., 1997). Long-term follow up of these mice demonstrated a survival ratio of 5/6 after one year. Pathological analysis revealed invasion of the submucosal layer by tumour cells in about 50% of the tumours which were then diagnosed as adenocarcinomas. Since then, consequences of homozygous deletion of *Apc* using different Cre promoters have been studied in the intestine (Barker et al., 2009, Sansom et al., 2004). Sansom *et al*. employed the Cyp1A promoter which directs Cre activity in the epithelial cells to achieve inducible Cre mediated inactivation of *Apc* in the intestinal epithelium by β-naphthoflavone injection. Disruption of normal intestinal homeostasis, including increased proliferation, altered differentiation, decreased migration and enhanced levels of cell death along with rapid

nuclear localisation of β-catenin was reported. A similar intestinal phenotype was observed following inducible deletion of *Apc* using another epithelial cell-specific promoter-*VillinCreERT2* (Andreu et al., 2005). Cre activity using the *VillinCreERT2* model was induced by tamoxifen injection, resulting in recombination in the intestinal epithelium (el Marjou et al., 2004). However, homozygous deletion of *Apc* under the control of Villin- and Ah-Cre recombinases causes a severe intestinal phenotype (by as early as day 5) in these mice resulting in very short survival periods. Therefore, these mice do not develop tumours. A possible solution would be to use a promoter which is only expressed in a sub-population of epithelial cells, resulting in subset-specific gene recombination in cells, and not the entire epithelium. One such example is the *Lgr5CreERT2* system which targets recombination in the intestinal $Lgr5^{+}$ stem cells (Barker et al., 2007).

It is also important to note here that the *Lgr5CreERT2* system leads to mosaic expression of the CreERT2 protein, hence recombination does not occur in all the $Lgr5^{+}$ stem cells. Barker and colleagues studied the consequences of conditional deletion of *Apc* ($Apc^{flox/flox}$) in intestinal stem cells (ISCs) using the Lgr5-EGFP-IRES-CreERT2 knockin mice crossed to or $Apc^{flox/flox}$ mice (Cre activity induced by a single i.p. injection of tamoxifen) *versus* Cre mediated deletion of *Apc* in the short-lived transit amplifying (TA) cell population (AhCre $Apc^{flox/flox}$ mice, Cre activation induced by oral administration of β-Naphthoflavone). Loss of *Apc* in ISCs resulted in tumour formation at around 4-5 weeks, however, no adenomas were observed when *Apc* was inactivated in the TA cells, implying that the ISCs are the cells of origin of intestinal cancer. Targeting the intestinal stem cells to model colon cancer development allows to precisely study the early stages of tumourigenesis in mice.

Numerous studies have now shown that mutation of *APC* is a crucial early event in tumourigenesis and the contribution of other oncogenes/tumour suppressor genes are often only revealed in the context of an *Apc* mutation. A number of studies have investigated the role of other genes in an APC deficient setting in mouse models of CRC (Table 5.2). Sansom and colleagues studied the role of *K-ras*, a gene mutated in 40-50% of CRCs at a relatively early stage (Bos et al., 1987), and observed that mutation in *K-ras* alone has no effect on intestinal homeostasis (Sansom et al., 2006). However, combining *Apc* loss and oncogenic mutation of *K-ras* was shown to accelerate tumourigenesis and resulted in increased invasiveness in the intestine. Out of the 100 tumours analysed in the β-naphthoflavone inducible $AhCre^{+/T}$ $K\text{-}ras^{+/LSLV12}$ $Apc^{+/flox}$ triple mutants, 17 tumours showed morphological evidence of invasion into the smooth muscle layer and were diagnosed as adenocarcinomas.

p53 has been postulated to be involved in more advanced stages of colorectal carcinogenesis (Fearon and Vogelstein, 1990). However, loss of *p53* alone is not sufficient to initiate intestinal tumourigenesis (Schwitalla et al., 2013). In addition, Reed and colleagues studied the consequences of *p53* deficiency upon *Apc* loss in the intestine and reported that the aberrant phenotype observed following *Apc* inactivation (rapid nuclear localisation of β-catenin, perturbed cell death, proliferation) is not significantly altered by loss of p53, suggesting that *p53* status has little impact on the initiating stages of this disease (Reed et al., 2008). Loss of *Pten*, a tumour suppressor gene which is mutated in 5-14% of CRCs (Berg et al., 2010), has no effect on normal intestinal homeostasis but accelerates tumourigenesis when coupled with *Apc* deficiency (Marsh et al., 2008). *AhCreERT* $Pten^{flox/flox}$ $Apc^{flox/+}$ mice developed adenocarcinomas which invaded through the muscularis propria of the small intestinal wall and into the peritoneal serosa. This was in contrast to the lesions observed in the *AhCreERT*

Pten$^{+/+}$ *Apc*$^{flox/+}$ control mice, which were benign and non-invasive intramucosal adenomas. Although *APC* is one of the major drivers of colorectal tumourigenesis, these studies reinforce the contribution of other genes to cancer development.

Table 5.2 Examples of genes studied in context of different Apc mutations with description of the location of adenomas and effect on tumour burden and invasion. Adapted from a review by Young *et al*. (Young et al., 2013)

Model	Gene mutated	Phenotype	Reference
Apc$^{min/+}$	Smad3	Increase in number of adenomas, particularly in the distal colon	(Sodir et al., 2006)
Apc$^{min/+}$	Ephb2	Presence of invasive intestinal adenomas	(Batlle et al., 2005)
Apc$^{min/+}$	Ephb3	Presence of invasive intestinal adenomas and increase in size and number of polyps in the colon	(Batlle et al., 2005)
Apc$^{1638N/+}$	TGF-β receptor II	No significant difference in the number of neoplastic lesions than *Apc*$^{1638N/+}$ but with drastic increase in proportion of lesions categorised as advanced, high grade adenocarcinomas	(Munoz et al., 2006)
Apc$^{\Delta 716/+}$	Smad4	Presence of small intestinal adenomas that invade into the stroma	(Takaku et al., 1998)
Apc$^{flox/+}$	Pten and K-ras	Presence of more invasive tumours	(Davies et al., 2014)
Apc$^{flox/flox}$	K-ras	Accelerated intestinal tumourigenesis and presence of invasive adenomas	(Sansom et al., 2006)
Apc$^{flox/flox}$	p53	Little or no impact on intestinal tumourigenesis	(Reed et al., 2008)
Apc$^{flox/flox}$	Pten	Rapid development of adenocarcinoma	(Marsh et al., 2008)
Apc$^{flox/flox}$	C-myc	Loss of *C-myc* rescues the phenotypes associated with inactivation of *Apc*	(Sansom et al., 2007)

Experimental data in Chapter-3 demonstrated that SNAI1 is upregulated in CRC and its expression correlates with ISCs markers. Previous studies in our laboratory have shown that SNAI1 co-localises with LGR5 in mouse small intestine (Horvay et al., 2011) and ectopic expression of *Snai1* in the small intestinal tissue promotes expansion of the ISC population and increased proliferation in these mice (Horvay et al., 2015). However, in context of cancer, very little is known about the role of *Snai1* particularly in the early stages of colorectal tumourigenesis. Activation of *Snai1* expression in the epidermis has been shown to cause epidermal hyperproliferation and induction of spontaneous tumours in the skin (De Craene et al., 2014). Furthermore, expression of *Snai1* in a skin-specific *p53*-null background (Cre mediated deletion of exons 2-10 in the germline, $Trp53^{flox/flox}$) results in accelerated tumourigenesis and more aggressive carcinosarcomas which metastasised to the lungs. Endogenous expression of SNAI1 and SNAI2 have been studied in context of breast cancer by FACS sorting $Snai1^{+}$ and $Snai2^{+}$ cells using knockin IRES-YFP reporters for *Snai1* and *Snai2* (Ye et al., 2015). Snai1-YFP expression was detected in early-stage mammary gland lesions in a transgenic mouse model of mammary cancer. Although SNAI1 is absent in normal mammary epithelial cells, its expression has been shown to be tightly associated with a tumour-initiating cell phenotype in breast cancer (Ye et al., 2015). Although *Snai1* has been essentially described as a critical driver of tumour metastasis, these recent data suggest that it may also play a critical role in driving tumour initiation.

5.1.2 Mouse models used in the study

5.1.2.1 *Lgr5-EGFP-IRES-CreERT2*

Lgr5-EGFP-IRES-CreERT2 is an inducible Cre recombinase (Cre is bound to the mutated ligand-binding domain of the oestrogen receptor) that allows visualisation of $Lgr5^{+}$ stem cells and also mediates recombination of target genes in the $Lgr5^{+}$ cells at any chosen time (Barker et al., 2007). The *Lgr5* promoter drives the expression of the EGFP cassette that allows intestinal stem cells to be traced (Figure 5.3). The inducible system allows Cre recombinase to be translocated into the nucleus of the $Lgr5^{+}$ intestinal stem cells to induce recombination. The *Lgr5CreERT2* model has been previously used to induce loss of *Apc* in the $Lgr5^{+}$ stem cells in the small intestine and colon. We took advantage of the mosaic pattern of Cre activity associated with the Lgr5 promoter to induce *Apc* deletion. *Lgr5CreERT2* $Apc^{flox/flox}$ have been shown to survive up to 36 days (Barker et al., 2009) and this allows examination of polyp formation in its early stages.

Figure 5.3 Schematic diagram showing the *Lgr5CreERT2* construct. UTR, untranslated region; EGFP, enhanced green fluorescent protein; IRES, internal ribosome entry site.

5.1.2.2 *Cdx2CreERT2*

Cdx2CreERT2 is an inducible Cre recombinase driver (Figure 5.4) which directs Cre activity and subsequent deletion of the floxed target sequence in the large intestine (Feng et al., 2013).

These mice were utilised in this chapter to direct polyp formation in the colon following loss of *Apc* and *Snai1* up-regulation.

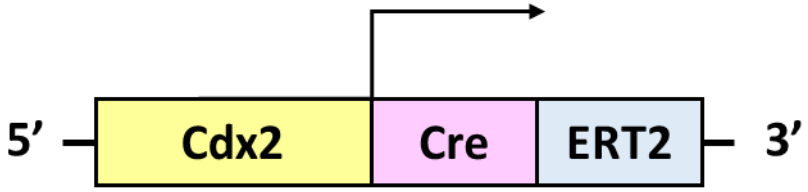

Figure 5.4 Schematic representation of the *Cdx2CreERT2* construct.

5.1.2.3 *Apc$^{flox/flox}$*

Inactivation of *Apc* was achieved by using a conditional allele where a pair of loxP sites were inserted into introns 13 and 14 of the *Apc* gene (Shibata et al., 1997). Cre-mediated recombination deletes a region encompassing exon 14 of *Apc* which produces a frameshift mutation at codon 580, resulting in a truncated non-functional protein (Figure 5.5). Loss of *Apc* was induced in different intestinal cell populations in mice using both the Lgr5Cre and Cdx2Cre driver lines.

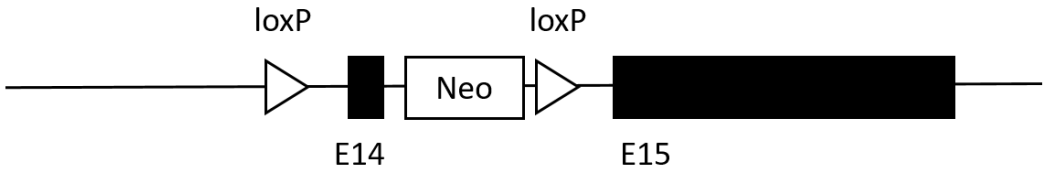

Figure 5.5 Schematic diagram showing the structure of the conditionally targeted allele of *Apc^{580s}*.

5.1.2.4 *Rosa26Snai1*

As discussed in the previous chapters, these mice were generated by conditionally targeting the ROSA26 locus. The construct contains a STOP cassette flanked by two LoxP sites, a *Snai1*

cassette and an IRES-eGFP cassette in exon 1 (Figure 5.6). Cre mediated deletion of the STOP cassette enables transcription of the Snai1-IRES-eGFP mRNA (Nyabi et al., 2009). To study *Snai1* function during early stages of tumourigenesis, *Snai1* up-regulation was coupled with loss of *Apc* in mice using two different intestine-specific Cre drivers.

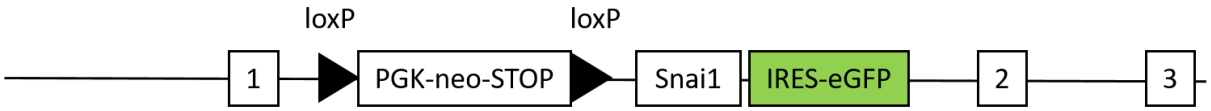

Figure 5.6 Schematic diagram showing the structure of the conditionally targeted *ROSA26* allele.

5.1.3 Significance of this study

Numerous studies so far have proposed that *Snai1* plays a role in cancer metastasis as it is one of the key regulators of epithelial-mesenchymal transition (EMT). However, its role in the early stages of tumourigenesis still needs to be explored. Inducing concomitant loss of *Apc* and *Snai1* up-regulation specifically in the ISCs will help us understand the role of *Snai1* in early stages of intestinal tumourigenesis. This study investigates whether *Snai1* expression is sufficient to accelerate initiation of intestinal polyposis in *Apc* deficient mice.

5.1.4 Hypothesis

This chapter investigates the hypothesis that upregulation of *Snai1* during the initiating stages of intestinal polyposis accelerates polyp formation and polyp growth.

5.2 Results

5.2.1 Analysis of polyp formation in *Lgr5CreERT2 Apc$^{flox/flox}$* (control) and *Lgr5CreERT2 Apc$^{flox/flox}$ RosaSnai1* (test) mice

Conditional deletion of *Apc* in the intestinal stem cell population using the *Lgr5-EGFP-IRES-CreERT2* knockin mice has been previously shown to result in formation of polyps throughout the small intestine and colon (Barker et al., 2009). Cohorts of *Lgr5CreERT2 Apc$^{flox/flox}$* control and *Lgr5CreERT2 Apc$^{flox/flox}$ RosaSnai1* test mice were injected with four daily injections of tamoxifen. Cre-mediated recombination was expected to result in deletion of *Apc* (control and test group) along with expression of the *Snai1* transgene (test group only) in the Lgr5^{+} stem cells in the small intestine and colon. Small intestinal and colonic tissues were harvested on day 36. Polyp formation was observed throughout the intestinal tract in both control and test groups (Figure 5.7) as expected.

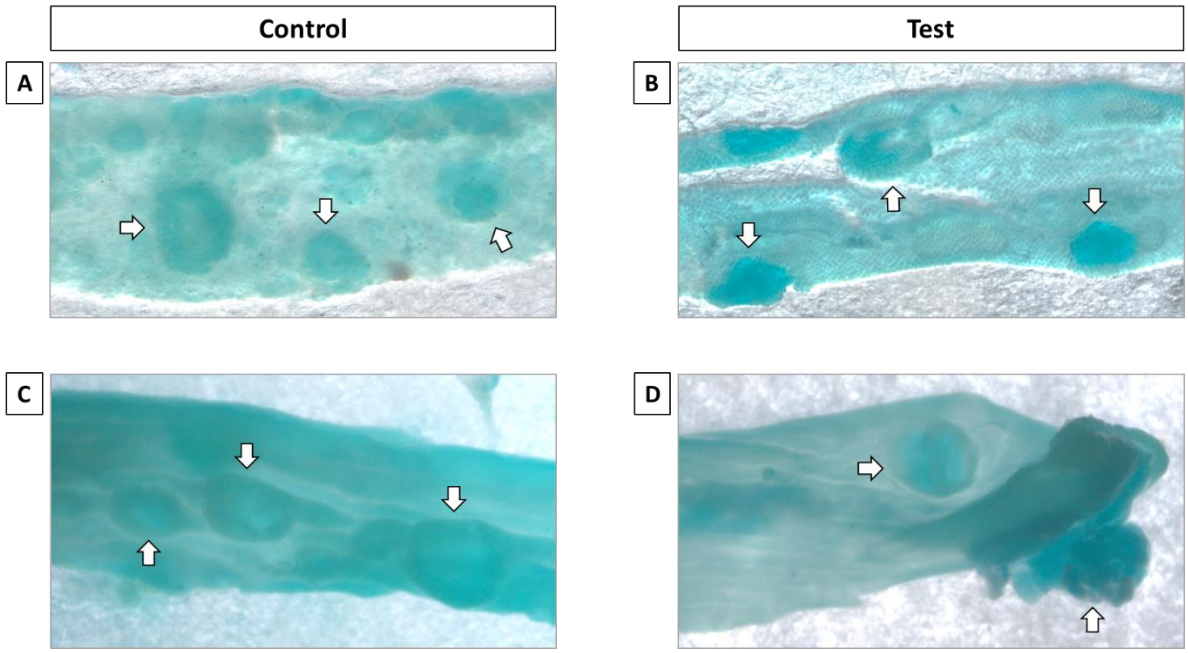

Figure 5.7 Representative images of polyps found in *Lgr5CreERT2 Apc*$^{flox/flox}$ control mice (A) small intestinal and (C) colonic tissue and *Lgr5CreERT2 Apc*$^{flox/flox}$ *RosaSnai1* test (B) small intestine and (D) colon. On day 36 post induction with tamoxifen, intestinal tissues were stained with methylene blue to highlight polyps (marked by white arrows). Both control and test mice developed numerous polyps throughout the small intestine and colon. Magnification 6.4x.

The number of polyps along the intestinal tract was quantified and we observed that it was highest in the distal end of the small intestine in both control and test mice (Figure 5.8 (A)), suggesting highest recombination efficiency in this region of the intestinal tract. However, coupling *Apc* loss with a conditional activation of the *Snai1* transgene in the intestinal stem cell population in mice did not accelerate polyp formation. There was no significant difference in the number of polyps observed in the colonic tissues isolated from test mice when compared to the control group (Figure 5.8 (A) and (B)). Similar results were found in the proximal and distal regions of the small intestinal tissues, where no significant difference in polyp number was observed in different parts of the small intestine in the test *versus* control mice. Overall, majority of the polyps in both control and test groups were localised in the

small intestinal tissues rather than colon. This is similar to other reports using this Cre model but does not accurately model adenoma formation in FAP patients where adenomas predominantly form in the colon (Table 5.3).

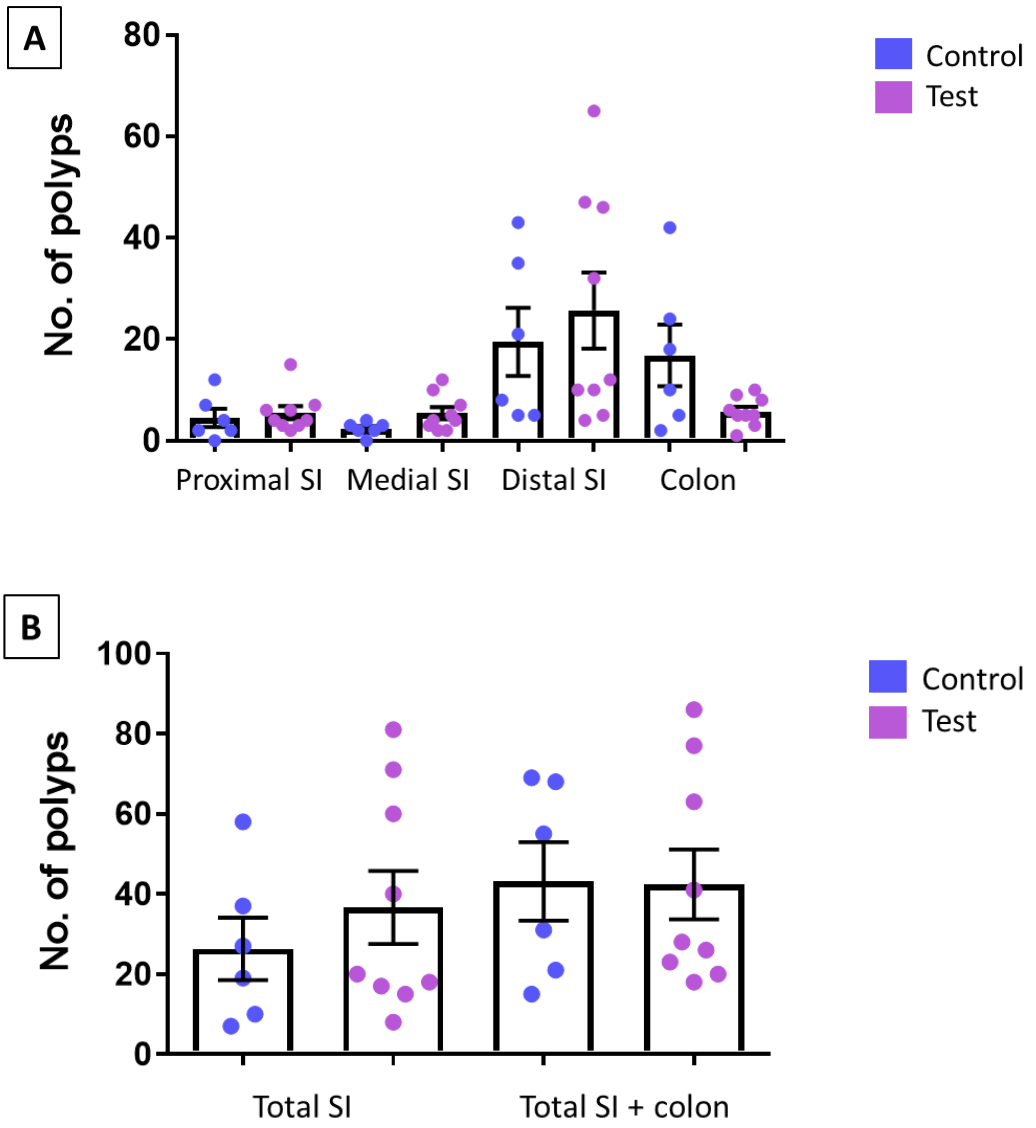

Figure 5.8 Potential *Snai1* overexpression has no effect on the number of polyps formed in the test mice. Average number of polyps in (A) different parts of small intestine and colon and (B) overall small intestine and small intestine and colon combined in control (n=6) and test groups (n=9). No significant difference in polyp number was observed between control and test tissues. Data was analysed by (A) two-way ANOVA and (B) unpaired t-test and is represented as the mean ± SEM.

Table 5.3 Summary of localisation of polyps in the intestinal tract in control and test mice

Mouse genotype	Number of polyps					
	Proximal SI	Medial SI	Distal SI	Colon	Total no. of polyps per SI	Total no. of polyps
Lgr5CreERT2 Apc$^{fl/fl}$	12	3	43	10	58	68
	7	4	8	2	19	21
	4	2	21	42	27	69
	2	3	5	5	10	15
	2	0	5	24	7	31
	0	2	35	18	37	55
Lgr5CreERT2 Apc$^{fl/fl}$ RosaSnai1	4	4	10	5	18	23
	7	3	5	5	15	20
	3	4	10	9	17	26
	2	2	4	10	8	18
	6	2	32	1	40	41
	15	10	46	6	71	77
	6	7	47	3	60	63
	3	5	12	8	20	28
	4	12	65	5	81	86

5.2.2 *Snai1* transgene does not affect polyp growth

In order to assess the effects of *Snai1* expression on growth of polyps in the intestinal tract, polyp size was measured. As the number of polyps observed was highest in the distal small intestine, size of polyps present in the distal small intestine and colon was measured. Interestingly, polyps present in the distal SI of both control and test mice were significantly larger ($p<0.05$) than their colonic counterparts (Figure 5.9 (A) and (B)). On the other hand, no significant difference in the average polyp size was observed when comparing control versus test polyps in the distal small intestine and colon (Figure 5.10 (A) and (B)). Data were analysed by unpaired t-test and $p<0.05$ was considered as significant. This suggests that *Snai1* overexpression in polyps may not be sufficient to accelerate their growth in either the small intestine or colon.

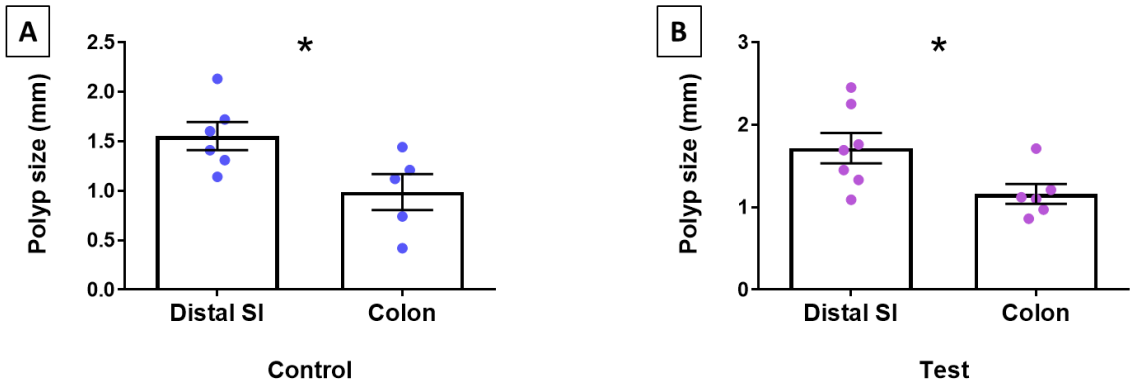

Figure 5.9 Distal small intestine is the site for larger polyps. Average polyp diameter (mm) in (A) control (p=0.03) and (B) test (p=0.03) distal SI (n=6 and 7 respectively) and colonic (n=5 and 6 respectively) tissues. Data were analysed by unpaired t-test for both distal SI and colon and represented as the mean ± SEM.

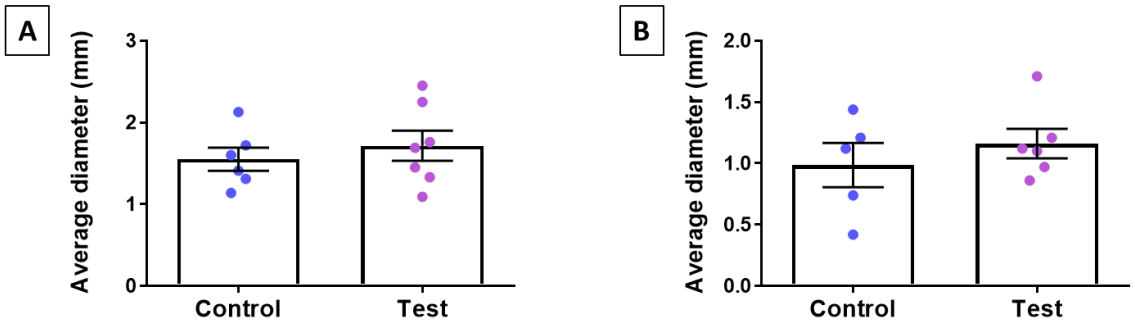

Figure 5.10 *Snai1* overexpression does not affect polyp growth in the distal SI and colon. Average polyp diameter in (A) distal SI and (B) colon in control (n=6 and 5 respectively) vs test (n=7 and 6 respectively) mice. No significant difference in polyp growth was observed in both distal SI and colon. Data were analysed by unpaired t-test and represented as the mean ± SEM.

5.2.3 *Snai1* transgene does not favour growth of either small or large polyps

Although the average polyp size was not affected by *Snai1* overexpression in the test group, sub-grading polyps into three groups based on size (small, medium and large) was conducted in order to determine whether *Snai1* affects the initial growth of small lesions or supports the growth of large polyps. No significant difference in polyp growth was observed when comparing small, medium and large polyps in the control and test group in both the distal SI and colonic tissues (Figure 5.11 (A) and (B)). Data were analysed by unpaired t-test and $p<0.05$ was considered as significant.

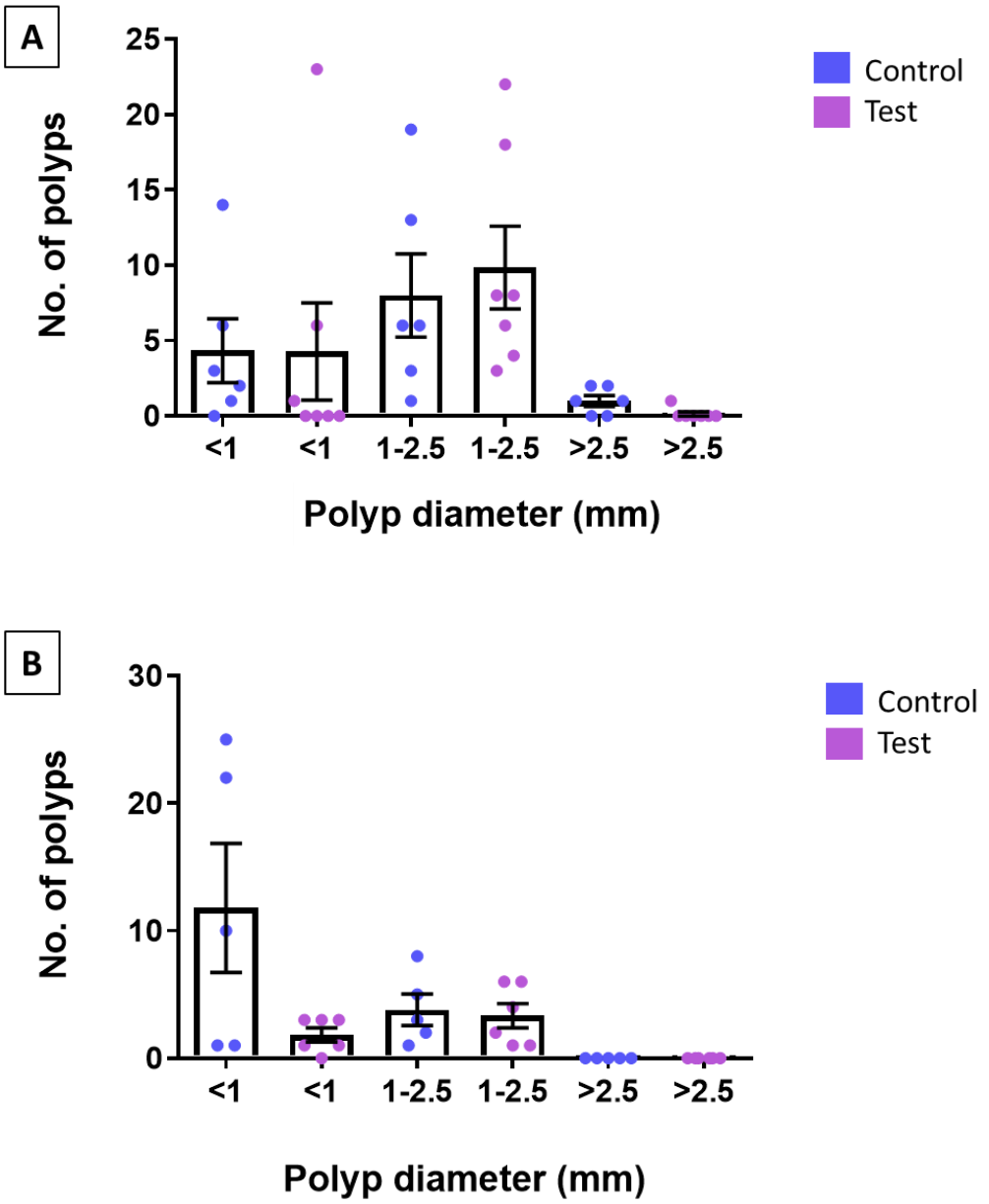

Figure 5.11 *Snai1* transgene does not favour growth of polyps in either distal SI or colon. Sub-grading polyps in (A) distal SI (n=6 and 7 respectively) and (B) colon (n=5 and 6 respectively) into three groups (small, <1 mm; medium, 1-2.5 mm; large >2.5 mm) based on size. Data were analysed by unpaired t-test and represented as the mean ± SEM.

5.2.4 Analysis of *Snai1* expression in polyps formed in the colon

To confirm *Snai1* upregulation in test mice, polyps observed in the colonic tissues of control and test mice (n=3 each) were dissected using a surgical blade and processed for RNA extraction followed by reverse transcription. The expression of *Snai1* and *β-actin*, a housekeeper gene, was analysed by PCR (Figure 5.12). As previously determined, a *Snai1* overexpressing small intestinal sample was used as positive control and a sample without cDNA was used as negative control. PCR analysis revealed that the cDNA transcribed from RNA isolated from the polyps in control and test groups was of poor quality and hence could not be amplified. Droplet Digital PCR (ddPCR) analysis examining the expression of *Snai1* in the control and test polyps revealed similar results as the *Snai1* expression could not be detected in these samples. This may be due to the quality of RNA isolated from the paraffin fixed tissues. Due to these technical issues, *Snai1* overexpression in the *Lgr5CreERT2 Apc*$^{flox/flox}$ *RosaSnai1* experimental group could not be confirmed by PCR. Histological analysis of polyp tissues by immunofluorescence using an anti-GFP antibody to detect Snai1-eGFP revealed detection of very few GFP^{+} cells in polyps indicating that there may not be a sufficient up-regulation of *Snai1* expression in these tissues using the *Lgr5CreERT2* model (Figure 5.13). As I could not confirm effective up-regulation of *Snai1* in this model, the function of *Snai1* in modulating polyp formation could not be accurately determined. I, therefore, decided to examine another model for this study.

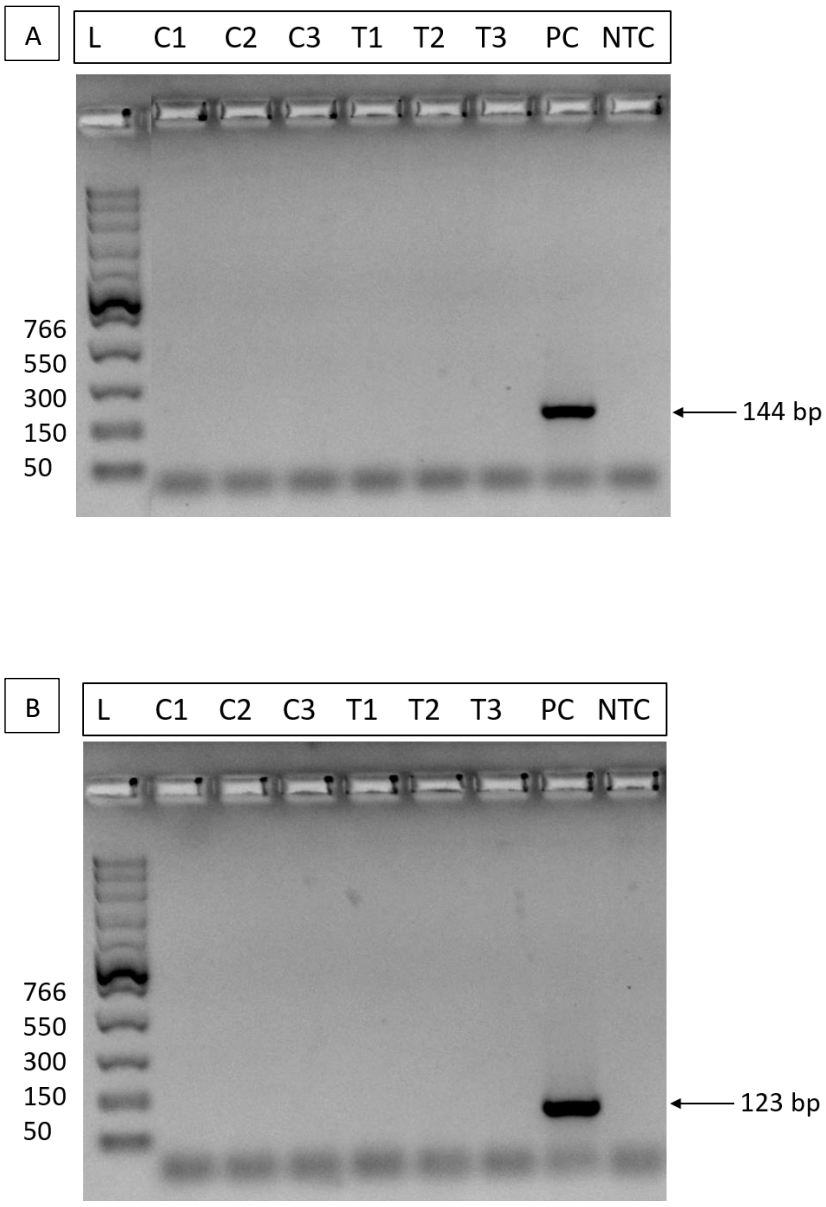

Figure 5.12 PCR analysis of cDNA from polyps dissected from control (C1, C2, C3) and test (T1, T2, T3) groups examining the expression of (A) *Snai1* and (B) *β-actin* compared to positive control (PC) and no template control (NTC). Failure to amplify the housekeeper gene (β-actin) in both control and test polyps may be due to poor quality of the cDNA samples.

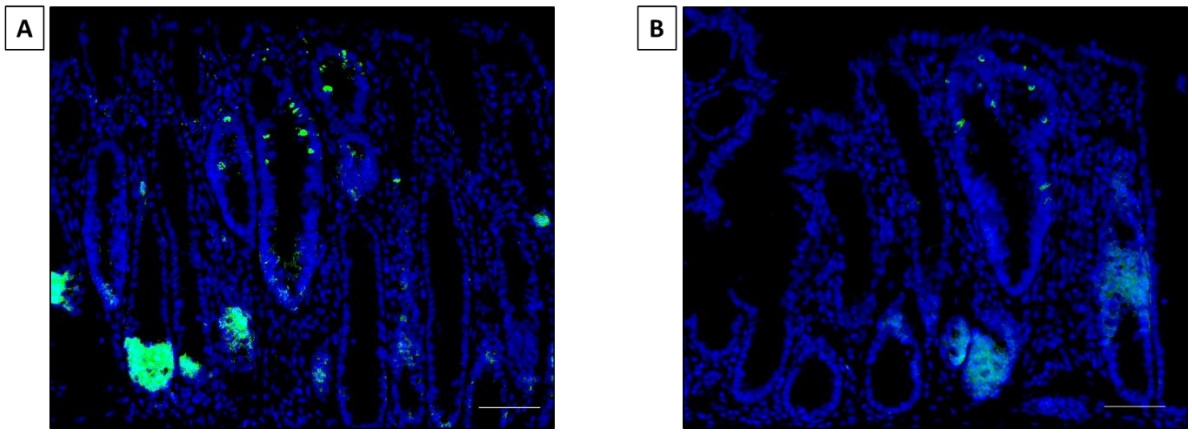

Figure 5.13 Insufficient *Snai1* up-regulation in *Lgr5CreERT2 Apc$^{flox/flox}$ RosaSnai1* mice. Representative fluorescent images of colonic polyps cross-sections from two different test mice showing Snai1-eGFP^{+} (green) cells counterstained with DAPI (blue). Scale bars 50 µm.

5.2.5 Analysis of polyp formation in *Cdx2CreERT2 Apc$^{flox/flox}$ RosaSnai1* mice

The above observations indicate that the Lgr5-Cre driver directs polyp formation preferentially in the small intestine with relatively fewer polyps formed in the colon. More importantly, this system failed to induce sufficient *Snai1* up-regulation in the polyps. Hence, a more colon-specific promoter, Cdx2, was chosen for analyses of *Snai1* function in colonic polyposis in mice. Control *Cdx2CreERT2 Apc$^{flox/flox}$* and test *Cdx2CreERT2 Apc$^{flox/flox}$ RosaSnai1* mice were injected with three daily doses of tamoxifen. Tissues were harvested when mice developed symptoms of sickness (average day 27) including loss of body weight, abdominal swelling, hunched appearance and/or rectal bleeding. Polyps were harvested from *Cdx2CreERT2 Apc$^{flox/flox}$ RosaSnai1* colon tissues expressing the *Snai1* transgene and compared to *Cdx2CreERT2 Apc$^{flox/flox}$* control polyps. Of note, no polyp growth was observed in the small intestinal tissues. To analyse *Snai1* expression in the control and test colonic polyps, ddPCR was performed using RNA isolated from snap frozen polyps. No significant up-regulation of *Snai1* expression was observed in polyps collected from the test group compared to control

(Figure 5.14). One possible explanation for this could be that the proportion of Snai1^{+} cells in the test polyps chosen for ddPCR analysis may be very limited, as a result expression of the *Snai1* transgene may be diluted. Hence, the overall expression of *Snai1* in the test polyps was comparable to the controls.

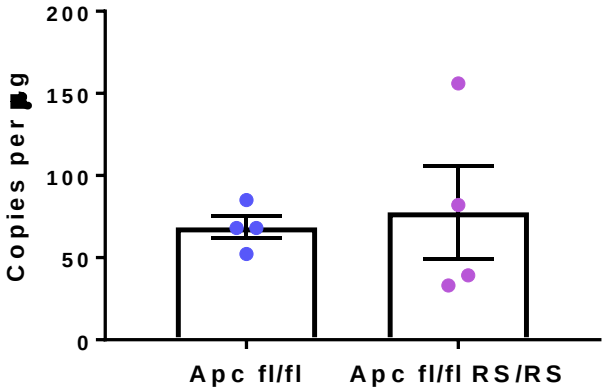

Figure 5.14 ddPCR analysis revealed that control and test polyps exhibited no significant difference in *Snai1* expression. *Snai1* mRNA expression in test group (*Cdx2CreERT2 Apc$^{flox/flox}$ RS/RS*) compared to control (*Cdx2CreERT2 Apc$^{flox/flox}$*), p = 0.7702 (n = 4 each). Data was analysed by unpaired t-test and is represented as the mean ± SEM.

As *Snai1* up-regulation in the polyps could not be confirmed at the RNA level, I decided to investigate whether SNAI1-expressing cells could be detected in the polyps. The RosaSnai1 construct contains an eGFP cassette which allows visualisation of cells with up-regulated SNAI1 via GFP expression. Histological examination of colonic tissues in the test group was carried out in order to assess the presence of the *Snai1* transgene in polyps. Indeed, *Snai1* transgene expression was detected in polyps indicated by expression of GFP (Snai1-eGFP) analysed by immunofluorescence (Figure 5.15). Expression of Snai1-eGFP allows tracing of

the recombined cells within a polyp and has proven highly valuable in the current study in the analyses of specific regions within polyps which express the *Snai1* transgene.

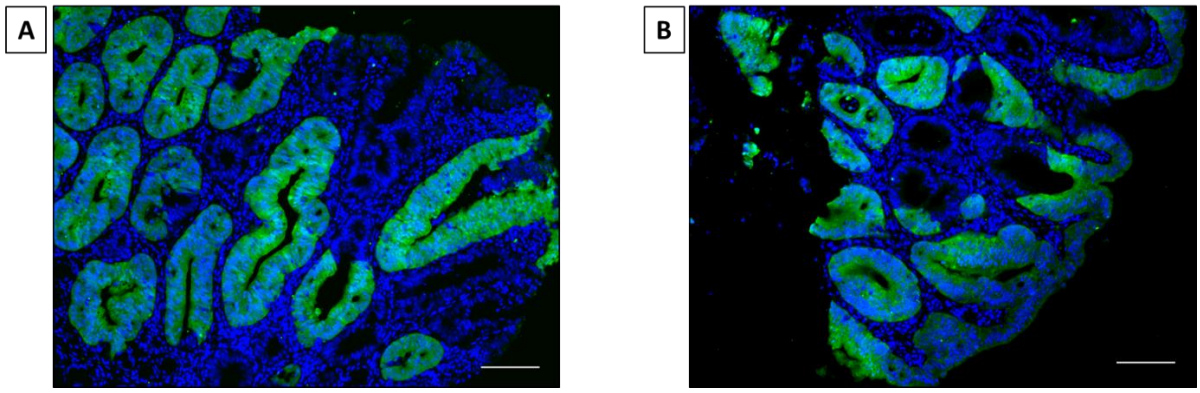

Figure 5.15 Successful *Snai1* up-regulation in polyps. Representative fluorescent images showing *Snai1*-eGFP transgene expression in colonic tissue cross-sections from *Cdx2CreERT2 Apc$^{flox/flox}$ RosaSnai1* mice. Sections were incubated with an anti-GFP antibody and counter-stained with DAPI. Scale bars 50 µm.

Following successful demonstration that *Snai1* expression could be induced in test tissues, the quantification of polyp number throughout the length of the colon was conducted in both control (n = 4) and *Snai1* transgene-expressing (n = 6) mice. Overall, the test mice presented with a higher number of polyps in the colon with an average of 46 polyps compared to 35 polyps for the control group, however, this difference was not significant as shown in Figure 5.16.

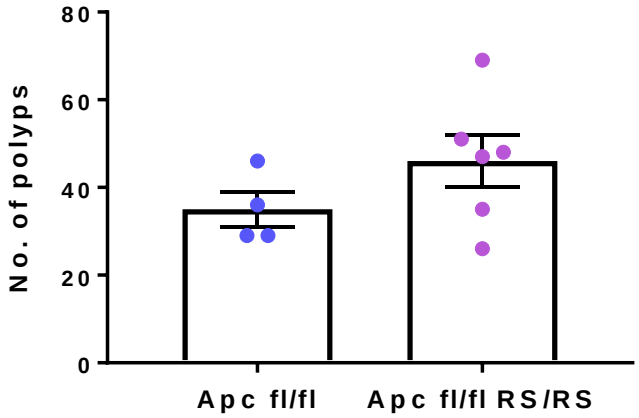

Figure 5.16 *Snai1* transgene expression does not affect polyp count in the colon. No significant difference (p=0.1669) in number of polyps in control (n=4) versus test (n=6) mice was observed. Data was analysed by unpaired t-test and is represented as the mean ± SEM.

5.2.6 Expression of *Snai1* transgene results in larger polyps

To determine if *Snai1* transgene affects polyp growth, diameter of polyps formed in both control and test colonic tissues was measured by imaging of whole mount preparations of colons from mice. The diameter of polyps was measured using AxioVision Rel. 5.0 software as described in Chapter 2 (Section 2.8). Overall, polyps over-expressing *Snai1* were significantly bigger in size compared to the control polyps (p= 0.0467) (Figure 5.18). The average polyp diameter in the test group was 0.58 mm, which was slightly higher than the average diameter of control polyps (0.48 mm). Data was analysed by student's unpaired t-test and $p<0.05$ was considered as significant. Representative images showing polyps formed in the colon of control and test mice are shown in Figure 5.17.

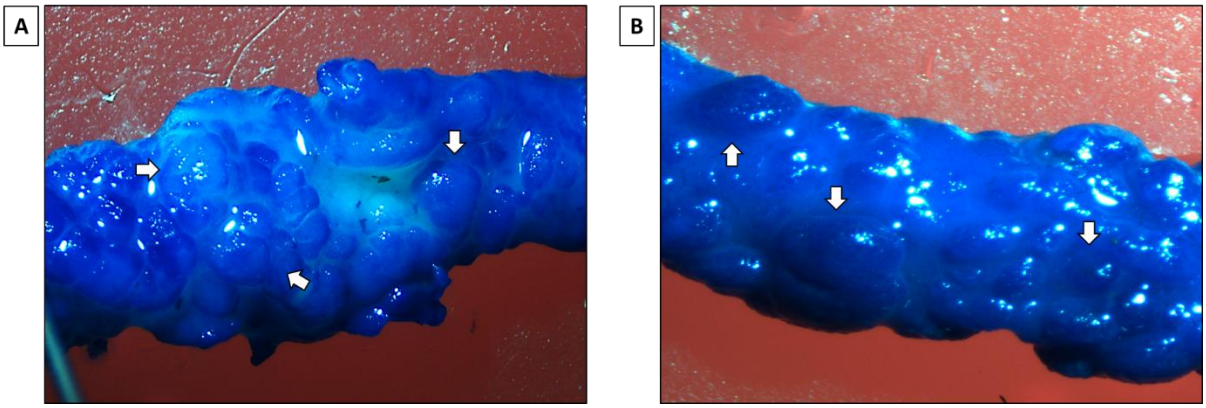

Figure 5.17 Representative images of colonic tissues with polyps isolated from (A) *Cdx2CreERT2 Apc*$^{flox/flox}$ (control) and (B) *Cdx2CreERT2 Apc*$^{flox/flox}$ *RS/RS* (test) mice. Tissues were harvested from the animals around the day 30 time-point and stained with methylene blue prior to imaging. Numerous polyps (marked by white arrows) were observed in both groups. Magnification 6.4x.

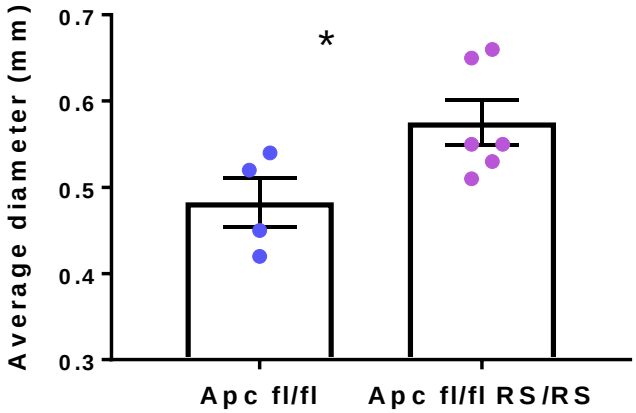

Figure 5.18 Expression of *Snai1* transgene promotes growth of polyps. Significantly larger polyps (p = 0.0467) were observed in colonic tissues of test mice (n=6) overexpressing *Snai1* compared to control mice (n=4). Data was analysed by unpaired t-test and is represented as the mean ± SEM.

5.2.7 Analysis of cell proliferation in mice expressing the *Snai1* transgene

As shown above, mice expressing the *Snai1* transgene formed larger polyps. Hence, the next step was to examine cell proliferation in these mice. Two hours prior to culling, mice were injected with BrdU to enable analysis of cell proliferation in these mice. Upon staining with anti-BrdU and anti-GFP antibody (and counter-staining with DAPI), the number of $BrdU^+$ cells was counted in the polyps. On comparing the number of actively proliferating cells in recombined (GFP^+) versus non-recombined (GFP^-) regions within test polyps, it was found that regions expressing the *Snai1* transgene harboured a significantly higher number of $BrdU^+$ cells while regions of the polyps negative for the *Snai1* transgene had fewer proliferating cells (Figures 5.19 and 5.20). The average number of $BrdU^+$ cells per 0.01 mm^2 of GFP^+ polyp area was 76 cells whereas for GFP^- polyps the average number of $BrdU^+$ cells was 65. Data was analysed by student's paired t-test and $p<0.05$ was considered as significant. Figure 5.20 (A) and (B) shows representative images of colonic polyps from a test animal expressing the Snai1 transgene and stained for BrdU, GFP and DAPI.

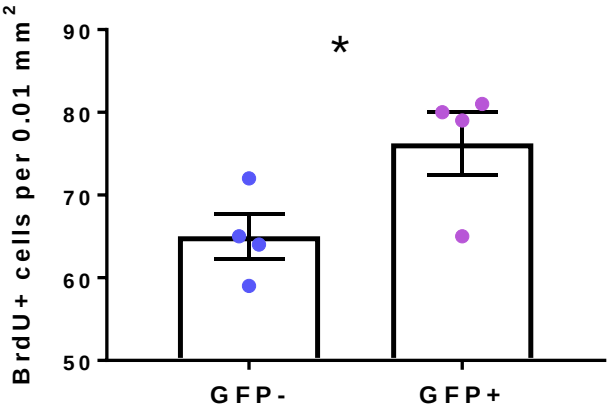

Figure 5.19 Over-expression of *Snai1* in polyps promotes cell proliferation. Number of $BrdU^+$ proliferative cells per 0.01 mm^2 GFP^- versus GFP^+ polyp area (n= 4). Data was analysed by paired t-test and is represented as the mean ± SEM.

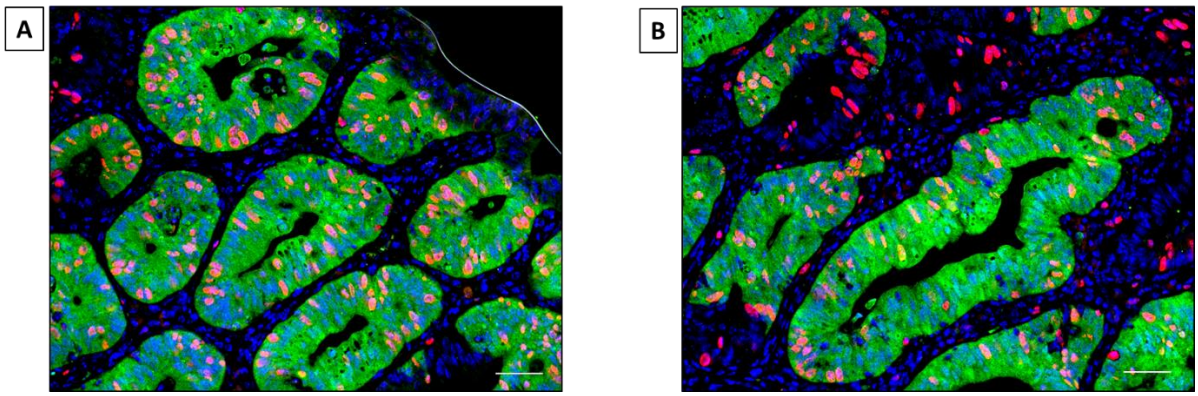

Figure 5.20 Polyp regions over-expressing *Snai1* harbour more proliferative cells. Representative co-immunofluorescence images of colonic polyps from two different mice (A) and (B) showing the $BrdU^+$ proliferative cells (red) and Snai1-$eGFP^+$ expressing cells (green) counterstained with DAPI (blue). Scale bars 20 µm.

5.3 Discussion

5.3.1 Caveats of the mouse models

The *Apc*$^{flox/flox}$ mouse model of colon cancer has proven advantageous over the *Apc*$^{min/+}$ mice as it allows for inactivation of the *Apc* gene at a known time-point, thus enabling investigation into the early stages of intestinal tumourigenesis. However, these mouse models do not completely recapitulate the human CRC phenotype. A commonly encountered problem is the failure to produce advanced and metastatic tumours in these mice. This is in part due to the short lifespan of mice and also the high tumour burden which these mutations lead to. Another fundamental issue in modelling CRC in mice is the location of tumours formed. Bowel cancer patients develop tumours predominantly in the colon whereas loss of *Apc* in these mice results in formation of a high number of tumours in the small intestine.

It is important to note that selective silencing of the mutant allele occurs in the *Lgr5-EGFP-IRES-CreERT2* mice which leads to mosaic pattern of the CreERT2 protein expression in intestinal crypts (Barker et al., 2007), resulting in target sequence deletion only in approximately 10% of Lgr5^{+} stem cells. In addition, the *Lgr5CreERT2* transgene is expressed at a much lower frequency in the mouse colon than it is in the small intestinal crypts (Barker et al., 2007). This explains the differences in number of polyps observed in the small intestinal and colonic tissues arising due to higher recombination efficiencies in the small intestine compared to the colon in both control and test groups.

Although homozygous deletion of *Apc* in mice under the control of the Lgr5-Cre enables study of the early stages of polyposis, the majority of these polyps are localised in the small intestine (Barker et al., 2009). This was confirmed by findings in this study. Barker and colleagues have

also reported differences in kinetics of clone formation in the small intestine and colon using the *Lgr5CreERT2-Rosa26-lacZ* mice (Barker et al., 2007). Tamoxifen induced Cre activity in $Lgr5^{+}$ stem cells results in irreversible LacZ expression in the progeny of the recombined stem cells. Day 5 post tamoxifen induction, LacZ staining in the colon was still restricted to the crypt bottom, whereas, in the small intestinal crypts $LacZ^{+}$ cells were detected relatively higher along the length of the crypts. This implies that the colon stem cells are more quiescent than their small intestinal counterparts. Another possible explanation for this distribution could be the difference in the number of $Lgr5^{+}$ stem cells present in small intestine and colonic tissues in mice. Short-term clonal tracing analysis of individually labelled $Lgr5^{hi}$ cells (using a *Lgr5-EGFP-IRES-creERT2* allele in conjunction with the R26R-Confetti reporter) has revealed that crypts of the small intestine contain, on an average, 14 $Lgr5^{hi}$ cells (Snippert et al., 2010). Although similar experiments in the mouse colon have not been performed so far, it has been suggested that there relatively fewer $Lgr5^{+}$ stem cells in the colon (Barker et al., 2007). A higher number of $Lgr5^{+}$ cells in the small intestine increases the number of probable recombination events that can occur, resulting in higher number of polyps when *Apc* is inactivated in these cells in mice. A more recent study using the *Lgr5CreERT2* mice reported localisation of adenomas in the small intestine of mice overexpressing RSPO3 (a secreted protein that potentiates *Wnt* signalling in the intestine) as compared to the colon (Hilkens et al., 2016). In the set of experiments conducted in my study, the distal site of the small intestine was found to have the highest number of polyps. There was also no definitive evidence that *Snai1* expression was efficiently induced in polyps using this model. This is possibly due to the expression level of the Cre recombinase driven by the Lgr5 promoter. Overall, the *Lgr5CreERT2* model was not an effective way to examine co-operation between

Apc and *Snai1* in promoting tumorigenesis in the colon. In order to accurately model CRC in mice, it is important to specifically target recombination in the colon. I therefore chose a different model to investigate the co-operation of *Apc* and *Snai1* in polyp formation.

The Cdx2P-NLS-Cre has been reported to preferentially target recombination in the colon (Hinoi et al., 2007). Hinoi *et al*. assessed somatic activation of the floxed *Apc* allele in the gastrointestinal tract of *Cdx2Cre Apc$^{flox/+}$* and *VillinCre Apc$^{flox/+}$* mice. In the *Cdx2Cre Apc$^{flox/+}$* mice the Cre targeted *Apc* allele was found to be present along with the wild-type *Apc* allele in normal mucosa from distal small intestine to the rectum, whereas, in *VillinCre Apc$^{flox/+}$* mice the *Apc* allele was present from the duodenum to the rectum. Furthermore, the majority of adenomas formed in the *Cdx2Cre Apc$^{flox/+}$* mice were found in the large intestine as compared to the *VillinCre Apc$^{flox/+}$* mice which mostly developed small intestinal adenomas. Not only did the *Cdx2Cre Apc$^{flox/+}$* mice develop more tumours in the colon, these tumours were relatively more invasive as compared to their *VillinCre Apc$^{flox/+}$* counterparts. Tamoxifen induced Cre activity has been studied in *Cdx2CreERT2* mice carrying the EYFP reporter construct (Feng et al., 2013). EYFP expression was found in epithelial cells from terminal ileum to rectum with the strongest induction of Cre activity in the caecum and proximal colon. These studies confirm the colon-specific activity of Cre under the Cdx2 promoter. As shown in Chapter 4, tamoxifen induced Cre activity using the Cdx2 promoter directs recombination in the proximal colon. Experiments in this chapter demonstrated loss of *Apc* directed by tamoxifen inducible *Cdx2CreERT2* led to formation of numerous polyps in the colon. No polyp growth was observed in the small intestinal tissues. The majority of colonic polyps were found in the proximal part of the colon. Furthermore, although not induced at high levels, cells expressing the *Snai1* transgene could be detected by reference to GFP expression in polyps of test mice

containing both the floxed *Apc* alleles and the *Snai1* transgene. For the studies conducted here, the *Cdx2CreERT2* model was much more effective than the *Lgr5CreERT2* model.

5.3.2 Expression of *Snai1* transgene enhances polyp growth

There is evidence supporting the involvement of *Snai1* in cancer progression *in vitro*, yet very little is known about the contribution of *Snai1* to the early onset of epithelial cancers *in vivo*. Functions of endogenously encoded SNAI1 and SNAI2 in context of breast cancer pathogenesis have been investigated using knock-in IRES-YFP reporters for *Snai1* and *Snai2* (Ye et al., 2015). Snai1-YFP expression was shown to be present in early-stage lesions whereas the relative frequency of Snai2-YFP^{+} cells was markedly reduced in these lesions compared to normal tissue. De Craene et al. employed a mouse model (K14-Snai1) with skin-specific expression of an HA-tagged SNAI1 protein (tagged to distinguish the transgene from endogenous SNAI1), to demonstrate that *Snai1* transgenic mice develop spontaneous skin tumours (De Craene et al., 2014). These studies suggest that *Snai1* plays a role in the early stages of tumourigenesis.

In our hands, no significant difference was observed in either polyp number or polyp growth in the *Lgr5CreERT2 Apc$^{flox/flox}$ RosaSnai1* test group compared to the *Lgr5CreERT2 Apc$^{flox/flox}$* controls. The lack of sufficient *Snai1* transgene expression in the test group explains the absence of a *Snai1*-mediated phenotype in these mice.

Inducing loss of *Apc* under the control of the tamoxifen inducible *Cdx2CreERT2* promoter in both the *Cdx2CreERT2 Apc$^{flox/flox}$* control and *Cdx2CreERT2 Apc$^{flox/flox}$ RosaSnai1* test groups resulted in polyp formation predominantly in the proximal region of the colon with relatively fewer polyps in the distal colon in both experimental groups. Although in the context of

intestinal polyposis there was no significant increase in expression of *Snai1* at the mRNA level (detected by ddPCR) in the test group, expression of the *Snai1* transgene (Snai1-eGFP) was clearly visible in the polyps at the protein level by immunofluorescence indicating successful *Snai1* up-regulation. Using the *RosaSnai1* construct (Nyabi et al., 2009) has proven advantageous in the current study as the eGFP cassette, located downstream of Snai1-IRES, permits visualisation of recombined cells. This has been a breakthrough as previously it has been a challenge to visualise and/or locate cells over-expressing *Snai1*, as no specific anti-SNAI1 antibodies are available. It is interesting to note here that expression of the *Snai1* transgene (Snai1-eGFP) was not observed in all the polyps, and if detected, was only visible in patches. This was not expected as these polyps essentially originate from cells which have undergone recombination and hence have lost *Apc* so it would also be expected that the *Snai1* transgene would be activated in these cells. One possible explanation for this could be that these recombined cells somehow are able to silence the *Snai1* transgene, leading to both loss of Snai1 and GFP expression. Alternatively, it may be possible that Cre recombinase targets the *Apc* alleles more efficiently than the *Snai1* transgene, producing a limited number of recombined cells carrying both a non-functional *Apc* gene and a *Snai1* transgene which could explain why GFP-negative regions within polyps were observed. Nevertheless, expression of the *Snai1* transgene led to formation of larger polyps in the colon which may be due to an increase in cell proliferation as indicated by the number of $BrdU^+$ cells in the polyps. No difference in polyp number between the control and test groups was observed suggesting that *Snai1* may not be affecting the initiation of polyps but could play a role in driving tumourigenesis.

p53, a tumour suppressor gene, induces apoptosis by eliminating cells subjected to different forms of stress. Tumour formation in the skin-specific *Snai1* transgenic mice has been studied in a *p53*-deficient setting (De Craene et al., 2014). Not only did the *K14-Snail K14Cre Trp53*$^{flox/flox}$ mice develop more aggressive tumours characterised by presence of epithelial and mesenchymal features, tumourigenesis was much more rapid with a decrease in the median latency period in these mice as compared to the K14-Snail controls. This suggests that *Snai1* expression and loss of *p53* play a synergistic role in initiating tumours, most likely by allowing cells with DNA damage to survive. The same could be applied to the present study where no effects of *Snai1* expression (in conjunction with *Apc* loss) on polyp number were observed. As tumour progression is a result of accumulation of mutations, it may be possible that loss of a commonly mutated gene in CRC like *p53* may be required in addition to *Snai1* up-regulation to give rise to a more aggressive phenotype in these mice. This could be a future avenue of investigation.

Taken together, results in this chapter suggest that *Apc* loss alone is sufficient to induce the majority of changes that occur at the earliest stages of polyposis. *Snai1* transgene expression results in increase in cell proliferation in polyps. This suggests that *Snai1* mutation during earlier stages of tumourigenesis is likely to support accelerated tumourigenesis. It would be interesting to see whether an additional genetic manipulation, which prevents DNA damaged cells to be eliminated by apoptosis such as *p53* loss, has any additive effects on cell proliferation and whether it is required to produce a more aggressive phenotype in mice.

5.3.3 Chapter Conclusion

The data in this chapter highlights the need and importance of closely modelling CRC in mouse models. *Snai1* transgene expression combined with loss of *Apc* is sufficient to accelerate polyp growth in mice. It may be possible that an intervention like loss of the tumour suppressor gene *p53* may be required in combination with loss of *Apc* and *Snai1* up-regulation for development of an aggressive phenotype in these mice. Further analysis is required to examine the extent of invasion of tumour cells into the intestinal wall. Additional studies are required to define the contributory role of *Snai1* in intestinal tumourigenesis.

Chapter 6 - General discussion

Chapter 6 – General discussion

6.1 Introduction

Findings from work in this thesis highlight the role of *SNAIL* family members, in particular SNAI1, in CRC. Up-regulation of *SNAI1* and its association with expression of ISC markers in colorectal tumours suggest a possible functional role of SNAI1 in the regulation of stem cells within tumours. *SNAI1* up-regulation during early stages of colorectal tumour progression suggests *SNAI1* may play a role during earlier stages on tumourigenesis. Furthermore, examination of up-regulation of *SNAI1* in *in vivo* and *in vitro* systems suggests that SNAI1 triggers different downstream mechanisms in different settings. Based on these observations I have proposed a model of *Snai1* function in the colonic epithelium.

6.2 Main findings

6.2.1 *SNAI1* is up-regulated in CRC and its expression correlates with ISC marker expression and early stage tumours

I have been able to confirm *SNAI1* up-regulation in CRC, which has previously been reported (Roy et al., 2005). Correlation analyses revealed positive association of *SNAI1* expression with expression of ISC markers *LGR5*, *EPHB2* and *BMI1* in colorectal tumours suggesting that these genes may be working in harmony with *SNAI1* in CRC. As the expression of SNAI1 has been shown to induce cancer stem cell-like properties in other tissues of epithelial origin (Mani et

al., 2008), it may be possible that SNAI1 induces stem cell-like properties in non-stem cells or regulates the CSC population in colorectal tumours. Up-regulation of *SNAI1* was observed in earlier stages, i.e. stages T2 and T3, of colorectal tumourigenesis within the patient cohort examined. It was previously believed that SNAI1 plays a role in advanced stage tumours as these tumours undergo EMT during metastasis. However, my data indicates that *SNAI1* also contributes to development of tumours during earlier stages. It could be possible that there is a critical requirement of *SNAI1* up-regulation by tumour cells during invasion into the deeper layers of the intestinal wall which occurs in stages T2 and T3 tumours. As such, further analyses is required to assess localisation of SNAI1 expression in these tumours.

6.2.2 Alterations in *SNAIL* genes are associated with lower overall survival of patients with CRC

I utilised an online resource, cBioPortal for Cancer Genomics, to compare my findings to a larger cohort of colorectal tumours. In a cohort of 629 CRC patients, *SNAIL* genes were altered in 133 (21%) patients with the majority of these alterations resulting in either amplification or up-regulation at the mRNA or protein level. A large proportion of *SNAI1* alterations occurred in patients with stage T2 or T3 tumours. This concurs with our findings in the Cabrini CRC patient cohort where *SNAI1* was significantly up-regulated in T2 and T3 stage tumours. A previous study has reported association of *Snai1* up-regulation in the skin with development of spontaneous tumours in mice (De Craene et al., 2014). These findings reinforce the notion that SNAI1 plays an important role in earlier stages of tumourigenesis. Furthermore, patients with altered *SNAIL* family genes have a significantly reduced overall survival period compared to patients with wild-type *SNAIL* genes. Overall, data presented in Chapter 3 suggest that

SNAI1 plays a critical role during initial stages of tumourigenesis and is associated with induction of invasive characteristics in colorectal tumours.

6.2.3 Characterisation of different intestinal tissue-specific promoters for manipulation of gene expression

Three different intestinal tissue-specific Cre drivers were utilised in this thesis to study the effects of *Snai1* up-regulation in the colonic epithelial tissues in mice. Significant variations in recombination efficiency were identified in the colonic epithelium using the tamoxifen inducible VillinCre, Lgr5Cre and Cdx2Cre promoters. The *VillinCreERT2* model resulted in higher recombination efficiency in the small intestine with relatively poor efficiency in the colon. Very high up-regulation of *Snai1* was observed in the small intestine while the over-expression of *Snai1* observed in the colon was relatively very low. This is in contrast to previous studies where the recombination under the control of the Villin promoter has been shown to result in sufficient expression of the transgene in the colonic epithelium (Eckmann et al., 2008, Schwitalla et al., 2013). However, there have been studies that have reported inefficient recombination in the colon using the *VillinCreERT2* model (Andreu et al., 2005, el Marjou et al., 2004), which are in agreement with our study. These inconsistencies observed in efficiency of recombination using the VillinCre promoter could be due to different genetic backgrounds of mice used in these studies or environmental influences in different animal facilities. Similar expression of Cre activity was observed using the *Lgr5CreERT2* mice where loss of *Apc* in the $Lgr5^{+}$ stem cells resulted in formation of polyps predominantly in the small intestine. This is likely due to the relatively lower frequency of the *Lgr5CreERT2* transgene expression in the colon compared to the small intestine, as demonstrated by Barker *et al*. (Barker et al., 2007). Furthermore, differences in kinetics of clone formation in the small

intestine and colon using the *Lgr5CreERT2* model have been reported (Barker et al., 2007) suggesting that the colonic Lgr5^{+} stem cells are more quiescent, which further explains the differences in recombination efficiency observed in the small intestine and colon in this study. My results demonstrate efficient recombination using the *Cdx2CreERT2* model as indicated by sufficient *Snai1* transgene expression in proximal colon in both normal colonic epithelium and during intestinal polyposis. These differences in recombination efficiency observed using different Cre drivers should be taken into account when choosing mouse lines for studying gene function in the colon.

6.2.4 *In vivo* up-regulation of *Snai1* increases cell proliferation in normal colonic epithelium and during intestinal polyposis in mice

Downstream effects of SNAI1 up-regulation observed in CRC remain largely unknown. This study evaluated the consequences of SNAI1 over-expression in colonic epithelial tissues *in vivo* using different transgenic mouse models. Using the *RosaSnai1* mice (Nyabi et al., 2009), the Snai1^{+} recombined cells marked by expression of GFP could be traced which proved highly valuable. In normal epithelium, *Snai1* up-regulation resulted in enhanced cell proliferation in the crypts. However, *Snai1* transgene expression was not sufficient to induce polyposis in these mice. The *Apc$^{flox/flox}$* mouse model of intestinal polyposis was utilised along with conditional activation of *Snai1* transgene expression, resulting in formation of polyps over-expressing SNAI1. Indeed, the enhanced cell proliferation observed in normal tissues was replicated in *Apc$^{flox/flox}$* mice. Polyp growth was accelerated, driven by increase in proliferation of the tumour cells. These findings, along with those observed in the human colorectal tumours (discussed above), implicate a functional role of SNAI1 in driving cell proliferation

during the early stages of tumour development. Furthermore, no activation of EMT was observed following up-regulation of SNAI1 in these contexts.

6.2.5 *In vitro* up-regulation of *Snai1* activates EMT in colonic stem cells

To assess the effect of *Snai1* up-regulation in a pure epithelial cell population, colonic organoid cultures were utilised. Data presented in Chapter 4 reveals for the first time successful up-regulation of *Snai1* in mouse colonic organoids. Successful transfection in organoids using TAT-Cre recombinase was confirmed by analysing expression of GFP by flow cytometry. Following *Snai1* up-regulation, we FACS-sorted two cell populations enriched for ISCs, one recombined ($CD24^{med}/GFP^{+}$) and the other non-recombined ($CD24^{med}/GFP^{-}$) and re-seeded in Matrigel. While the GFP^{-} cells gave rise to spherical organoids, the GFP^{+} cells lost their epithelial characteristics, confirmed by loss of *Lgr5* expression, and acquired a mesenchymal phenotype. This suggests activation of EMT in the stem cells as a result of *Snai1* up-regulation. Further validation by analysing the expression of mesenchymal markers is required. Nevertheless, these findings suggest SNAI1 expression, in the up-regulated state, is sufficient to alter the epithelial characteristics of cells *in vitro*. The cells expressing higher levels of SNAI1 were isolated by FACS in this experiment which produced cultures where the majority of cells were expressing SNAI1. This would produce tissue with a higher threshold of SNAI1 which may explain the differences observed between the *in vitro* and *in vivo* experiments.

6.3 Proposed model of SNAI1 function in the colonic epithelium

Based on the data presented in this thesis, I have proposed a model of potential SNAI1 function during different stages of colorectal tumour development (Figure 6.1). This is based

on findings in human primary colorectal tumours, mouse models and *in vitro* organoid cultures to development of human CRC. SNAI1 plays a critical role during both initial stages of tumour formation as well as metastasis. According to the proposed model, SNAI1, at normal levels of expression regulates and supports survival of the the ISC population. Tumour initiation then occurs and following up-regulation of *Wnt* signalling, SNAI1 is up-regulated in T-stage 2 and 3 tumours. At these stages, the main function of SNAI1 is regulation of proliferation of tumour cells including CSCs. Further up-regulation of SNAI1 occurs in CSCs in stage T3 tumours transitioning into stage T4. During the transition of tumours from T3 to T4 stage, SNAI1 causes further expansion of the CSC population which results in subsequent 'switching off' of proliferation, like a negative feedback loop. Up-regulation of SNAI1 is sustained by tumour cells through to T-stage 4 where tumour cells including CSCs lose their epithelial identity and adopt a mesenchymal morphology (referred to as EMT) for migration to nearby organs (or metastasis). Hence, my model proposes potentially different roles of SNAI1 based on the stage of tumour development. However, this is speculative at the moment and a deeper understanding of SNAI1 function is crucial for further validation.

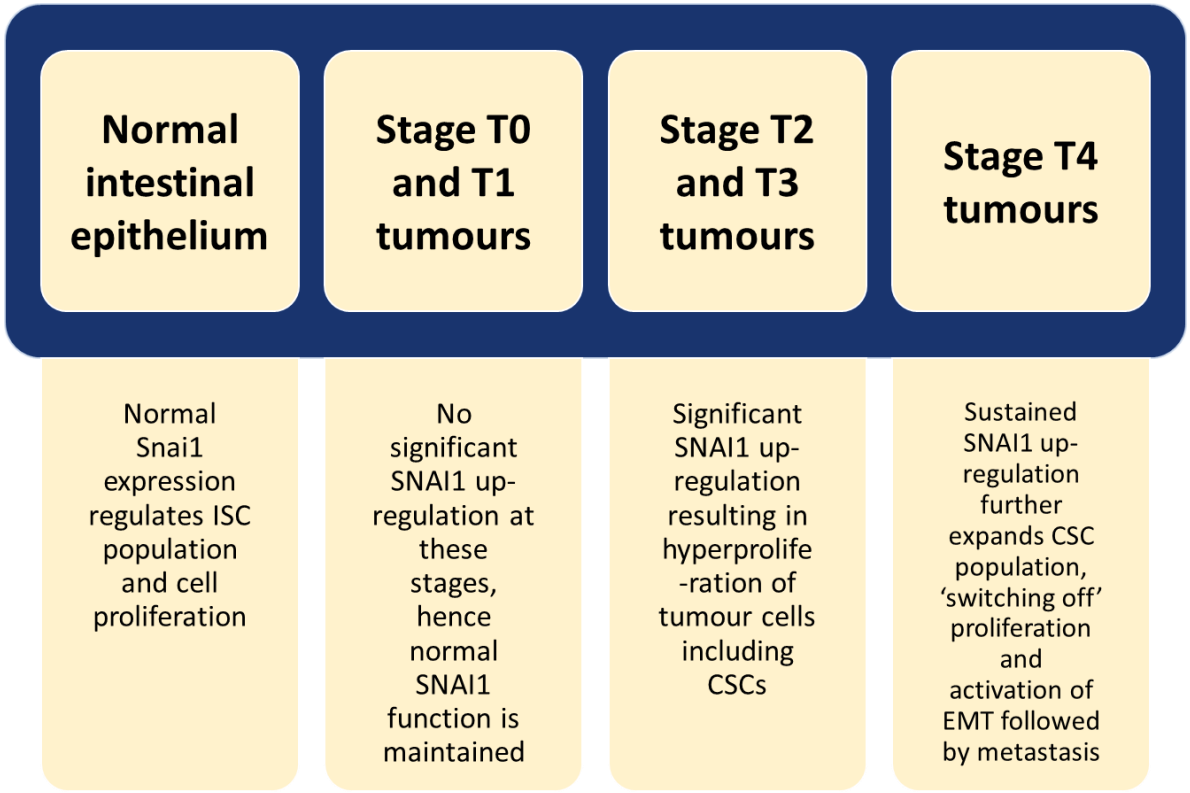

Figure 6.1 Proposed model for SNAI1 function in the colonic epithelium. In the normal intestinal epithelium, *Snai1* functions as a regulator of stem cell proliferation and this function is maintained during development of T0 and T1 tumours as SNAI1 expression is comparable to normal epithelium. Up-regulation of *SNAI1* in T2 and T3 tumours results in hyperproliferation of CSCs and adjoining tumour cells. Sustained SNAI1 up-regulation in T4 tumours kicks in a negative feedback loop which shuts down proliferation of tumour cells. Activation of EMT occurs at this stage resulting in subsequent tumour cell migration and metastasis.

6.4 Future directions

6.4.1 Localisation of SNAIL expression in colorectal tumours

While I observed *SNAI1* over-expression and its correlation with ISC markers in colorectal tumours, further investigation is required to assess its localisation within the tumours. It is still unclear whether SNAI1 is expressed in the epithelial cell compartment in tumours and whether its expression co-localises with ISC markers within tumours. Due to lack of robust anti-SNAI1 antibodies, I attempted to investigate this subject by designing SNAI1 RNA probes for in situ hybridisation (ISH) and tested a dual staining protocol (dual ISH/IHC) using an anti-EPHB2 antibody. However, these attempts were unsuccessful and no conclusions could be drawn. Further investigations are necessary in order to define a more specific function of SNAI1 during tumourigenesis. In addition, CSC populations can be isolated from tumours by flow cytometry using CSC markers like EPHB2 and examined for enrichment of SNAI1 in these tumour cell subsets.

6.4.2 Examining the ISC population following SNAI1 up-regulation in the colonic epithelium

Balanced levels of *Wnt* signalling are critical for regulation of the stem cell population and maintenance of intestinal homeostasis. I observed down-regulation of ISC markers following *Snai1* over-expression in the mouse colonic epithelium. It is unclear whether this down-regulation occurred as a result of decrease in number of stem cells or an overall reduction in the expression of ISC markers as a result of decrease in levels of WNT signalling in these cells. Investigating the immediate effects of SNAI1 up-regulation and quantification of ISC population at earlier time-points could further identify the down-stream effects of SNAI1 over-expression.

6.4.3 Examining SNAI1 function in mouse model of intestinal polyposis

We observed presence of larger polyps driven by increase in cell proliferation following SNAI1 up-regulation in *Apc*$^{flox/flox}$ mice. It remains unclear whether these polyps differed in pathology compared to the control polyps. Examination of histopathological features of these tumours is essential to understand the mechanism of *Snai1* function in tumourigenesis. Additional loss of a tumour suppressor gene like *p53* may highlight the role of *Snai1* in tumour development as *p53* is an important pro-apoptotic gene and its loss would protect the mutated cells from apoptosis thereby, potentially rise to an aggressive tumour phenotype.

6.5 Conclusion

Data presented in this thesis highlights the potential role of SNAIL proteins in regulation of CSCs in CRC along with insight into the down-stream effects of SNAI1 up-regulation observed in colorectal tumours.

References

AL-HAJJ, M., WICHA, M. S., BENITO-HERNANDEZ, A., MORRISON, S. J. & CLARKE, M. F. 2003. Prospective identification of tumorigenic breast cancer cells. *Proc Natl Acad Sci U S A,* 100**,** 3983-8.

ALBERGA, A., BOULAY, J. L., KEMPE, E., DENNEFELD, C. & HAENLIN, M. 1991. The snail gene required for mesoderm formation in Drosophila is expressed dynamically in derivatives of all three germ layers. *Development,* 111**,** 983-92.

ALEXANDRE, C., BAENA-LOPEZ, A. & VINCENT, J. P. 2014. Patterning and growth control by membrane-tethered Wingless. *Nature,* 505**,** 180-5.

ANDREU, P., COLNOT, S., GODARD, C., GAD, S., CHAFEY, P., NIWA-KAWAKITA, M., LAURENT-PUIG, P., KAHN, A., ROBINE, S., PERRET, C. & ROMAGNOLO, B. 2005. Crypt-restricted proliferation and commitment to the Paneth cell lineage following Apc loss in the mouse intestine. *Development,* 132**,** 1443-51.

AOKI, K. & TAKETO, M. M. 2007. Adenomatous polyposis coli (APC): a multi-functional tumor suppressor gene. *J Cell Sci,* 120**,** 3327-35.

ARNOLD, M., SIERRA, M. S., LAVERSANNE, M., SOERJOMATARAM, I., JEMAL, A. & BRAY, F. 2017. Global patterns and trends in colorectal cancer incidence and mortality. *Gut,* 66**,** 683-691.

AUSTRALIAN INSTITUTE OF, H. & WELFARE 2018. Cancer in Australia: Actual incidence data from 1982 to 2013 and mortality data from 1982 to 2014 with projections to 2017. *Asia Pac J Clin Oncol,* 14**,** 5-15.

BAKER, S. J., PREISINGER, A. C., JESSUP, J. M., PARASKEVA, C., MARKOWITZ, S., WILLSON, J. K., HAMILTON, S. & VOGELSTEIN, B. 1990. p53 gene mutations occur in combination with 17p allelic deletions as late events in colorectal tumorigenesis. *Cancer Res,* 50**,** 7717-22.

BARKER, N. & CLEVERS, H. 2006. Mining the Wnt pathway for cancer therapeutics. *Nat Rev Drug Discov,* 5**,** 997-1014.

BARKER, N., RIDGWAY, R. A., VAN ES, J. H., VAN DE WETERING, M., BEGTHEL, H., VAN DEN BORN, M., DANENBERG, E., CLARKE, A. R., SANSOM, O. J. & CLEVERS, H. 2009. Crypt stem cells as the cells-of-origin of intestinal cancer. *Nature,* 457**,** 608-11.

BARKER, N., VAN ES, J. H., KUIPERS, J., KUJALA, P., VAN DEN BORN, M., COZIJNSEN, M., HAEGEBARTH, A., KORVING, J., BEGTHEL, H., PETERS, P. J. & CLEVERS, H. 2007. Identification of stem cells in small intestine and colon by marker gene Lgr5. *Nature,* 449**,** 1003-7.

BATLLE, E., BACANI, J., BEGTHEL, H., JONKHEER, S., GREGORIEFF, A., VAN DE BORN, M., MALATS, N., SANCHO, E., BOON, E., PAWSON, T., GALLINGER, S., PALS, S. & CLEVERS, H. 2005. EphB receptor activity suppresses colorectal cancer progression. *Nature,* 435**,** 1126-30.

BERG, M., DANIELSEN, S. A., AHLQUIST, T., MEROK, M. A., AGESEN, T. H., VATN, M. H., MALA, T., SJO, O. H., BAKKA, A., MOBERG, I., FETVEIT, T., MATHISEN, O., HUSBY, A., SANDVIK, O., NESBAKKEN, A., THIIS-EVENSEN, E. & LOTHE, R. A. 2010. DNA sequence profiles of the colorectal cancer critical gene set KRAS-BRAF-PIK3CA-PTEN-TP53 related to age at disease onset. *PLoS One,* 5**,** e13978.

BEROUD, C. & SOUSSI, T. 1996. APC gene: database of germline and somatic mutations in human tumors and cell lines. *Nucleic Acids Res,* 24**,** 121-4.

BJERKNES, M. & CHENG, H. 1999. Clonal analysis of mouse intestinal epithelial progenitors. *Gastroenterology,* 116**,** 7-14.

BJERKNES, M. & CHENG, H. 2002. Multipotential stem cells in adult mouse gastric epithelium. *Am J Physiol Gastrointest Liver Physiol,* 283**,** G767-77.

BLANCO, M. J., MORENO-BUENO, G., SARRIO, D., LOCASCIO, A., CANO, A., PALACIOS, J. & NIETO, M. A. 2002. Correlation of Snail expression with histological grade and lymph node status in breast carcinomas. *Oncogene,* 21**,** 3241-6.

BOS, J. L., FEARON, E. R., HAMILTON, S. R., VERLAAN-DE VRIES, M., VAN BOOM, J. H., VAN DER EB, A. J. & VOGELSTEIN, B. 1987. Prevalence of ras gene mutations in human colorectal cancers. *Nature,* 327**,** 293-7.

BOSMAN, F. T., CARNEIRO, F., HRUBAN, R. H. & THEISE, N.D. EDS 2010. Carcinoma of the colon and rectum. *WHO classification of tumours of the digestive system*

4th ed.: IARC Press.

CANCER GENOME ATLAS, N. 2012. Comprehensive molecular characterization of human colon and rectal cancer. *Nature,* 487**,** 330-7.

CANO, A., PEREZ-MORENO, M. A., RODRIGO, I., LOCASCIO, A., BLANCO, M. J., DEL BARRIO, M. G., PORTILLO, F. & NIETO, M. A. 2000. The transcription factor snail controls epithelial-mesenchymal transitions by repressing E-cadherin expression. *Nat Cell Biol,* 2**,** 76-83.

CARVER, E. A., JIANG, R., LAN, Y., ORAM, K. F. & GRIDLEY, T. 2001. The mouse snail gene encodes a key regulator of the epithelial-mesenchymal transition. *Mol Cell Biol,* 21**,** 8184-8.

CAVENEE, W. K., HANSEN, M. F., NORDENSKJOLD, M., KOCK, E., MAUMENEE, I., SQUIRE, J. A., PHILLIPS, R. A. & GALLIE, B. L. 1985. Genetic origin of mutations predisposing to retinoblastoma. *Science,* 228**,** 501-3.

CERAMI, E., GAO, J., DOGRUSOZ, U., GROSS, B. E., SUMER, S. O., AKSOY, B. A., JACOBSEN, A., BYRNE, C. J., HEUER, M. L., LARSSON, E., ANTIPIN, Y., REVA, B., GOLDBERG, A. P., SANDER, C. & SCHULTZ, N. 2012. The cBio cancer genomics portal: an open platform for exploring multidimensional cancer genomics data. *Cancer Discov,* 2**,** 401-4.

CHEN, J. S., HSIEH, P. S., CHIANG, J. M., YEH, C. Y., TSAI, W. S., TANG, R., CHANGCHIEN, C. R. & WU, R. C. 2010. Clinical outcome of signet ring cell carcinoma and mucinous adenocarcinoma of the colon. *Chang Gung Med J,* 33**,** 51-7.

CHEN, Y. & GRIDLEY, T. 2013. Compensatory regulation of the Snai1 and Snai2 genes during chondrogenesis. *J Bone Miner Res,* 28**,** 1412-21.

CHENG, H. & LEBLOND, C. P. 1974. Origin, differentiation and renewal of the four main epithelial cell types in the mouse small intestine. V. Unitarian Theory of the origin of the four epithelial cell types. *Am J Anat,* 141**,** 537-61.

CHRISTOFORI, G. 2010. Snail1 links transcriptional control with epigenetic regulation. *EMBO J,* 29**,** 1787-9.

DAVIES, E. J., MARSH DURBAN, V., MENIEL, V., WILLIAMS, G. T. & CLARKE, A. R. 2014. PTEN loss and KRAS activation leads to the formation of serrated adenomas and metastatic carcinoma in the mouse intestine. *J Pathol,* 233**,** 27-38.

DE CRAENE, B., DENECKER, G., VERMASSEN, P., TAMINAU, J., MAUCH, C., DERORE, A., JONKERS, J., FUCHS, E. & BERX, G. 2014. Epidermal Snail expression drives skin cancer initiation and progression through enhanced cytoprotection, epidermal stem/progenitor cell expansion and enhanced metastatic potential. *Cell Death Differ,* 21**,** 310-20.

DE FRUTOS, C. A., VEGA, S., MANZANARES, M., FLORES, J. M., HUERTAS, H., MARTINEZ-FRIAS, M. L. & NIETO, M. A. 2007. Snail1 is a transcriptional effector of FGFR3 signaling during chondrogenesis and achondroplasias. *Dev Cell,* 13**,** 872-83.

ECKMANN, L., NEBELSIEK, T., FINGERLE, A. A., DANN, S. M., MAGES, J., LANG, R., ROBINE, S., KAGNOFF, M. F., SCHMID, R. M., KARIN, M., ARKAN, M. C. & GRETEN, F. R. 2008. Opposing functions of IKKbeta during acute and chronic intestinal inflammation. *Proc Natl Acad Sci U S A,* 105**,** 15058-63.

EL MARJOU, F., JANSSEN, K. P., CHANG, B. H., LI, M., HINDIE, V., CHAN, L., LOUVARD, D., CHAMBON, P., METZGER, D. & ROBINE, S. 2004. Tissue-specific and inducible Cre-mediated recombination in the gut epithelium. *Genesis,* 39**,** 186-93.

FAN, X. S., WU, H. Y., YU, H. P., ZHOU, Q., ZHANG, Y. F. & HUANG, Q. 2010. Expression of Lgr5 in human colorectal carcinogenesis and its potential correlation with beta-catenin. *Int J Colorectal Dis,* 25**,** 583-90.

FEARNHEAD, N. S., BRITTON, M. P. & BODMER, W. F. 2001. The ABC of APC. *Hum Mol Genet,* 10**,** 721-33.

FEARON, E. R. & VOGELSTEIN, B. 1990. A genetic model for colorectal tumorigenesis. *Cell,* 61**,** 759-67.

FENG, Y., SENTANI, K., WIESE, A., SANDS, E., GREEN, M., BOMMER, G. T., CHO, K. R. & FEARON, E. R. 2013. Sox9 induction, ectopic Paneth cells, and mitotic spindle axis defects in mouse colon adenomatous epithelium arising from conditional biallelic Apc inactivation. *Am J Pathol,* 183**,** 493-503.

FERRARI-AMOROTTI, G., FRAGLIASSO, V., ESTEKI, R., PRUDENTE, Z., SOLIERA, A. R., CATTELANI, S., MANZOTTI, G., GRISENDI, G., DOMINICI, M., PIERACCIOLI, M., RASCHELLA, G., CHIODONI, C., COLOMBO, M. P. & CALABRETTA, B. 2013. Inhibiting interactions of lysine demethylase LSD1 with snail/slug blocks cancer cell invasion. *Cancer Res,* 73**,** 235-45.

FODDE, R. & BRABLETZ, T. 2007. Wnt/beta-catenin signaling in cancer stemness and malignant behavior. *Curr Opin Cell Biol,* 19**,** 150-8.

FODDE, R., KUIPERS, J., ROSENBERG, C., SMITS, R., KIELMAN, M., GASPAR, C., VAN ES, J. H., BREUKEL, C., WIEGANT, J., GILES, R. H. & CLEVERS, H. 2001. Mutations in the APC tumour suppressor gene cause chromosomal instability. *Nat Cell Biol,* 3**,** 433-8.

GALIATSATOS, P. & FOULKES, W. D. 2006. Familial adenomatous polyposis. *Am J Gastroenterol,* 101**,** 385-98.

GAO, J., AKSOY, B. A., DOGRUSOZ, U., DRESDNER, G., GROSS, B., SUMER, S. O., SUN, Y., JACOBSEN, A., SINHA, R., LARSSON, E., CERAMI, E., SANDER, C. & SCHULTZ, N. 2013. Integrative analysis of complex cancer genomics and clinical profiles using the cBioPortal. *Sci Signal,* 6**,** pl1.

GARBER, J. E., GOLDSTEIN, A. M., KANTOR, A. F., DREYFUS, M. G., FRAUMENI, J. F., JR. & LI, F. P. 1991. Follow-up study of twenty-four families with Li-Fraumeni syndrome. *Cancer Res,* 51**,** 6094-7.

GAVERT, N. & BEN-ZE'EV, A. 2007. beta-Catenin signaling in biological control and cancer. *J Cell Biochem,* 102**,** 820-8.

GOARDON, N., MARCHI, E., ATZBERGER, A., QUEK, L., SCHUH, A., SONEJI, S., WOLL, P., MEAD, A., ALFORD, K. A., ROUT, R., CHAUDHURY, S., GILKES, A., KNAPPER, S., BELDJORD, K., BEGUM, S., ROSE, S., GEDDES, N., GRIFFITHS, M., STANDEN, G., STERNBERG, A., CAVENAGH, J., HUNTER, H., BOWEN, D., KILLICK, S., ROBINSON, L.,

PRICE, A., MACINTYRE, E., VIRGO, P., BURNETT, A., CRADDOCK, C., ENVER, T., JACOBSEN, S. E., PORCHER, C. & VYAS, P. 2011. Coexistence of LMPP-like and GMP-like leukemia stem cells in acute myeloid leukemia. *Cancer Cell,* 19**,** 138-52.

GRACZ, A. D., FULLER, M. K., WANG, F., LI, L., STELZNER, M., DUNN, J. C., MARTIN, M. G. & MAGNESS, S. T. 2013. Brief report: CD24 and CD44 mark human intestinal epithelial cell populations with characteristics of active and facultative stem cells. *Stem Cells,* 31**,** 2024-30.

GREGORIEFF, A. & CLEVERS, H. 2005. Wnt signaling in the intestinal epithelium: from endoderm to cancer. *Genes Dev,* 19**,** 877-90.

GRODEN, J., THLIVERIS, A., SAMOWITZ, W., CARLSON, M., GELBERT, L., ALBERTSEN, H., JOSLYN, G., STEVENS, J., SPIRIO, L., ROBERTSON, M. & ET AL. 1991. Identification and characterization of the familial adenomatous polyposis coli gene. *Cell,* 66**,** 589-600.

GROSS, J. C., CHAUDHARY, V., BARTSCHERER, K. & BOUTROS, M. 2012. Active Wnt proteins are secreted on exosomes. *Nat Cell Biol,* 14**,** 1036-45.

GUILLEMOT, F., NAGY, A., AUERBACH, A., ROSSANT, J. & JOYNER, A. L. 1994. Essential role of Mash-2 in extraembryonic development. *Nature,* 371**,** 333-6.

GUINNEY, J., DIENSTMANN, R., WANG, X., DE REYNIES, A., SCHLICKER, A., SONESON, C., MARISA, L., ROEPMAN, P., NYAMUNDANDA, G., ANGELINO, P., BOT, B. M., MORRIS, J. S., SIMON, I. M., GERSTER, S., FESSLER, E., DE SOUSA, E. M. F., MISSIAGLIA, E., RAMAY, H., BARRAS, D., HOMICSKO, K., MARU, D., MANYAM, G. C., BROOM, B., BOIGE, V., PEREZ-VILLAMIL, B., LADERAS, T., SALAZAR, R., GRAY, J. W., HANAHAN, D., TABERNERO, J., BERNARDS, R., FRIEND, S. H., LAURENT-PUIG, P., MEDEMA, J. P., SADANANDAM, A., WESSELS, L., DELORENZI, M., KOPETZ, S., VERMEULEN, L. & TEJPAR, S. 2015. The consensus molecular subtypes of colorectal cancer. *Nat Med,* 21**,** 1350-6.

GUO, W., KECKESOVA, Z., DONAHER, J. L., SHIBUE, T., TISCHLER, V., REINHARDT, F., ITZKOVITZ, S., NOSKE, A., ZURRER-HARDI, U., BELL, G., TAM, W. L., MANI, S. A., VAN OUDENAARDEN, A. & WEINBERG, R. A. 2012. Slug and Sox9 cooperatively determine the mammary stem cell state. *Cell,* 148**,** 1015-28.

HAGGAR, F. A. & BOUSHEY, R. P. 2009. Colorectal cancer epidemiology: incidence, mortality, survival, and risk factors. *Clin Colon Rectal Surg,* 22**,** 191-7.

HALBERG, R. B., KATZUNG, D. S., HOFF, P. D., MOSER, A. R., COLE, C. E., LUBET, R. A., DONEHOWER, L. A., JACOBY, R. F. & DOVE, W. F. 2000. Tumorigenesis in the multiple intestinal neoplasia mouse: redundancy of negative regulators and specificity of modifiers. *Proc Natl Acad Sci U S A,* 97**,** 3461-6.

HAO, H. X., XIE, Y., ZHANG, Y., CHARLAT, O., OSTER, E., AVELLO, M., LEI, H., MICKANIN, C., LIU, D., RUFFNER, H., MAO, X., MA, Q., ZAMPONI, R., BOUWMEESTER, T., FINAN, P. M., KIRSCHNER, M. W., PORTER, J. A., SERLUCA, F. C. & CONG, F. 2012. ZNRF3 promotes Wnt receptor turnover in an R-spondin-sensitive manner. *Nature,* 485**,** 195-200.

HARDY, R. G., VICENTE-DUENAS, C., GONZALEZ-HERRERO, I., ANDERSON, C., FLORES, T., HUGHES, S., TSELEPIS, C., ROSS, J. A. & SANCHEZ-GARCIA, I. 2007. Snail family transcription factors are implicated in thyroid carcinogenesis. *Am J Pathol,* 171**,** 1037-46.

HE, S., ZHOU, H., ZHU, X., HU, S., FEI, M., WAN, D., GU, W., YANG, X., SHI, D., ZHOU, J., ZHOU, J., ZHU, Z., WANG, L., LI, D. & ZHANG, Y. 2014. Expression of Lgr5, a marker of

intestinal stem cells, in colorectal cancer and its clinicopathological significance. *Biomed Pharmacother,* 68**,** 507-13.

HILKENS, J., TIMMER, N. C., BOER, M., IKINK, G. J., SCHEWE, M., SACCHETTI, A., KOPPENS, M. A., SONG, J. Y. & BAKKER, E. R. 2016. RSPO3 expands intestinal stem cell and niche compartments and drives tumorigenesis. *Gut*.

HINDSON, B. J., NESS, K. D., MASQUELIER, D. A., BELGRADER, P., HEREDIA, N. J., MAKAREWICZ, A. J., BRIGHT, I. J., LUCERO, M. Y., HIDDESSEN, A. L., LEGLER, T. C., KITANO, T. K., HODEL, M. R., PETERSEN, J. F., WYATT, P. W., STEENBLOCK, E. R., SHAH, P. H., BOUSSE, L. J., TROUP, C. B., MELLEN, J. C., WITTMANN, D. K., ERNDT, N. G., CAULEY, T. H., KOEHLER, R. T., SO, A. P., DUBE, S., ROSE, K. A., MONTESCLAROS, L., WANG, S., STUMBO, D. P., HODGES, S. P., ROMINE, S., MILANOVICH, F. P., WHITE, H. E., REGAN, J. F., KARLIN-NEUMANN, G. A., HINDSON, C. M., SAXONOV, S. & COLSTON, B. W. 2011. High-throughput droplet digital PCR system for absolute quantitation of DNA copy number. *Anal Chem,* 83**,** 8604-10.

HINOI, T., AKYOL, A., THEISEN, B. K., FERGUSON, D. O., GREENSON, J. K., WILLIAMS, B. O., CHO, K. R. & FEARON, E. R. 2007. Mouse model of colonic adenoma-carcinoma progression based on somatic Apc inactivation. *Cancer Res,* 67**,** 9721-30.

HORVAY, K., CASAGRANDA, F., GANY, A., HIME, G. R. & ABUD, H. E. 2011. Wnt signaling regulates Snai1 expression and cellular localization in the mouse intestinal epithelial stem cell niche. *Stem Cells Dev,* 20**,** 737-45.

HORVAY, K., JARDE, T., CASAGRANDA, F., PERREAU, V. M., HAIGH, K., NEFZGER, C. M., AKHTAR, R., GRIDLEY, T., BERX, G., HAIGH, J. J., BARKER, N., POLO, J. M., HIME, G. R. & ABUD, H. E. 2015. Snai1 regulates cell lineage allocation and stem cell maintenance in the mouse intestinal epithelium. *EMBO J,* 34**,** 1319-35.

HUGEN, N., BROWN, G., GLYNNE-JONES, R., DE WILT, J. H. & NAGTEGAAL, I. D. 2016. Advances in the care of patients with mucinous colorectal cancer. *Nat Rev Clin Oncol,* 13**,** 361-9.

HUGEN, N., VERHOEVEN, R. H., LEMMENS, V. E., VAN AART, C. J., ELFERINK, M. A., RADEMA, S. A., NAGTEGAAL, I. D. & DE WILT, J. H. 2015. Colorectal signet-ring cell carcinoma: benefit from adjuvant chemotherapy but a poor prognostic factor. *Int J Cancer,* 136**,** 333-9.

HWANG, W. L., JIANG, J. K., YANG, S. H., HUANG, T. S., LAN, H. Y., TENG, H. W., YANG, C. Y., TSAI, Y. P., LIN, C. H., WANG, H. W. & YANG, M. H. 2014. MicroRNA-146a directs the symmetric division of Snail-dominant colorectal cancer stem cells. *Nat Cell Biol,* 16**,** 268-80.

HWANG, W. L., YANG, M. H., TSAI, M. L., LAN, H. Y., SU, S. H., CHANG, S. C., TENG, H. W., YANG, S. H., LAN, Y. T., CHIOU, S. H. & WANG, H. W. 2011. SNAIL regulates interleukin-8 expression, stem cell-like activity, and tumorigenicity of human colorectal carcinoma cells. *Gastroenterology,* 141**,** 279-91, 291 e1-5.

HYNGSTROM, J. R., HU, C. Y., XING, Y., YOU, Y. N., FEIG, B. W., SKIBBER, J. M., RODRIGUEZ-BIGAS, M. A., CORMIER, J. N. & CHANG, G. J. 2012. Clinicopathology and outcomes for mucinous and signet ring colorectal adenocarcinoma: analysis from the National Cancer Data Base. *Ann Surg Oncol,* 19**,** 2814-21.

IACOPETTA, B. 2003. TP53 mutation in colorectal cancer. *Hum Mutat,* 21**,** 271-6.

INOUE, A., SEIDEL, M. G., WU, W., KAMIZONO, S., FERRANDO, A. A., BRONSON, R. T., IWASAKI, H., AKASHI, K., MORIMOTO, A., HITZLER, J. K., PESTINA, T. I., JACKSON, C.

W., TANAKA, R., CHONG, M. J., MCKINNON, P. J., INUKAI, T., GROSVELD, G. C. & LOOK, A. T. 2002. Slug, a highly conserved zinc finger transcriptional repressor, protects hematopoietic progenitor cells from radiation-induced apoptosis in vivo. *Cancer Cell,* 2**,** 279-88.

IRELAND, H., KEMP, R., HOUGHTON, C., HOWARD, L., CLARKE, A. R., SANSOM, O. J. & WINTON, D. J. 2004. Inducible Cre-mediated control of gene expression in the murine gastrointestinal tract: effect of loss of beta-catenin. *Gastroenterology,* 126**,** 1236-46.

JANSSON, L., KIM, G. S. & CHENG, A. G. 2015. Making sense of Wnt signaling-linking hair cell regeneration to development. *Front Cell Neurosci,* 9**,** 66.

JARDE, T., KASS, L., STAPLES, M., LESCESEN, H., CARNE, P., OLIVA, K., MCMURRICK, P. J. & ABUD, H. E. 2015. ERBB3 Positively Correlates with Intestinal Stem Cell Markers but Marks a Distinct Non Proliferative Cell Population in Colorectal Cancer. *PLoS One,* 10**,** e0138336.

JARDÉ, T., KERR, G., AKHTAR, R. & ABUD, H. E. 2018. Modelling Intestinal Carcinogenesis Using In Vitro Organoid Cultures. *In:* JENKINS, B. J. (ed.) *Inflammation and Cancer: Methods and Protocols.* New York, NY: Springer New York.

JEN, J., POWELL, S. M., PAPADOPOULOS, N., SMITH, K. J., HAMILTON, S. R., VOGELSTEIN, B. & KINZLER, K. W. 1994. Molecular determinants of dysplasia in colorectal lesions. *Cancer Res,* 54**,** 5523-6.

JIANG, R., LAN, Y., NORTON, C. R., SUNDBERG, J. P. & GRIDLEY, T. 1998. The Slug gene is not essential for mesoderm or neural crest development in mice. *Dev Biol,* 198**,** 277-85.

JOHNSTONE, C. N., WHITE, S. J., TEBBUTT, N. C., CLAY, F. J., ERNST, M., BIGGS, W. H., VIARS, C. S., CZEKAY, S., ARDEN, K. C. & HEATH, J. K. 2002. Analysis of the regulation of the A33 antigen gene reveals intestine-specific mechanisms of gene expression. *J Biol Chem,* 277**,** 34531-9.

JONES, R. J., MATSUI, W. H. & SMITH, B. D. 2004. Cancer stem cells: are we missing the target? *J Natl Cancer Inst,* 96**,** 583-5.

KADARI, A., LU, M., LI, M., SEKARAN, T., THUMMER, R. P., GUYETTE, N., CHU, V. & EDENHOFER, F. 2014. Excision of viral reprogramming cassettes by Cre protein transduction enables rapid, robust and efficient derivation of transgene-free human induced pluripotent stem cells. *Stem Cell Res Ther,* 5**,** 47.

KAJITA, M., MCCLINIC, K. N. & WADE, P. A. 2004. Aberrant expression of the transcription factors snail and slug alters the response to genotoxic stress. *Mol Cell Biol,* 24**,** 7559-66.

KALLURI, R. & WEINBERG, R. A. 2009. The basics of epithelial-mesenchymal transition. *J Clin Invest,* 119**,** 1420-8.

KINZLER, K. W., NILBERT, M. C., SU, L. K., VOGELSTEIN, B., BRYAN, T. M., LEVY, D. B., SMITH, K. J., PREISINGER, A. C., HEDGE, P., MCKECHNIE, D. & ET AL. 1991. Identification of FAP locus genes from chromosome 5q21. *Science,* 253**,** 661-5.

KINZLER, K. W. & VOGELSTEIN, B. 1996. Lessons from hereditary colorectal cancer. *Cell,* 87**,** 159-70.

KINZLER, K. W. & VOGELSTEIN, B. 1997. Cancer-susceptibility genes. Gatekeepers and caretakers. *Nature,* 386**,** 761, 763.

KLEIST, B., XU, L., LI, G. & KERSTEN, C. 2011. Expression of the adult intestinal stem cell marker Lgr5 in the metastatic cascade of colorectal cancer. *Int J Clin Exp Pathol,* 4**,** 327-35.

KNAB, L. M., EBINE, K., CHOW, C. R., RAZA, S. S., SAHAI, V., PATEL, A. P., KUMAR, K., BENTREM, D. J., GRIPPO, P. J. & MUNSHI, H. G. 2014. Snail cooperates with Kras G12D in vivo to increase stem cell factor and enhance mast cell infiltration. *Mol Cancer Res,* 12**,** 1440-8.

KOEPPEN, B. M. & STANTON, B. A. 2008. *Berne & Levy Physiology*.

KOO, B. K., SPIT, M., JORDENS, I., LOW, T. Y., STANGE, D. E., VAN DE WETERING, M., VAN ES, J. H., MOHAMMED, S., HECK, A. J., MAURICE, M. M. & CLEVERS, H. 2012. Tumour suppressor RNF43 is a stem-cell E3 ligase that induces endocytosis of Wnt receptors. *Nature,* 488**,** 665-9.

KORZELIUS, J., NAUMANN, S. K., LOZA-COLL, M. A., CHAN, J. S., DUTTA, D., OBERHEIM, J., GLASSER, C., SOUTHALL, T. D., BRAND, A. H., JONES, D. L. & EDGAR, B. A. 2014. Escargot maintains stemness and suppresses differentiation in Drosophila intestinal stem cells. *EMBO J,* 33**,** 2967-82.

KOSINSKI, C., LI, V. S., CHAN, A. S., ZHANG, J., HO, C., TSUI, W. Y., CHAN, T. L., MIFFLIN, R. C., POWELL, D. W., YUEN, S. T., LEUNG, S. Y. & CHEN, X. 2007. Gene expression patterns of human colon tops and basal crypts and BMP antagonists as intestinal stem cell niche factors. *Proc Natl Acad Sci U S A,* 104**,** 15418-23.

KRESO, A., VAN GALEN, P., PEDLEY, N. M., LIMA-FERNANDES, E., FRELIN, C., DAVIS, T., CAO, L., BAIAZITOV, R., DU, W., SYDORENKO, N., MOON, Y. C., GIBSON, L., WANG, Y., LEUNG, C., ISCOVE, N. N., ARROWSMITH, C. H., SZENTGYORGYI, E., GALLINGER, S., DICK, J. E. & O'BRIEN, C. A. 2014. Self-renewal as a therapeutic target in human colorectal cancer. *Nat Med,* 20**,** 29-36.

KUO, K. T., CHOU, T. Y., HSU, H. S., CHEN, W. L. & WANG, L. S. 2012. Prognostic significance of NBS1 and Snail expression in esophageal squamous cell carcinoma. *Ann Surg Oncol,* 19 Suppl 3**,** S549-57.

LABONNE, C. & BRONNER-FRASER, M. 2000. Snail-related transcriptional repressors are required in Xenopus for both the induction of the neural crest and its subsequent migration. *Dev Biol,* 221**,** 195-205.

LI, D. W., TANG, H. M., FAN, J. W., YAN, D. W., ZHOU, C. Z., LI, S. X., WANG, X. L. & PENG, Z. H. 2010. Expression level of Bmi-1 oncoprotein is associated with progression and prognosis in colon cancer. *J Cancer Res Clin Oncol,* 136**,** 997-1006.

LIN, Y., WU, Y., LI, J., DONG, C., YE, X., CHI, Y. I., EVERS, B. M. & ZHOU, B. P. 2010. The SNAG domain of Snail1 functions as a molecular hook for recruiting lysine-specific demethylase 1. *EMBO J,* 29**,** 1803-16.

LINNEKAMP, J. F., HOOFF, S. R. V., PRASETYANTI, P. R., KANDIMALLA, R., BUIKHUISEN, J. Y., FESSLER, E., RAMESH, P., LEE, K., BOCHOVE, G. G. W., DE JONG, J. H., CAMERON, K., LEERSUM, R. V., RODERMOND, H. M., FRANITZA, M., NURNBERG, P., MANGIAPANE, L. R., WANG, X., CLEVERS, H., VERMEULEN, L., STASSI, G. & MEDEMA, J. P. 2018. Consensus molecular subtypes of colorectal cancer are recapitulated in in vitro and in vivo models. *Cell Death Differ*.

LOPEZ-ARRIBILLAGA, E., RODILLA, V., PELLEGRINET, L., GUIU, J., IGLESIAS, M., ROMAN, A. C., GUTARRA, S., GONZALEZ, S., MUNOZ-CANOVES, P., FERNANDEZ-SALGUERO, P.,

RADTKE, F., BIGAS, A. & ESPINOSA, L. 2015. Bmi1 regulates murine intestinal stem cell proliferation and self-renewal downstream of Notch. *Development,* 142**,** 41-50.
LUGLI, A., SPICHTIN, H., MAURER, R., MIRLACHER, M., KIEFER, J., HUUSKO, P., AZORSA, D., TERRACCIANO, L., SAUTER, G., KALLIONIEMI, O. P., MOUSSES, S. & TORNILLO, L. 2005. EphB2 expression across 138 human tumor types in a tissue microarray: high levels of expression in gastrointestinal cancers. *Clin Cancer Res,* 11**,** 6450-8.
LV, T., YUAN, D., MIAO, X., LV, Y., ZHAN, P., SHEN, X. & SONG, Y. 2012. Over-expression of LSD1 promotes proliferation, migration and invasion in non-small cell lung cancer. *PLoS One,* 7**,** e35065.
MADISEN, L., ZWINGMAN, T. A., SUNKIN, S. M., OH, S. W., ZARIWALA, H. A., GU, H., NG, L. L., PALMITER, R. D., HAWRYLYCZ, M. J., JONES, A. R., LEIN, E. S. & ZENG, H. 2010. A robust and high-throughput Cre reporting and characterization system for the whole mouse brain. *Nat Neurosci,* 13**,** 133-40.
MALATERRE, J., CARPINELLI, M., ERNST, M., ALEXANDER, W., COOKE, M., SUTTON, S., DWORKIN, S., HEATH, J. K., FRAMPTON, J., MCARTHUR, G., CLEVERS, H., HILTON, D., MANTAMADIOTIS, T. & RAMSAY, R. G. 2007. c-Myb is required for progenitor cell homeostasis in colonic crypts. *Proc Natl Acad Sci U S A,* 104**,** 3829-34.
MANDRIOTA, S. J., TURNER, K. J., DAVIES, D. R., MURRAY, P. G., MORGAN, N. V., SOWTER, H. M., WYKOFF, C. C., MAHER, E. R., HARRIS, A. L., RATCLIFFE, P. J. & MAXWELL, P. H. 2002. HIF activation identifies early lesions in VHL kidneys: evidence for site-specific tumor suppressor function in the nephron. *Cancer Cell,* 1**,** 459-68.
MANI, S. A., GUO, W., LIAO, M. J., EATON, E. N., AYYANAN, A., ZHOU, A. Y., BROOKS, M., REINHARD, F., ZHANG, C. C., SHIPITSIN, M., CAMPBELL, L. L., POLYAK, K., BRISKEN, C., YANG, J. & WEINBERG, R. A. 2008. The epithelial-mesenchymal transition generates cells with properties of stem cells. *Cell,* 133**,** 704-15.
MARSH, V., WINTON, D. J., WILLIAMS, G. T., DUBOIS, N., TRUMPP, A., SANSOM, O. J. & CLARKE, A. R. 2008. Epithelial Pten is dispensable for intestinal homeostasis but suppresses adenoma development and progression after Apc mutation. *Nat Genet,* 40**,** 1436-44.
MATANO, M., DATE, S., SHIMOKAWA, M., TAKANO, A., FUJII, M., OHTA, Y., WATANABE, T., KANAI, T. & SATO, T. 2015. Modeling colorectal cancer using CRISPR-Cas9-mediated engineering of human intestinal organoids. *Nat Med,* 21**,** 256-62.
MAUNOURY, R., ROBINE, S., PRINGAULT, E., LEONARD, N., GAILLARD, J. A. & LOUVARD, D. 1992. Developmental regulation of villin gene expression in the epithelial cell lineages of mouse digestive and urogenital tracts. *Development,* 115**,** 717-28.
MCCLANAHAN, T., KOSEOGLU, S., SMITH, K., GREIN, J., GUSTAFSON, E., BLACK, S., KIRSCHMEIER, P. & SAMATAR, A. A. 2006. Identification of overexpression of orphan G protein-coupled receptor GPR49 in human colon and ovarian primary tumors. *Cancer Biol Ther,* 5**,** 419-26.
MERLOS-SUAREZ, A., BARRIGA, F. M., JUNG, P., IGLESIAS, M., CESPEDES, M. V., ROSSELL, D., SEVILLANO, M., HERNANDO-MOMBLONA, X., DA SILVA-DIZ, V., MUNOZ, P., CLEVERS, H., SANCHO, E., MANGUES, R. & BATLLE, E. 2011. The intestinal stem cell signature identifies colorectal cancer stem cells and predicts disease relapse. *Cell Stem Cell,* 8**,** 511-24.
MICCHELLI, C. A. & PERRIMON, N. 2006. Evidence that stem cells reside in the adult Drosophila midgut epithelium. *Nature,* 439**,** 475-9.

MIYOSHI, Y., ANDO, H., NAGASE, H., NISHISHO, I., HORII, A., MIKI, Y., MORI, T., UTSUNOMIYA, J., BABA, S., PETERSEN, G. & ET AL. 1992a. Germ-line mutations of the APC gene in 53 familial adenomatous polyposis patients. *Proc Natl Acad Sci U S A,* 89**,** 4452-6.

MIYOSHI, Y., NAGASE, H., ANDO, H., HORII, A., ICHII, S., NAKATSURU, S., AOKI, T., MIKI, Y., MORI, T. & NAKAMURA, Y. 1992b. Somatic mutations of the APC gene in colorectal tumors: mutation cluster region in the APC gene. *Hum Mol Genet,* 1**,** 229-33.

MOHAMMAD, H. P., SMITHEMAN, K. N., KAMAT, C. D., SOONG, D., FEDEROWICZ, K. E., VAN ALLER, G. S., SCHNECK, J. L., CARSON, J. D., LIU, Y., BUTTICELLO, M., BONNETTE, W. G., GORMAN, S. A., DEGENHARDT, Y., BAI, Y., MCCABE, M. T., PAPPALARDI, M. B., KASPAREC, J., TIAN, X., MCNULTY, K. C., ROUSE, M., MCDEVITT, P., HO, T., CROUTHAMEL, M., HART, T. K., CONCHA, N. O., MCHUGH, C. F., MILLER, W. H., DHANAK, D., TUMMINO, P. J., CARPENTER, C. L., JOHNSON, N. W., HANN, C. L. & KRUGER, R. G. 2015. A DNA Hypomethylation Signature Predicts Antitumor Activity of LSD1 Inhibitors in SCLC. *Cancer Cell,* 28**,** 57-69.

MOODY, S. E., PEREZ, D., PAN, T. C., SARKISIAN, C. J., PORTOCARRERO, C. P., STERNER, C. J., NOTORFRANCESCO, K. L., CARDIFF, R. D. & CHODOSH, L. A. 2005. The transcriptional repressor Snail promotes mammary tumor recurrence. *Cancer Cell,* 8**,** 197-209.

MOOLENBEEK, C. & RUITENBERG, E. J. 1981. The "Swiss roll": a simple technique for histological studies of the rodent intestine. *Lab Anim,* 15**,** 57-9.

MORIN, P. J., SPARKS, A. B., KORINEK, V., BARKER, N., CLEVERS, H., VOGELSTEIN, B. & KINZLER, K. W. 1997. Activation of beta-catenin-Tcf signaling in colon cancer by mutations in beta-catenin or APC. *Science,* 275**,** 1787-90.

MOSER, A. R., PITOT, H. C. & DOVE, W. F. 1990. A dominant mutation that predisposes to multiple intestinal neoplasia in the mouse. *Science,* 247**,** 322-4.

MOSER, A. R., SHOEMAKER, A. R., CONNELLY, C. S., CLIPSON, L., GOULD, K. A., LUONGO, C., DOVE, W. F., SIGGERS, P. H. & GARDNER, R. L. 1995. Homozygosity for the Min allele of Apc results in disruption of mouse development prior to gastrulation. *Dev Dyn,* 203**,** 422-33.

MUNOZ, J., STANGE, D. E., SCHEPERS, A. G., VAN DE WETERING, M., KOO, B. K., ITZKOVITZ, S., VOLCKMANN, R., KUNG, K. S., KOSTER, J., RADULESCU, S., MYANT, K., VERSTEEG, R., SANSOM, O. J., VAN ES, J. H., BARKER, N., VAN OUDENAARDEN, A., MOHAMMED, S., HECK, A. J. & CLEVERS, H. 2012. The Lgr5 intestinal stem cell signature: robust expression of proposed quiescent '+4' cell markers. *EMBO J,* 31**,** 3079-91.

MUNOZ, N. M., UPTON, M., ROJAS, A., WASHINGTON, M. K., LIN, L., CHYTIL, A., SOZMEN, E. G., MADISON, B. B., POZZI, A., MOON, R. T., MOSES, H. L. & GRADY, W. M. 2006. Transforming growth factor beta receptor type II inactivation induces the malignant transformation of intestinal neoplasms initiated by Apc mutation. *Cancer Res,* 66**,** 9837-44.

MURRAY, S. A., CARVER, E. A. & GRIDLEY, T. 2006. Generation of a Snail1 (Snai1) conditional null allele. *Genesis,* 44**,** 7-11.

MURRAY, S. A., ORAM, K. F. & GRIDLEY, T. 2007. Multiple functions of Snail family genes during palate development in mice. *Development,* 134**,** 1789-97.

NAGASE, H., MIYOSHI, Y., HORII, A., AOKI, T., OGAWA, M., UTSUNOMIYA, J., BABA, S., SASAZUKI, T. & NAKAMURA, Y. 1992. Correlation between the location of germ-line

mutations in the APC gene and the number of colorectal polyps in familial adenomatous polyposis patients. *Cancer Res,* 52**,** 4055-7.
NAGASE, H. & NAKAMURA, Y. 1993. Mutations of the APC (adenomatous polyposis coli) gene. *Hum Mutat,* 2**,** 425-34.
NEFZGER, C. M., JARDE, T., ROSSELLO, F. J., HORVAY, K., KNAUPP, A. S., POWELL, D. R., CHEN, J., ABUD, H. E. & POLO, J. M. 2016. A Versatile Strategy for Isolating a Highly Enriched Population of Intestinal Stem Cells. *Stem Cell Reports,* 6**,** 321-9.
NIETO, M. A. 2002. The snail superfamily of zinc-finger transcription factors. *Nat Rev Mol Cell Biol,* 3**,** 155-66.
NIETO, M. A., SARGENT, M. G., WILKINSON, D. G. & COOKE, J. 1994. Control of cell behavior during vertebrate development by Slug, a zinc finger gene. *Science,* 264**,** 835-9.
NYABI, O., NAESSENS, M., HAIGH, K., GEMBARSKA, A., GOOSSENS, S., MAETENS, M., DE CLERCQ, S., DROGAT, B., HAENEBALCKE, L., BARTUNKOVA, S., DE VOS, I., DE CRAENE, B., KARIMI, M., BERX, G., NAGY, A., HILSON, P., MARINE, J. C. & HAIGH, J. J. 2009. Efficient mouse transgenesis using Gateway-compatible ROSA26 locus targeting vectors and F1 hybrid ES cells. *Nucleic Acids Res,* 37**,** e55.
ONUMA, K., OCHIAI, M., ORIHASHI, K., TAKAHASHI, M., IMAI, T., NAKAGAMA, H. & HIPPO, Y. 2013. Genetic reconstitution of tumorigenesis in primary intestinal cells. *Proc Natl Acad Sci U S A,* 110**,** 11127-32.
POTTEN, C. S. 1977. Extreme sensitivity of some intestinal crypt cells to X and gamma irradiation. *Nature,* 269**,** 518-21.
POWELL, A. E., WANG, Y., LI, Y., POULIN, E. J., MEANS, A. L., WASHINGTON, M. K., HIGGINBOTHAM, J. N., JUCHHEIM, A., PRASAD, N., LEVY, S. E., GUO, Y., SHYR, Y., ARONOW, B. J., HAIGIS, K. M., FRANKLIN, J. L. & COFFEY, R. J. 2012. The pan-ErbB negative regulator Lrig1 is an intestinal stem cell marker that functions as a tumor suppressor. *Cell,* 149**,** 146-58.
POWELL, S. M., ZILZ, N., BEAZER-BARCLAY, Y., BRYAN, T. M., HAMILTON, S. R., THIBODEAU, S. N., VOGELSTEIN, B. & KINZLER, K. W. 1992. APC mutations occur early during colorectal tumorigenesis. *Nature,* 359**,** 235-7.
RAD, R., CADINANOS, J., RAD, L., VARELA, I., STRONG, A., KRIEGL, L., CONSTANTINO-CASAS, F., ESER, S., HIEBER, M., SEIDLER, B., PRICE, S., FRAGA, M. F., CALVANESE, V., HOFFMAN, G., PONSTINGL, H., SCHNEIDER, G., YUSA, K., GROVE, C., SCHMID, R. M., WANG, W., VASSILIOU, G., KIRCHNER, T., MCDERMOTT, U., LIU, P., SAUR, D. & BRADLEY, A. 2013. A genetic progression model of Braf(V600E)-induced intestinal tumorigenesis reveals targets for therapeutic intervention. *Cancer Cell,* 24**,** 15-29.
REED, K. R., MENIEL, V. S., MARSH, V., COLE, A., SANSOM, O. J. & CLARKE, A. R. 2008. A limited role for p53 in modulating the immediate phenotype of Apc loss in the intestine. *BMC Cancer,* 8**,** 162.
ROY, H. K., SMYRK, T. C., KOETSIER, J., VICTOR, T. A. & WALI, R. K. 2005. The transcriptional repressor SNAIL is overexpressed in human colon cancer. *Dig Dis Sci,* 50**,** 42-6.
SANGIORGI, E. & CAPECCHI, M. R. 2008. Bmi1 is expressed in vivo in intestinal stem cells. *Nat Genet,* 40**,** 915-20.
SANSOM, O. J., MENIEL, V., WILKINS, J. A., COLE, A. M., OIEN, K. A., MARSH, V., JAMIESON, T. J., GUERRA, C., ASHTON, G. H., BARBACID, M. & CLARKE, A. R. 2006. Loss of Apc allows phenotypic manifestation of the transforming properties of an endogenous K-ras oncogene in vivo. *Proc Natl Acad Sci U S A,* 103**,** 14122-7.

SANSOM, O. J., MENIEL, V. S., MUNCAN, V., PHESSE, T. J., WILKINS, J. A., REED, K. R., VASS, J. K., ATHINEOS, D., CLEVERS, H. & CLARKE, A. R. 2007. Myc deletion rescues Apc deficiency in the small intestine. *Nature,* 446**,** 676-9.

SANSOM, O. J., REED, K. R., HAYES, A. J., IRELAND, H., BRINKMANN, H., NEWTON, I. P., BATLLE, E., SIMON-ASSMANN, P., CLEVERS, H., NATHKE, I. S., CLARKE, A. R. & WINTON, D. J. 2004. Loss of Apc in vivo immediately perturbs Wnt signaling, differentiation, and migration. *Genes Dev,* 18**,** 1385-90.

SASAKI, N., SACHS, N., WIEBRANDS, K., ELLENBROEK, S. I., FUMAGALLI, A., LYUBIMOVA, A., BEGTHEL, H., VAN DEN BORN, M., VAN ES, J. H., KARTHAUS, W. R., LI, V. S., LOPEZ-IGLESIAS, C., PETERS, P. J., VAN RHEENEN, J., VAN OUDENAARDEN, A. & CLEVERS, H. 2016. Reg4+ deep crypt secretory cells function as epithelial niche for Lgr5+ stem cells in colon. *Proc Natl Acad Sci U S A,* 113**,** E5399-407.

SATO, T., STANGE, D. E., FERRANTE, M., VRIES, R. G., VAN ES, J. H., VAN DEN BRINK, S., VAN HOUDT, W. J., PRONK, A., VAN GORP, J., SIERSEMA, P. D. & CLEVERS, H. 2011. Long-term expansion of epithelial organoids from human colon, adenoma, adenocarcinoma, and Barrett's epithelium. *Gastroenterology,* 141**,** 1762-72.

SATO, T., VRIES, R. G., SNIPPERT, H. J., VAN DE WETERING, M., BARKER, N., STANGE, D. E., VAN ES, J. H., ABO, A., KUJALA, P., PETERS, P. J. & CLEVERS, H. 2009. Single Lgr5 stem cells build crypt-villus structures in vitro without a mesenchymal niche. *Nature,* 459**,** 262-5.

SAUER, B. & HENDERSON, N. 1988. Site-specific DNA recombination in mammalian cells by the Cre recombinase of bacteriophage P1. *Proc Natl Acad Sci U S A,* 85**,** 5166-70.

SCHEEL, C. & WEINBERG, R. A. 2012. Cancer stem cells and epithelial-mesenchymal transition: concepts and molecular links. *Semin Cancer Biol,* 22**,** 396-403.

SCHMIDT, D. M. & MCCAFFERTY, D. G. 2007. trans-2-Phenylcyclopropylamine is a mechanism-based inactivator of the histone demethylase LSD1. *Biochemistry,* 46**,** 4408-16.

SCHUIJERS, J., JUNKER, J. P., MOKRY, M., HATZIS, P., KOO, B. K., SASSELLI, V., VAN DER FLIER, L. G., CUPPEN, E., VAN OUDENAARDEN, A. & CLEVERS, H. 2015. Ascl2 acts as an R-spondin/Wnt-responsive switch to control stemness in intestinal crypts. *Cell Stem Cell,* 16**,** 158-70.

SCHWITALLA, S., ZIEGLER, P. K., HORST, D., BECKER, V., KERLE, I., BEGUS-NAHRMANN, Y., LECHEL, A., RUDOLPH, K. L., LANGER, R., SLOTTA-HUSPENINA, J., BADER, F. G., PRAZERES DA COSTA, O., NEURATH, M. F., MEINING, A., KIRCHNER, T. & GRETEN, F. R. 2013. Loss of p53 in enterocytes generates an inflammatory microenvironment enabling invasion and lymph node metastasis of carcinogen-induced colorectal tumors. *Cancer Cell,* 23**,** 93-106.

SEFTON, M., SANCHEZ, S. & NIETO, M. A. 1998. Conserved and divergent roles for members of the Snail family of transcription factors in the chick and mouse embryo. *Development,* 125**,** 3111-21.

SESHAGIRI, S., STAWISKI, E. W., DURINCK, S., MODRUSAN, Z., STORM, E. E., CONBOY, C. B., CHAUDHURI, S., GUAN, Y., JANAKIRAMAN, V., JAISWAL, B. S., GUILLORY, J., HA, C., DIJKGRAAF, G. J., STINSON, J., GNAD, F., HUNTLEY, M. A., DEGENHARDT, J. D., HAVERTY, P. M., BOURGON, R., WANG, W., KOEPPEN, H., GENTLEMAN, R., STARR, T. K., ZHANG, Z., LARGAESPADA, D. A., WU, T. D. & DE SAUVAGE, F. J. 2012. Recurrent R-spondin fusions in colon cancer. *Nature,* 488**,** 660-4.

SHIBATA, H., TOYAMA, K., SHIOYA, H., ITO, M., HIROTA, M., HASEGAWA, S., MATSUMOTO, H., TAKANO, H., AKIYAMA, T., TOYOSHIMA, K., KANAMARU, R., KANEGAE, Y., SAITO, I., NAKAMURA, Y., SHIBA, K. & NODA, T. 1997. Rapid colorectal adenoma formation initiated by conditional targeting of the Apc gene. *Science,* 278**,** 120-3.

SHIN, N. R., JEONG, E. H., CHOI, C. I., MOON, H. J., KWON, C. H., CHU, I. S., KIM, G. H., JEON, T. Y., KIM, D. H., LEE, J. H. & PARK, D. Y. 2012. Overexpression of Snail is associated with lymph node metastasis and poor prognosis in patients with gastric cancer. *BMC Cancer,* 12**,** 521.

SHPITZ, B., HAY, K., MEDLINE, A., BRUCE, W. R., BULL, S. B., GALLINGER, S. & STERN, H. 1996. Natural history of aberrant crypt foci. A surgical approach. *Dis Colon Rectum,* 39**,** 763-7.

SLEEMAN, K. E., KENDRICK, H., ASHWORTH, A., ISACKE, C. M. & SMALLEY, M. J. 2006. CD24 staining of mouse mammary gland cells defines luminal epithelial, myoepithelial/basal and non-epithelial cells. *Breast Cancer Res,* 8**,** R7.

SMITH, K. J., JOHNSON, K. A., BRYAN, T. M., HILL, D. E., MARKOWITZ, S., WILLSON, J. K., PARASKEVA, C., PETERSEN, G. M., HAMILTON, S. R., VOGELSTEIN, B. & ET AL. 1993. The APC gene product in normal and tumor cells. *Proc Natl Acad Sci U S A,* 90**,** 2846-50.

SNIPPERT, H. J., VAN DER FLIER, L. G., SATO, T., VAN ES, J. H., VAN DEN BORN, M., KROON-VEENBOER, C., BARKER, N., KLEIN, A. M., VAN RHEENEN, J., SIMONS, B. D. & CLEVERS, H. 2010. Intestinal crypt homeostasis results from neutral competition between symmetrically dividing Lgr5 stem cells. *Cell,* 143**,** 134-44.

SODIR, N. M., CHEN, X., PARK, R., NICKEL, A. E., CONTI, P. S., MOATS, R., BADING, J. R., SHIBATA, D. & LAIRD, P. W. 2006. Smad3 deficiency promotes tumorigenesis in the distal colon of ApcMin/+ mice. *Cancer Res,* 66**,** 8430-8.

SONG, N., POGUE-GEILE, K. L., GAVIN, P. G., YOTHERS, G., KIM, S. R., JOHNSON, N. L., LIPCHIK, C., ALLEGRA, C. J., PETRELLI, N. J., O'CONNELL, M. J., WOLMARK, N. & PAIK, S. 2016. Clinical Outcome From Oxaliplatin Treatment in Stage II/III Colon Cancer According to Intrinsic Subtypes: Secondary Analysis of NSABP C-07/NRG Oncology Randomized Clinical Trial. *JAMA Oncol,* 2**,** 1162-9.

SOUTHALL, T. D. & BRAND, A. H. 2009. Neural stem cell transcriptional networks highlight genes essential for nervous system development. *EMBO J,* 28**,** 3799-807.

TAKAHASHI, H., ISHII, H., NISHIDA, N., TAKEMASA, I., MIZUSHIMA, T., IKEDA, M., YOKOBORI, T., MIMORI, K., YAMAMOTO, H., SEKIMOTO, M., DOKI, Y. & MORI, M. 2011. Significance of Lgr5(+ve) cancer stem cells in the colon and rectum. *Ann Surg Oncol,* 18**,** 1166-74.

TAKAKU, K., OSHIMA, M., MIYOSHI, H., MATSUI, M., SELDIN, M. F. & TAKETO, M. M. 1998. Intestinal tumorigenesis in compound mutant mice of both Dpc4 (Smad4) and Apc genes. *Cell,* 92**,** 645-56.

UCHIDA, H., YAMAZAKI, K., FUKUMA, M., YAMADA, T., HAYASHIDA, T., HASEGAWA, H., KITAJIMA, M., KITAGAWA, Y. & SAKAMOTO, M. 2010. Overexpression of leucine-rich repeat-containing G protein-coupled receptor 5 in colorectal cancer. *Cancer Sci,* 101**,** 1731-7.

VAN DER FLIER, L. G., HAEGEBARTH, A., STANGE, D. E., VAN DE WETERING, M. & CLEVERS, H. 2009a. OLFM4 is a robust marker for stem cells in human intestine and marks a subset of colorectal cancer cells. *Gastroenterology,* 137**,** 15-7.

VAN DER FLIER, L. G., SABATES-BELLVER, J., OVING, I., HAEGEBARTH, A., DE PALO, M., ANTI, M., VAN GIJN, M. E., SUIJKERBUIJK, S., VAN DE WETERING, M., MARRA, G. & CLEVERS, H. 2007. The Intestinal Wnt/TCF Signature. *Gastroenterology,* 132**,** 628-32.

VAN DER FLIER, L. G., VAN GIJN, M. E., HATZIS, P., KUJALA, P., HAEGEBARTH, A., STANGE, D. E., BEGTHEL, H., VAN DEN BORN, M., GURYEV, V., OVING, I., VAN ES, J. H., BARKER, N., PETERS, P. J., VAN DE WETERING, M. & CLEVERS, H. 2009b. Transcription factor achaete scute-like 2 controls intestinal stem cell fate. *Cell,* 136**,** 903-12.

VAN NES, J. G., DE KRUIJF, E. M., PUTTER, H., FARATIAN, D., MUNRO, A., CAMPBELL, F., SMIT, V. T., LIEFERS, G. J., KUPPEN, P. J., VAN DE VELDE, C. J. & BARTLETT, J. M. 2012. Co-expression of SNAIL and TWIST determines prognosis in estrogen receptor-positive early breast cancer patients. *Breast Cancer Res Treat,* 133**,** 49-59.

VISVADER, J. E. & LINDEMAN, G. J. 2012. Cancer stem cells: current status and evolving complexities. *Cell Stem Cell,* 10**,** 717-28.

VLACHOGIANNIS, G., HEDAYAT, S., VATSIOU, A., JAMIN, Y., FERNANDEZ-MATEOS, J., KHAN, K., LAMPIS, A., EASON, K., HUNTINGFORD, I., BURKE, R., RATA, M., KOH, D. M., TUNARIU, N., COLLINS, D., HULKKI-WILSON, S., RAGULAN, C., SPITERI, I., MOORCRAFT, S. Y., CHAU, I., RAO, S., WATKINS, D., FOTIADIS, N., BALI, M., DARVISH-DAMAVANDI, M., LOTE, H., ELTAHIR, Z., SMYTH, E. C., BEGUM, R., CLARKE, P. A., HAHNE, J. C., DOWSETT, M., DE BONO, J., WORKMAN, P., SADANANDAM, A., FASSAN, M., SANSOM, O. J., ECCLES, S., STARLING, N., BRACONI, C., SOTTORIVA, A., ROBINSON, S. P., CUNNINGHAM, D. & VALERI, N. 2018. Patient-derived organoids model treatment response of metastatic gastrointestinal cancers. *Science,* 359**,** 920-926.

YASUI, K., SHIMAMURA, M., MITSUTAKE, N. & NAGAYAMA, Y. 2013. SNAIL induces epithelial-to-mesenchymal transition and cancer stem cell-like properties in aldehyde dehydroghenase-negative thyroid cancer cells. *Thyroid,* 23**,** 989-96.

YE, X., TAM, W. L., SHIBUE, T., KAYGUSUZ, Y., REINHARDT, F., NG EATON, E. & WEINBERG, R. A. 2015. Distinct EMT programs control normal mammary stem cells and tumour-initiating cells. *Nature,* 525**,** 256-60.

YOKOYAMA, K., KAMATA, N., FUJIMOTO, R., TSUTSUMI, S., TOMONARI, M., TAKI, M., HOSOKAWA, H. & NAGAYAMA, M. 2003. Increased invasion and matrix metalloproteinase-2 expression by Snail-induced mesenchymal transition in squamous cell carcinomas. *Int J Oncol,* 22**,** 891-8.

YOKOYAMA, K., KAMATA, N., HAYASHI, E., HOTEIYA, T., UEDA, N., FUJIMOTO, R. & NAGAYAMA, M. 2001. Reverse correlation of E-cadherin and snail expression in oral squamous cell carcinoma cells in vitro. *Oral Oncol,* 37**,** 65-71.

YOUNG, M., ORDONEZ, L. & CLARKE, A. R. 2013. What are the best routes to effectively model human colorectal cancer? *Mol Oncol,* 7**,** 178-89.

ZANDER, M. A., CANCINO, G. I., GRIDLEY, T., KAPLAN, D. R. & MILLER, F. D. 2014. The Snail transcription factor regulates the numbers of neural precursor cells and newborn neurons throughout mammalian life. *PLoS One,* 9**,** e104767.

ZHANG, J., LIU, W. L., TANG, D. C., CHEN, L., WANG, M., PACK, S. D., ZHUANG, Z. & RODGERS, G. P. 2002. Identification and characterization of a novel member of olfactomedin-related protein family, hGC-1, expressed during myeloid lineage development. *Gene,* 283**,** 83-93.